THE ROLE OF AMP-KINASE IN REGULATING AND REMODELING ADIPOCYTE METABOLISM

MANDEEP PINKY GAIDHU

A DISSERTATION SUBMITTED TO THE FACULTY OF GRADUATE STUDIES IN PARTIAL FULFILMENT OF THE REQUIREMENTS FOR THE DEGREE OF

DOCTOR OF PHILOSOPHY

GRADUATE PROGRAM IN KINESIOLOGY AND HEALTH SCIENCE
YORK UNIVERSITY
TORONTO, ONTARIO

JUNE 2011

Your file Votre référence
ISBN: 978-0-494-80545-9
Our file Notre référence
ISBN: 978-0-494-80545-9

ABSTRACT

Since obesity is characterized by excessive accumulation of white adipose tissue (WAT), remodeling adipocyte metabolism to promote energy dissipation versus storage has become of great therapeutic interest. AMP-kinase (AMPK) has emerged as a potential candidate for mediating these processes, since its activation causes suppression of anabolic pathways and promotes fatty acid (FA) oxidation. Previous data from our lab demonstrated that acute activation of AMPK elicits tissue-specific effects, however chronic activation of this enzyme remains to be elucidated with regards to glucose and lipid metabolism in WAT.

We investigated the role of AMPK on various metabolic parameters in the WAT of rodents using the pharmacological agonist AICAR in both *in vitro* and *in vivo* systems. We show evidence of time-dependent effects of chronic AICAR-induced AMPK activation on lipolysis, which involves antagonistic modulation of hormone-sensitive lipase (HSL) and adipose triglyceride lipase (ATGL). Additionally, we demonstrate that exposure of adipocytes for 15h to AICAR increased the expression of proteins involved in oxidative metabolism and an increase in FA oxidation. Chronic *in vivo* administration of AICAR supported these observations with increased mitochondrial content in subcutaneous and visceral WAT depots. Importantly, our *in vivo* work showed marked reductions in all WAT depots, an effect that was accompanied by increased spontaneous physical activity and energy expenditure. Conversely, in a diet-induced obesity model we observed a reduction in AMPK activity in WAT depots and corresponding reductions in

FA oxidation, suggesting impaired activity of this enzyme exists under pathophysiological conditions.

The fat-reducing effects of chronic AMPK activation are compatible with the inhibitory effect of this enzyme on glucose uptake in WAT. We clearly demonstrate the inhibitory effects of AICAR-induced AMPK activation are due to impaired phosphorylation of Akt-substrate of 160kDa (AS160) and a decrease in GLUT4 translocation to the plasma membrane, and this effect is mediated by AMPKα1 signaling.

In summary, our data suggest a role for AMPK in remodeling adipocyte metabolism by up-regulating pathways that stimulate energy dissipation versus lipid storage. These findings identify AMPK as a potential target for the development of therapies for the treatment of obesity and its related metabolic disorders.

ACKNOWLEDGEMENTS

ROnCo© mantra: That's just how we *roll.*

Dr. Rolando Ceddia: I never thought that a random email from a professor at York University would turn into a 6-year stint as your grad student! Thank you for trusting me with your ideas, for believing in my ability as a scientist, and for *never* settling for mediocrity. From 2005 as a Masters student to finishing my PhD from your lab, I leave with absolutely no regrets during my time under your supervision. I know saying thank you will never be able to express my gratitude for you, but I hope that this document says it on my behalf. This dissertation is dedicated to you, for your ideas and passion for science. I hope it makes you a fraction as proud as you've made me.

Dr. Sergiu Fediuc: I have no doubt that you and I will be co-authors for life and friends for eternity. I'm proud to call you Vanilla, my "brotha from anotha motha".

Dr. Robert Perry: Roberts, your friendship in the last few years has been nothing short of wonderful – and necessary. Thanks for being a friend, colleague, sound-board, and coffee-mate. I also can't believe I met someone who's mind is deeper in the gutter than mine. Nice to know I'm not alone.

Dr. Andrea Frontini: Who knew rats could fly?! *Mama mia, soltanto in Italia!* You are a gifted scientist and an amazing person. I am grateful that I had the opportunity to meet and work with you – even on your days with God.

Steven ('Steamin' – you have a question?), Kathryn ('Bumblebee'), Fawad ('Fawads' my protégé) and Sanaz ('Bare & Darin'): You guys are <u>all</u> trouble, but 100% worth it. Thank you for your assistance and comic relief.

Nicole Anthony and Mandy So: My sincerest gratitude for your help with experiments and your friendship beyond the lab bench.

Drs. S. Cinti and T. Kadowaki: For allowing me to conduct research in their labs abroad and the wonderful collaborative experiences.

Supervisory committee: Thank you for your valuable input.

Other labmates - too numerous to name: All equally appreciated.

My family: Thanks for not always questioning what I'm still doing in school, even though I know it's killing you not to ask.

Mango: My rock - always there for me. Thank you for your unconditional love.

Aubrey Reid: The only thing more difficult than being a grad student is being in a relationship with one. Thank you for being so patient, understanding, and for always offering to edit my work. For all the times you were voluntarily in the lab on weekends, holidays, and nights to help with experiments and just to be there with me – I know I am fortunate to have you to love. Thanks for sticking around.

TABLE OF CONTENTS

LIST OF TABLES AND FIGURES

LIST OF ABBREVIATIONS

α-AR	Alpha adrenoreceptor
AC	Adenylyl cyclase
ACC	Acetyl-CoA carboxylase
ACL	ATP-citrate lyase
ADP	Adenosine diphosphate
AICAR	5-aminoimidazole-4-carboxamide-1-beta-d-ribofuranoside
AMP	Adenosine monophosphate
AMPK	AMP-activated protein kinase
AS160	Akt/PKB substrate of 160 kDa
ATGL	Adipose triglyceride lipase (or desnutrin, or calcium-independent phospholipase A2 isoform zeta (iPLA2ζ))
ATP	Adenosine triphosphate
β-AR	Beta-adrenoceptor
cAMP	Cyclic AMP
CBS	Cystathionine-β-synthase
CE	Cholesterol ester
CGI-58	Comparative gene identification-58 (or α/β hydrolase domain-containing protein 5 (ABHD5))
CoA	Coenzyme A
CPT-1	Carnitine palmitoyltransferase isoform 1
DAG	Diacylglycerol
DGAT	DAG acyltransferase
FA/NEFA	Fatty acid/non-esterified fatty acid (FA and NEFA are used interchangeably)
FA-CoA	Fatty acyl-CoA
FAS	FA synthase
FTP	FA transport protein
GBD	Glycogen-binding domain
GLUT4	Glucose transporter isoform 4
GyK	Glycerol kinase
G-3-P	Glycerol-3-phosphate
G-6-P	Glucose-6-phosphate
GPAT	G-3-P acyltransferase
GPDH	G-3-P dehydrogenase
HFD	High fat diet
HSL	Hormone-sensitive lipase
IL-6	Interleukin-6
IRS-1	Insulin receptor substrate isoform 1
LDL	Low density lipoprotein
MAG	Monoacylglycerol

MAGL	MAG lipase
NEFA/FA	Non-esterified FA (NEFA and FA are used interchangeably)
OAA	Oxaloacetate
PEPCK-C	Phosphoenolpyruvate carboxykinase (cytosolic isoform)
PDE-3	Phosphodiesterase isoform 3
PI3-K	Phosphatidylinositol 3-kinase
PP	Protein phosphatase
PPARα	Peroxisome proliferator-activated receptor isoform alpha
PPARγ	PPAR isoform gamma
PGC-1α	PPARγ coactivator-1 α
PKA	Protein kinase A
PKB	Protein kinase B (or Akt)
Peri-A	Perilipin A
SC	Subcutaneous
TAG	Triacylglycerol
TNF-α	Tumor necrosis factor α
TZD	Thiazolidindione
T2D	Type 2 diabetes
VC	Visceral
WAT	White adipose tissue
ZMP	5-aminoimidazole-4-carboxamide-1-β-D-ribofuronosil-5'-monophosphate

CHAPTER 1: INTRODUCTION

Obesity rates in Canada have risen over the past 25 years, with the prevalence of obesity (defined as having a body mass index (BMI) of 30 kg/m^2 or more) reaching 24.1% amongst Canadian adults in 2007-2009 (1). Unfortunately, a substantial number of Canadian youth are also part of this trend with obesity rates among adolescents tripling from 1978 to 2004 (2), which is particularly alarming since this condition often persists into adulthood. For both adults and adolescents, the current obesity epidemic is at least partially attributed to decreased physical activity coupled with excessive energy intake from high sugar and fat-laden "convenience" or fast food.

The burden of obesity on the Canadian healthcare system has been substantial, particularly in the last decade. Recent estimates on the direct costs of obesity on healthcare reached $5.9 billion in 2006, accounting for 4.1% of the total federal healthcare budget (3). Approximately $2.0 billion was attributed to overweight individuals (defined as having a BMI of 27 or greater) while $3.9 billion was due to the obese population (3). Direct costs included medical, psychological, and psychiatric diagnoses and treatment of comorbidities that were strongly linked to obesity (3). These include, but are not limited to: type 2 diabetes, cardiovascular disease, several types of cancer, sleep apnea, and osteoarthritis. As research in the field of bariatrics progresses, identification of new comorbidities will add to the current costs inflicted by obesity. Additionally, these numbers do not even include the indirect expenses to the healthcare system, which include loss of wages and reduced productivity in the working sector. Therefore, implementation of health policies and interventions in order to prevent or

counteract obesity are necessary for both the health and well-being of Canadians, and for the economic "health" of the health care system.

Currently, the most common prescription to try and counteract obesity is a regimen of exercise and diet, which is generally effective in the short-term. Unfortunately, long-term success rates of this therapy are low, where 90-95% of adults and children who lose weight gain it back within 1-2 years (4). This is due to hormonal and physiological changes that up-regulate mechanisms of food intake and reduces the basal metabolic rate under conditions of chronic negative energy balance to maintain weight at a "set-point" and prevent continuous weight loss (5). Understanding the protective mechanisms that are activated under these conditions will help in developing new therapies and identify new targets for treating obesity and its related comorbidities. Novel approaches could involve either increasing energy expenditure or reducing food intake, while bypassing energy sparing mechanisms in order to maintain long-term weight loss. To date, there are no pharmacological or surgical treatments for obesity that are at the same time effective and free of undesirable and dangerous side effects. Almost all appetite suppressants (i.e. diethylproprion, fenfluramine) are modified amphetamines that alter the brain chemistry in order to reduce hunger, but also tend to foster anxiety, depression, and suicidal thoughts (6,7). Increasing energy expenditure through consumption of products containing ephedrine alkaloids was popular in North America. Unfortunately, it had such adverse effects to the cardiovascular and central nervous system of users that the compound is now banned as a weight loss agent (8,9). Therefore, identifying targets and developing therapies for treating obesity that are not accompanied by unacceptable side

effects will reduce the risk of associated comorbidities, and improve the health and lives of Canadians. In this context, it is important to identify strategies and molecular targets to overcome energy-sparing mechanisms in order to improve the outcome of weight loss programs.

CHAPTER 2: LITERATURE REVIEW

2.1. White adipose tissue (WAT)

2.1.1. Structure and distribution

The WAT is the major energy reservoir in mammals and plays a critical role in the maintenance of whole-body energy homeostasis. The WAT is composed of 35-75% white adipocytes, with the remaining being comprised of stromal vasculature tissue containing fibroblasts, endothelial cells, blood cells, macrophages, pericytes, and preadipocytes among others (10). White adipocytes are specialized and differentiated spherical cells with a great capacity to store lipids in the form of triacylglycerides (TAGs) for subsequent release of fatty acids (FAs) under conditions of high metabolic demand (i.e. exercise) or negative energy balance (i.e. food restriction). Once the adipocyte has reached a mature appearance of a single lipid droplet (unilocular adipocytes) surrounded by a rim of cytoplasm and offset nucleus, cell size can continue to increase from less than 10μm to nearly 200μm in diameter, mostly by increases in TAG storage (10). White adipocytes have a small number of thin and elongated mitochondria with randomly oriented cristae (10). Other organelles such as Golgi complex, rough and smooth endoplasmic reticulum, and lysosomes are poorly developed in these cells (10).

WAT is distributed throughout the body in subcutaneous (SC) and visceral (VC) regions. SC tissue lies beneath the dermis, while VC adipose tissue resides within the body cavity. In mice and rats, the SC depots account for about 60-70% of the adipose organ. The remaining parts of the organ (30-40%) form several VC depots in the thorax, abdomen, and limbs (10). In humans, 80% of the total WAT exists as SC while the

remaining 20% corresponds to the VC component (11). It is important to note that the VC fat depots in humans correspond to those described above for rodents, except that the omental depot is much more developed and epididymal fat is not found in the former. Despite these depot-specific differences, the morphology of human adipose tissues is identical to that of mice and rats (10).

2.1.2. Main functions

From a metabolic perspective, the main classical functions of white adipocytes are: **a)** lipid synthesis and storage from a variety of substrates; and **b)** TAG breakdown (lipolysis) and exportation of FAs (10,12). However, adipocytes also express and secrete various factors (adipokines) that exert autocrine, paracrine, and endocrine effects in the body (12). These adipokines relay information to the CNS regarding energy availability in the organism and make continuous adjustments in food intake and energy expenditure (13,). Therefore, the WAT is currently viewed as a multifunctional organ that has the ability to regulate the metabolic rate of various organs and tissues, as well as whole-body substrate metabolism and energy homeostasis (12,13).

2.1.2.1. Energy storage

A primary function of adipocytes is the storage of excess energy in the highly efficient form of TAGs, where 1g of lipid yields 9 kCal/g compared to glucose or protein which yields approximately 4 kCal/g. Fat is stored as neutral TAGs in the adipocyte, which requires esterification of circulating FAs with a glycerol backbone. As the name implies, TAG consist of a 3-carbon glycerol backbone with 3 FAs attached by ester

bonds. Therefore, glycerol synthesis within the adipocyte is crucial for lipid esterification and storage as TAG. This process depends fundamentally on the uptake of glucose and conversion of this substrate into glycerol-3-phosphate (G-3P) (14). A considerable fraction of glucose (20-30%) under normal conditions is used for producing intracellular G-3P (14) since the enzyme glycerol kinase (GyK) is present in very low amounts in adipose tissue (15). Efficient glucose transport requires the hormone insulin, which triggers a series of intracellular events resulting in the translocation of glucose transporter 4 (GLUT4) to the plasma membrane for facilitation of glucose uptake in skeletal muscle and white adipose tissue (16) (Figure 2-1). Briefly, insulin is secreted by pancreatic β-cells under conditions of high plasma glucose, i.e. post-prandially. Insulin binds to the insulin receptor (IR) and is autophosphorylated. This results in an interaction with insulin receptor substrate 1 (IRS-1) (17,18) allowing the IR to phosphorylate IRS-1 at multiple tyrosine residues. The phosphotyrosine residues of IRS-1 then interact with the p85 sub-unit of phosphatidylinositol 3-kinase (PI3-K), thereby recruiting the p110 catalytic subunit of this enzyme to the plasma membrane where it converts phosphatidylinositol (3,4) biphosphate (PIP_2) into phosphatidylinositol (3,4,5) triphosphate (PIP_3) (17,18). Activation of the PI3-K pathway by insulin leads to rapid increase of PIP_3 and activation phosphatidylinositol-dependent kinases 1 and 2 (PDK1/2), also located on the plasma membrane. The latter directly activates downstream mediators, such as Akt/protein kinase B (Akt/PKB), via phosphorylation on serine and threonine residues (17,18) (Figure 2-1). Phosphorylation of Akt then targets

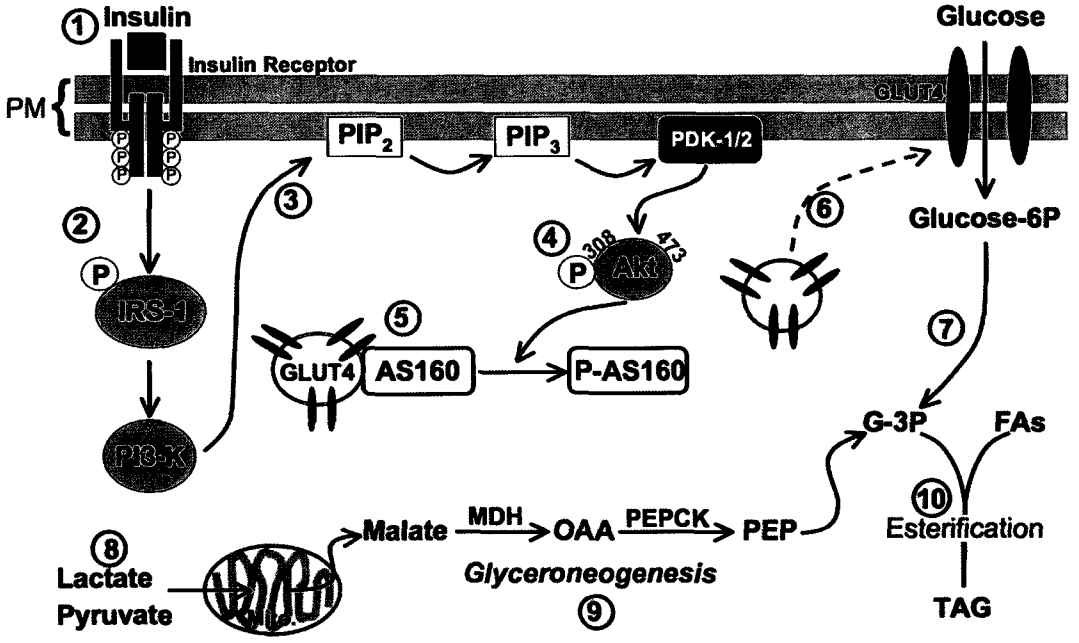

Figure 2-1. Schematic representation of the intracellular signaling steps of insulin-stimulated glucose uptake and glyceroneogenesis. **(1)** Insulin binds to its receptor, which is subsequently autophosphorylated. This facilitates phosphorylation of tyrosine residues on IRS-1 **(2)** and activates PI3-K. PI3-K converts PIP_2 to PIP_3 **(3)**, subsequently activating PDK-1/2 and targets Akt for phosphorylation/activation at Thr308 and Ser473 residues, respectively **(4)**. Under basal conditions, AS160 promotes intracellular retention of GLUT4-containing vesicles **(5)**. However, once phosphorylated by Akt under insulin-stimulated conditions AS160 is inactivated and allows GLUT4 vesicles to translocate, dock, and fuse with the plasma membrane **(6)**. This allows glucose to enter the cell, where it is promptly phosphorylated and enters the glycolytic pathway **(7)**. In adipocytes, glucose is primarily used to generate glycerol-3-phosphate (G-3P) in order to esterify FAs. Alternatively, non-carbohydrate precursors (i.e. lactate, pyruvate) **(8)** can be metabolized and converted to G-3P through the process of glyceroneogenesis **(9)**. Up to 3 FAs can be esterified to the G-3P backbone to generate TAG for neutral lipid storage **(10)**. PM, plasma membrane; Mito, mitochondria; MDH, malate dehydrogenase.

the Akt Substrate of 160kDa (AS160). AS160 contains six potential phosphomotifs allowing it to be phosphorylated by Akt at these residues upon insulin stimulation (19). AS160 has been identified as a protein containing a **G**TPase-**a**ctivating **p**rotein (GAP) domain towards members of the Rab protein family (20). Rabs are small G-proteins that participate in vesicle movement and fusion with target membranes (21). It has been proposed that the GAP domain of AS160 acts on Rab proteins stimulating the conversion of GTP into GDP, rendering Rab inactive (21). However, upon insulin stimulation, the activity of the AS160 GAP domain is inhibited, increasing the amount of GTP-bound Rab allowing translocation of GLUT4 vesicles to dock and fuse with the plasma membrane (22) (Figure 2-1). This results in exocytosis of the vesicle's contents, and GLUT4 is fused to plasma membrane to allow glucose transport into the cell. Although GLUT4 is the most insulin-sensitive isoform of the GLUT family, GLUT1 is also modestly stimulated by insulin by about 1.5-fold relative to basal levels (16). GLUT1 is ubiquitously expressed in many tissues, including muscle and adipose tissues, and accounts for the majority of basal levels of glucose uptake.

In addition to using glucose to produce G-3P, non-glucose derived precursors such as lactate and pyruvate can also be utilized in a process termed glyceroneogenesis (Figure 2-1). This is particularly important under conditions such as fasting, where FAs released from the WAT inevitably return to the adipocyte to be re-esterified. In this scenario, the limited amount of glucose under fasting conditions is spared for use by the central nervous system (CNS). Therefore, these conditions require glyceroneogenesis to generate G-3P for FA esterification. For this process to take place, non-glucose derived substrates

(i.e.lactate) enter the mitochondria and are converted into malate via malate dehydrogenase. Malate exits the mitochondria and enters the cytosol, where malate is converted into oxaloacetate (OAA). OAA is acted on by phosphoenolpyruvate carboxykinase (PEPCK), the rate limiting enzyme for glyceroneogenesis (Figure 2-1). PEPCK converts OAA into phosphoenolpyruvate (PEP) and through a series of intracellular biochemical reactions, produces G-3P. The importance of PEPCK in WAT in the recycling and re-esterification of FAs is demonstrated by adipose tissue-specific PEPCK knockout mice that display lipodystrophy (23), while overexpression of the enzyme fosters an obese phenotype (24). When considering that high levels of non-esterified FAs (NEFAs) are hallmarks of metabolic diseases such as insulin resistance and type 2 diabetes, the role of PEPCK in glyceroneogenesis is important for normalizing plasma NEFA levels, and maintaining energy homeostasis.

One source of FAs comes from dietary fats. When ingested, the majority of fat is carried to the small intestine to be broken down. At this stage, fats are emulsified by bile salts in the duodenum and converted by the enterocytes into lipid-protein complexes called lipoproteins, more specifically chylomicrons (25). These lipoproteins enter the lymphatic system, which shuttles these lipid-rich particles to the circulatory system. Chylomicrons are acted on by lipoprotein lipase (LPL) that mobilizes FAs so they can be taken up by the adipocyte by either diffusion through the plasma membrane or via proteins that facilitate FA transport into the adipocyte (26,27). FAs are then available to be esterified by G-3P for storage as neutral TAG molecules. The remnants of the chylomicrons are processed in the liver (15).

Alternatively, adipocytes also have the machinery in place to undergo *de novo* FA synthesis under conditions where glucose influx into the adipocyte is high (i.e. post-prandially). This process begins with the conversion of glucose into pyruvate, which is then decarboxylated in the mitochondria and converted to acetyl-CoA. The latter undergoes a condensation reaction with oxaloacetate to form citrate in the Kreb's cycle. Citrate exits the mitochondrion and can be cleaved by ATP-citrate lyase (ACL) to form oxaloacetate and acetyl-CoA in the cytoplasm (28). Subsequently, acetyl-CoA carboxylase (ACC) uses acetyl-CoA as a substrate to produce malonyl-CoA, a 3-carbon molecule (29),(30). The fatty acid synthase (FAS) complex then initiates FA synthesis via a condensation reaction between acetyl-CoA and malonyl-CoA (34), resulting in a 4-carbon molecule and the release of a CO_2 molecule during the reaction. In order to make a long-chain fatty acid (LCFA), several condensation reactions follow, each time adding 2-carbons from a malonyl-CoA molecule and releasing a CO_2 molecule. Once a 16-carbon chain is produced, a thioesterase cleaves the bond linking the carbon chain with the FAS complex, and completes the *de novo* lipogenic pathway. Once palmitate is produced, it can be modified by increasing the length of the carbon chain through the action of elongases (i.e. stearate, 18 carbons) as well as through introduction of double bonds via desaturases to produce unsaturated FAs (i.e. oleate, 18 carbons with one double bond). Subsequently, three of these newly formed FAs are esterified with G-3P to form TAG. The TAGs then merge with the large central droplet, making the adipocyte larger (31).

2.1.2.2. Regulation of lipolysis in the adipose tissue

Lipolysis occurs when the body's glucose stores are low, during periods of fasting (32), and/or exercise (33). In these conditions, FAs become the major substrate for energy production in most peripheral tissues and organs, sparing glucose to be utilized by the central nervous system (32). In this context, the adipocyte takes the role of exporting FAs to other organs for oxidation during glucose deficit conditions (34). In order for this to occur, lipolysis must take place within the adipocyte to breakdown stored TAGs for glycerol and FA exportation (Figure 2-2). This process is stimulated under conditions such as exercise and fasting, where catecholamines such as epinephrine and norepinephrine are produced and released by either the adrenal glands or by post-ganglionic sympathetic fibres. Epinephrine is predominately produced and secreted by the adrenal glands and enters the circulatory system whereas norepinephrine is the primary neurotransmitter for sympathetic nerve fibres. Both catecholamines produce similar responses with respect to increasing lipolysis, and are delivered to tissues through the endocrine system or via direct sympathetic innervation of the WAT. To stimulate lipolysis, catecholamines bind to a β-adrenergic receptors (β-ARs) located on the surface of the adipocyte (34) (Figure 2-2). Three different isoforms of β-ARs exist in WAT. While β1 and β2 are predominately expressed in humans, β3 is responsible for the majority of the effects in rodents (35). Binding of catecholamines to the β-AR induces an intracellular cascade mediated by the G-stimulatory-protein coupled receptor (G_sPCR) and its effector adenylate cyclase (34) that increase cyclic AMP (cAMP) production. This leads to the activation of Protein Kinase A (PKA) and phosphorylation of several

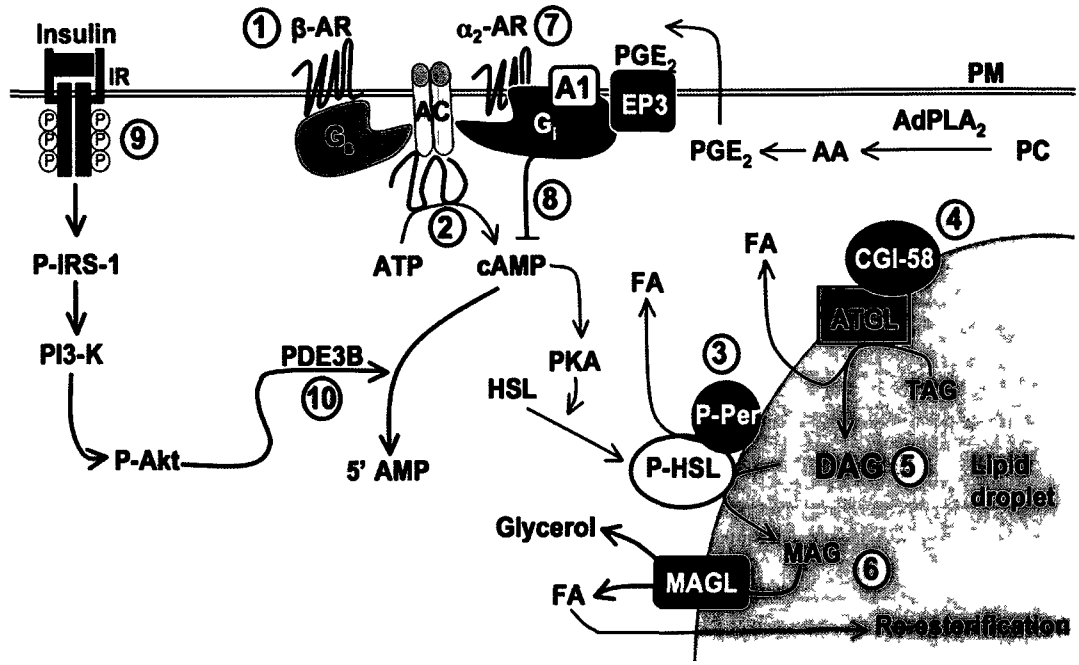

Figure 2-2. Regulation of lipolysis in adipocytes. When catecholamines are released they bind to β-ARs **(1)** coupled to G-stimulatory proteins that subsequently activates adenylate cyclase (AC) to generate cAMP **(2)**. High levels of cAMP activate PKA and phosphorylates both HSL and perilipin (Peri) **(3)**. Perilipin is associated with CGI-58 under basal conditions, however when phosphorylated, it dissociates from CGI-58 and promotes fragmentation of the lipid droplet to allow lipase access for hydrolysis to occur. The first step of TAG hydrolysis requires ATGL to associate with CGI-58 **(4)**, which act together to liberate the first FA from the TAG molecule generating DAG **(5)**. P-HSL translocates to the lipid droplet to breakdown DAGs, generating MAG **(6)**. The last step of lipolysis requires the constitutively active MAG lipase to release the final FA and glycerol backbone that originally held the TAG together. FAs are exported to peripheral tissues, or re-enter the adipocyte to be either re-esterified or metabolized. Mechanisms also exist to inhibit lipolysis, including presence of α2-ARs, adenosine A1, and EP3 prostaglandin receptors **(7)** that are coupled to G-inhibitory proteins. Binding of ligands to these receptors inhibits cAMP production **(8)** and subsequently the lipolytic cascade. Lipoysis is also potently inhibited through insulin signaling **(9)**. Phosphorylation of the downstream target Akt activates phosphodiesterase-3B (PDE3B), an enzyme that inactivates cAMP by converting it into 5'AMP **(10)**.

downstream targets including perilipin A, a protein located exclusively on the surface of the adipocyte lipid droplet (Figure 2-2). Perilipin has been demonstrated to serve a dual role by acting as a protective barrier for the lipid droplet under basal conditions, while also being necessary for propagating the catecholamine-induced lipolytic response (36). Under basal conditions, perilipin coats the lipid drop in association with comparative gene identification 58 (CGI-58; also known as abhydrolase domain containing protein 5) (37-39). Once phosphorylated at serines residues 492 and 517, perilipin dissociates from CGI-58 and causes fragmentation and dispersion of lipid droplets (40). This provides lipases greater access to TAG molecules in order for hydrolysis to occur. CGI-58 that is dissociated from perilipin interacts with adipose triglyceride lipase (ATGL) to activate this enzyme and initiate lipolysis by removing the first FA from a TAG molecule through a hydrolysis reaction (41). The removal of a FA from TAG generates the intermediate diacylglycerol (DAG) (Figure 2-2), a reaction that is facilitated by adipose triglyceride lipase (ATGL). ATGL has been described as a TAG-specific lipase, and has recently been shown to be the rate-limiting step of the lipolytic pathway (42). In fact, ATGL null mice show ectopic deposition of WAT in many organs, including the heart, causing cardiac dysfunction and premature death (43).

Currently, hormone sensitive lipase (HSL) is the only hydrolase that has been identified as a DAG lipase. In fact, in HSL null mice, the inability to breakdown DAGs causes accumulation of this intermediate within the WAT (44). When PKA is active, it phosphorylates HSL at key serine residues (563, 659, and 660 in rat, and 552, 640, 650 in humans) (45) and facilitates its translocation to the lipid droplet (46). Simultaneously,

phosphorylation of perilipin at serine residues 8, 222, and 276 in rodents has also been demonstrated to be critical for recruitment of HSL to perilipin-coated droplets (47). Therefore, PKA phosphorylation of both HSL and perilipin is required for the breakdown of DAG. Once DAG has been cleaved to produce monoacylglycerol (MAG), a constitutively active MAG lipase releases the final FA and the glycerol backbone that originally held the TAG together (48) (Figure 2-2). While the liver metabolizes glycerol molecules, FAs are conjugated with serum albumin and transported through the circulatory system. Once in the circulation, FAs are taken up by peripheral tissues (i.e. heart muscle, liver, skeletal muscle, etc) and enter several different pathways or re-enter the adipocyte for re-esterification (26).

Under resting or basal conditions, lipolysis is suppressed and fat stores are preserved for potential future episodes of increased energy demand. The most potent inhibitor of lipolysis in WAT is insulin, which phosphorylates and activates phosphodiesterase 3B (PDE3B). When activated, PDE3B converts cAMP to the inactive 5'AMP and prevents the activation of downstream targets that promote lipolysis (Figure 2-2). Adipocytes also express α2 adrenergic G-inhibitory-protein coupled receptors (G_iPCR) (Figure 2-2). Contrary to β-ARs, catecholamine-induced activation of α2-ARs inhibits adenylate cyclase and prevents the lipolytic cascade. Binding studies indicate that epinephrine has a greater affinity for α2 receptors compared to norepinephrine, although both hormones display greater binding affinity to α2 receptors than to β1 and β2-AR isoforms (35). Interestingly, despite these observations, the effect of β-adrenergic

stimulation predominates under catecholamine-stimulated conditions. This appears to be linked with the absence or abundance of the β3-AR, and the ratio between these receptors and the α2-ARs (35). The dual presence of these antagonistic receptors plays an important role in different physiological conditions. Under resting circumstances, low levels of catecholamines preferentially bind to α2-ARs and inhibit lipolysis. On the other hand, during conditions where there are high levels of sympathetic activity, β-ARs are highly operative and activation of these receptors overrides the inhibitory effect of α2-ARs on lipolysis. Therefore, the interplay between β- and α2-ARs is important in regulating fat cell function with respect to lipolysis under basal and catecholamine-stimulated conditions.

It has been well established that prostaglandins and adenosine are produced by the WAT and serve as paracrine/autocrine inhibitors of lipolysis. Of the prostaglandins, prostaglandin E_2 (PGE_2) is released in the highest levels by adipose tissue (49). Its synthesis requires the WAT-specific adipose phospholipase A_2 ($AdPLA_2$) to convert phosphatidylcholine into arachadonic acid, the main precursor for prostaglandin synthesis (49) (Figure 2-2). Once PGE_2 is synthesized, it is secreted by the WAT and acts as the primary ligand for the E-prostanoid 3 receptor (EP3) located on the cell membrane of adipocytes (50). EP3 is coupled to G_i protein receptors and inhibits cAMP production, thereby exerting an anti-lipolytic effect (50) (Figure 2-2). Also released by the WAT and other cells in the body, adenosine acts via its receptors (adenosine 1, A1 and adenosine 2, A2 receptors) that are coupled to inhibitory and stimulatory GPCRs, respectively (Figure

2-2). A1 receptors are highly expressed in mature adipocytes making adenosine a potent inhibitor of lipolysis (51). On the other hand, A2 receptors are less abundant in fully differentiated adipocytes (51) and do not seem to exert important regulatory roles in WAT lipolysis.

2.1.2.3. Endocrine function of adipose tissue

Once considered a mere energy reservoir, it is now clear that the WAT has the ability to secrete bioactive molecules collectively referred to as adipokines. These adipocyte-derived proteins act at both the local and systemic levels and play important roles in many metabolic processes, including steroid synthesis, inflammation, as well as in glucose and lipid transport (52). In particular, leptin, adiponectin, tumor necrosis factor α (TNFα), and interleukin 6 (IL-6) have been demonstrated to play important roles in regulating insulin action and whole-body energy homeostasis (52).

Leptin

With respect to whole-body energy homeostasis, leptin seems to be the most influential adipokine. Leptin is a 16 kDa peptide hormone that was identified in 1994 as the circulating hormone that could transmit information to the central nervous system (CNS) regarding the energy stores in the body (53). Circulating leptin levels are directly proportional to the amount of WAT present in the body. This hormone signals to the CNS to regulate food intake and energy expenditure accordingly. The impact of leptin on energy homeostasis has been well demonstrated in mice lacking a functional form of leptin (*ob/ob* mice). These animals exhibit hyperphagia, reduced energy expenditure,

obesity, and insulin resistance (54). These abnormalities were eradicated with the administration of exogenous leptin (54), which gave great promise to the role of leptin as the "anti-obesity hormone". However, this idea was quickly dispelled with the discovery that obese humans and various animal models of diet-induced obesity had high circulating levels of leptin without the accompanying anorexic effects, indicating the presence of leptin resistance (55-57). The cause of leptin resistance is not clearly understood, although hypotheses on defects in leptin signaling and transport across the blood-brain-barrier are currently being investigated (58).

The effects of leptin require cell-surface receptors expressed in both the periphery and CNS. Five splice variants of the leptin receptor (LepR) exist (denoted as *a* to *e*), however the long form of LepR (variant b) seems to mediate the majority of the effects of leptin through the JAK2-STAT3 (**Ja**nus **k**inase **2**-**s**ignal **t**ransducer and **a**ctivator of **t**ranscription **3**) pathway (Figure 2-3). Once leptin binds to LepRb, which exists as homodimerized transmembrane gp130 molecules, the JAK2 kinases constitutively associated with the cytoplasmic portion of the receptor are activated. This allows JAK to phosphorylate the receptor cytoplasmic domains, creating docking sites for src-homology 2 (SH2)-containing signaling proteins, such as STAT3. Located in the cytoplasm under resting conditions, STAT3 docks onto LepRb and is phosphorylated at tyrosine residue 705 (59). STAT3 then dimerizes and migrate to the nucleus where the complex activates a variety of genes such as the anorexigenic peptide proopiomelanocortin (POMC) as well as up-regulation of suppressor of cytokine signaling 3 (SOCS3). The latter works as

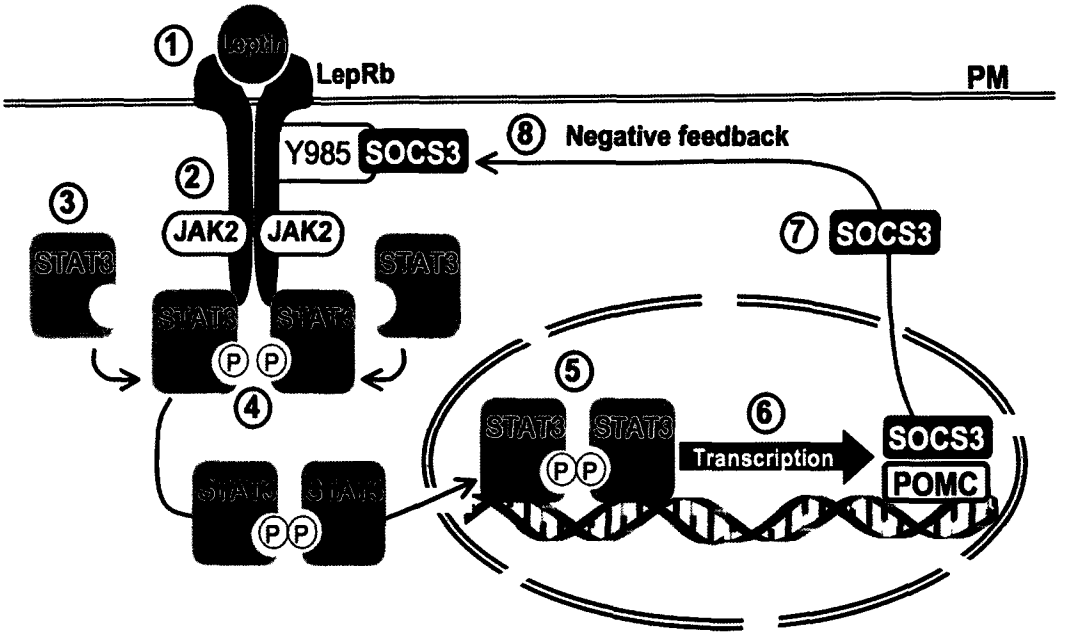

Figure 2-3. Leptin signaling via STAT3 in the hypothalamus. Leptin binds to its homodimerized receptor **(1)** and activates the JAK2 kinases located on the cytoplasmic portion of LepRb **(2)**. This allows STAT3, which are normally in the cytoplasm **(3)**, to dock onto the LepRb where they are phosphorylated and able to dimerize **(4)**. Once dimerized, STAT3 enters the nucleus **(5)** and promotes expression of many genes **(6)**, including POMC and SOCS3. SOCS3 exits the nucleus **(7)** and acts as a negative feedback mechanism by phosphorylating the tyrosine 985 (Y985) residue on LepRb **(8)**. This prevents leptin signaling through the JAK2-STAT3 pathway.

a negative feedback regulator through binding to phosphorylated tyrosine residue 985 on LepRb and prevents leptin signaling through STAT3 (60) (Figure 2-3). Leptin receptors are present in various hypothalamic nuclei. Neurons in the arcuate nucleus release neuropeptides and neurotransmitters to second-order neurons within the hypothalamus that regulate food intake and energy expenditure in response to upstream signals. LepRb is found on neurons expressing both orexigenic and anorexigenic agents. Neuropeptide Y (NPY) and agouti-related protein (AgRP) are two neuropeptides that are co-expressed in hypothalamic neurons and are clearly linked with increased feeding behaviour. Exogenous NPY injections into the hypothalamus of Sprague-Dawley rats induced hyperphagia and obesity (61), while ablation of NPY/AgRP neurons in mice promoted a lean, hypophagic phenotype, with a total body fat reduction of ~53% (62). In the same hypothalamic nuclei reside neurons co-expressing anorexigenic agents such as POMC and cocaine and amphetamine regulated transcript (CART). POMC is the pre-prohormone for melanocyte stimulating hormone (MSH), which acts on melanocortin receptors in the hypothalamus to decrease food intake and up-regulate energy expenditure. Since both NPY/AgRP and POMC/CART neurons express the leptin receptor, leptin controls food intake by regulating these neurons simultaneously (63). Briefly, leptin inhibits NPY/AgRP neurons while stimulating POMC/CART neurons. When leptin levels are low (reduced adiposity), there is no inhibition of the NPY/AgRP neurons, which stimulates feeding behaviour, and simultaneously prevents activation of POMC/CART neurons in order to decrease energy expenditure. On the contrary, when leptin levels are high (increased adiposity), leptin signaling inhibits the NPY/AgRP while

stimulating POMC/CART neurons, resulting in decreased food intake and increased energy expenditure (64). The action of leptin on these neurons is crucial in the regulation of feeding and whole-body energy expenditure. Disruption of the leptin receptor in POMC/CART neurons attenuates the actions of leptin and results in mild-obesity (65). Ablation of NPY partially reverses hyperphagia and promotes energy expenditure in *ob/ob* mice (66). Altogether, leptin signaling in the hypothalamus to NPY/AgRP and POMC/CART expressing neurons is necessary to convey information regarding the body's energy stores and allows for changes in food intake and energy expenditure accordingly.

The intricate regulation of leptin signaling is required in order to ensure energy homeostasis is maintained. Although leptin levels do not seem to be acutely regulated with fasting or re-feeding, it is clear that this hormone functions largely within the long-term system and influences the quantity of food consumed relative to the amount of energy expended (58,67). This is particularly relevant when we consider the role of leptin during diet and exercise induced weight loss. Under these conditions of chronic negative energy balance, low leptin levels exert orexigenic effects by stimulating food intake and decreasing energy expenditure (68). The role of leptin in these processes is a major obstacle for long-term weight loss, and reduces the efficacy of currently used strategies (diet and exercise) for the reduction of fat mass. Therefore, understanding the regulation and signaling of leptin under conditions of reduced adiposity are important to identify long-term treatments for obesity that are safer and more effective than the ones currently available.

Adiponectin

Adiponectin is a 30kDa protein uniquely mainly expressed by mature, differentiated adipocytes and is involved in whole-body insulin sensitivity. The hormone exists as hexamers arranged in multimeric structures of low, middle and high molecular weights, although the latter form has been implicated in exerting the most potent insulin sensitizing effects (69). Reductions in plasma adiponectin levels are consistently reported in obese humans, primates, and rodent models as well as diseased states associated with insulin resistance such as cardiovascular disease (70). Constant infusion of recombinant adiponectin in both lipoatrophic and obese mouse models (*db/db* and KKA^{y} mice) ameliorated hyperglycemia and insulin resistance in these animals (71). Replenishment of adiponectin in obese humans has been considered as a treatment strategy for treating insulin resistance and type 2 diabetes. In fact, some of the insulin-sensitizing effects of thiazolidinediones (TZDs) have been attributed the ability of these anti-diabetic drugs to increase adiponectin release by the WAT (72).

The actions of adiponectin are mediated by specific receptors denominated AdipoR1 and AdipoR2 (70,73). These G-protein coupled receptors share 67% sequence homology and are expressed abundantly in skeletal muscle and liver, respectively (74). Transcriptional regulation of AdipoR1/R2 occurs rapidly, where fasting and feeding increases and reduces mRNA levels of these receptors, respectively. Since expression seemed to be nutritionally regulated, experiments were conducted to assess whether insulin was involved in this process. Studies using streptozotocin-treated mice to render them hypoinsulinemic showed increased expression of AdipoR1/R2 in skeletal muscle,

and this effect was reversed with exogenous insulin administration, indicating that insulin negatively regulates expression of the adiponectin receptors. Therefore, it was not surprising when decreased expression of AdipoR1 and AdipoR2 was observed in skeletal muscle and WAT of hyperinsulinemic *ob/ob* mice. These findings indicate that obesity not only reduces circulating adiponectin, but also down-regulates the relative expression of the receptors for this adipokine (75). The latter is particularly detrimental, since targeted disruption of AdipoR1 and AdipoR2 *in vivo* results in insulin resistance and reverses the beneficial effects of adiponectin on glucose homeostasis (74). The end result is a positive feedback cycle of reduced adiponectin levels, leading to insulin resistance and hyperinsulinemia, which invariably reduces expression of AdipoR1/R2, further exacerbating the insulin resistant condition.

TNFα

TNFα is expressed and produced primarily by macrophages; however adipocytes and stromovascular cells within the WAT also express this cytokine (76). The receptors for TNFα exist as membrane bound and soluble forms, both of which are expressed in the WAT (77). TNFα was originally described as a cytokine that induced cachexia, and then subsequently implicated in the development of insulin resistance (78,79). In fact, studies have shown that obese rodents and humans have increased plasma levels of TNFα that are positively correlated with adiposity (79). This is supported by studies in mice lacking TNFα or its receptors (80) showing improvement in insulin sensitivity and reduction in circulating plasma FAs. In WAT, TNFα exerts its effects by downregulating

the expression of genes involved in adipogenesis, lipogenesis, and uptake of FAs and glucose (79,81). These effects of TNFα are invariably accompanied by increases in plasma FAs and have been associated with insulin resistance. In fact, TNFα interferes directly with insulin signaling by phosphorylating serine resides of IRS-1 and 2. This, in turn, prevents insulin-induced phosphorylation of tyrosine residues that are required for the action of this hormone (78). Therefore, the effects of TNFα appear to have direct implications for the ability of the WAT to respond to the anti-lipolytic effect of insulin. This contributes to increase circulating FAs and impairment of insulin signaling in other tissues such as skeletal muscle and liver, with major detrimental effects on whole-body glucose homeostasis.

IL-6

Similar to TNFα, IL-6 is a cytokine that circulates in levels positively correlated with fat mass and acts on receptors that have the same structure and homology as LepRb (82). Approximately 15-30% of IL-6 is derived from the stromovascular fraction of the WAT, while the remaining is secreted from other tissues, notably skeletal muscle (83). The precise relationship between IL-6 and obesity remains unclear and controversial due to the pleiotropic effects of this cytokine on peripheral tissues and the CNS. Because of its positive correlation with fat mass, it was considered that elevated levels of IL-6 in the plasma were a predictor of insulin resistance (83,84). Indeed, studies in liver (85) and adipose tissue have demonstrated that IL-6 imposes negative effects on insulin signaling by reducing expression of insulin receptor signaling components (85,86), inhibiting

adipogenesis (87), and decreasing adiponectin secretion (88). Chronic IL-6 treatment of 3T3-L1 adipocytes also shows blunted phosphorylation of the insulin receptor and IRS-1 in response to insulin stimulation (86). At the same time, IL-6 stimulates WAT lipolysis, further contributing to increased levels of plasma FAs that are associated with insulin resistance (89,90). However, a study using IL-6 deficient mice demonstrated that these animals developed mature-onset obesity that was partly reversed by IL-6 replacement, suggesting that a lack of IL-6 could lead to metabolic disorders (91). In fact, a positive role of IL-6 in glucose metabolism is compatible with the marked increases in circulating IL-6 levels that occur after exercise bouts (92). Studies in cultured L6 myotubes provide further evidence that, contrary to the effects in liver and WAT, IL-6 promoted FA oxidation and glucose uptake (93). Importantly, acute infusion of IL-6 into healthy humans has been shown to either enhance or have no negative effect on insulin-stimulated glucose disposal in humans (93,94), supporting the notion that IL-6 could have beneficial effects on insulin sensitivity at least in skeletal muscle.

When assessing the role of IL-6 in the CNS, levels of this cytokine were inversely proportional to fat mass, contrary to the positive correlation seen in the periphery (95). These observations are corroborated with studies in mice and rats where intracerebroventricular injections of IL-6 reduced body weight as well as fat pad mass after 14 days of treatment (96). This was mediated by decreased food intake and increased energy expenditure (96), suggesting that the central effects of IL-6 have different effects on energy homeostasis when compared to liver and WAT.

2.2. Brown Adipose Tissue (BAT)

BAT is a highly vascularized tissue composed primarily of brown adipocytes ranging from 10-50μm in diameter. Contrary to white fat cells, brown adipocytes are multilocular cells composed of numerous small lipid droplets with a centralized nucleus. The cytoplasmic portion of the cell is primarily occupied with large mitochondria, which confer the brown colour to the tissue (97). The main function of BAT is to generate heat through non-shivering thermogenesis. This response is typically triggered in rodents when these animals are exposed to temperatures that fall below thermoneutrality, leading to increased sympathetic nervous system activity in the highly innervated BAT. The generation of heat by brown adipocytes is possible because these cells express uncoupling protein 1 (UCP-1), which uncouples oxidative phosphorylation from ATP synthesis (98). It does so by shuttling protons across the mitochondrial membrane to produce heat instead of ATP. Since BAT is highly vascularized, it allows adequate blood flow to distribute the heat generated by this tissue to other parts of the body.

BAT is present throughout the lifespan of rodents (99). Until recently, BAT in humans was considered to be present only in infants and children, serving a negligible role in thermogenesis attributed to this tissue in adults (99). However, recent studies using ^{18}F-fluorodeoxyglucose positron emission tomography/computed tomography (PET/CT) imaging techniques identified physiologically relevant amounts of BAT localized in the anterior neck and the thoracic regions close to the heart in adult humans (99). Immunohistochemical and immunofluorescence analyses of adipose tissue biopsies from these areas confirmed the presence of UCP-1 positive multilocular cells (99,100).

Importantly, the amount of BAT present in adult humans appears to be inversely related to body mass index, suggesting that it may have a protective effect against obesity (100).

2.2.1. Differentiation of BAT versus WAT

Since WAT and BAT share many common features, the pursuit for mechanisms that regulated the differentiation of these two tissue types has been of great interest. In particular, because the BAT has the ability to dissipate energy and could potentially exert an anti-obesity effect. In this context, it has been demonstrated that both WAT and BAT require the peroxisome proliferator and activated receptor γ (PPARγ) for differentiation to occur (101,102). However, there are several major factors that have been identified as key regulators in driving brown versus white adipocyte differentiation. One of the first transcriptional regulators largely expressed in brown but almost undetectable in white fat cells was PPARγ co-activator 1α (PGC-1α) (103). PGC-1α has been identified as a key player in regulating adaptive thermogenesis and as a master regulator of mitochondrial biogenesis and oxidative metabolism, particularly in BAT and skeletal muscles (104). This is supported by studies in PGC-1α knock out mice showing reduced tolerance to cold in these animals (105). On the other hand, ectopic expression of PGC-1α in WAT induces the expression of various mitochondrial genes, including the one coding for UCP-1 (104,106). Interestingly, while depletion of PGC-1α appears to affect mitochondrial biogenesis and thermogenesis, the mass of BAT and expression of BAT-specific genes are not markedly altered. This led to speculation that another factor was required to induce the BAT phenotype. Recently, the zinc finger protein PRD1-BF-1-

RIZ1 homologous domain containing 16 (PRDM16) was identified as the factor that drove commitment towards the brown fat lineage (107). Knockdown of PRDM16 in brown fat precursors resulted in a loss of brown fat characteristics and reduced mRNA levels of BAT-specific genes including UCP-1, cell death-inducing DNA fragmentation factor alpha-like effector A (CIDE-A), and type 2 deiodinase (107). Since WAT and BAT were originally believed to arise from common precursors, it was speculated that ablation of PRDM16 in BAT precursors would result in a phenotype that would promote fat accumulation in a pattern similar to WAT. Surprisingly, the phenotype that emerged was that of myoblasts, indicating that PRDM16 drives brown adipocyte differentiation from a progenitor that expresses myoblast markers (108,109). In fact, technology using genetic fate mapping indicate that brown adipocytes arise from precursors that express *Myf5*, previously thought to be exclusively expressed in myogenic cells (109). Furthermore, ectopic expression of PRDM16 in C_2C_{12} myoblasts resulted in activation of the brown adipogenic program (109). Interestingly, transgenic expression of PRDM16 in white fat depots *in vivo* as well as in cultured white adipocyte precursors activates a robust BAT phenotype including the induction of PGC-1α and UCP-1 (109,110). This indicates that despite being expressed in different progenitor cells, PRDM16 is a powerful inducer of the brown adipocyte program. Importantly, PRDM16 expression is not effective in eliciting these changes after adipogenic differentiation has occurred (107), suggesting that PRDM16 establishes the brown adipocyte program at an early stage of BAT differentiation, but it is unable to change it.

Mutational analysis of PRDM16 indicates that its actions do not require direct

DNA binding for activation of brown fat adipogenesis, but rather acts through protein-protein interactions. PRDM16 interacts with a variety of transcription factors including PPARα, PPARγ, and the transcriptional complex CCAAT/enhancer-binding proteins (C/EBPs) for brown adipocyte differentiation to occur (108). With respect to the latter, ablation of C/EBPβ in mice suppressed the ability of PRDM16 to exert its brown adipogenic effects (108). Interestingly, it has also been shown that transcriptional control of brown adipocytes relies partially on the interaction of PRDM16 with the co-activator PGC-1α (108). Since the importance of PGC-1α in regulating mitochondrial biogenesis and UCP-1 expression in BAT has been well established, these findings help to explain the actions of PRDM16 in BAT development.

2.2.2. Plasticity between WAT and BAT depots

The term "adipose organ" was first used to better understand the coexistence of WAT and BAT, two tissues with markedly distinct functions and properties (97). It is now clear that adipocytes have the phenotypic plasticity to be converted from an energy storing to an energy-dissipating compartment, despite being a terminally differentiated cells. The term "transdifferentiation" was coined based on studies that identified the conversion of white into brown adipocytes and vice versa in response to different biological demands (111). This was observed in studies where mice were chronically exposed to cold (112,113), stimulated with β-adrenergic agonists (114,115), and treated with various TZDs (116,117). These studies showed increased presence of multilocular and UCP-1 positive cells in the WAT. Interestingly, this adaptation to environmental

stimuli is reversed under exposure to warm environments (10). Since UCP-1 is a hallmark of brown adipocytes, it was initially thought that white adipocytes were switched to a brown adipogenic program. However, recent literature has determined that there are developmental and molecular differences between classical brown adipocytes (i.e. interscapular region) and those that reside within WAT depots (107,109). Evidence now suggests that the phenomenon of transdifferentiation is not a complete switch to brown adipocytes, but rather an induction of "brown-like" characteristics within the WAT (118) (Figure 2-4). One study reported that it was a subset (~10%) of adipocytes within the WAT that elicited the ability to acquire a broad, but incomplete, array of brown adipocyte-specific genes (118). The induction of mitochondrial biogenesis is also seen in white adipocytes exposed to these conditions, which is an important aspect of the acquisition of a "brown-like" phenotype (118). This subset population of fat cells was termed "brite" (**br**own in wh**ite**) adipocytes, and still retained expression of the homeobox protein Hoxc9, a white adipocyte cell autonomous marker (118). This suggests that white and "brite" adipocytes arise from a common precursor (Figure 2-4). Importantly, despite the fact that these cells did not express myogenin or PRDM16, they were capable of UCP-1-dependent thermogenesis. Therefore, physiological or pharmacological remodeling of white adipocytes towards a "brown-like" phenotype clearly takes place in the absence of classical brown-adipocyte markers (Figure 2-4). In fact, it has been repeatedly demonstrated that white adipocytes have the biochemical oxidative machinery to dissipate energy within themselves (31,119). *In vivo* studies have demonstrated that when exposed to adenovirus-induced hyperleptinemia, white

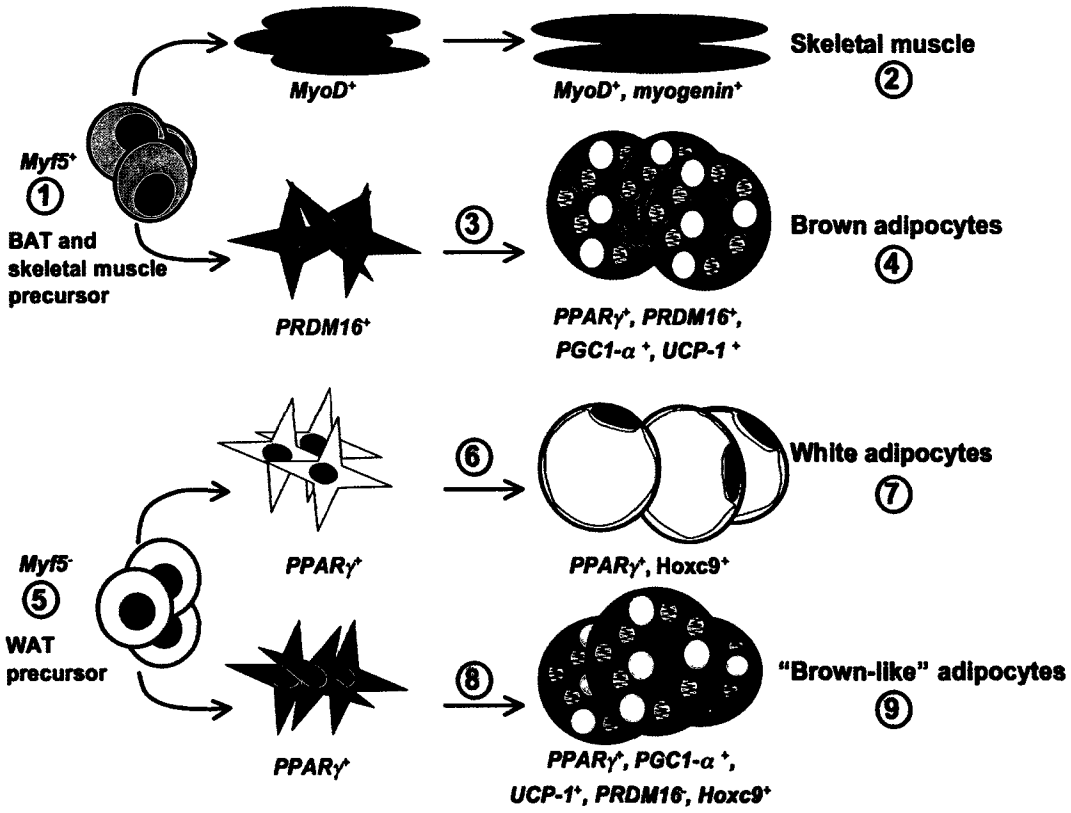

Figure 2-4. Molecular distinctions between white and brown adipocytes. Brown adipocytes arise from the same progenitor as skeletal muscle and are *Myf5*$^+$ **(1)**. When Myf5 and MyoD are simultaneously expressed, cells are driven towards differentiation as skeletal muscle **(2)**. When these precursors express PRDM16 **(3)**, cells differentiate into classical brown adipocytes that also express *PPARγ, PGC-1α, and UCP-1* **(4)**. White adipocytes arise from a *Myf5*$^-$ precursor **(5)**. When these cells express PPARγ **(6)**, they are normally differentiated into mature white adipocytes **(7)**. However, if these cells are subjected to different stimuli such as cold exposure or β-adrenergic stimulation, they can being to express markers characteristic of brown adipocytes such as *PGC-1α*, *UCP-1* while still retaining expression of white adipocyte markers (i.e. *Hoxc9*) **(8)**. Importantly, although these "brown-like" adipocytes are also capable of thermogenesis, they still do not express *PRDM16* **(9)**.

adipocytes can be rapidly transformed into very effective "fat burning machines" (119), suggesting that WAT can undergo a change in phenotype to resemble BAT. Additionally, isolated adipocytes chronically exposed to leptin increased glucose and FA oxidation within the fat cells that was accompanied by an increase in uncoupling protein-2 (UCP2) expression, which has similar sequence homology to UCP-1 (120). These increases in intra-adipocyte combustion of fat were characterized by elevated mitochondrial content and thermogenic proteins, and decreased expression of lipogenic enzymes (106,119). Other *in vitro* and *in vivo* studies on human and mouse adipose tissues (106), have shown that adipocytes over-expressing PGC-1α increases the expression of UCP-1. Furthermore, ectopic expression of UCP-1 specifically in WAT prevents genetically induced obesity in mice by increasing thermogenesis and effectively reducing fat mass (121). Thus, it is interesting that WAT has the ability to transform into an oxidative compartment (106). Altogether, these functional and structural transformations of white adipocytes confer high metabolic versatility to fat tissue with important therapeutic implications for the treatment of obesity and its related metabolic disorders.

2.3. Obesity

Characterized by the excessive accumulation of white adipose tissue, the prevalence of obesity has reached epidemic proportions worldwide and it is a major risk factor for a number of debilitating conditions including heart disease, type 2 diabetes (T2D), and even certain types of cancer. The current non-pharmacological strategies

available to treat obesity involve a regimen of diet and exercise in order to acquire a condition of chronic negative energy balance that induces fat loss. Although relatively effective in the short term, these approaches frequently lead to poor long-term weight loss results (90 to 95% of adults and children who lose weight gain it back) (4), suggesting that attempts to alter body weight is opposed by systems of energy homeostasis that up-regulate food intake and decrease metabolic rate in order to maintain an individualized weight "set point". Overcoming this defensive mechanism has become a major obstacle in the treatment of obesity and pharmacological therapies targeted towards reducing fat mass have been unsuccessful to date due to detrimental side effects (122).

2.3.1. Adipose tissue lipolysis and insulin resistance

Expansion of adipose tissue occurs two ways: 1) hypertrophy of existing adipocytes, and 2) hyperplasia, or increasing the number of fat cells. In obesity, both have been shown to occur in all WAT depots regardless of anatomical location. In particular, increased adipocyte size has been correlated with serum insulin concentrations, whole-body insulin resistance, and increased risk of developing T2D (123). Adipocytes isolated from obese non-diabetic individuals indicate that larger fat cells size show impaired insulin-stimulated glucose uptake compared to smaller cells in lean controls (123,124). Interestingly, adipocytes isolated from diabetic individuals exhibit insulin resistance regardless of cell size (125), suggesting that defects in the insulin signaling cascade occur prior to adipocyte enlargement. This could be caused by increased secretion of inflammatory mediators (i.e. TNFα, IL-6, etc.) by macrophages infiltrated in WAT that

promote insulin resistance, as well as changes in expression or activation of proteins involved in insulin signaling.

It is hypothesized that insulin resistance in adipocytes is a protective mechanism to prevent cell death, since bigger adipocytes are more fragile and susceptible to rupture (126). Therefore, once storage within the adipocyte reaches a certain capacity, it prevents further uptake of FAs and leaves them in the circulation. Additionally, since insulin is a potent anti-lipolytic hormone in the WAT, insulin-resistant adipocytes exhibit increased rates of basal lipolysis, further increasing circulating levels of FAs (125). Circulating levels of FAs in obese individuals under resting conditions can reach levels of 600-800μM, while lean individuals are generally in the 200-400μM range (127). Subsequently, under conditions such as obesity when the WAT can no longer expand to accommodate additional FAs and glucose through either hypertrophy or proliferation/differentiation of new adipocytes, the FAs in circulation are diverted towards other tissues, such as skeletal muscle and liver. However, if FAs are not oxidized in these tissues in response to an increased flux of substrate, lipid accumulation occurs in tissues not originally meant to store large amounts of fat. This ectopic lipid deposition that occurs in skeletal muscles and liver is particularly detrimental, since fat content in these tissues is invariably associated with insulin resistance and the development of type 2 diabetes (128). The skeletal muscle comprises between 30-45% of total body mass depending on age and sex (129), and has been estimated to account for ~80% of insulin stimulated glucose disposal (130). Thus, the toxic effects of FAs (lipotoxicity) on skeletal muscle have important implications for whole-body glucose homeostasis. Insulin

resistance in the liver results in impaired suppression of hepatic glucose output (131) and exacerbates hyperglycemic conditions since the skeletal muscle is unable to uptake glucose.

The mechanism by which FAs induce insulin resistance was first described by Randle and colleagues as the "glucose-fatty acid cycle" and was based on the notion of substrate competition (132) (Figure 2-5A). The hypothesis proposes that relative availability of glucose and FAs determines which substrate will be utilized for energy production. When high levels of FAs exist, this substrate is preferentially oxidized resulting in subsequent production of acetyl-CoA and NADH in the mitochondria (Figure 2-5A). This leads to inhibition of pyruvate dehydrogenase further preventing metabolism of glucose. Additionally, the elevated condensation of acetyl-CoA and oxaloacetate into citrate increases the exit of the latter metabolite into the cytoplasm. Increased cytoplasmic concentrations of citrate inhibit phosphofructokinase, the rate-limiting enzyme of glycolysis (Figure 2-5A). By preventing glycolysis from proceeding, it was postulated that increased intracellular glucose-6-phosphate (G-6P) levels would prevent further entry of glucose into the cell. However, the absence of accumulation of intracellular G-6P as predicted by this model led to interest in other potential mechanisms of FA-induced insulin resistance (133,134). It has been shown that an increase in intracellular FA metabolites can inhibit glucose uptake in a manner dependent on phosphorylation of proteins in the insulin-signaling pathway (135,136) (Figure 2-5B). In particular, it has been demonstrated that elevated plasma FA concentrations results in the intracellular production and accumulation of ceramides, fatty acyl-CoAs, and DAG

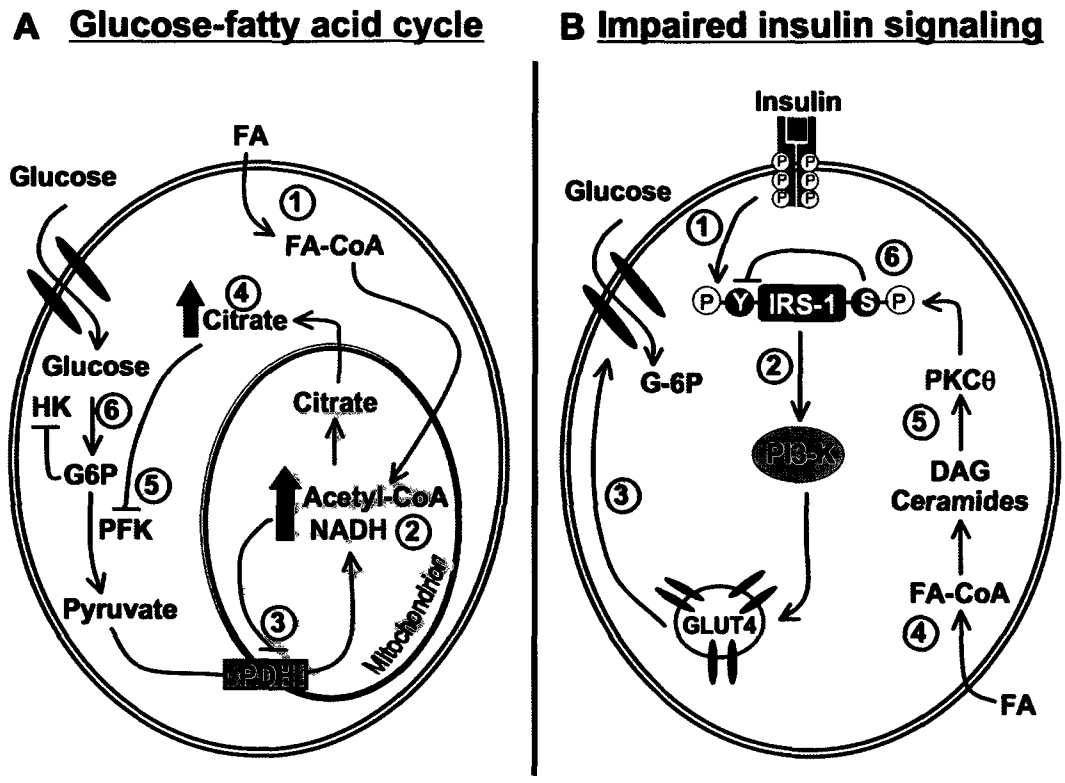

Figure 2-5. Mechanisms of FA induced insulin resistance. **[A]** The "glucose-fatty acid" cycle hypothesis proposes that competition between glucose and FAs determines which substrate will be utilized for energy production. Under conditions such as obesity where circulating FAs are increased, FAs enter the cell where they are activated through acylation **(1)**. This allows the FA-CoA to enter the mitochondrion where they are oxidized and increase production of acetyl-CoA and NADH **(2)**. This inhibits pyruvate dehydrogenase (PDH) **(3)** and promotes the production of citrate **(4)**. Citrate enters the cytoplasm where its accumulation inhibits phosphofructokinase (PFK) **(5)** and increases build-up of glucose-6-phosphate (G6P). Hexokinase (HK) activity is subsequently suppressed G6P accumulation **(6)**, not allowing retention of glucose inside of the cell for metabolic processes. **[B]** Normally, when insulin binds to its receptor it phosphorylates tyrosine (denoted Y) residues on IRS-1 **(1)** and triggers a signaling cascade **(2)** that translcoates GLUT4-vesicles to the plasma membrane **(3)**, facilitating glucose uptake. However, when circulating FA levels are elevated, FAs enter the cell and are converted into FA metabolites (i.e. DAGs, ceramides) **(4)**. These metabolites activate PKCθ **(5)** that subsequently phosphorylates serine (denoted S) residues on IRS-1. Serine phosphorylation prevents phosphorylation of tyrosine residues on IRS-1, and results in impaired insulin signaling **(6)**.

within the skeletal muscle (137). These FA metabolites act as signaling molecules that activate protein kinase C θ (PKCθ) (135,136) (Figure 2-5B). PKCθ phosphorylates serine/threonine residues on IRS-1/2 and prevents phosphorylation at tyrosine residues required for insulin signaling. Downstream targets of insulin signaling such as PI3-kinase activation is also observed to be impaired, indicating that the ability of IRS-1/2 to be phosphorylated is a critical mediator of glucose uptake via insulin (135,136). Based on these observations, an alternative explanation for the FA-induced insulin resistance in skeletal muscle has been put forward. Instead of substrate competition ("glucose-fatty acid cycle") leading to reduced glucose uptake and metabolism, it is the impairment of insulin signaling caused by intracellular accumulation of intermediates of lipid metabolism that suppress glucose uptake in skeletal muscle cells. These effects of increased circulating FAs would also impair the ability of insulin to signal in hepatocytes to inhibit glucose production by the liver.

2.3.2. Impaired catecholamine-induced lipolysis in obesity

In contrast to basal lipolysis being elevated, *in vivo* experiments in humans (138,139) and rodents (140,141) have demonstrated that catecholamine-induced lipolysis is blunted in obesity, a condition sometimes referred to as catecholamine resistance (142). It has been postulated that a blunted response to catecholamines occurs as an adaptive response that counteracts the insulin resistant state in obesity (142). The underlying mechanisms are not clear, although studies have suggested that SC adipocytes from obese men have reduced β2-AR density and increased α2-AR content (138). However, a

thorough analysis of the AR distribution in the obese condition as well as of the relative importance of each type of receptor still remains to be performed. Interestingly, expression and content of HSL in SC fat of obese men has reportedly been decreased (143). This could at least partially explain the blunted lipolytic response to catecholamines, since HSL plays an important role in the process of DAG hydrolysis. In fact, WAT from ATGL and HSL null mice both display blunted lipolysis in response to isoproterenol or epinephrine (43,44). Additionally, perilipin knockout mice also show blunted lipolysis *in vivo*, which is similar to the phenotype seen in HSL knockout mice (36,144).

The production of PGE_2 has been shown to be upregulated in obese rodents and humans, and this is in line with increased expression and activity of $AdPLA_2$ (49,145). Since PGE_2 binds to the EP3 receptor coupled to a G_i protein, increased levels of this prostaglandin may also contribute to a reduction in cAMP levels and therefore blunted β-adrenergic stimulated lipolysis.

2.3.3. Regional adiposity - Subcutaneous versus visceral WAT

Most adipose tissue (~80%) is localized in the subcutaneous area (11,146); however, the proportion of SC and VC depots to total body fat varies with sex, age, physical activity levels, and nutritional status (147). VC adipose tissue has been estimated to account for ~20% of total body fat in men but only 6% women (148). Cadaver dissection studies (age range 55-94 years) indicate that VC corresponds to 16.8% and 12.9% of total body adipose tissue in men and women, respectively (149). In obese

patients, especially those with abdominal obesity, VC accounts for a much higher proportion of the total body fat (150).

From a functional perspective, SC and VC adipose tissue have the biochemical machinery necessary to either store or release of FAs depending on the nutritional status. However, despite the fact that SC fat is the major component of total fat mass, it is VC adiposity that has been consistently linked to many facets of the metabolic syndrome, including glucose intolerance, hypertension, dyslipidemia, and insulin resistance (151). One common explanation for the detrimental effects of VC adiposity is the highly metabolic nature of this fat depot, particularly in regards to lipolysis. VC fat has been demonstrated to elicit higher lipolytic rates and to be less responsive to the anti-lipolytic effect of insulin than SC (152-154). The major contributing factors accounting for the differences in lipolytic activity of SC and VC WAT occur at the receptor and post-receptor levels (155). VC depots have an ratio of β:α2 adrenergic receptors when compared to SC fat depots (155,156). Additionally, the affinity of insulin to its receptor is lower in VC versus SC adipocytes, which results in reduced autophosphorylation of the insulin receptor (154). This limits the insulin-mediated activation of PDE3B, which serves as a potent inhibitor of lipolysis by degrading cAMP within the cell.

Variations in lipase activity between VC and SC fat depots have also been investigated, but the literature currently available is conflicting and precludes a definitive answer as to whether these differences contribute to depot-specific lipolytic activity. Studies in rats indicate that epididymal and retroperitoneal fat pads have ~2-fold greater HSL mRNA and protein levels compared to SC fat, suggesting that HSL could be a

contributing factor to regional differences in lipolytic activity (157,158). However, another study in human fat cells found that LPL and HSL mRNA levels were not different between SC and omental fat depots of lean subjects, although increased levels in omental fat were detected in obese subjects (159). One study in human adipocytes classified as having either 'low' or 'high' lipolytic acitivity while controlling for cell size found that cells with higher lipolytic activity had elevated HSL mRNA and activity. However, this study did not compare VC and SC fat depots (160). Examination of ATGL mRNA in humans showed no differences in omental versus SC fat in either lean or obese individuals (159), although rats under fasting conditions showed an increase in ATGL mRNA in retroperitoneal and mesenteric fat depots versus SC (158). Due to the conflicting results in the literature in both human and rodent studies, it is unclear whether the different lipolytic activities observed in various fat depots are dependent on differences in lipase expression/activity.

Despite the fact that VC fat exhibits greater lipolytic activity, approximately 70% of FAs circulating systemically are derived from the SC fat depots (161). This is interesting since VC adiposity was found to be specifically associated with metabolic alterations in obese men and women (151). Because VC fat, specifically omental and mesenteric fat depots, drain directly into the portal vein, the "portal hypothesis" was developed as an attempt to explain the detrimental effects of VC adiposity despite its relatively low contribution to circulating FAs. The portal hypothesis proposes that an increased flux of FAs into the liver causes detrimental effects in this organ (128). This has been attributed to the high lipolytic activity of VC fat, since all factors released from

this fat depot are drained directly into the portal vein. Consequently, the liver ends up being exposed to a much higher concentration of FAs than what is found in the systemic circulation (128). This condition may lead to pronounced lipotoxic effects, ultimately impairing the ability of insulin to suppress hepatic glucose production. Additionally, enlargement of VC WAT results in elevated secretion of inflammatory cytokines such as TNFα and IL-6, which further worsens the insulin resistant condition in the liver.

Importantly, proper regulation of glucose homeostasis depends not only on the liver responsiveness to insulin, but also on the sensitivity of skeletal muscle to this hormone and the ability to uptake and store large amounts of glucose. In fact, it has been estimated that skeletal muscle is responsible for 70-80% of whole-body insulin-stimulated glucose disposal (130) and is considered the most important site of insulin resistance. There is now compelling evidence that elevated circulating levels of NEFAs causes impairment of insulin signaling in skeletal muscle and greatly contributes to the pathogenesis of type 2 diabetes (127,162). Additionally, since SC fat depots also exhibit insulin resistant and increased basal lipolysis in obesity, the fat derived from SC lipolysis should also be seen as critical for inducing lipotoxicity and for the development of insulin resistance and type 2 Diabetes.

2.4. AMP-kinase (AMPK)

2.4.1. Structure and regulation

AMPK is a well-conserved heterotrimeric enzyme composed of a catalytic (α) and two regulatory subunits (β and γ) (Figure 2-6). Multiple isoforms of each mammalian subunit exist (α1, α2, β1, β2, γ1-γ3) and are differentially expressed in various tissues.

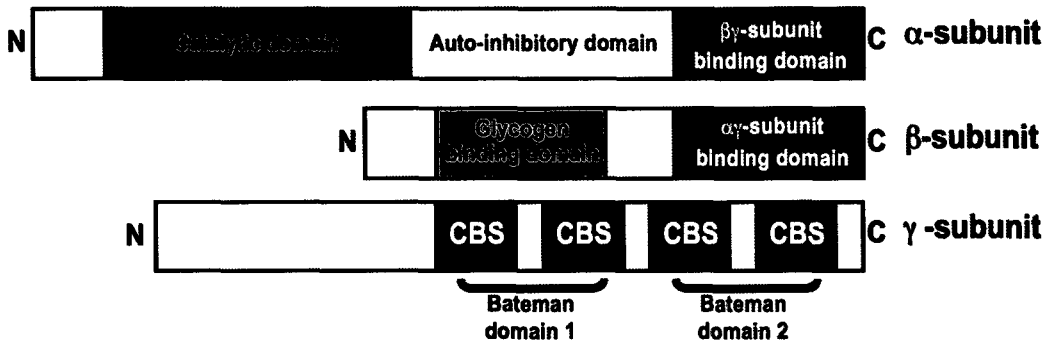

Figure 2-6. Structure of AMPK. AMPK is a heterotrimeric enzyme composed of α, β, and γ subunits. There are two isoforms of the α-subunit, and both contain the catalytic domain where AMPK is phosphorylated at Thr172 by upstream kinases. It also contains a domain where β and γ subunits can bind and interact with the α subunit. Two isoforms also exist for the β-subunit, which contains a glycogen binding domain and an αγ-subunit binding domain. The γ subunit has 3 isoforms of varying lengths which all contain 4 CBS sequences where AMP, ADP, and ATP can bind. The CBS sequences are found in tandem pairs called Bateman domains. N and C denote the N- and C-terminus, respectively.

The existence of various isoforms of each subunit enables the potential formation of 12 heterotrimer combinations that are thought to exhibit differences in subcellular localization and signaling functions (163). The N-terminus portion of the α catalytic subunit has a serine/threonine protein kinase domain, while the C-terminal region contains the β1-binding domain required for the formation of the heterotrimer complex (164) (Figure 2-6). The β subunit serves as a scaffold that allows the assembly of the αβγ complex, and also contains the glycogen binding domain (GBD), which is a member of the isoamylase-N domain family usually found in enzymes that metabolize the α1→6 branch of glycogen and starch (165). Recent studies provide evidence that the existence of the GBD allows AMPK to also act as a cellular sensor of glycogen that regulates the rate of synthesis and breakdown of this fuel source (165). The γ subunit of AMPK has four cystathionine β-synthase sequence repeats (CBS domains), which are small motifs found in tandem pairs also referred to as Bateman domains (Figure 2-6). The CBS sequences provide sites for the binding of the regulatory nucleotides AMP, ADP and ATP (166,167). AMPK is activated by stresses that cause depletion of ATP leading to increased binding of AMP and ADP (i.e. exercise, fasting). This is a result of ATP hydrolysis, which is rapidly converted into AMP via the adenylate kinase reaction. In fact, studies in adenylate kinase-deficient mice have demonstrated that a reduction in AMP formation results in impaired AMPK phosphorylation (168). Therefore, it is the AMP:ATP ratio within the cell that is critical in regulating AMPK activity (163). ATP has also been demonstrated to bind to the CBS domain and inactivate AMPK either directly or indirectly by preventing binding of

AMP. It has been reported that ATP binds with a lower affinity than AMP or ADP and in a mutually exclusive manner (169). These observations help to explain how AMPK can be activated under physiological conditions with small increases in AMP and ADP despite high intracellular ATP levels. With the use of N-methylanthraniloyl (mant)-labelled probes for AMP and ATP, Xiao *et al* (166) demonstrated that under physiological conditions AMPK mainly exists in its inactive form in complex with Mg-ATP, which is much more abundant than either AMP or ADP. Based on these findings, even when activated under metabolic stress only a small proportion of AMPK will be activated or bound to AMP, but these small changes induce a large enough increase in AMPK activity that allows for functional alterations in metabolism to occur.

The interaction of AMP with CBS domains exerts a direct allosteric effect that increases up to 10-fold the activity of AMPK, whereas the binding of ADP does not elicit this effect (167). Recent evidence indicates that binding of ADP to CBS domains plays an important role in preventing dephosphorylation of the Thr172 residue on AMPKα by inhibiting the action of protein phosphatases, particularly protein phosphatase 2C (PP2C) (167). Likewise, AMP also elicits a protective effect against dephosphorylation. Support from this comes from studies using an *in vitro* system with purified AMPK, upstream kinases, and phosphatase, which found that AMP was not able to increase phosphorylation of AMPK (170). However, elevated AMP levels in response to stress inhibited PP2C, thereby preventing dephosphorylation of AMPK at Thr172 (170). By preventing the action of PP2C, increased AMP allows for the accumulation and potentiation of AMPK activity. AMP also promotes the phosphorylation of a critical

threonine residue (Thr-172) within the kinase domain of the α-catalytic subunit, which further activates AMPK by up to 100-fold, accounting for the majority of its activity (170). Therefore, the combined effect of AMP and upstream kinases on AMPK activation is estimated to elicit up to ~1000-fold increase in enzyme activity (170). The tumor suppressor LKB1 (a dysfunctional kinase in Peutz-Jeghers syndrome) was described as the main kinase of AMPK. LKB1 forms a complex with STRAD and MO25 (171,172) and all three subunits are required for full activity (173). It has been shown that activity of LKB1 is not altered with contraction, phenformin, or 5-aminoimidazole-4-carboxamide-1-β-D-ribofuranotide (AICAR) in skeletal muscle, suggesting that this AMPK kinase is constitutively active (174). Interestingly, it has been shown in cell lines lacking LKB1 that alternative kinases can activate AMPK, particularly Ca^{2+}/calmodulin-dependent protein kinase kinase β (CaMKKβ), linking increases in intracellular Ca^{2+} to AMPK activation (175). A third kinase, transforming growth factor-β-activated protein kinase (TAK1) activates AMPK (176), and its physiological role seems to mediate autophagy induced by tumour necrosis factor-related apoptosis-inducing ligand (TRAIL)-triggered apoptosis preferentially in cancer cells (177).

2.4.2. The role of AMPK in lipolysis

Since a primary function of adipose tissue is delivery of substrate for ATP production in peripheral tissues, the majority of studies investigating the role of AMPK in adipose tissue have focused on the effects of this enzyme on lipolysis. The initial evidence of a regulatory role for AMPK in adipocyte lipolysis came from the observation

that hormone sensitive lipase (HSL), an important intermediary enzyme involved in lipolysis, was phosphorylated by AMPK. Studies *in vitro* indicated that phosphorylation of HSL by AMPK occurs on a serine residue that antagonizes phosphorylation of HSL by PKA (178), causing suppression of β-adrenergic stimulated lipolysis. Based on these *in vitro* studies, it was proposed that AMPK activation would exert an antilipolytic effect in adipocytes. However, while several studies (179,180) have reported an inhibitory effect of AMPK on adipocyte lipolysis, others (181,182) have found that activation of this kinase caused the opposite effect. In this scenario, whether AMPK exerted an anti- or pro-lipolytic role in adipocytes became a controversial issue. This was particularly evident when considering that acute and chronic exercise bouts increase catecholamine release, lipolysis, and AMPK activation in the adipose tissue (182). Therefore, an anti-lipolytic role for AMPK seemed counterintuitive, since during exercise levels of FAs are significantly increased and not reduced in the circulation. These disparities were subsequently reconciled by observations that AMPK was activated in adipocytes as a consequence of lipolysis and was proposed to function as a mechanism that limits TAG breakdown in WAT in order to spare energy (183). The rationale for this is based on the fact that if FAs released by lipolysis are not oxidized either within the adipocyte or in other tissues, they are re-esterified into TAGs in the fat cells, creating an energy-consuming "futile cycle" (184). Therefore, AMPK activation as a consequence of lipolysis has been proposed to restrain energy depletion through its reciprocal anti-lipolytic effect in WAT. This is supported by studies showing that AICAR-induced AMPK activation potently suppresses glycerol release by isolated visceral and

subcutaneous rat adipocytes, an effect that is prevented by pre-treatment with the AMPK inhibitor Compound C (179). Furthermore, adipocytes from AMPKα1 knockout mice exhibit increased lipolysis, indicating an anti-lipolytic role of this enzyme (180).

As originally proposed by Garton et al (178), the mechanism by which AMPK inhibits lipolysis seems to be via suppression of PKA-mediated phosphorylation of key HSL serine residues. In fact, upon catecholamines binding to β-adrenergic receptors, a cascade of events lead to activation of PKA, which in turn phosphorylates HSL at Ser 563, 660, and 659 residues leading to activation of this lipase. It has been shown that phosphorylation of HSL at the Ser565 residue by AMPK prevents phosphorylation of the PKA-targeted serine residues, thereby impairing lipolysis (178). Both acute and prolonged AICAR-induced AMPK activation in rat adipocytes increases Ser565 phosphorylation, and this is accompanied by a potent suppression of phosphorylation at the HSL Ser563 and 660 residues under both basal and epinephrine-stimulated conditions (179). The inhibitory effect of AICAR on lipolysis and phosphorylation of Ser563 and 660 are reversed when cells were pre-treated with Compound C (179). These findings indicate that AMPK inhibits HSL activity by regulating key phosphorylation sites on this enzyme (179). *In vivo* studies have also indicated that acute AICAR infusions in diabetic rats decrease whole-body lipolysis (185), an effect that can be attributed to inhibition of HSL phosphorylation.

Although the effects of AMPK on regulating lipolysis through HSL have been well documented, it still remains to be determined whether or not this kinase also plays a role in modulating ATGL activity. A recent study examined the role of the AMPKα2

subunit in the nematode *C. elegans* (186). The data suggest that this subunit is responsible for inhibiting ATGL and preserving lipid stores during diapause. This serves as a mechanism to increase lifespan of the *C. elegans* larvae, while deletion of the AMPKα1 subunit did not affect the phenotype (186). Since major differences exist between mammalian models and the use of multicellular eukaryotic nematodes, it is difficult to translate these findings to rodents and humans. Future studies are warranted to unravel the potential role of AMPK in regulating ATGL activity and the effects that this may have on lipid metabolism.

2.4.3. Regulation of glucose metabolism by AMPK

Studies in skeletal muscle have demonstrated that activation of AMPK through muscle contractions or by pharmacological agents leads to a significant increase in glucose uptake (187). This effect was demonstrated to be independent of insulin and mediated by increased plasma membrane GLUT4 content (188). Although the signaling mechanisms involved in the regulation of basal and insulin-stimulated glucose uptake are very similar in skeletal muscle cells and adipocytes, the role of AMPK activation in regulating this process in the latter is still controversial. Studies in differentiated 3T3-L1 adipocytes have shown that exposure of these cells to the AMPK agonist AICAR stimulated GLUT4 translocation to the plasma membrane. This was also accompanied by increased basal glucose uptake, which was prevented when cells were pre-treated with the PI3-kinase inhibitor wortmannin, suggesting a cross-talk between the AMPK and insulin-signaling pathways (189). However, assessment of insulin-stimulated glucose

uptake revealed that this variable was inhibited by AICAR in 3T3-L1 adipocytes, an effect that could not be prevented by pre-incubation of these cells with wortmannin. Furthermore, the phosphorylation states of the insulin receptor substrate 1 (IRS-1) and of the downstream signaling target protein kinase B (PKB) were unaltered with AICAR treatment (190), suggesting that a signaling step downstream of PKB could be targeted by AMPK. Studies from our lab have consistently demonstrated that glucose uptake in primary rat adipocytes is potently inhibited by AICAR under both basal and insulin-stimulated conditions (191). These findings indicate that clear differences exist between fully differentiated primary adipocytes and 3T3-L1 cells with regards to the role of AMPK in the regulation of glucose uptake. The mechanisms underlying these differences still remain to be fully elucidated, but could be due to the presence of different AMPK isoforms in primary and 3T3-L1 adipocytes. These could exert distinct regulatory effects on specific steps of the signaling cascade involved in the regulation of basal and insulin-stimulated glucose uptake in primary and 3T3-L1 adipocytes.

A major step involved in the regulation of GLUT4 translocation in adipocytes that could affect the ability of these cells to uptake glucose is the downstream target of PKB known as AS160. In fact, it has been found in skeletal muscle that AS160 is a converging point of the AMPK and insulin signaling pathways. *In vitro* contraction and AICAR treatment of isolated extensor digitorum longus (EDL) muscle induced phosphorylation of AS160 in a wortmannin-insensitive manner (22). Additionally, muscle incubations using the EDL and tibialis anterior from animals deficient in AMPK signaling showed that this kinase is required for contraction-induced AS160 phosphorylation (192).

Therefore, it could be that AS160 is distinctly regulated by AMPK in skeletal muscle and primary adipocytes, since activation of this kinase leads to stimulation and inhibition of glucose uptake in the former and latter, respectively.

The opposite effects of AMPK on glucose uptake in adipocyte versus skeletal muscle seem counterintuitive. However, the inhibitory role of AMPK on adipocyte glucose uptake and metabolism may serve as a mechanism that conserves adipocyte energy content while still providing substrate for energy production in peripheral tissues. The rationale is that the costly process of FA re-esterification into TAG in adipocytes relies on glucose metabolism for the production of glycerol 3-phosphate, since glycerol kinase activity is negligible in WAT (193). Therefore, by suppressing glucose uptake and its metabolism AMPK not only prevents energy consumption through FA re-esterification, but also facilitates the exportation of FAs to be used as substrate for energy production in other peripheral tissues. This is particularly important under conditions of stress and increased energy demand, which are also known to induce AMPK activation in the WAT. This hypothesis is compatible with observations that short-term activation of AMPK markedly reduced glucose and FA uptake and the incorporation of glucose and palmitate into lipids in adipocytes (191).

2.4.4. Regulation of fatty acid oxidation by AMPK

The majority of the literature regarding how AMPK regulates FA oxidation refers to the role of this kinase in skeletal muscle. It has been well documented that phosphorylation and activation of AMPK facilitates phosphorylation and inactivation of acetyl-CoA carboxylase (ACC) (Figure 2-7). There are two isoforms of ACC (ACC1 and

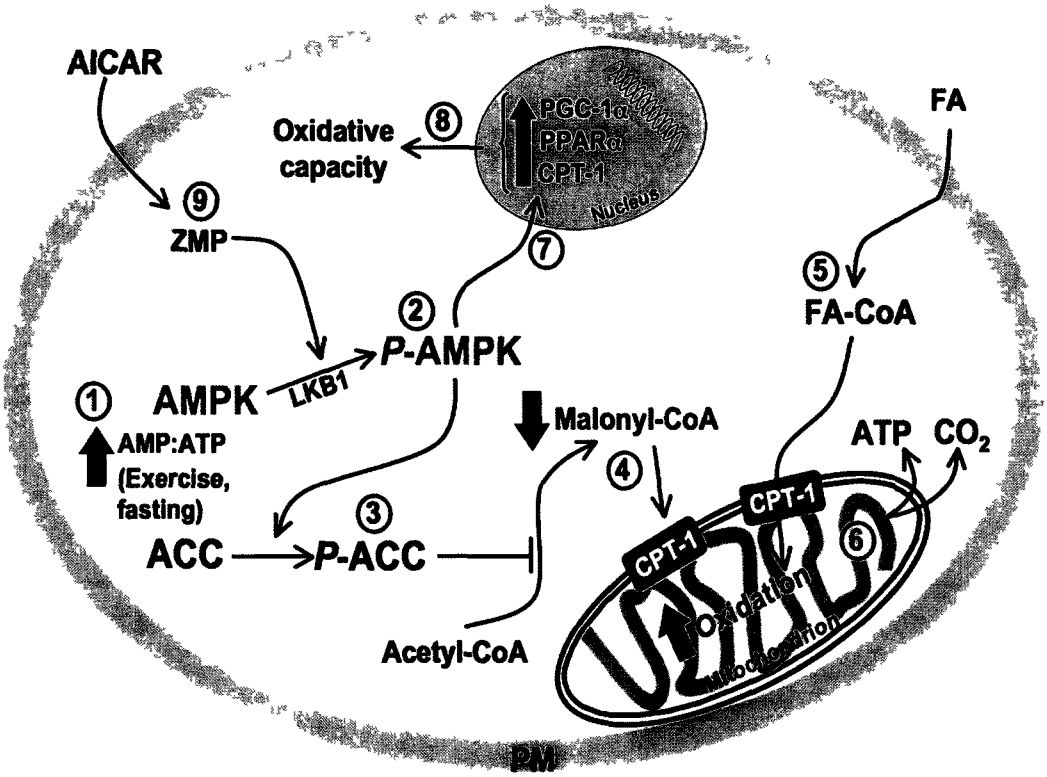

Figure 2-7. Regulation of fatty acid oxidation by AMPK. Under conditions such as exercise and fasting, an increase in the AMP:ATP ratio induces allosteric activation of AMPK **(1)**. This makes AMPK a better substrate for its upstream kinases (i.e. LKB1) to phosphorylate and increase its activity **(2)**. Once activated, AMPK phosphorylates and inactivates ACC **(3)**, which prevents the conversion of acetyl-CoA into malonyl-CoA. The resulting low malonyl-CoA levels disinhibit CPT-1 **(4)** and permits FA entry into the mitochondria **(5)** where they are oxidized to produce ATP and CO_2 **(6)**. Chronic AMPK activation has also been demonstrated to increase expression of genes involved in mitochondrial biogenesis **(7)**, ultimately leading to increased oxidative capacity of the cell **(8)**. Activation of AMPK can also occur pharmacologically using AICAR, a cell permeable adenosine analog that enters the cell where it is promptly phosphorylated into ZMP **(9)**. ZMP serves as an AMP mimetic and activates AMPK without altering the AMP:ATP ratio.

ACC2), which are encoded by separate genes and display distinct tissue distributions (194). ACC1 is primarily expressed in adipose tissue and liver, whereas ACC2 is predominantly expressed in heart and muscle (195). Inhibition of ACC by phosphorylation suppresses the formation of malonyl-CoA in the *de novo* lipid synthesis pathway. A reduction in intracellular malonyl-CoA increases carnitine palmitoyltransferase 1 (CPT-1) activity and facilitates the import of long chain fatty acids (LCFAs) into the mitochondrial matrix, where they can be oxidized to produce ATP (196). Evidence for this comes from rats injected with AICAR, which causes a decrease in malonyl-CoA levels in skeletal muscle, liver, and adipose tissue presumably through activation of AMPK and inhibition of ACC (197,198). Additionally, AICAR- and contraction-induced AMPK activation has been shown to increase the activity of malonyl-CoA decarboxylase (MCD), which degrades malonyl-CoA and prevents inhibition of CPT-1 (199). However, other groups have noted that MCD is not a direct substrate of AMPK (200), therefore the relationship between these two enzymes requires further investigation. The important role of AMPK in the regulation of FA oxidation is further substantiated in studies using ACC2 knockout ($ACC2^{-/-}$) mice, which have elevated levels of FA oxidation due to reduced malonyl-CoA (201). These $ACC2^{-/-}$ mice also have reduced fat mass and low accumulation of hepatic lipids compared to wild type mice (201). Furthermore, $ACC2^{-/-}$ mice are protected against diet-induced obesity and have increased insulin sensitivity, presumably through a decrease in ectopic lipid deposition (202,203).

Although it has been documented that FA oxidation in skeletal muscle is reduced

in obesity, the role of AMPK in regulating oxidation under conditions of elevated FAs is unclear. Exposure of up to 8h of L6 rat myotubes to elevated levels of palmitic acid (100μM-800μM) commonly found in obese states, impaired FA oxidation in a time- and concentration-dependent manner despite AMPK and ACC phosphorylation (204), suggesting alterative mechanisms are responsible for down-regulating oxidation in these conditions. Impairment of the AMPK pathway has been reported in human cultured skeletal muscle cells from obese subjects, which show a reduction in AMPK activation and FA oxidation compared to their lean counterparts (205). Interestingly, stimulation of AMPK activity using AICAR or adiponectin in myotubes increased AMPK activity, however was unable to recover the effects on ACC phosphorylation or on FA oxidation (205). These studies suggest that in diseases states such as obesity where FA levels are high, there may be lipotoxic effects that either suppress maximal AMPK activity or prevent downstream proteins in this pathway from exerting anti-diabetic effects, allowing intracellular accumulation of lipids and the development of insulin resistance. Repairing or targeting downstream targets of this pathway may be a potential therapy to stimulate oxidation in order to prevent/alleviate ectopic deposition of lipids, particularly in skeletal muscle where this condition leads to insulin resistance. It could also be that the abundance of FAs under conditions such as obesity overrides any regulatory mechanisms (i.e. AMPK) that control substrate metabolism under normal conditions. For example, the acute elevation of circulating FAs during exercise is accompanied by increased whole-body fat oxidation. However, under conditions of chronically elevated FAs such as in obesity, the oxidative machinery cannot process the excessive FAs available. This may

result in ectopic lipid deposition and cause deleterious effects that would prevent the oxidative machinery from functioning properly, despite activation of the AMPK pathway.

In addition to its acute metabolic effects, it has also been demonstrated that chronic activation of AMPK causes alterations in gene expression, and this is compatible with observations that the α2 isoform is localized in the nucleus of various cell types (206). It is now clear that AMPK activation plays a critical role in initiating mitochondrial biogenesis (207-210). A direct cause-effect relationship between AMPK and induction of mitochondrial biogenesis was revealed in mice exposed to β-guanidinopropionic acid (GPA), a pharmacological method of depleting intracellular phosphocreatine and ATP concentrations (210). This study indicated that energy depletion with GPA increased CaMK IV and PGC-1α as expected, but this effect was abolished in transgenic mice expressing DN-AMPKα2 in skeletal muscle (210). Additionally, recent studies have revealed that AMPK is required to phosphorylate PGC-1α directly in order to mediate its effects on mitochondrial function and content (211). Recent work published by Cantó et al (209) indicate both *in vitro* and *in vivo* that in skeletal muscle, AMPK controls the expression of genes such as PGC-1α by acting in coordination with the NAD^+-dependent type III deacetylase sirtuin 1 (SIRT1). Deacetylation of PGC-1α by SIRT1 results in its activation, and allows PGC-1α to upregulate the expression of oxidative enzymes (209). Similarly to AMPK, SIRT1 activity is increased under conditions such as exercise and fasting, where FA oxidation is increased causing a subsequent elevation of NAD^+ levels (212,213). In fact, when SIRT1 was knocked down in C_2C_{12} myotubes, AICAR-induced

expression of genes related to mitochondrial metabolism was markedly attenuated, indicating a clear link between AMPK and SIRT1 with respect to activation of PGC-1α (209). When AMPK-targeted phosphorylation sites on PGC-1α were mutated, general SIRT1 activity was not altered; however, PGC-1α deacetylation was impaired. These findings provide evidence that direct phosphorylation of PGC-1α makes it a specific target for deacetylation by SIRT1 (209). The interdependent regulation between AMPK and SIRT1 provides a finely tuned mechanism to control the action of PGC-1α in regulating FA metabolism through expression of key genes that regulate oxidation.

While there have been extensive studies on the regulation of FA metabolism by AMPK in skeletal muscle, there is limited information regarding the metabolic fate of FAs under conditions of either acute or chronic AMPK activation in adipocytes. In fact, the importance of investigating the role of AMPK in WAT is highlighted by the fact that this enzyme exerts tissue-specific effects with respect to metabolism. Work in primary adipocytes acutely exposed to AICAR indicated that contrary to what has been shown in skeletal muscle, activation of AMPK inhibits intra-adipocyte FA oxidation (191). The decrease in FA oxidation is likely an effect due to limited substrate availability, since FA uptake is also suppressed in AICAR-treated adipocytes. When considering the role of WAT in whole-body energy metabolism it is compatible that under conditions of higher energy demand, adipocytes would prevent FA uptake and oxidation in order to spare energy for more metabolically active tissues such as skeletal muscle and liver (191).

Although acute AMPK activation can rapidly suppress glucose and FA uptake

and metabolism in adipocytes, chronic AMPK activation has been associated with major alterations in gene expression, which may affect the ability of adipocytes to process glucose and FAs in a similar manner. Therefore, investigation of chronic AMPK activation in WAT is necessary to see whether the tissue-specific effects of acute AMPK activation remain after alterations in gene expression may have occurred. Interestingly, the observation that prolonged AMPK activation facilitates mitochondrial biogenesis to increase FA oxidation in skeletal muscle (209,210) gives insight into potential therapeutic targets to treat obesity by increasing FA oxidation and reducing fat stores in adipocytes (191). Indirect evidence of the role of AMPK in promoting FA oxidation after chronic activation is documented in studies where white adipocytes of hyperleptinemic rats were accompanied by increases in PGC-1α, uncoupling protein (UCP)-1, and AMPK activity in WAT (119). These findings suggested that induction of oxidative genes and acquisition of a brown adipocyte phenotype could be achieved through chronic pharmacological activation of AMPK in WAT. Physiological activation of AMPK using exercise and adrenaline has also demonstrated an up-regulation of PGC-1α mRNA in rat adipose tissue (214). In fact, a recent study indicated that mice injected with AICAR showed increased UCP-1 expression and induced accumulation of brown adipocytes within the WAT (215). These data suggest that AMPK could be a target for the conversion of WAT into a more "BAT-like phenotype", which opens up a new possibility for the treatment of obesity and its related metabolic disorders. However, more studies are required to address the effects of chronic AMPK activation on remodeling WAT towards a more oxidative tissue.

2.4.5. Effects of adipokines on AMPK activation

Adiponectin and leptin are two important hormones released by adipocytes that have been associated with dysfunctional metabolic alterations present in obesity and type 2 diabetes. The concentration of leptin in the blood is directly proportional to fat mass, and this hormone plays a critical role in regulating food intake, energy expenditure and neuroendocrine function (216). Several obese and insulin resistant murine models such as *ob/ob* (lacking functional leptin) or *db/db* (lacking functional leptin receptors) mice strongly indicate that leptin plays a critical role in regulating fat mass and the development of insulin resistance (54,217). Although the effects of leptin on food intake and energy balance are primarily mediated through the action of this hormone in the CNS, there is a large body of evidence demonstrating that leptin also increases glucose disposal and FA oxidation by acting directly in skeletal muscle and adipose tissue (119,120,218-222). Minokoshi *et al* (223) have shown that the expression of a dominant-negative form of AMPK in H-2Kb muscle cells abolished the direct peripheral effects of leptin. Although the direct energy dissipating effects of leptin could lead to reduced fat accumulation and increase glucose disposal, it does not seem to be the case in human obesity. In fact, compared to lean individuals obese people have much higher levels of circulating leptin, indicating impaired ability to respond to this hormone (67). Thus, obese individuals face the obstacle of overcoming leptin resistance, which seems to prevent the peripheral effects of AMPK activation. In this context, an attractive therapeutic alternative that has emerged involves targeting AMPK directly in order to

facilitate its downstream anti-diabetic effects, while bypassing the limitations imposed by impaired leptin-receptor-mediated signaling.

Unlike most adipokines, the concentration of adiponectin in the blood is inversely related to fat mass, where healthy individuals have high circulating adiponectin and obese patients exhibit lower levels of this hormone (224). Furthermore, the expression of AdipoR1 and AdipoR2 is reduced in obesity, which negatively affects adiponectin sensitivity in these individuals (73). This is problematic, since AMPK activation by adiponectin requires binding to AdipoR1/R2 to exert its metabolic effects, such as glucose uptake and FA oxidation in the liver and in muscle (74,225). However, other studies have also suggested that impaired adiponectin signaling in obesity is not a result of reduced receptors, but a downstream defect in this pathway that reduces AMPK activity (205).

2.4.6. Role of AMPK in adipocyte proliferation and differentiation

Compatible with the role of AMPK in shutting down anabolic pathways when activated, it has been demonstrated in preadipocytes as well as in various other cell lines that activation of this kinase potently inhibits cell proliferation (226-230). Treatment of 3T3-L1 cells either as fibroblasts or in the early stages of differentiation with AMPK agonists also inhibits clonal expansion in a dose-dependent manner (229,230). Notably, the effect of AMPK on cell proliferation has been well demonstrated in cancer cell lines where activation of AMPK using AICAR has been shown to arrest the cell cycle in the S-phase by inducing expression of genes involved in halting cell cycle progression (i.e. p21,

p27, p53) (226,227). Inhibition of AMPK activity through expression of dominant-negative AMPK, shRNA, or treatment with iodotubercidin reverses the effects of AICAR, indicating that these are indeed AMPK-mediated (226,227). Reduced clonal expansion of 3T3-L1 adipocytes with AMPK activation is accompanied by large reductions in neutral lipid content and suppresses transcription factors PPARγ1/2, C/EBPα, adipocyte differentiation and determination factor 1 (ADD1), and sterol-regulatory element binding protein 1c (SREBP1c) that are necessary for adipogenesis to occur (226,227). Expression of late adipogenic markers is also inhibited with AMPK activation, including expression of ACC and FAS (226,227). Interestingly, once adipocytes are differentiated activation of AMPK does not seem to reverse adipogenesis since there is no alteration in the expression of PPARγ1/2, C/EBPα, and SREBP1c (226,227). Rather, there seems to be a decrease in the pre-existing adipocyte size through reduced expression of proteins involved in TAG synthesis such as glycerol-3-phosphate and diacylglycerol acyltransferases (GPAT and DGAT, respectively).

Although AMPK inhibits white adipocyte differentiation, a recent study in cultured brown adipocytes suggests a different role for this enzyme in regulating brown fat cell differentiation (215). When activated during the later stages of the differentiation process, AMPK was found to be necessary for inhibition of the mammalian target of rapamycin (mTOR), which stimulates protein synthesis and cell growth via multiple mechanisms including phosphorylation of S6 kinase. Importantly, AMPK-dependent inhibition of mTOR was required for brown adipocyte differentiation to take place (215).

2.4.7. Effects of AMPK on the hypothalamus

Regulation of AMPK in the hypothalamus occurs via alterations in nutritional and hormonal signals. Under fasting conditions AMPK is activated in the hypothalamus (specifically the arcuate and paraventricular nuclei) and promotes food intake while refeeding elicits the opposite effect (231). Similarly to the periphery, AMPK activation in the hypothalamus promotes phosphorylation and inactivation of ACC. This results in low levels of malonyl-CoA that in turn elicits anorectic effects in the hypothalamus. Inhibition of FAS through intracerebroventricular (i.c.v.) administration of cerulinin increases malonyl-CoA levels and subsequently decreases food intake and body weight, while increasing energy expenditure (232). Additionally, expression of orexigenic neuropeptides NPY and AgRP are reduced (232,233), while POMC and CART expression are increased in response to elevated malonyl-CoA levels (234). The signaling mechanisms by which malonyl-CoA regulates these processes are not clear. It could be that malonyl-CoA interacts directly with a yet unidentified signaling protein that regulates expression of these neuropeptides. Alternatively, it has been demonstrated that malonyl-CoA binds to and inhibits CPT-1c, the brain specific isoform of this protein, which may mediate the effects of malonyl-CoA in the CNS (235). Indeed, CPT-1c knockout mice exhibit reductions in food intake and body weight (236). Paradoxically, the presence of CPT-1c protects against the effects of a high fat diet, suggesting a more complex role for CPT-1c in regulating whole body energy balance (236).

Since leptin plays a critical role in food intake, there was interest in examining whether this hormone could regulate AMPK in the hypothalamus. In contrast to

peripheral tissues, intraperitoneal (i.p.) and i.c.v. injections of leptin substantially reduced phosphorylation of this enzyme as well as ACC in the hypothalamus (237,238). In contrast, injection of ghrelin, a gut peptide hormone that has been shown to induce feeding, increased phosphorylation and activity of AMPK relative to saline treated controls (237). The role of AMPK was further substantiated in a mouse model where constitutively active (CA) and a dominant negative (DN) version of AMPKα1 and α2 increased and decreased food intake, respectively (231). Furthermore, leptin injections in the CA-AMPK mice did not attenuate food intake or body weight, indicating that suppression of AMPK activity in the hypothalamus is required for the anorexigenic effects of leptin (231). Importantly, activation of AMPK in the hypothalamus was accompanied by increases in expression of NPY and AgRP in the arcuate nucleus (231). A recent study was done where AMPKα2 was knocked out in either POMC (POMCα2KO) or AgRP (AgRPα2KO) expressing neurons to establish whether these neuronal populations required AMPK activity (239). AgRPα2KO mice developed a lean phenotype with increased insulin sensitivity, an anticipated result since AMPK stimulates food intake as does AgRP. On the other hand POMCα2KO mice exhibited an obese phenotype. This was at odds with the initial role for AMPK, since removal of its enzymatic activity should have promoted anorexigenic effects. These results suggest that rather than acting as a general energy sensor in the hypothalamus, AMPK may play a specific role in different populations of neurons (239). The divergent roles of AMPK in POMC and AgRP neurons indicate a complex role for AMPK in the hypothalamus.

In addition to feeding, a role for AMPK as a glucose sensor in the ventromedial hypothalamus (VMH) has recently emerged. Under hypoglycemic conditions, AMPK is activated in the VMH, an area of the brain that has been known to increase hepatic glucose production. The injection of AICAR into the VMH nucleus to mimic fasting/hypoglycemia increased AMPK activity and hepatic glucose production (240,241). Conversely, inhibition of AMPK attenuated these responses, resulting in severe and prolonged hypoglycemia (241,242). This indicates that AMPK mediates counterregulatory mechanisms in response to alterations in glucose availability to the brain. Additionally, POMCα2KO mice displayed a deficiency in responding to alterations in extracellular glucose levels, suggesting that the interaction of AMPK and POMC is required for proper glucose sensing in the hypothalamus (239).

2.4.8. Clinical applications of AMPK activation

From a clinical perspective, AICAR has been administered to humans intravenously as "acadesine" to ameliorate ischaemic reperfusion injury after myocardial infarction associated with coronary artery bypass graft surgery (243). Acadesine is a purine nucleoside analog that enters the cell and is rapidly phosphorylated into ZMP, which is an AMP mimetic. Although the precise mechanism is unclear, acadesine increases the endogenous pool of adenosine to allow increased blood flow while inhibiting platelet aggregation and neutrophil activation (244,245). Whether this cardioprotective effect of acadesine is mediated by the activation of AMPK remains controversial. It has been reported that acadensine does not act on adenosine receptors located on the plasma

membrane (190,246), although it has been demonstrated in rat brain slices that this compound does compete with adenosine for uptake into cells (246). Regardless of the mechanisms of actions, the efficacy of acadesine has been tested in stage III of clinical trials, which indicate that unlike the use of adenosine, this drug is site- and event-specific, thereby preventing unwanted side effects. Interestingly, one noted side effect of acadesine is the lowering of plasma glucose levels, which in hindsight can now be attributed to AMPK facilitated glucose disposal into skeletal muscle, as well as to suppression of hepatic glucose production (247,248). In fact, recent studies in healthy men and type 2 diabetic humans indicated that intravenous infusion of AICAR reduces plasma glucose levels by stimulating 2-deoxyglucose uptake into skeletal muscle and by lowering hepatic glucose output (249,250). Diabetic patients also exhibited lowered levels of NEFAs in the plasma, presumably through reduced adipose tissue lipolysis and/or increased FA oxidation in skeletal muscle (249). However, AICAR infusion in either lean or diabetic individuals was not accompanied by an increase in AMPK phosphorylation. These findings suggest that either a small change in AMPK activity is enough to stimulate glucose uptake in skeletal muscle or that this drug acts via AMPK-independent pathways. It is clear that the controversy regarding the mechanism of action of acadesine with respect to treating obesity requires more detailed clinical trials.

The effect of acadesine in humans illustrates the potential of AMPK as an important therapeutic target for metabolic disease, but poor bioavailability of acadesine for chronic treatment of metabolic disease is a major obstacle (245). Currently, only acute intravenous administration of acadesine has been demonstrated to reach circulation when

measured in whole blood, whereas comparable oral doses of this drug elicited <5% bioavailability (251); therefore further research is required to optimize agents that can be administered to the general population without invasive procedures requiring hospitalization.

The classical insulin-sensitizing effects of thiazolidinediones (TZDs) have been described to occur through chronic activation of PPARγ in white adipose tissue through increased adipogenesis and increasing levels of adiponectin (252,253). However, it has been demonstrated in differentiated L6 myotubes and isolated muscle that these drugs can rapidly activate AMPK and elicit PPARγ-independent effects (254,255). In these studies, the downstream effects compatible with AMPK activation were observed including increased FA oxidation, and insulin-independent increases in glucose uptake (254,255). Rats treated *in vivo* with pioglitazone have increased AMPK activation in liver and adipose tissue and this is accompanied by a reduction in malonyl-CoA levels, which suggests enhanced fat oxidation in these tissues (256). This is compatible with the notion that reduced hepatic lipid accumulation seen in patients administered pioglitazone (257) may be partially due to increased phosphorylation of AMPK and promotion of FA oxidation. TZDs can also activate AMPK indirectly by increasing adiponectin levels, which would promote FA oxidation in skeletal muscle and liver (225). In fact, when phosphorylation of AMPK was assessed after pioglitazone injections in adiponectin knock out *ob/ob* mice, it was attenuated relative to the *ob/ob* control, suggesting that TZDs activate AMPK through adiponectin-dependent mechanisms (258).

The biguanide drug metformin alleviates hyperglycemia in type 2 diabetics primarily through suppression of gluconeogenesis in the liver (248) and also by stimulating glucose uptake into skeletal muscle (259). Increased FA oxidation via AMPK in the liver and skeletal muscle have been documented with metformin treatment (260), suggesting that this drug has pleiotropic effects through AMPK activation and explains the high efficacy of metformin treatment for type 2 diabetes. The use of metformin and TZDs in combination provides the most substantial improvement in glycemia and the lipid profile when compared to treatment with either drug alone (261). It has been demonstrated that metformin inhibits complex I in the respiratory chain in mitchondria, causing a rise in AMP levels and an increase in AMPK activity (262). Recent studies now suggest that TZDs also work in this manner, indicating that anti-diabetic agents are working through a similar mechanism of action (263). Several novel small molecule AMPK activators have recently been shown to activate this enzyme via different mechanisms, including inhibition of complex I respiration, direct activation, and some with unknown modes of action (please refer to (264) for a comprehesive review of these compounds). A particular AMPK agonist of interest is from a class of drugs called thienpyridones referred to as A769662, which has improved specificity for AMPK and does not significantly interfere with a large number of protein kinases involved in metabolism such as glycogen phosphorylase, fructose-1,6-bisphosphatase, and Akt (265). Injection of A769662 into *ob/ob* mice activated the AMPK/ACC pathway, leading to lowered glucose levels and reduced fat content in the liver (265). Importantly, since A769662 is not an adenosine analog, it does not bind to CBS domains on the γ subunit (265). It activates AMPK

allosterically through interacting with the β-subunit glycogen binding domain (GBD) and γ-subunit as shown in mutation studies (266). These studies have demonstrated that partial and complete deletions of the GBD and mutations of residues on the γ1 subunit that interact with the carbohydrate-binding loop proximal to the GBD are required for A769662-mediated AMPK activation. Importantly, it preferentially activates AMPK complexes containing the β1 subunit, highlighting the ability of this drug to target specific combinations of heterotrimers (266). Since the β1 subunit is expressed primarily in liver, the insulin-sensitizing effect of A769662 is thought to be mainly due to suppression of glucose production and FA oxidation within this organ (265). However, the same obstacle seen with acadesine arises since bioavailability of A769662 is only ~7% (265). Therefore a drug that exhibits more favourable pharmacokinetics still needs to be developed and investigated.

A natural remedy such as berberine, an alkaloid isolated from Chinese herbs, has been extensively used in natural medicine to treat gut-infections, although more recently to treat hyperglycemia and dyslipidemia (267). It was recently reported by Turner et al (267) that berberine inhibits complex I respiration. Furthermore, through the use of a cell model deficient in LKB1 signaling, they show that berberine requires AMPK activity to exert its metabolic effects on glucose and lipid homeostasis (267). Although berberine requires high oral doses to be effective, this study indicates that derivatives of berberine can be designed to reduce the amount required to achieve efficacy (267). Similarly, resveratrol, a compound found in grapes and red wine, has been demonstrated to

increased AMPK activity by increasing the AMP:ATP ratio in the cell (268). This effect was thought to be in combination of SIRT1 and AMPK activity (269), however later studies using AMPKα1 and α2 knockout mice indicated that AMPK was the central target mediated the metabolic effects of resveratrol (270). When added as a supplement to high-calorie diets administered to mice, resveratrol improved blood lipid profiles, increased survival, and fatty liver disease (268,271-273), ultimately enhancing overall health of these animals. Specifically, the downstream effects of AMPK activation included increased insulin sensitivity and glucose uptake in skeletal muscle and increased mitochondrial content (272). Since resveratrol can be administered efficiently through the diet, the delivery of small molecule activators of AMPK is an attainable goal for the development of treatments for obesity and metabolic disease.

CHAPTER 3: OBJECTIVES AND HYPOTHESES

OBJECTIVE #1 (Chapter 4): To investigate the effects of prolonged AICAR-induced AMPK activation on lipid partitioning and the potential molecular mechanisms involved in these processes in adipocytes.

Hypotheses:

1) Chronic AMPK activation will increase expression and content of proteins involved in oxidative metabolism (i.e. PGC-1α, PPARα, PPARδ, CPT-1) and cause a subsequent increase in FA oxidation.
2) Lipolysis will be suppressed due to AMPK-mediated inhibition of HSL phosphorylation and activity.

OBJECTIVE #2 (Chapter 5): To investigate the molecular mechanisms by which diet-induced obesity dysregulates lipid metabolism and whether AMPK is involved in these processes in adipocytes from visceral (VC) and subcutaneous (SC) fat depots.

Hypotheses:

1) The activity of the lipolytic machinery will be increased in VC compared to SC fat depots.
2) Blunted catecholamine-induced lipolysis in both VC and SC fat depots under conditions of diet-induced obesity will be mediated by impaired HSL phosphorylation.
3) The inhibitory effect of AMPK on HSL activity will be disrupted in VC and SC adipose tissue under conditions of diet-induced obesity.

OBJECTIVE #3 (Chapter 6): To investigate the molecular mechanisms by which AICAR-induced AMPK activation inhibits basal and insulin-stimulated glucose uptake in primary rat adipocytes.

Hypotheses:

1) AMPK activation inhibits basal and insulin-stimulated phosphorylation of the Akt substrate of 160 kDa (AS160) and GLUT4 translocation in adipocytes.
2) Disruption of AMPKα1 signaling will reverse the inhibitory effects of AICAR-induced AMPK activation on glucose uptake in primary adipocytes.

OBJECTIVE #4 (Chapter 7): To determine the functional and structural alterations in VC and SC fat depots, as well as the adaptive responses in whole-body energy balance induced by chronic *in vivo* systemic AMPK activation.

Hypotheses:

1) Increased mitochondrial content and a greater number of multilocular and UCP-1 positive adipocytes within the WAT will be accompanied by elevated rates of FA oxidation with chronic AMPK activation.
2) Adiposity will be reduced by chronic AMPK activation.
3) Reductions in adiposity will activate energy-sparing mechanisms, causing reduction in whole-body resting energy expenditure.
4) Systemic AICAR treatment will increase hypothalamic AMPK activation and trigger whole-body energy-sparing mechanisms.

CHAPTER 4:

Prolonged AICAR-induced AMP-kinase activation promotes energy dissipation in white adipocytes: Novel mechanisms integrating HSL and ATGL

Mandeep P. Gaidhu, Sergiu Fediuc, Nicole M. Anthony, Mandy So, Mani Mirpourian, Robert L.S. Perry, Rolando B. Ceddia.

School of Kinesiology and Health Science – York University, Toronto, ON, Canada

Contribution of authors:

MPG organized and conducted all experiments, and wrote the manuscript. SF, NMA, MS, MM, and RLS assisted with time-sensitive experiments. RBC designed and assisted with experiments and edited the manuscript.

Keywords: Obesity, AMPK, ATGL, HSL, PGC-1α, adipocytes, fatty acid oxidation.

A version of this manuscript has been published in the *Journal of Lipid Research.* The copyright policy automatically grants permission for authors reusing published material in the Journal of Lipid Research in a thesis or dissertation.

(**Gaidhu MP**, Fediuc S, Anthony NM, So M, Mirpourian M, Perry RL, Ceddia RB. Prolonged AICAR-induced AMP-kinase activation promotes energy dissipation in white adipocytes: novel mechanisms integrating HSL and ATGL. ***J Lipid Res***. 50:704-15, 2009).

ABSTRACT

This study was designed to investigate the effects of prolonged activation of AMP-activated protein kinase (AMPK) on lipid partitioning and the potential molecular mechanisms involved in these processes in white adipose tissue (WAT). Rat epididymal adipocytes were incubated with AICAR (0.5mM) for 15h. Also, epididymal adipocytes were isolated 15h after AICAR was injected (i.p. 0.7g/kg b.w.) in rats. Adipocytes were utilized for various metabolic assays and for determination of gene expression and protein content. Time-dependent *in vivo* plasma non-esterified fatty acid (FA) concentrations were determined. AICAR treatment significantly increased AMPK activation, inhibited lipogenesis, and increased FA oxidation. This was accompanied by up-regulation of peroxisome proliferator-activated receptor (PPAR)α, PPARδ, and PPARγ-coactivator-1α (PGC-1α) mRNA levels. Lipolysis was first suppressed, but then increased both *in vitro* and *in vivo* with prolonged AICAR treatment. Exposure to AICAR increased adipose triglyceride lipase content (ATGL) and FA release, despite inhibition of basal and epinephrine-stimulated hormone sensitive lipase (HSL) activity. Here, we provide evidence that prolonged AICAR-induced AMPK activation can remodel adipocyte metabolism by up-regulating pathways that favor energy dissipation versus lipid storage in WAT. Additionally, we show novel time-dependent effects of AICAR-induced AMPK activation on lipolysis, which involves antagonistic modulation of HSL and ATGL.

INTRODUCTION

Obesity is a major risk factor for metabolic disorders such as Type 2 Diabetes and cardiovascular disease and it is characterized by the excessive accumulation of fat in the white adipose tissue. In this context, physiological and/or pharmacological strategies aimed towards increasing fatty acid (FA) oxidation and energy dissipation in adipocytes have become of great therapeutic interest (274). One enzyme that has emerged as a potential target for dissipation of fat stores is AMP-activated protein kinase (AMPK). This enzyme functions as an energy sensor and is activated in response to changes to the AMP:ATP ratio in the cell (274,275). Upon activation, AMPK switches on catabolic pathways to produce ATP in an attempt to restore cellular energy homeostasis. One pathway that is central to the integrated effects of AMPK in peripheral tissues is the stimulation of FA oxidation (274,275), which could be of great relevance for the treatment of obesity and metabolic syndrome. However, currently very little is known regarding the effects of AMPK activation on glucose and lipid metabolism in WAT. We have recently reported that acute (1h) AICAR-induced AMPK activation in isolated rat adipocytes caused a reduction in glucose and FA uptake with concomitant reduction in oxidation of these substrates (191). This is contrary to the effects previously described in skeletal muscle (254), indicating that AMPK regulates glucose and lipid metabolism in a tissue-specific manner. Importantly, although acute AMPK activation can rapidly suppress glucose and FA uptake and metabolism in adipocytes (191), chronic AMPK activation has been associated with major alterations in gene expression, which might powerfully affect the ability of adipocytes to process glucose and FAs. In fact, it has been

demonstrated that AMPKα2 is localized in the nuclei of many cells and is involved in the regulation of gene expression (206). Support for this comes from correlative *in vivo* studies reporting that chronic AMPK activation in hyperleptinemic rats is associated with increased expression of PGC-1α, higher mitochondrial content, up-regulation of uncoupling proteins (UCPs), elevated expression of enzymes involved in β-oxidation, such as carnitine palmitoyl transferase 1 and acetyl-CoA oxidase, and decreased expression of lipogenic enzymes (acetyl-CoA carboxylase and fatty acid synthase) in WAT (119,276). Observations from these studies suggest that since hyperleptinemia depletes body fat without increasing plasma FA levels, the up-regulation of genes involved in oxidative metabolism were responsible for enhanced intra-adipocyte oxidation (119,222). Even though these studies show that AMPK phosphorylation is increased by hyperleptinemia, a direct cause-effect relationship between AMPK activation and these metabolic changes in adipocytes has not been established (119,222). Importantly, the effects of hyperleptinemia require the presence of a functional leptin receptor that engages many downstream targets, not specifically AMPK. In order to extend the knowledge on the role of AMPK activation in adipocyte metabolism, we tested whether chronic activation of AMPK causes alterations in gene expression that promote energy dissipation rather than storage in adipocytes. This is particularly important because potential pharmacological strategies for the treatment of obesity and its related metabolic disorders by selectively targeting adipose tissue AMPK activation will be chronic rather than acute in nature. Therefore, in order to test whether or not chronic activation of AMPK can lead to metabolic alterations that promote energy

dissipation in WAT, we performed *in vivo* and *in vitro* studies to assess various parameters as well as the potential mechanisms involved in the regulation of glucose and lipid metabolism by AMPK in adipocytes. Here, we provide novel evidence that chronic AICAR-induced AMPK activation causes a potent anti-lipogenic effect by increasing the expression of PGC-1α, PPARα, and PPARδ, by suppressing FA uptake, and by promoting oxidation of this substrate in rat white adipocytes. Chronic AICAR-induced AMPK activation also increased ATGL content and FA release, despite the fact that basal and epinephrine-stimulated HSL phosphorylation and activity was suppressed in adipocytes. Our data indicate that, through chronic AMPK activation, WAT metabolism can be remodeled towards energy dissipation and this may be of great relevance for the treatment of obesity and its related metabolic disorders.

MATERIALS AND METHODS

Reagents - 5'-aminoimidasole-4-carboxamide-1-beta-d-ribofuranoside (AICAR) was purchased from Toronto Research Chemicals, Inc. (Toronto, Ontario, Canada); cardiolipin, *E. coli* DAG kinase, DETAPAC, DTNB, di-'isononyl' phthalate, epinephrine, FA-free bovine serum albumin (BSA), free glycerol determination kit, glucose oxidase kit, MTT toxicology assay kit, octyl-β-glucoside, oxaloacetic acid, palmitic acid, phenylethylamine, silica coated TLC plates, and SYBR green were obtained from Sigma; [1-^{14}C]diolein, [9,10-^{3}H]triolein, [U-^{14}C]glycerol and [γ-^{32}P]ATP was purchased from American Radiolabeled Chemicals, Inc. (St. Louis, MO); D-[U-^{14}C]glucose, [1-^{14}C]pyruvic acid, and [1-^{14}C]palmitic acid was from GE Healthcare

Radiochemicals (Quebec City, Quebec, Canada), and human insulin (Humulin) was from Eli Lilly. Non-esterified fatty acid (NEFA) kit was from Wako Chemicals. Lactate oxidase kit was from Trinity Biotech. RNeasy Lipid Extraction Kit was from Qiagen. Superscript II and Taq polymerase was from Invitrogen. DNase kit was from Ambion. Tripalmitin, triolein, and *sn*-1,2-dioleoylglycerol standards were purchased from Nu Check Prep (Elysian, MN). Phosphatidic acid standard was from Avanti Polar Lipids (Alabaster, AL). Specific antibodies against phospho-AMPK, AMPK, acetyl-CoA carboxylase (ACC), hormone sensitive lipase (HSL), phospho-HSL (all residues), and adipose triglyceride lipase (ATGL) were from Cell Signaling Technology Inc. (Beverly, MA). Phospho-ACC was antibody was from Upstate (Charlottesville, VA). PEPCK-1 and GAPDH were from Abcam (Cambridge, MA). PGC-1α was from Cayman Chemicals (Ann Arbor, MI). All other chemicals were of the highest grade available.

Animals and isolation of primary adipocytes - Male albino rats (Wistar strain), weighing 150 - 200g, were maintained on a 12/12-h light/dark cycle at 22°C and fed (*ad libitum*) standard laboratory chow. The experimental protocol was approved by the York University Animal Care Ethics Committee. Rat epididymal fat pads were quickly removed, finely minced, and digested at 37°C for 30min in DMEM containing type II collagenase (1mg/ml). The digested tissue was filtered through a nylon mesh, and washed 3 times with DMEM supplemented with 1% fetal bovine serum (FBS), 1% antibiotic/antimycotic, 50μg/mL gentamycin, and 15mM HEPES (DMEM-1% FBS) (191). Cells were re-suspended in DMEM-1% FBS, and incubated in the absence or

presence of AICAR (0.5mM) for 15h prior to assaying for various metabolic parameters. The amount of AICAR was chosen for our *in vitro* studies was based on a dose response with concentrations of 0, 0.25, 0.5, 1, and 2mM, where AMPK activation was detectable using 0.5mM.

MTT assay for cytotoxicity - The MTT (3-[4,5-dimethylthiazol-2-yl]-2,5-diphenyl tetrazolium bromide) cytotoxicity test was performed according to manufacturer's instruction with slight modifications as described by Canovà et al (277). Briefly, cells were incubated for 15h in the absence or presence of AICAR (2mM). Subsequently, cells were re-suspended in serum and phenol red-free DMEM and cultivated for 2h in MTT work solution, consisting of a final concentration of 500 μg/ml MTT. The resulting purple formazan crystals were solubilized using the solution provided, and measured spectrophotometrically at 540nm.

Measurement of glycerol kinase (GyK) activity - Adipocytes were incubated for 15h in the presence of either AICAR (0.5mM) or Rosiglitazone (1μM). Control cells received only vehicle (DMEM-1% FBS or DMSO). After incubation, cells were snap-frozen in liquid nitrogen and prepared for measurement of GyK activity (253). Briefly, 150μL of extraction buffer (50 mM HEPES, 40 mM KCl, 11 mM $MgCl_2$, 1 mM EDTA, 1 mM dithiothreitol, pH 7.8) was added to cells, which were then vortexed and sonicated for complete lysis. Homogenates were centrifuged and the infranatant containing GyK was collected. Samples of the extract containing 10μg of total protein were added to 75μL assay buffer containing 5μCi/mL of U-[^{14}C]glycerol (~30μM), for 3h at 37°C. The

reaction was terminated by the addition of 150μL of 97% ethanol, 3% methanol (253). Seventy-five microlitres of the alcohol-treated reaction mixture were spotted onto DE-81 Whatman filters and allowed to air dry before being washed with distilled water overnight. Filters were dried again, and counted for radioactivity (253).

Measurement of glycerol, glucose, and pyruvate incorporation into lipids - For glycerol, glucose, and pyruvate incorporation into lipids, adipocytes (~2 x 10^5) were pre-incubated with AICAR for 15h and subsequently exposed for 1h to either [U-^{14}C]glycerol (0.5μCi/ml; ~30μM), D-[U-^{14}C]glucose (0.5μCi/mL, with 5.5mM unlabeled D-glucose), or [1-^{14}C]pyruvic acid (0.1μCi/mL, with 10μM unlabeled pyruvate) to allow incorporation of these substrates into total lipids (191,254). Subsequently, lipids were extracted using Doles method (278), and assessed for radioactivity (191,254).

Incorporation of [1-^{14}C]palmitic acid into TAGs – After the 15h incubation in the absence or presence of AICAR, adipocytes (~2 x 10^5) were incubated in the presence of 0.2mM palmitic acid and 0.2μCi/mL of labeled [1-^{14}C]palmitic acid for 1h to allow incorporation of palmitate into lipids (221). Subsequently, lipids were extracted by the method of Bligh and Dyer (279) with a few modifications. Briefly, cells were lysed in 0.5mL of methanol with vigorous vortexing, and lipids were extracted by adding 1.5mL of a chloroform:methanol solution (1:2, v/v) and incubated on ice for 1h. Subsequently, 0.5mL of each chloroform and 0.2M NaCl were added to the tubes, and phases were separated by centrifugation. The bottom phase was removed and washed with 0.5mL each of methanol and NaCl. The lower phase was extracted and evaporated under a

constant stream of N_2. Lipids were then re-suspended in 40μL of a chloroform:methanol solution (2:1) and 5μL was spotted onto a silica-coated glass thin layer chromotography (TLC) plate with triacylglycerol standards (tripalmitin and triolein). Lipids were separated with n-hexane/ethyl ether/acetic acid (70:30:1) as solvent and visualized using iodine vapor. The spots corresponding to the triacylglycerol (TAG) standards were scraped off and counted for radioactivity.

Palmitate Uptake - Palmitate uptake was assayed as described previously (191) with a few modifications. Briefly, fat cells (2×10^5) were re-suspended to a lipocrit of 30% and incubated either in the absence or presence of AICAR for 15h. Subsequently, palmitic acid uptake was assayed in KRB containing [1-^{14}C]palmitic acid (0.2μCi/mL) and non-labeled palmitate (30μM) conjugated with FA-free albumin in a molar ratio of 1 (~0.7% albumin). After cells had been exposed to the assay buffer for 3min, an aliquot (240μL) of the cell suspension was transferred to microtubes containing 100μL of cold di-'isononyl' phthalate and quickly centrifuged (13,000 rpm for 30s) to separate the cells from the radiolabeled incubation medium and to terminate the reaction. Microtubes were cut through the oil phase and cells transferred to scintillation vials to be counted for radioactivity. Non-specific transport was determined in the same conditions, except that ice-cold assay buffer was added to the cells and immediately centrifuged (time zero). Non-specific values were subtracted from all conditions.

Determination of lipolysis and the production of $^{14}CO_2$ from exogenous and endogenous [1-^{14}C]palmitic acid - Lipolysis was determined after AICAR-treated adipocytes (~2 x 10^5) had been incubated for 75min in the absence or presence of epinephrine (100nM final concentration) or vehicle (0.5M HCl). An aliquot of the media (400μL) was collected and analyzed for glycerol and non-esterified FA (NEFA) release using commercially available kits from Sigma Aldrich and Wako Chemicals, respectively. The oxidation of exogenous palmitate by isolated adipocytes pre-incubated with AICAR for 15h was measured in Krebs Ringer buffer (KRB) containing 4% FA-free albumin in the presence of 0.2mM palmitic acid and 0.2μCi/mL of labeled [1-^{14}C]palmitic acid for 1h (191). For endogenous palmitate oxidation, cells were incubated in the absence or presence of AICAR for 15h. Subsequently, cells were pre-labeled with 1μCi/mL of [1-^{14}C]palmitic acid (18,221) for 30min, and then washed to eliminate any [1-^{14}C]palmitic acid that had not been incorporated into adipocytes. Cells were then incubated in KRB containing 4% FA-free albumin, and $^{14}CO_2$ was collected as previously described for measurement of oxidation (191).

Citrate synthase activity – Citrate synthase activity was assayed with adaptations to the method described by Alp *et al* (280). Adipocytes (6 x 10^6) were lysed in buffer (25mM Tris-HCl, 1mM EDTA, pH 7.4), centrifuged, and the infranatant was collected. An aliquot containing ~20μg of protein was added to the assay buffer (50mM Tris-HCl, pH 8.1, 0.2mM DTNB, 0.1mM Acetyl-CoA, 0.5mM oxaloacetate) and absorbance was

measured over 10min in a spectrophotometer at 412nm. The assay control contained all components except the sample, and its value was subtracted from all conditions.

Quantification of diacylglycerol (DAG) content – DAG levels were quantified by a modified enzymatic method described by Preiss *et al* (281), which is based on the principle of DAG phosphorylation and conversion into phosphatidic acid. Briefly, control and AICAR-treated adipocytes (1×10^5) were lysed and lipids were extracted as described above. Lipids were dried under N_2 gas, and solubilized in 80μL of a 7.5% octyl-β-D-glucoside, 5mM cardiolipin in 1mM DETAPAC solution using brief sonication. Subsequently, 60μL of reaction buffer (100 mM imidazole HCl, pH 6.6, 100 mM NaCl, 25 mM $MgCl_2$, and 2 mM EGTA), 10μL of 20mM DTT in 1mM DETAPAC, and 10μL of DAG kinase solution (~4μg per reaction) was added to 10μL of solubilized lipids. Reactions were initiated with the addition of 10μL of ATP solution (final concentrations 1mM ATP and 2μCi of [γ-^{32}P]ATP per reaction) and allowed to proceed at 25°C for 30min. The reaction was terminated with the addition of 2mL of cold chloroform:methanol (1:2) solution, followed by 1mL of 0.2M NaCl and 2mL of chloroform. Tubes were vortexed, and after separation of phases, the lower phase was carefully extracted and placed into fresh test tubes. Lipids were dried under N_2 gas and solubilized in 50μL of 5% methanol in chloroform. Five microliters of the lipid was spotted onto a silica-coated glass plate, and separated using a solvent composed of chloroform, acetone, methanol, acetic acid, and distilled water (50:20:10:10:5, v/v/v/v/v). As a standard, cold phosphatidic acid (25μg) was spotted onto the plate. Lipids were

visualized using iodine vapour, and corresponding spots were scraped off and radioactivity was counted. For absolute quantification of DAG, a standard curve with known amounts of *sn*-1,2-dioleoylglycerol was assayed concurrently with samples for each experiment. Non-specifics were treated the same as standards and samples, except that no lipid was present. Non-specific values were subtracted from all values.

Western blot analysis - AICAR-treated and control adipocytes (1×10^7) were stimulated with epinephrine (100nM) for the final 30min of the 15h incubation-period. For time-course analyses, cells were exposed to AICAR for 0, 1, 2, 4, 8, and 15h. Cells were then immediately snap-frozen in liquid nitrogen and lysed in buffer composed of 25mM Tris-HCl and 25mM NaCl, (pH 7.4), 1mM $MgCl_2$, 2.7mM KCl, 1% NP-40, and protease and phosphatase inhibitors (0.5mM Na_3VO_4, 1mM NaF, 1μM leupeptin, 1μM pepstatin, 1μM okadaic acid, and 20mM PMSF) (191,282). Cell lysates were centrifuged, the infranatant was collected, and an aliquot was used to determine protein concentration using the Bradford method. Sample preparation and SDS-PAGE conditions were performed as previously described (191). All primary antibodies were used in a dilution of 1:1000 with the exception of AMPK (1:500), PGC-1α (1:200), and GAPDH (1:5000).

Quantitative PCR (q-PCR) analysis - Total RNA was isolated from adipocytes using the RNeasy kit, followed by DNase treatment in order to remove gDNA carry-over. Primers were designed using the software PrimerQuest (IDT, USA) based on probe sequences available at the Affymetrix database (NetAffx™ Analysis Center, http:// www.affymetrix.com/analysis) for each given gene. Real-time PCR reactions were

carried out at amplification conditions as follows: 95°C (3 min); 40 cycles of 95°C (10 s), 65°C (15 s), 72°C (20 s); 95°C (15 s), 60°C (15 s), 95°C (15 s). qPCR was performed using the ABI Prism® 7900HT Sequence Detection System (Applied Biosystems, Perkin Elmer, USA). All genes were normalized to the control gene GAPDH and β-actin, and values are expressed as fold increases relative to control. Primers sequences are shown in Table 4-2.

In vivo treatment - Rats were given a single i.p. injection of either saline or AICAR (0.7g/kg b.w.). The dosage was chosen based on previous *in vivo* rat studies that used between 0.5 – 1.0 g/kg b.w. for chronic AICAR injections (283-285). Fifteen hours later, epididymal fat pads from each group were extracted, and adipocytes were isolated for analysis of palmitate oxidation (191) or protein expression by Western blotting. For *in vivo* glucose and NEFA determination, animals were injected with either saline or AICAR and blood samples from the saphenous vein were collected at various time points. An 8h time-course was chosen for *in vivo* studies to avoid the effects of circadian rhythm on lipolytic rate (286). Glucose concentration was determined by the glucose oxidase method using a commercially available kit from Sigma.

HSL and TAG lipase activity - Activity of HSL was measured as established by Fredrikson *et al* (287). Briefly, after treatment with AICAR for 15h, cells were stimulated with epinephrine (100nM) for 75min. Subsequently, cells were lysed in 2 volumes of homogenization buffer (287) and centrifuged for 45min (4°C, 11,000g). An aliquot (~100μg of protein) of the infranatant was incubated with assay buffer containing a final

concentration of 7.5mM unlabeled diolein (DO) and 0.5μCi/mL of labeled [1-^{14}C]diolein at 37°C for 10min. This substrate is a commercially available diacylglycerol that liberates a labeled [1-^{14}C]oleic acid in the presence of HSL activity (287). The reaction was terminated with the addition of 3.25mL of extraction buffer and 1.05mL of a 0.1M K_2CO_3, 0.1M boric acid solution (287). Tubes were centrifuged (800*g*) and 1mL from the upper phase, which contains the liberated [1-^{14}C]oleic acid, was extracted and counted for radioactivity. Determination of TAG lipase activity was identical to measurement of HSL activity, except the assay buffer contained 5mM unlabeled triolein and 0.5μCi/mL of labeled [9,10-^{3}H]triolein as a substrate.

Statistical Analysis – Statistical analyses were performed by unpaired t-tests or using either one- or two-way analysis of variance with Tukey-Kramer multiple comparison post-hoc tests. The level of significance was set to $P<0.05$.

RESULTS

AMPK and ACC phosphorylation and content, PGC-1α content, cytotoxicity, palmitate uptake, palmitate oxidation, and citrate synthase activity. Adipocytes treated with AICAR elicited an increase in both phosphorylation and content of AMPK (Figure 4-1A). AICAR increased ACC phosphorylation while total ACC levels decreased relative to control values (Figure 4-1A). PGC-1α content clearly increased after 15h of AICAR treatment (Figure 4-1B). Measurement of cytoxicity revealed no difference between control and adipocytes exposed to AICAR for 15h (Figure 4-1C). Palmitate uptake

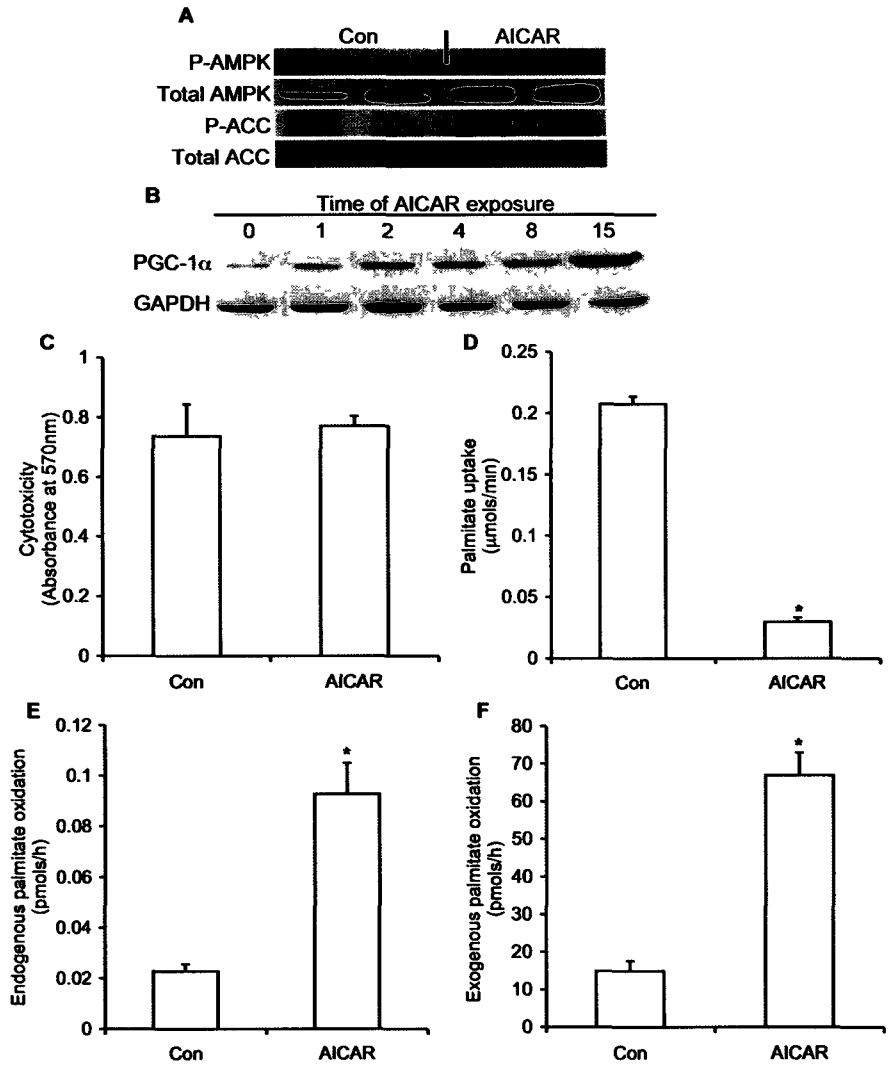

Figure 4-1. Effects of AICAR on content and phosphorylation of AMPK and ACC **(A)**, PGC-1α content **(B)**, cytotoxicity **(C)**, palmitate uptake **(D)**, and $^{14}CO_2$ production from [1-^{14}C]palmitic acid via endogenous **(E)** and exogenous **(F)** sources. Blots are representative of 3 independent experiments. Data for cytotoxicity, uptake, and oxidation are compiled from 4-5 independent experiments. Unpaired t-tests were performed for statistical analyses. *P<0.05 versus control (Con) conditions.

significantly decreased (~87%) in AICAR treated cells (Figure 4-1D), while oxidation of both endogenous and exogenous palmitate was elevated by ~6.6- and ~3-fold, respectively (Figure 4-1E-F). We have also tested whether or not the addition of L-carnitine to the incubation medium would modify the ability of fat cells to oxidize long-chain FAs. We exposed isolated adipocytes to AICAR for 15h in the absence or presence of carnitine (500μM). The addition of L-carnitine increased palmitate oxidation from 0.021 ± 0.004 to 0.058 ± 0.004 and from 0.052 ± 0.007 to 0.150 ± 0.004 nmols/h in control and AICAR-treated cells, respectively. These data indicate that, although the addition of L-carnitine to the incubation medium increased the absolute values of palmitate oxidation, it did not alter the AICAR-induced ~3.0-fold increase in the ability of adipocytes to oxidize palmitate. Compatible with the elevation in oxidation, AICAR treated cells also elicited an increase in citrate synthase activity by ~1.9-fold relative to control cells (Table 4-1).

Quantitative PCR analyses. Quantitative PCR analysis revealed that the mRNA levels of the α1 isoform of AMPK was not altered by AICAR treatment, while the expression of the α2 isoform increased by ~4.8-fold (Table 4-2). Additionally, mRNA levels of PGC-1α, PEPCK-1, PPARα, PPARδ, and PPARγ were increased by ~3.0-, ~7.0, ~3.7-, ~2.5, and ~2.8-fold, respectively, after AICAR treatment (Table 4-2). Enzymes involved in β-oxidation, such as carnitine palmitoyltransferase-1b (CPT-1b) and acetyl-CoA oxidase, were up-regulated by ~3.9- and 2.3-fold respectively. Expression of PEPCK-2, UCP-1, and UCP-2 remained unaltered with AICAR treatment (Table 4-2).

Condition	Citrate synthase activity (nmols/min/μg of protein)
Control	2.42 ± 0.53
AICAR	4.68 ± 0.36*

Table 4-1. Citrate synthase activity. Cells were incubated in the absence or presence of AICAR (0.5mM) for 15h, and protein was extracted for determination of citrate synthase activity. Values were corrected for μg of protein per sample. N=8 per group, with samples run in duplicate. Unpaired t-test was performed for statistical analysis. *P<0.05 versus Control.

Gene	Primer sequences (5' → 3') (F – Forward, R – Reverse)	Relative to control (Mean ± SE)
AMPKα1	F - ACCATTCTTGGTTGCCGAAACACC R- CCAAATGCCACTTTGCCTTCCGTA	1.03 ± 0.08
AMPKα2	F - CAGCCCTTGGGCATCTTTGCTAAT R - AAAGACCCTATGGCCAAAGCAAGG	4.79 ± 0.31*
PGC-1α	F - ACCGTAAATCTGCGGGATGATGGA R - CATTCTCAAGAGCAGCGAAAGCGT	3.04 ± 0.18*
PEPCK-1	F - TCCGAAGTTGGCATCTGACACTGA R - CTCACACACACATGCTCACACACA	7.02 ± 0.61*
PEPCK-2	F – AGGCTGGAAAGTGGAGTGTG R - GTGGAAGAGGCTGGTCAATG	0.71 ± 0.06
UCP-1	F – TCAACACTGTGGAAAGGGACGACT R - TCTGCCAGTATGTGGTGGTTCACA	1.29 ± 0.26
UCP-2	F – AGCACATCTCACTATGCCTCCTCA R - ACATTGGAGCTTGCTTTATGGGCG	0.73 ± 0.10
PPARα	F - TGCAGGTCATCAAGAAGACCGAGT R - TGTGCAAATCCCTGCTCTCCTGTA	3.70 ± 0.56*
PPARδ	F - AGACCTCAGGCAGATTGTCACAGA R - ACACTTTGTCAGCGACTGGGACTT	2.50 ± 0.33*
PPARγ	F - ACACTTTGTCAGCGACTGGGACTT R - AGACCTCAGGCAGATTGTCACAGA	2.97 ± 0.37*
COX-8	F - ATGGTTCCAGCAGGATGGGTCTTA R - AGCGTTTAATTGGCCTCTCAGGGA	2.18 ± 0.19*
COX-6	F - TTGCTGCTGCCTATAAGTTTGGCG R - AGTTCAGGAACACAGGTCAGCAGT	1.68 ± 0.13*
CPT-1a	F - ACGGACCCTCGTGATACAAACCAA R - AGCCAAGGCATCTCTGGATGTAGT	0.81 ± 0.18
CPT-1b	F - AGCCCTTAGGTGCCTATGTTTGGT R - ACAGCACTCTCGAAGTCCGCATTA	3.94 ± 0.56*
Acetyl-CoA oxidase	F - AGATTAGCCAGGAAAGCCGACCAT R - TCCTTCGTGGATGAAGTCCTGCAA	2.27 ± 0.15*
GAPDH	F - TGACTCTACCCACGGCAAGTTCAA R - ACGACATACTCAGCACCAGCATCA	N/A

Table 4-2. Quantatative PCR analyses. Total RNA was extracted from adipocytes after 15h of AICAR treatment and subsequently used for quantitative PCR analysis. GAPDH was used as the control gene. N=4-5 for each group. Samples were run in triplicates on the plate. *P<0.05 versus control.

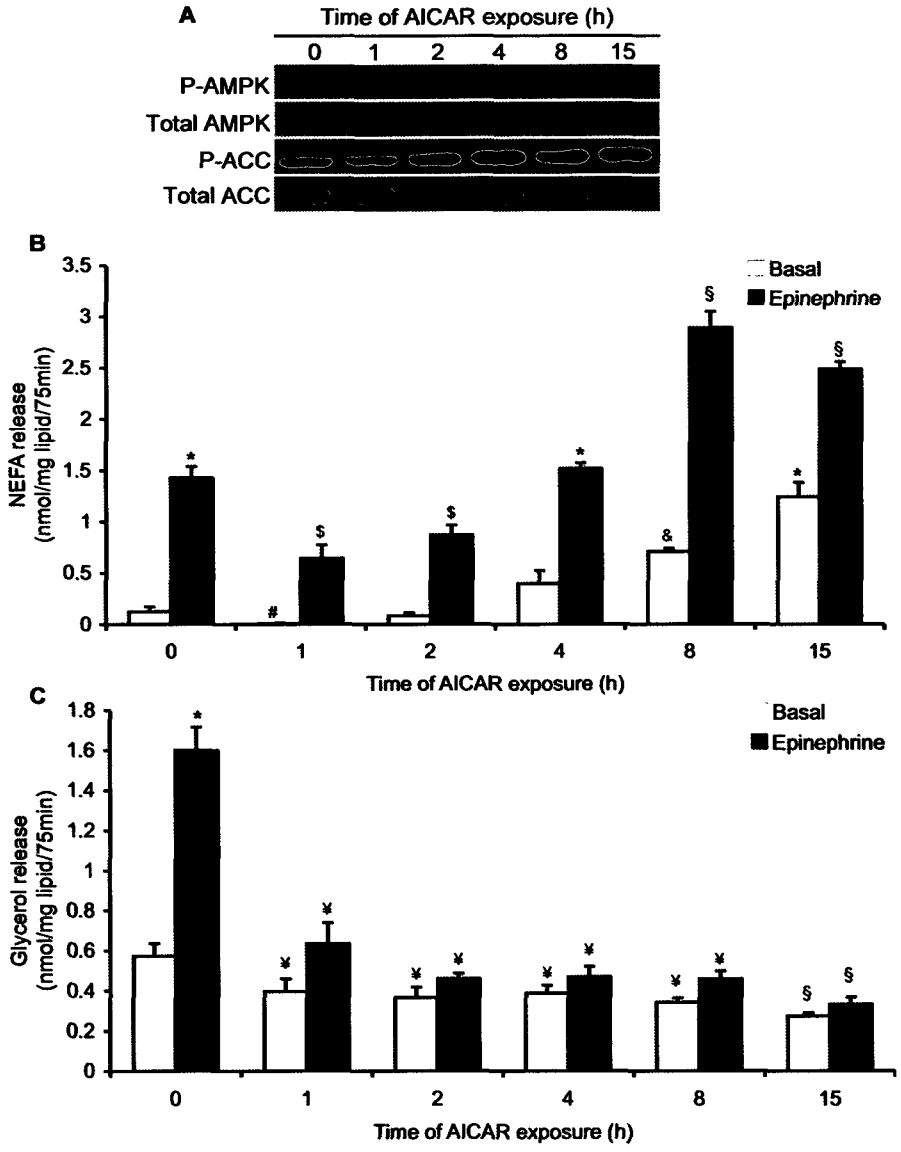

Figure 4-2. Time-dependent effects of AICAR on content and phosphorylation of AMPK and ACC from 0 to 15h **(A)**. Time-dependent effects of AICAR and epinephrine (Epi) on non-esterified FAs (NEFAs) **(B)** and glycerol release **(C)** *in vitro*. Blots are representative of 3 independent experiments. Data for NEFA and glycerol determination were compiled from 3 independent experiments. Two-way ANOVAs were performed for statistical analyses. * and $^{\#}P<0.05$ versus all other conditions; $^{\$}P<0.05$ versus 0, 4, 8, and 15h; $^{\&}P<0.05$ versus Basal 0, 1, 2, 4, 15h and Epi 8 and 15h; $^{\S}P<0.05$ versus all other conditions; $^{¥}P<0.05$ versus 0 and 15h.

In vitro lipolysis. NEFAs in the medium decreased after 1h and 2h of AICAR treatment under both basal (~95 and ~35%, respectively) and epinephrine stimulated (~55 and ~40%, respectively) conditions (Figure 4-2B). After 4, 8, and 15h of AICAR treatment, basal NEFA levels increased by ~3.2-, ~5.8-, and ~10-fold while under epinephrine-stimulated conditions this variable increased by ~1.1-, ~2-, and ~1.8-fold, respectively (Figure 4-2B). Glycerol release was suppressed at all time points remaining at ~50% and 20% of control values for basal and epinephrine conditions, respectively (Figure 4-2C).

PEPCK-1 content, GyK activity, and incorporation of palmitate, glucose, glycerol, and pyruvate into lipids. PEPCK-1 content was increased in a time-dependent manner with AICAR treatment (Figure 4-3A). Rosiglitazone was used as a positive control (253), and as expected, it significantly increased GyK activity by ~60% (Figure 4-3B). AICAR treatment did not change the activity of this enzyme (Figure 4-3B). AICAR treatment inhibited incorporation of palmitate, glucose, and glycerol into lipids by ~70, ~90 and ~35%, respectively (Figure 4-3C-E), while the incorporation of pyruvate into lipids remained unaffected (Figure 4-3F).

HSL content, phosphorylation, and activity, ATGL content, and TAG lipase activity. As expected, phosphorylation of HSL_{563} and HSL_{660} increased with epinephrine stimulation (Figure 4-4A). AICAR treatment inhibited phosphorylation of HSL_{563} and HSL_{660} under basal and epinephrine stimulated conditions (Figure 4-4A), while it increased phosphorylation of the HSL_{565} residue (Figure 4-4A). In cells exposed to AICAR, basal HSL activity significantly decreased by ~40 while the epinephrine-stimulated effect was

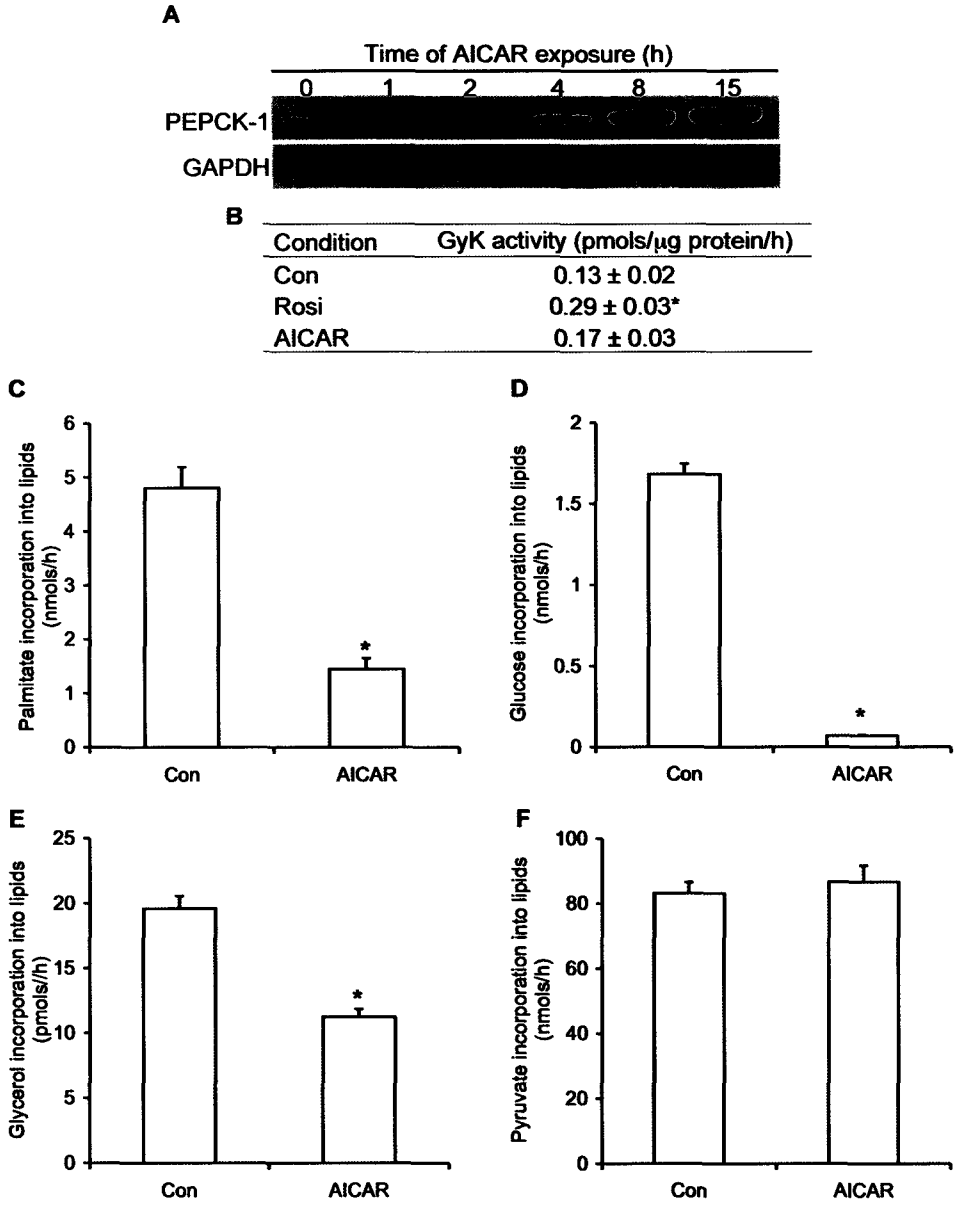

Figure 4-3. Measurement of PEPCK content by western blotting **(A)**, glycerol kinase (GyK) activity **(B)**, and the incorporation of palmitate **(C)**, glucose **(D)**, glycerol **(E)**, and pyruvate **(F)** into lipids. Rosiglitazone (Rosi; 1μM) was used as a positive control. PEPCK blot is representative of 2 independent experiments. All other data were compiled from 3-4 independent experiments. Unpaired t-tests and one-way ANOVAs were performed for statistical analyses. *P<0.05 versus Con.

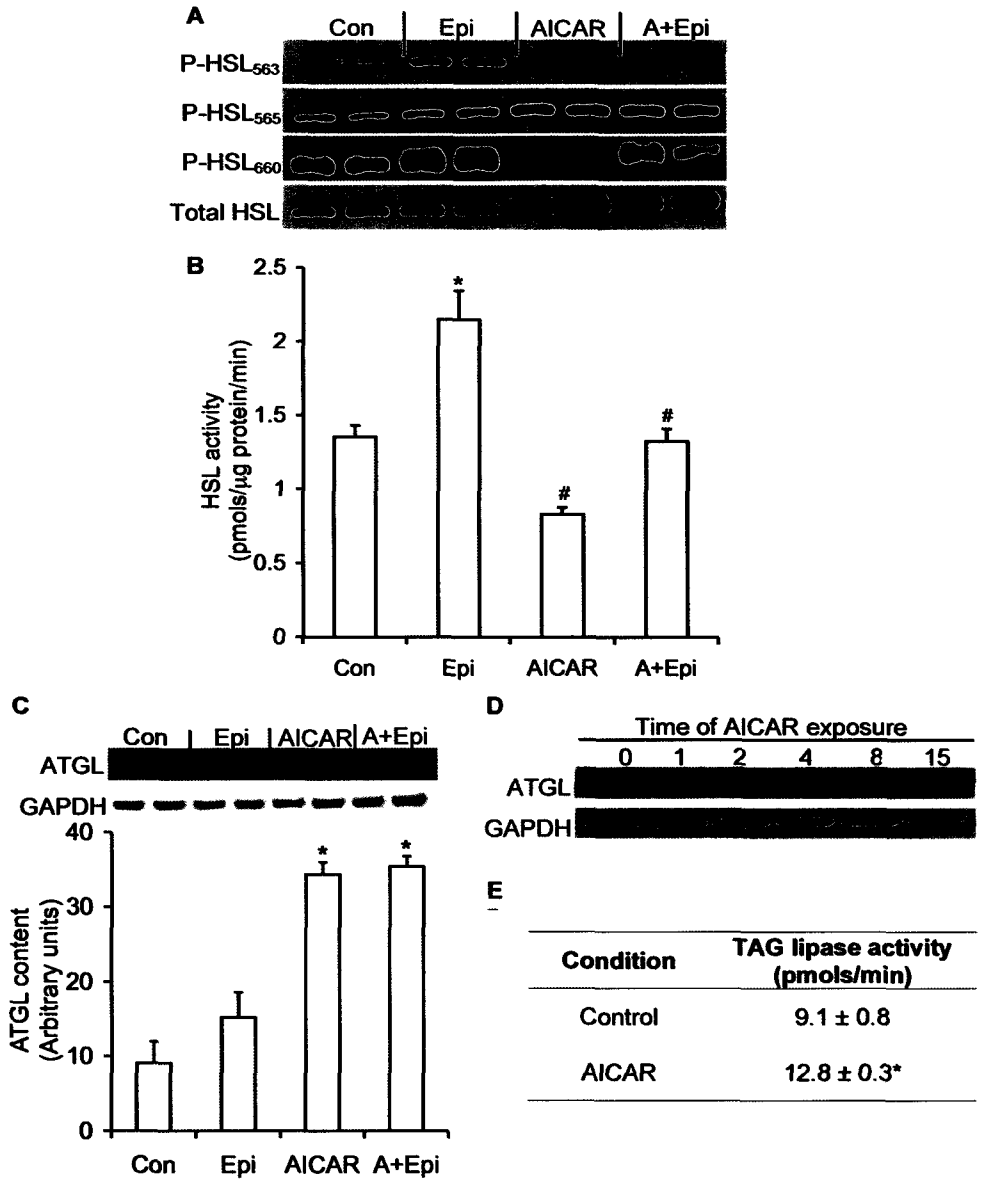

Condition	TAG lipase activity (pmols/min)
Control	9.1 ± 0.8
AICAR	12.8 ± 0.3*

Figure 4-4. Effects of AICAR, epinephrine (Epi), and AICAR plus epinephrine (A+Epi) on content and phosphorylation of HSL at serine residues 563, 565, and 660 **(A)**. Measurement of HSL activity **(B)**, ATGL content **(C)** and **(D)**, and TAG lipase activity **(E)**. Blots are representative of 3-4 independent experiments. Data for HSL activity were compiled from 3 independent experiments. One-way ANOVAs were performed for statistical analyses. *$P<0.05$ versus all other conditions; $^{\#}P<0.05$ versus Con and Epi.

suppressed by ~60% (Figure 4-4B), despite the fact that total HSL content increased by ~2-fold (Figure 4-4A). Furthermore, ATGL, which is a triacylglycerol (TAG)-specific lipase, showed a time-dependent increase in its content (Figure 4-4D), reaching ~4-fold greater than control values in AICAR treated cells (Figure 4-4C). TAG lipase activity was increased from 9.1 ± 0.8 to 12.8 ± 0.3 pmols/min in control versus AICAR treated cells, respectively (Figure 4-4E).

Time course of plasma glucose and NEFAs, measurement of AMPK/ACC phosphorylation, and determination of palmitate oxidation in WAT after AICAR-injection. Basal plasma NEFA concentrations decreased by ~55% 30min after AICAR injection (Figure 4-5A). However, NEFA release increased in a time dependent manner reaching values ~2.4- and ~2.1-fold higher than control at 4h and 8h, respectively (Figure 4-5A). Plasma glucose was significantly reduced from 6.6 to 4.2, 4.2, 4.2, 4.3, and 4.4mM after 30min, 1h, 2h, 4h, and 8h AICAR injection, respectively (Figure 4-5B). No alteration in plasma glucose was observed in saline-injected animals throughout the same time period (Figure 4-5B). AMPK phosphorylation increased by ~14-fold in epididymal fat tissue of AICAR injected animals, while total content of this protein was unchanged (Figure 4-5C). Palmitate oxidation was increased by ~2.2-fold in adipocytes isolated from epididymal fat pads of AICAR-treated rats (Figure 4-5D).

Measurement of cellular DAG levels. Quantification of DAG content showed similar levels in control versus AICAR-treated adipocytes (Figure 4-6).

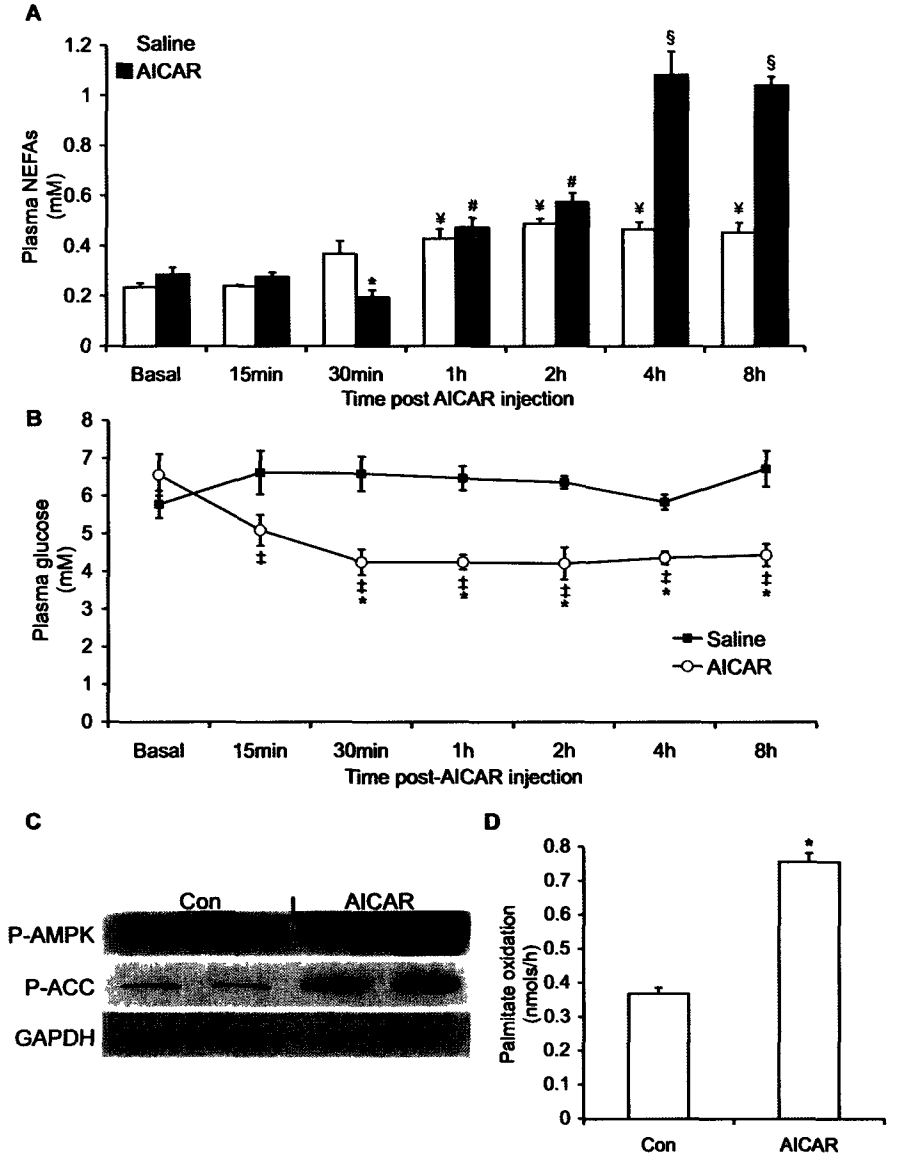

Figure 4-5. Time-course of NEFAs **(A)** and plasma glucose levels **(B)** after AICAR-injection. **(C)** Phosphorylation of AMPK and ACC, and **(C)** $^{14}CO_2$ production from [1-^{14}C]palmitic acid from epididymal fat pads of AICAR-injected rats (0.7g/kg bw). Blots are representative of 3 independent experiments. All other data were compiled from 3-4 independent experiments, n=12-15 for each condition. Unpaired t-tests and one-way ANOVAs were performed for statistical analyses. *P<0.05 versus Con and Basal values. $^{\#}$P<0.05 versus 0, 15, and 30min. $^{¥}$P<0.05 versus Con. §P<0.05 versus 0, 15min, 30min, 1h, and 2h. ‡P<0.05 versus relative saline control.

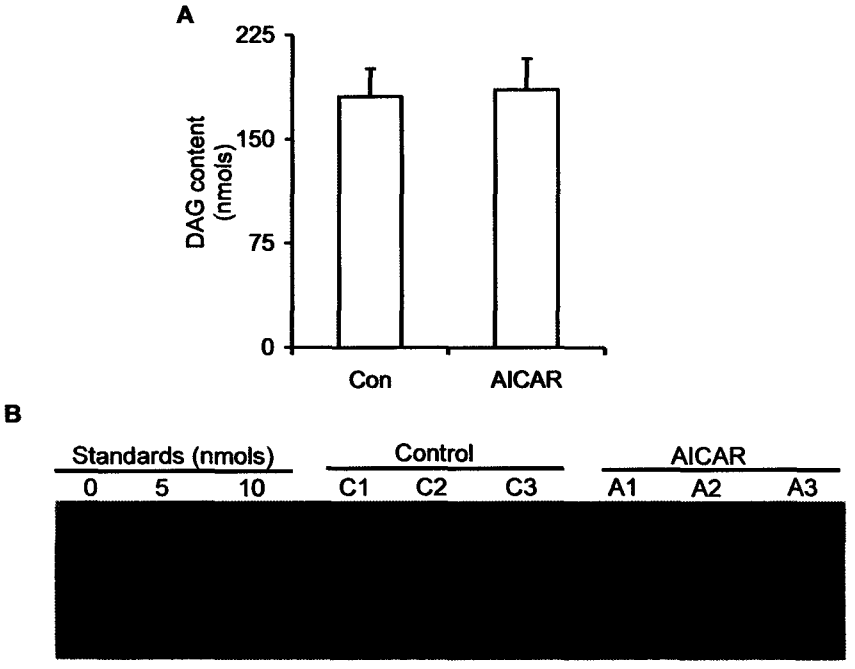

Figure 4-6. Quantification of cellular DAG levels **(A)** and representative TLC plate visualized by autoradiography **(B)**. C1-C3 and A1-A3 refer to control and AICAR samples, respectively. Data for DAG quantification is representative of 3 independent experiments, with n=9 for each condition. Unpaired t-test was used for statistical analysis.

DISCUSSION

Here, we demonstrate the novel findings that chronic AMPK activation remodels adipocyte metabolism by preventing TAG storage and by activating pathways that promote energy dissipation within the adipocyte. This is supported by a powerful suppression (~87%) in FA uptake and by an ~3.5- and 6-fold increase in exogenous and endogenous FA oxidation induced by AICAR, respectively. The expressions of AMPKα2, PGC-1α, PPARα, and PPARδ, which are directly implicated in the expression of enzymes of FA oxidation and mitochondrial biogenesis (119,211,276), were up-regulated after 15h of AICAR treatment. Additionally, mRNA of cytochrome C oxidases (COX6/8), CPT-1b, and acetyl-CoA oxidase, were up-regulated with AICAR treatment. Compatible with these findings is an elevation (~1.9-fold) in citrate synthase activity after 15h of AICAR treatment, indicating that metabolism is being diverted towards β-oxidation of FAs. Furthermore, the content of the lipogenic enzyme ACC was significantly reduced, while its phosphorylation state was increased. This is compatible with an increase in FA oxidation from *in vitro* and *in vivo* AICAR-treated adipocytes. We found that chronic AICAR-induced AMPK activation increased (~4.8-fold) the expression of the AMPKα2 subunit without affecting mRNA levels of the α1 isoform. This was also accompanied by a significant time-dependent increase in AMPK and PGC-1α contents, which is in line with the increase in FA oxidation observed in this study. The mRNA content of the lipogenic transcription factor PPARγ was significantly increased by AICAR treatment. However, our functional data clearly indicates that lipid

synthesis and storage is strongly inhibited in adipocytes exposed to AICAR. This may be explained by the fact that induction of PGC-1α by AMPK activation combined with an increase in PPARα and PPARδ expression is over-riding the potential lipogenic effects of PPARγ in AICAR treated white adipocytes.

A surprising finding of our study was that acute and chronic AICAR-induced AMPK activation suppressed glycerol release under basal and epinephrine-stimulated conditions. However, when we assessed lipolysis by measuring NEFAs in the medium, we found that it was initially reduced after AICAR treatment but progressively increased in a time-dependent manner, reaching values ~10- and ~1.8-fold higher than controls at 15h under basal and epinephrine-stimulated conditions, respectively. These findings were also reproduced *in vivo* when we determined the time-course of NEFAs in the plasma of AICAR-injected rats over an 8h time period. The reduction in glycerol release by adipocytes could have been because re-esterification of FAs was upregulated in cells chronically exposed to AICAR. In order to test this hypothesis, glycerol kinase (GyK) activity, PEPCK-1 expression, and the incorporation of palmitate, glucose, pyruvate, and glycerol into lipids were determined. We found that the activity of GyK was not affected in isolated adipocytes treated with AICAR, while the incorporation of glycerol into lipids was reduced by ~35%. Also, in line with these findings were the observations that glucose incorporation into lipids was powerfully suppressed with AICAR treatment, indicating a decrease in lipogenesis. Alternatively, re-esterification of FAs could also be occurring through glyceroneogenesis, leading to FA recycling in adipocytes (193). We found that the cytosolic form of PEPCK (PEPCK-1) mRNA levels were increased by 7-

fold, and protein levels were clearly enhanced with chronic AICAR treatment, suggesting up-regulation of glyceroneogenesis. However, the incorporation of palmitate into lipids indicated that even though the glyceroneogenic pathway could be up-regulated, re-esterification of FA was decreased by ~70% with AICAR treatment. This correlates with *in vivo* studies from our lab (unpublished data) and others (285) demonstrating that chronic AICAR injections in rats causes a decrease in fat mass (subcutaneous, epididymal, and retroperitoneal depots), further supporting a decrease in TG storage. Furthermore, our *in vitro* and *in vivo* measurements of NEFAs were still substantially increased after 15h of AICAR treatment, indicating a lack of FAs recycling back into TAG in the adipose tissue. Therefore, FA re-esterification could not account for the lower glycerol release observed after AICAR treatment. In this scenario, incomplete lipolysis could be occurring, which could justify the increase in NEFAs without a concomitant increase in glycerol release. To test this, we examined phosphorylation and activity of HSL. We found that chronic treatment of white adipocytes with AICAR significantly increased HSL phosphorylation at Ser565, while phosphorylation of the PKA-dependent Ser563 and Ser660 were powerfully suppressed, despite the fact that total HSL content was increased. Furthermore, this was accompanied by a significant reduction of ~40% in basal HSL activity and ~60% inhibition of epinephrine-induced HSL activation. Even though HSL plays an important role in lipolysis, another TAG-specific lipase called adipose triglyceride lipase (ATGL) has recently been identified. Ablation of ATGL significantly decreased the release of glycerol and FAs from fat cells (288,289); therefore, it has been proposed that complete hydrolysis of TAG in adipocytes requires

the expression and activation of both acyl hydrolases (290). Here, we provide evidence that AICAR-induced AMPK activation suppressed the activity of HSL, but promoted an ~4-fold increase in ATGL content in adipocytes. Although we were unable to obtain a direct measurement of ATGL activity, the increase in total TAG lipase activity (~40%) indicate that the increase in ATGL content must have facilitated the initiation of TAG hydrolysis but the inhibition of HSL activation may have restricted further breakdown of DAG. This is in line with the time-dependent elevation of FA release without a concomitant increase in glycerol levels observed in the present study. Measurement of DAG levels in the cell showed no differences between control and AICAR-treated cells. It could be that the accumulation of DAG in AICAR-treated cells is not sufficient to detect a difference after only 15h of treatment. In fact, studies using HSL knock-out mice indicate that only after 16 weeks DAG accumulation is detected in WAT of these mice (44). It is also possible that any excess DAG being produced may be diverted towards pathways where DAG molecules can be quickly converted into ceramides or various phospholipid molecules (291). Importantly, the assay used by us to quantify cellular DAG content is also suitable for measuring ceramide production, and we were not able to detect a significant amount of it in either control or AICAR treated cells. Therefore, the ultimate fate of DAG, if it is indeed accumulating and/or being shunted towards an alternative pathway, requires further investigation.

It is important to highlight that the effect of AICAR on FA release was time-dependent. Shortly after initiation of AICAR treatment, lipolysis was decreased as shown by NEFA release both *in vitro* and *in vivo*, which can be attributed to the rapid inhibition

by AMPK of HSL phosphorylation/activity. However, since changes in gene expression and protein content take longer to occur, the effects of increased ATGL content on lipolysis were evident only 4-6h after AICAR treatment. Previous studies have assessed the effect of AMPK activation on lipolysis in adipocytes *in vitro* (181,290,292,293) by measuring glycerol release and have reported conflicting results regarding whether AMPK is pro- or anti-lipolytic. Our data provide a novel mechanism by which AMPK exerts time-dependent effects on lipolysis, which could only be detected by measuring the release of both glycerol and NEFAs. Therefore, future studies investigating the role of prolonged AMPK activation in lipolysis should not rely on glycerol release as the sole indicator of TAG breakdown.

The elevated levels of NEFAs in AICAR-injected animals raise the possibility that chronic pharmacological activation of AMPK in WAT may lead to lipotoxicity and contribute to the development of insulin resistance. However, our data indicate that plasma glucose levels in fed animals significantly decreased (~35%) after AICAR injection, suggesting that glucose uptake in peripheral tissues was increased. Furthermore, the effect of AICAR on plasma glucose clearance was so potent that fasted animals had to be euthanized 1h after injection of this AMPK agonist due to severe hypoglycemia (data not shown). Also in line with these findings, several long-term *in vivo* studies using lean and diabetic rodent models have shown that AICAR-induced AMPK activation significantly reduces plasma glucose levels (185,284,294), indicating that despite elevated NEFA levels, glucose homeostasis is improved with treatment with this AMPK agonist. Additionally, activation of AMPK increases FA oxidation in

peripheral tissues such as liver and skeletal muscle (274), thereby exerting an anti-lipotoxic effect by preventing the accumulation of lipids in non-adipose tissues.

Even though lipolysis may be seen as a pathway that provides substrate for tissues to produce ATP and maintain cellular energy homeostasis, activation of AMPK has been proposed to limit lipolysis in WAT and actually spare energy (275). The rationale for this is based on the fact that if FAs released by lipolysis are not oxidized either within the adipocyte or in other tissues, they are recycled into TAGs in the fat cells creating a "futile cycle" (253). Therefore, AMPK activation as a consequence of lipolysis has been proposed to operate as a mechanism to restrain energy depletion in WAT (183). Based on our data, we propose that chronic AMPK activation remodels adipocyte metabolism, which may restrict energy depletion and increase ATP production. When acutely activated in the adipocyte, AMPK quickly inhibits HSL activity and also suppresses glucose and FA uptake (191). These rapid effects may be important to limit the excessive release of FAs and the potential energy cost of re-esterifying FAs that are not disposed of internally or peripherally (Figure 4-7). If chronically activated, AMPK also promotes alterations in gene expression that increase the ability of the cell to dispose of FAs internally through oxidation, facilitating ATP production and maintenance of intracellular energy homeostasis (Figure 4-7). In our experiments these chronic adaptations led to a net time-dependent increase *in vitro* and *in vivo* of FA release, indicating that the WAT can cope with internal energy challenges without compromising the provision of substrate for energy production in peripheral tissues. In summary, novel evidence is provided that through chronic pharmacological activation of AMPK, WAT metabolism

may be remodeled towards energy dissipation rather than storage. AMPK exerts these effects through distinct time-dependent regulation of HSL, ATGL, and by altering the expression of genes that promote lipid utilization versus storage in adipocytes. These mechanisms may be of great relevance for the treatment of obesity and Type 2 Diabetes.

ACKNOWLEDGEMENTS

This research was funded by the Natural Science and Engineering Research Council (NSERC), the Canadian Institute of Health Research (CIHR), and by the Canadian Diabetes Association (CDA) through operating grants awarded to RBC. RBC is also a recipient of the CIHR New Investigator Award. MPG was supported by a CIHR Canadian Graduate Scholarship - Doctoral Award. SF was supported by a doctoral NSERC Post Graduate Scholarship. Canadian Graduate Scholarships - Masters awards from CIHR and NSERC supported NMA and MS, respectively.

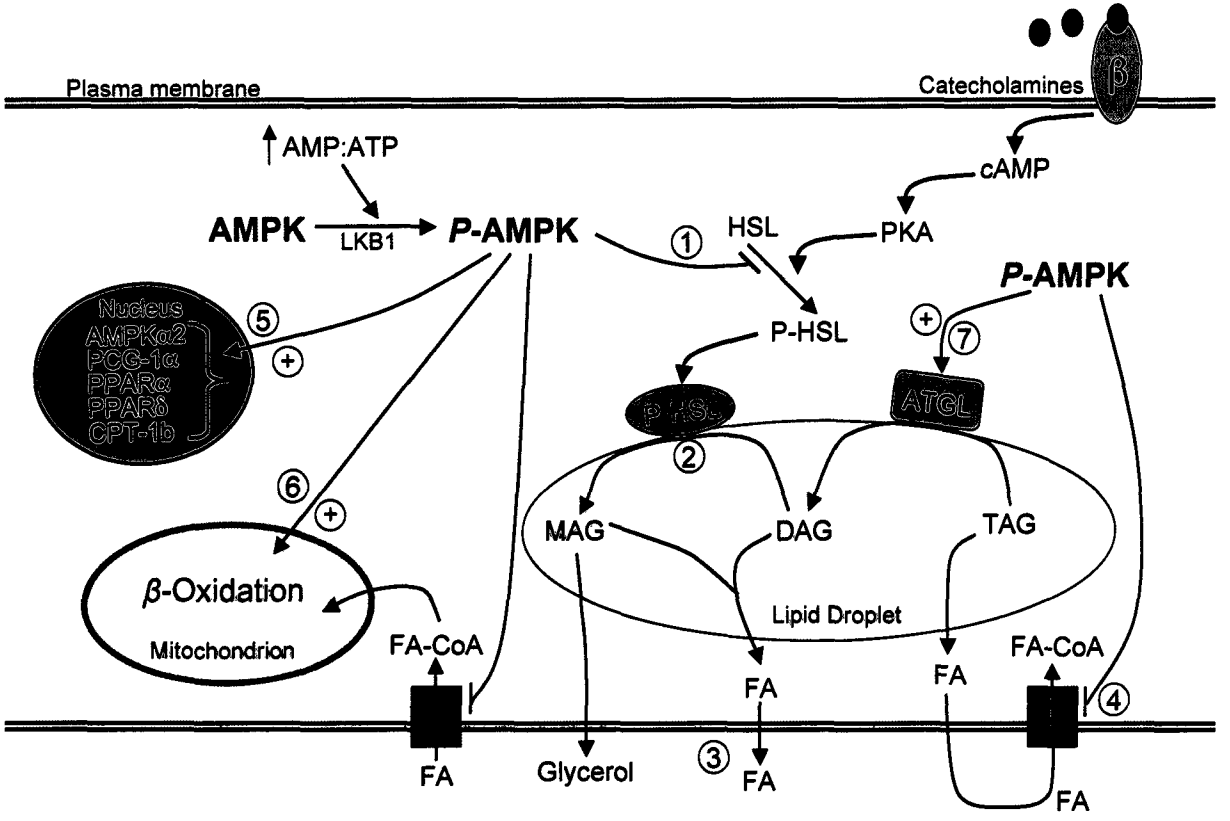

Figure 4-7. The role of AMPK activation in lipid metabolism in white adipocytes. Acute activation of AMPK inhibits HSL activity **(1)**, which prevents hydrolysis of DAG **(2)** and subsequent liberation of glycerol and FAs **(3)**. Acute and chronic pharmacological AMPK activation powerfully suppresses FA uptake **(4)**, conferring an anti-lipogenic role for AMPK in WAT. Furthermore, chronic AMPK activation up-regulates the expression of genes (PGC-1α, PPARα, PPARδ, CPT-1b) **(5)** that increase the ability of the cell to dispose of FAs intracellularly through β-oxidation **(6)**. ATGL content is also increased with AMPK activation **(7)** and catalyzes the hydrolysis of one FA from TAG. ⊕ and → denote stimulation; ⊣ denotes inhibition. LKB1, AMPK kinase.

CHAPTER 5:

Dysregulation of lipolysis and lipid metabolism in visceral and subcutaneous adipocytes by high-fat diet: The role of ATGL, HSL, and AMPK

Mandeep P. Gaidhu[1], Nicole M. Anthony[1], Prital Patel[1], Thomas J. Hawke[1,2], Rolando B. Ceddia[1]

[1] *Muscle Health Research Centre, York University, Toronto, Canada*

[2] *Pathology and Molecular Medicine, McMaster University, Hamilton, Canada*

Contribution of authors:

MPG organized and conducted all experiments, and wrote the manuscript. NMA and PP assisted with time-sensitive experiments and preparation. TJH provided animals and assisted with editing the manuscript. RBC designed and assisted with experiments and edited the manuscript.

Keywords: High-fat diet, adipose tissue, metabolism, adipose triglyceride lipase, hormone sensitive lipase, AMP-kinase

A version of this manuscript has been published in the *American Journal of Physiology – Cell Physiology* (Appendix C, Copyright Permission)

(Gaidhu MP, Anthony NM, Patel P, Hawke TJ, Ceddia RB. Dysregulation of lipolysis and lipid metabolism in visceral and subcutaneous adipocytes by high-fat diet: role of ATGL, HSL, and AMPK. *Am J Physiol Cell Physiol.* **298**: C961-71, 2010).

ABSTRACT

This study investigated the molecular mechanisms by which high-fat diet (HFD) dysregulates lipolysis and lipid metabolism in mouse epididymal (visceral, VC) and inguinal (subcutaneous, SC) adipocytes. Eight-weeks of HFD feeding increased adipose triglyceride lipase (ATGL) content and comparative gene identification-58 (CGI-58) expression, whereas hormone-sensitive lipase (HSL) phosphorylation and perilipin content were severely reduced. Adipocytes from HFD mice elicited increased basal but blunted epinephrine-stimulated lipolysis, and increased diacylglycerol content in both fat depots. Consistent with impaired adrenergic receptor signaling, HFD also increased adipose-specific phospholipase A_2 expression in both fat depots. However, inhibition of E-prostanoid 3 receptor increased basal lipolysis in control adipocytes, but failed to acutely alter the effects of HFD on lipolysis in both fat depots. In HFD visceral adipocytes, activation of adenylyl cyclases by forskolin increased HSL phosphorylation and surpassed the lipolytic response of control cells. However, in HFD subcutaneous adipocytes, forskolin induced lipolysis without detectable HSL phosphorylation, suggesting activation of an alternative lipase in response to HFD-induced suppression of HSL in VC and SC adipocytes. HFD also powerfully inhibited basal, epinephrine-, and forskolin-induced AMP-kinase (AMPK) activation as well peroxisome proliferator-activated receptor gamma co-activator-1α expression, citrate synthase activity, and palmitate oxidation in both fat depots. In summary, novel evidence is provided that defective adrenergic receptor signaling combined with up-regulation of ATGL and suppression of HSL and AMPK signaling mediate HFD-induced alterations in lipolysis

and lipid utilization in VC and SC adipocytes, which may play an important role in defective lipid mobilization and metabolism seen in diet-induced obesity.

INTRODUCTION

White adipose tissue (WAT) plays an important role in regulating whole-body energy homeostasis. One of its major roles is to release fatty acids (FAs) under conditions of negative energy balance or prolonged exercise to provide energy for peripheral tissues. The molecular machinery involved in triacylglycerol (TAG) breakdown and FA release works in an orderly and regulated fashion, conferring to WAT the capacity to respond to various feeding conditions and to the energy demands of the body. Importantly, conditions that lead to overeating and obesity disrupt normal regulation of WAT lipolysis. In fact, basal lipolysis has repeatedly been reported as elevated, while catecholamine-induced lipolysis is suppressed in obese humans and rodents (142). The classical mechanism to explain this condition is centered on the fact that the largely expanded WAT of obese subjects becomes resistant to insulin, impairing the major lipogenic and anti-lipolytic effects of this hormone (127,162,295). Obesity develops under conditions of chronic energy surplus, indicating that visceral (VC) and subcutaneous (SC) adipocytes must be able to deal with large amounts of lipids being delivered to the WAT. In this scenario, the ability of adipocytes to handle excess lipids via alterations in FA metabolism may play an important role in the adaptive responses of the WAT to obesity. Importantly, obesity is invariably accompanied by increased circulating levels of non-esterified fatty acids (NEFAs) (12,162,295,296), indicating that

the regulation of energy storage and mobilization of FAs from VC and SC adipocytes is defective. Although literature exists describing the differences between VC and SC fat depots with regards to eliciting distinct lipolytic rates (154,157,297), the cellular and molecular mechanisms responsible for these depot-specific characteristics still remain to be elucidated. This is particularly important since it is the excessive accumulation of VC adipose tissue (visceral obesity) that has been strongly correlated with the development of insulin resistance and type 2 diabetes (150,295). In this scenario, unraveling the molecular mechanisms involved in dysregulation of lipolysis and lipid metabolism in VC and SC WAT in obesity may be of great therapeutic relevance.

Lipolysis in the WAT of humans and rodents is regulated in a step-wise fashion by adipose triglyceride lipase (ATGL), hormone sensitive lipase (HSL), and monoacylglycerol lipase (MAGL) (295,298,299). The current model is that ATGL initiates lipolysis by cleaving the first FA from TAG and then HSL and MAGL act on diacyglycerol (DAG) and monoacylglycerol, respectively, releasing two additional FAs and one glycerol molecule (299). Therefore, the orchestrated activation of ATGL, HSL, and MAGL seems to be required for complete lipolysis to occur in adipocytes. Binding of agonists to the β-adrenergic receptors, coupled to adenylate cyclase via the stimulatory G protein, leads to an increase in cAMP and activation of protein kinase A (PKA) (31,295). In rat HSL, PKA phosphorylates serine residues 563, 659, and 660 (295,300,301), leading to translocation of HSL to the lipid droplet and to great enhancement of lipolysis. Phosphorylation of perilipin A, a protein associated with the lipid droplet, by PKA has also been demonstrated to be necessary for activation of HSL and for catecholamine-

induced lipolysis to occur. Conversely, the cellular energy sensor AMP-activated protein kinase (AMPK) has been demonstrated to phosphorylate serine 565 of HSL, which prevents PKA-mediated phosphorylation of this enzyme and impairs catecholamine-stimulated lipolysis (302). In this context, AMPK has been proposed to lower the release of FAs into the circulation, which could help preventing lipotoxicity in peripheral tissues as well as reduce the costly process of re-esterifying FAs in the WAT (179,183,303). ATGL activity is also stimulated by catecholamines, but the molecular mechanism(s) underlying this effect is unknown. Although ATGL can be phosphorylated on serine residues 404 and 428 by a yet unidentified kinase, this does not seem to affect the activity of this lipase. There is compelling evidence that the protein comparative gene identification-58 (CGI-58) drastically enhances ATGL-mediated TAG hydrolysis without affecting HSL activity (304). Under basal conditions, CGI-58 is also localized to the lipid droplet in association with perilipin A (288,304,305). Upon hormonal stimulation, PKA phosphorylates perilipin A at serine residues 492 and 517, resulting in CGI-58 dissociation (37). Once dissociated, CGI-58 interacts with ATGL and potently activates this TAG lipase (288,304,305). In fact, addition of CGI-58 to ATGL containing extracts enhances TAG hydrolase activity by ~20-fold (304). The current literature suggests that in lean rodents ATGL and HSL are the major lipases for TAG and DAG, respectively, and account for ~95% of lipase activity in murine WAT (288). Therefore, these molecular steps that regulate lipolysis can be potentially affected by obesity and also be distinctly regulated in VC versus SC WAT. However, very little is known about how diet-induced obesity affects HSL and ATGL content/activity as well as basal and

catecholamine-induced lipolysis in VC and SC WAT. Furthermore, although AMPK has been implicated in playing a role in regulating HSL and ATGL activity (179,183,303), its action on these major lipases has not been addressed in WAT under diet-induced obesity. Therefore, the present study was designed to address the effects of HFD-induced obesity on lipid metabolism within the adipocyte, specifically the roles of AMPK, HSL and ATGL in subcutaneous and visceral fat depots. Evidence is provided that dysregulation of lipolysis and lipid metabolism in VC and SC adipocytes of high-fat diet mice is mediated by defective adrenergic receptor signaling combined with up-regulation of ATGL and suppression of HSL and AMPK signaling. These findings give new insight into the importance of depot-specific regulation of lipolysis and also address the molecular mechanisms underlying dysfunctional adaptations that occur within the adipocyte with respect to lipid metabolism under conditions of diet-induced obesity and insulin resistance.

MATERIALS AND METHODS

Reagents - Epinephrine, FA-free bovine serum albumin (BSA), free glycerol determination kit, glucose oxidase kit, palmitic acid, and phenylethylamine were obtained from Sigma. [1-^{14}C]palmitic acid was from GE Healthcare Radiochemicals (Quebec City, Quebec, Canada). [γ-^{32}P]ATP and [9,10-^{3}H]triolein was from American Radiolabeled Chemicals (St. Louis, MO). RNeasy Lipid Extraction Kit was from Qiagen. Superscript II and Taq polymerase was from Bio-Rad Canada. DNase kit was from Ambion. Standard and high fat chow was obtained from LabDiets Inc. (Richmond, IN). All antibodies were

from Cell Signaling Technology Inc. (Beverly, MA) unless otherwise noted. Specific antibodies against phospho-ACC was from Upstate (Charlottesville, VA). Perilipin was from American Research Products (Belmont, MA). All other chemicals were of the highest grade available.

Animals and isolation of primary adipocytes – Eight-week old C57BL/6J male mice were maintained on a 12/12-h light/dark cycle at 22°C and fed *ad libitum* a standard laboratory chow for a 1 week acclimation period. Subsequently, the animals were randomly assigned to two groups: control and high-fat diet (HFD). Control animals received a standard chow diet containing 25% of kcal from fat (TestDiet; LabDiet Inc. Cat #5015), while the HFD group was fed a diet containing 60% of kcal from fat (TestDiet; LabDiet Inc. Cat #58Y1) for 8 weeks. A standard chow diet was used for the purpose of comparing the effects of a HFD to those mice fed a diet that supports normal growth and development. The inguinal and epididymal fat pads were used as representative of subcutaneous (SC) and visceral (VC) WAT, respectively. After the 8-week study period, SC and VC fat pads were carefully removed and used for adipocyte isolation as previously described (Chapter 4, page 74) with minor modifications (191). Briefly, VC and SC fat pads from control and HFD animals were extracted, weighed, then finely and carefully minced using microscissors. The minced tissue was transferred to plastic vials containing Krebs Ringer Buffer (KRB) supplemented with 30mM HEPES and collagenase (0.5mg/mL). After digestion and filtration, cells were re-suspended in KRBH-3.5% BSA, and allowed to equilibrate for 30min prior to use in experiments. The

procedures described herein have been adopted in order to prevent adipocyte lysis and to obtain fat cells that are viable and responsive to stimulation. This is confirmed by ~30- to 40-fold increases in control cells exposed to epinephrine. In order to distribute equal number of adipocytes in all treatment conditions, cell diameters and numbers were measured by the method of DiGirolamo and Fine (14).

Plasma measurements – Glucose and NEFA levels were measured as describe previously (Chapter 4, page 81). Plasma insulin was measured using an ELISA kit from Millipore.

Determination of lipolysis, and palmitate oxidation, uptake, and incorporation into triacylglycerols - Lipolysis was determined after adipocytes (1 x 10^5 cells) had been incubated with constant agitation (80 orbital strokes/min) for 75min in the absence or presence of epinephrine (100nM) or forskolin (10μM) (179) by measuring glycerol release (Chapter 4, page 78). For experiments using the EP3 receptor antagonist L826266, cells were pre-incubated with 10μM of the inhibitor for 2h prior to stimulation with epinephrine. Palmitate uptake, oxidation, and incorporation into TAGs was determined using standard protocols established in the laboratory (Chapter 4, pages 77-78).

Citrate synthase activity – Citrate synthase activity was assayed with adaptations to the method as described in Chapter 4, page 78.

Quantitative PCR (q-PCR) analysis – Real time PCR reactions were carried out according to the procedure noted in Chapter 4, page 80. Primers sequences are shown in

Table 5-3.

Western blot analysis – For whole-tissue samples, fat depots were extracted and immediately snap frozen in liquid nitrogen. Tissue (~100mg) was subsequently processed for western blot analyses (Chapter 4, page 80). For isolated adipocytes, cells were stimulated with forskolin (10μM) or epinephrine (100nM) for 30min prior to lysis with buffer as described above. To ensure sufficient solubilization of lipid droplet-associated proteins under basal and stimulated conditions, we validated our protein extraction protocol using an alternative buffer (1% SDS, 1mM EDTA, 1mM benzamidine, 20mM NaF, and protease and phosphatase inhibitors) for adipocyte protein extraction and achieved similar results under adrenergic stimulation. All primary antibodies were used in a dilution of 1:1000 with the exception of phospho-AMPK (1:500) and perilipin (1:2000).

Diacylglycerol (DAG) content and TAG Lipase activity - DAG levels were quantified by a modified enzymatic method (detailed in Chapter 4, page 79). TAG lipase activity was measured as established by Fredrikson *et al* and previously performed in our laboratory (Chapter 4, page 81).

Statistical analysis – Data are expressed as mean ± SEM. Statistical significance was set to $P<0.05$, and was calculated by using either t-test or analysis of variance (ANOVA) with Tukey-Kramer post-hoc comparisons. The statistical analyses performed for each data set is noted in the figure legends.

RESULTS

Body mass, fat mass, adipocyte diameter, and plasma measurements – Mice in the HFD group had an average of 36% greater body mass than control animals, which was accompanied by an increase of 3.0- and 2.8-fold in epididymal and inguinal fat pad mass, respectively (Table 5-1). This was compatible with a 1.67- and 1.59-fold increase in adipocyte diameters from the epididymal and inguinal fat pads from the HFD group, respectively (Table 5-1). Compared to control mice, the HFD group had significantly higher plasma levels of NEFAs, glucose and insulin (1.36-, 1.13-, and 2.26-fold, respectively), indicating that these animals were an appropriate model for diet-induced obesity and insulin resistance (Table 5-2).

Effects of HFD on HSL, AMPK and ACC phosphorylation and protein content of AMPK, ACC, HSL, ATGL, and perilipin in WAT – In order to assess the effects of HFD on major molecular mechanisms that regulate lipolysis in WAT, we examined phosphorylation of HSL on key serine residues as well as the protein content of ATGL and perilipin. Since AMPK has also been implicated in the regulation of HSL activity, the phosphorylation and content of this kinase and of its direct substrate, ACC, were determined. Phosphorylation of HSL at serine 563, 565, and 660 revealed that these variables were potently suppressed in the VC and SC adipose tissue of HFD mice, despite no change in total HSL protein content (Figure 5-1). Perilipin was decreased in both fat depots of HFD mice, although this effect was more pronounced in VC compared to SC adipose tissue. Conversely, the content of ATGL was markedly increased in both fat depots (Figure 5-1).

	Body weight (g)		Fat pad mass (g)		Adipocyte diameter (μm)	
Diet	**Baseline**	**8 weeks**	**Epididymal**	**Inguinal**	**Epididymal**	**Inguinal**
Con	22.7 ± 0.7	26.1 ± 0.7	0.84 ± 0.10	0.25 ± 0.03	79.4 ± 2.8	75.5 ± 4.4
HF	23.1 ± 0.6	35.4 ± 1.2*	2.55 ± 0.10*	0.70 ± 0.08*	133.0 ± 6.3*	119.9 ± 8.3*

Table 5-1: Body weight, fat mass, and adipocyte diameter. Epididymal and inguinal fat pads were extracted and used as representative tissues for visceral and subcutaneous fat depots. Body weight and fat pad mass was calculated from n=40-45 mice per group. Adipocyte diameter was calculated from n=10-14. Unpaired t-tests were used for statistical analyses. *P<0.05 indicates significance between Control vs. HF for that variable.

	Control	HF
NEFAs (mM)	0.39 ± 0.02	0.53 ± 0.04*
Glucose (mM)	14.35 ± 0.25	16.23 ± 0.73*
Insulin (ng/mL)	2.55 ± 0.18	5.76 ± 0.97*

Table 5-2: Plasma levels of NEFAs, glucose, and insulin from mice in a fed state. Data for NEFAs, glucose, and insulin were compiled from 36-40 mice per condition. Unpaired t-tests were used for statistical analyses. *P<0.05 indicates significance between Control vs. High Fat (HF) for that variable.

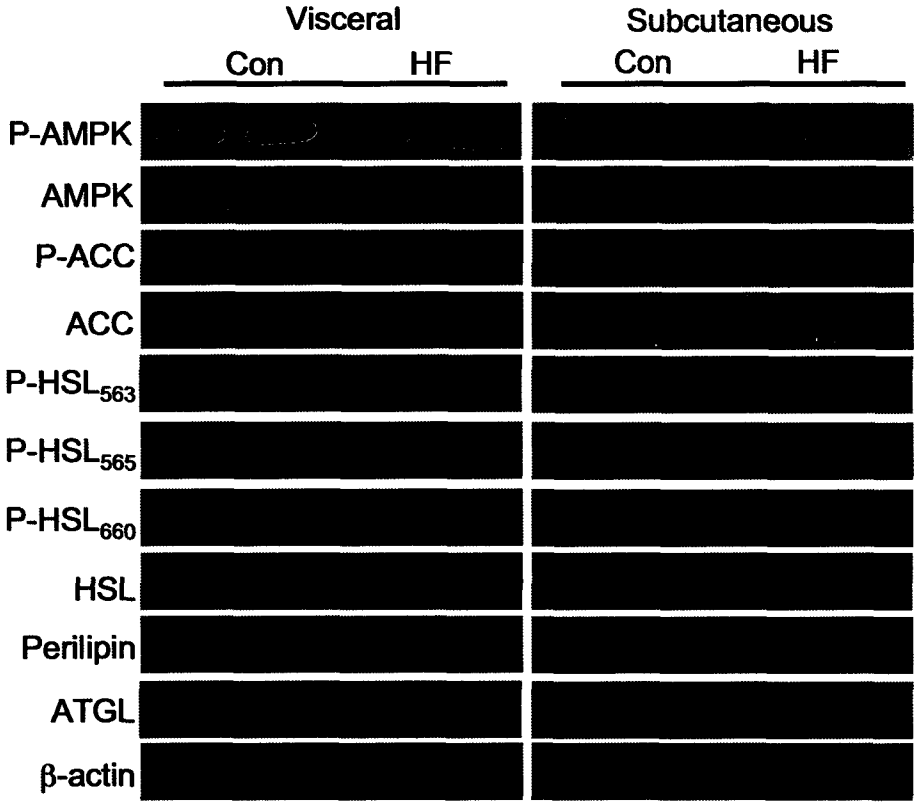

Figure 5-1. Phosphorylation of AMPK, ACC, and HSL, and protein content of AMPK, ACC, HSL, perilipin, and ATGL in white adipose tissue. After 8 weeks on either control (Con) or high-fat (HF) diet, VC and SC fat depots were extracted and processed for western blotting. β-actin was used as a loading control. Blots are representative of n = 4-6 for each condition.

Phosphorylation and content of AMPK and ACC was reduced in the VC and SC adipose tissue of HFD mice relative to control animals (Figure 5-1).

DAG content and TAG lipase activity in VC and SC fat depots – Since HSL phosphorylation was suppressed in VC and SC adipose tissue, we looked at DAG content and TAG lipase activity in these fat depots from control and HFD mice. DAG content increased by 2.5-fold in VC (Figure 5-2A) and by 2.9-fold in SC (Figure 5-2B) fat pads from HFD mice. TAG lipase activity increased by 1.4- and 2-fold in visceral and subcutaneous WAT from HF-diet mice, respectively (Figure 5-2C).

Lipolysis and phosphorylation of AMPK, ACC and HSL in VC and SC adipocytes exposed to forskolin and epinephrine – As expected, adipocytes from control mice exposed to epinephrine increased glycerol release from 0.52 ± 0.04 to 14.16 ± 0.44 nmols/75min/10^5 cells, and from 0.26 ± 0.03 to 10.49 ± 1.12 nmols/75min/10^5 cells in VC and SC adipocytes, respectively (Figure 5-3C-D). When treated with forskolin, glycerol release from VC and SC adipocytes of control mice reached 12.82 ± 0.48 and 15.61 ± 1.02 nmols/75min/10^5 cells, respectively (Figure 5-3C-D). HFD mice had increased basal lipolysis in VC and SC adipocytes by 2.3- and 2.9-fold, respectively, while epinephrine-stimulated lipolysis was blunted in both fat depots of HFD animals (Figure 5-3C-D). Treatment of HFD visceral adipocytes with forskolin increased lipolysis to levels above those of control visceral adipocytes (Figure 5-3C); however, only 83% of the lipolytic response was recovered in HFD subcutaneous cells by this agent (Figure 5-3D). In order to assess the potential mechanisms by which HFD induced these alterations

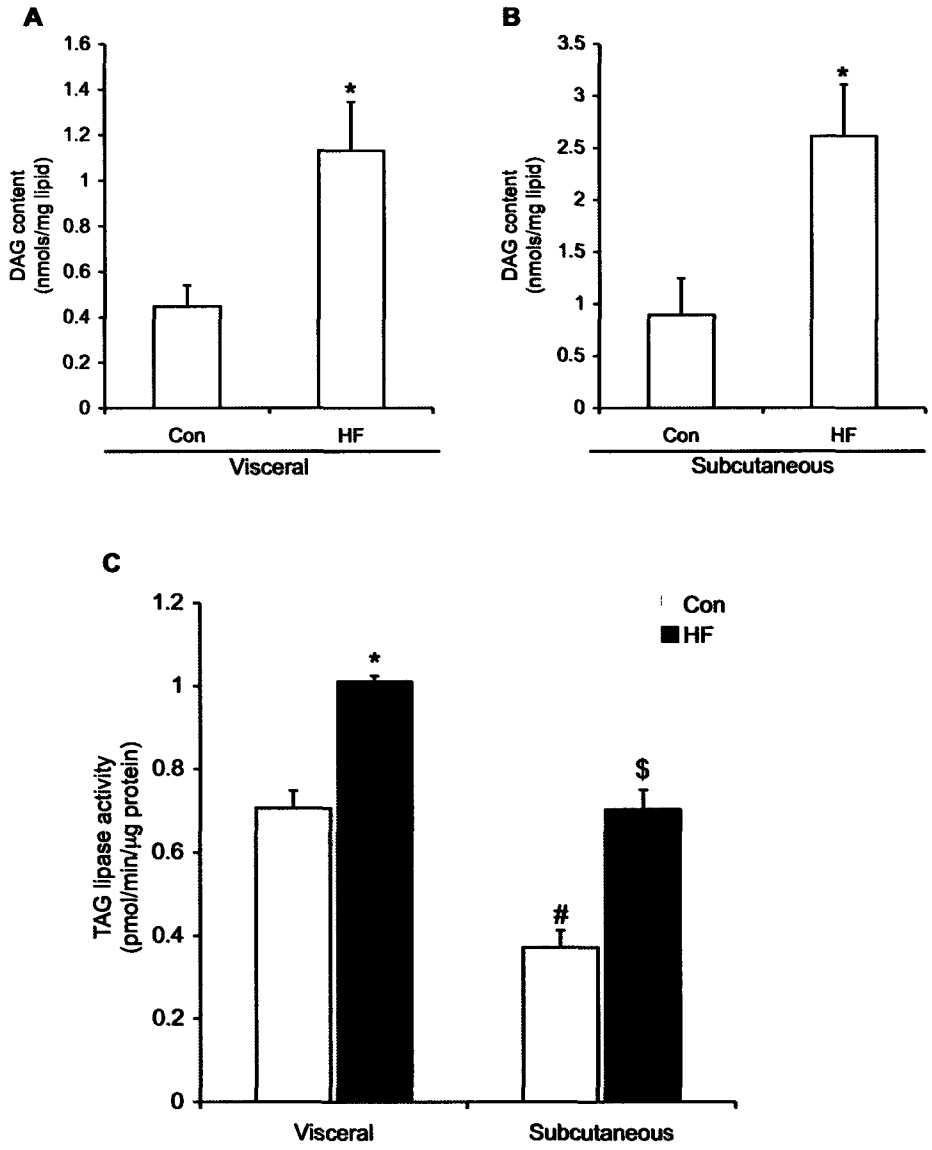

Figure 5-2. Diacylglycerol (DAG) content in VC (**A**) and SC (**B**) adipose tissues from control (Con) and high-fat (HF) diet mice for 8 weeks. TAG lipase activity in adipose tissue from Con and HF diet mice **(C)**. Data compiled from 4-6 mice from each condition. Unpaired t-test or two-way ANOVA with Tukey-Kramer post-hoc test was used for statistical analyses. Different symbols denote statistical differences between all other conditions, where $P<0.05$.

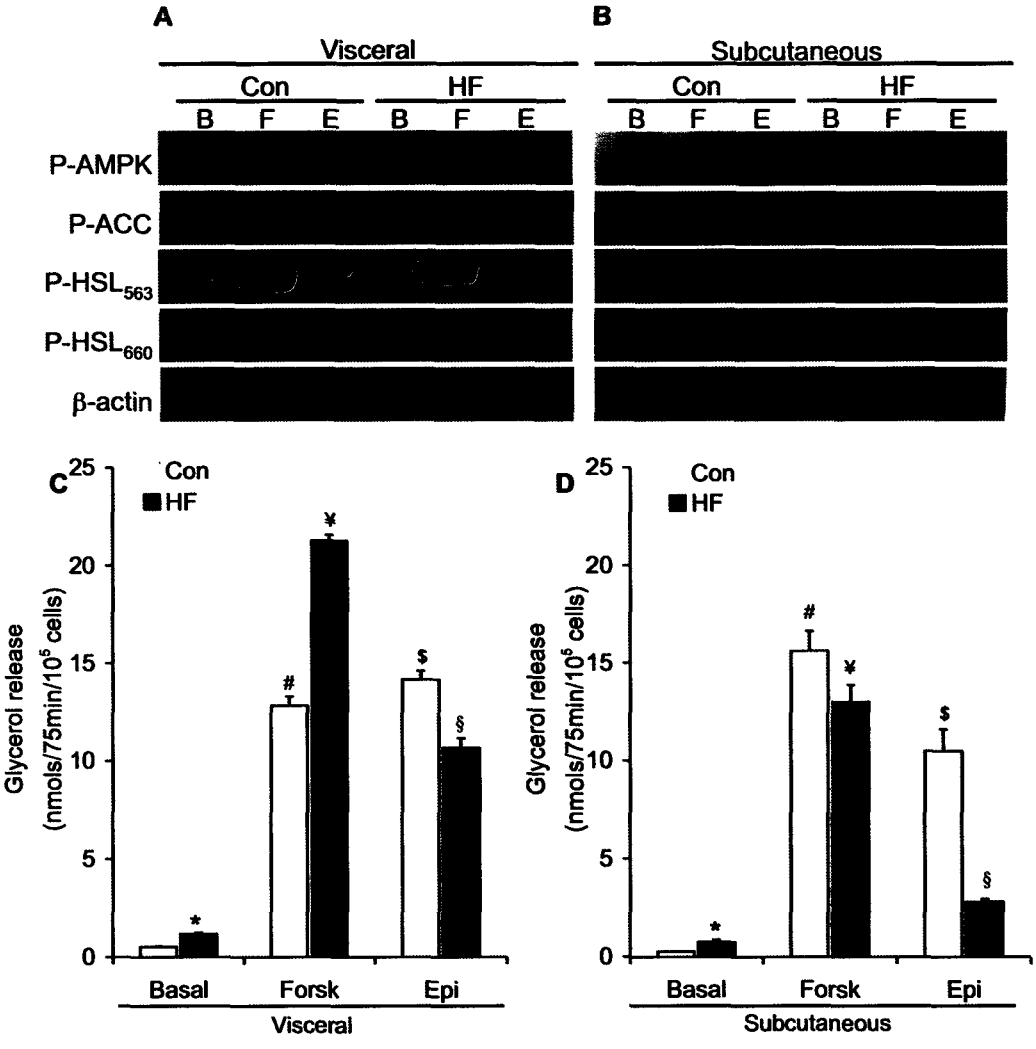

Figure 5-3. Determination of AMPK, ACC, and $HSL_{Ser563/660}$ phosphorylation under basal (B; vehicle), forskolin (F; 10μM), and epinephrine (E; 100nM) conditions in VC **(A)** and SC **(B)** adipocytes from control (Con) and high-fat (HF) diet mice. Blots are representative of 3 independent experiments. Glycerol release was measured under basal, forskolin (Forsk), and epinephrine (Epi)-stimulated conditions in VC **(C)** and SC **(D)** adipocytes from Con and HF mice. Data compiled from 3 independent experiments with quadruplicates for each condition. Two-way ANOVAs were used for statistical analyses. Different symbols denote statistical differences between all other conditions, where $P<0.05$.

in lipolysis, we looked at key proteins involved in the regulation of this pathway. As expected, phosphorylation of AMPK, ACC, and HSL serine 563 and 660 in VC and SC adipocytes from control mice was increased in response to forskolin and epinephrine (Figure 5-3A). In HFD VC adipocytes, forskolin- and epinephrine-induced phosphorylation of AMPK and ACC was blunted. Although forskolin was able to increase $HSL_{Ser563/660}$ phosphorylation back to control levels, the epinephrine effect on this variable remained suppressed in HFD VC adipocytes (Figure 5-3A). In HFD SC fat cells, phosphorylation of AMPK and ACC in response to forskolin and epinephrine was also impaired. Furthermore, contrary to observations in visceral adipocytes, phosphorylation of HSL in subcutaneous fat cells of the HFD mice was so low that it could not be detected by western blot under basal, forskolin-, or epinephrine-stimulated conditions (Figure 5-3B), despite the fact that total HSL content was unaltered (Figure 5-1) and these cells elicited a significant lipolytic response when exposed to these agents (Figure 5-3D).

The effects of the specific EP3 receptor inhibitor, L826266, on VC and SC adipocyte lipolysis – In an attempt to unravel the mechanisms by which HSL was inhibited under basal and epinephrine-stimulated conditions, we blocked the E-prostanoid 3 (EP3) receptor with the drug L826266 in both VC and SC adipocytes from control and HFD mice. The EP3 receptor inhibitor increased basal lipolysis from 0.52 ± 0.04 to 0.97 ± 0.10 nmols/75min/10^5 cells and from 0.26 ± 0.03 to 1.60 ± 0.27 nmols/75min/10^5 cells in VC and SC adipocytes from control animals, respectively. However, it did not affect basal

lipolysis in VC (1.18 ± 0.07 to 1.48 ± 0.14 nmols/75min/10^5 cells) and SC (0.76 ± 0.11 to 0.72 ± 0.09 nmols/75min/10^5 cells) adipocytes from HFD animals. Similarly, L826266 did not have any effect on the epinephrine response from VC and SC adipocytes from either control or HFD mice.

Effect of HFD on palmitate uptake, incorporation into triacylglycerols, oxidation, and citrate synthase activity – Since TAG breakdown was defective with HFD and was differentially regulated in VC versus SC adipocytes, we also assessed whether parameters involved in lipid metabolism were altered in both fat depots. As expected, insulin elicited a 1.2-fold increase in palmitate uptake by VC adipocytes from control mice (Figure 5-4A). However, palmitate uptake by VC adipocytes from HFD mice decreased by 26% and 37% under basal and insulin-stimulated conditions relative to control VC adipocytes, respectively (Figure 5-4A). In SC adipocytes from HFD mice, suppression in both basal and insulin-stimulated palmitate uptake (17% and 28%, respectively) was also observed when compared to control SC fat cells (Figure 5-4B). Despite a reduction in palmitate uptake, palmitate incorporation into triacylglycerols increased above controls by 1.7-fold in VC (Figure 5-4C) and by 1.5-fold in SC (Figure 5-4D) adipocytes from HFD mice. Palmitate oxidation was decreased in both VC and SC adipocytes from HFD mice by ~64% and 75%, respectively (Figure 5-5A-B). In line with these changes, citrate synthase activity was also reduced by 46% in VC and by 63% in SC adipocytes from HFD mice (Figure 5-5C).

Analysis of gene expression in VC and SC fat depots by Quantitative PCR – We utilized

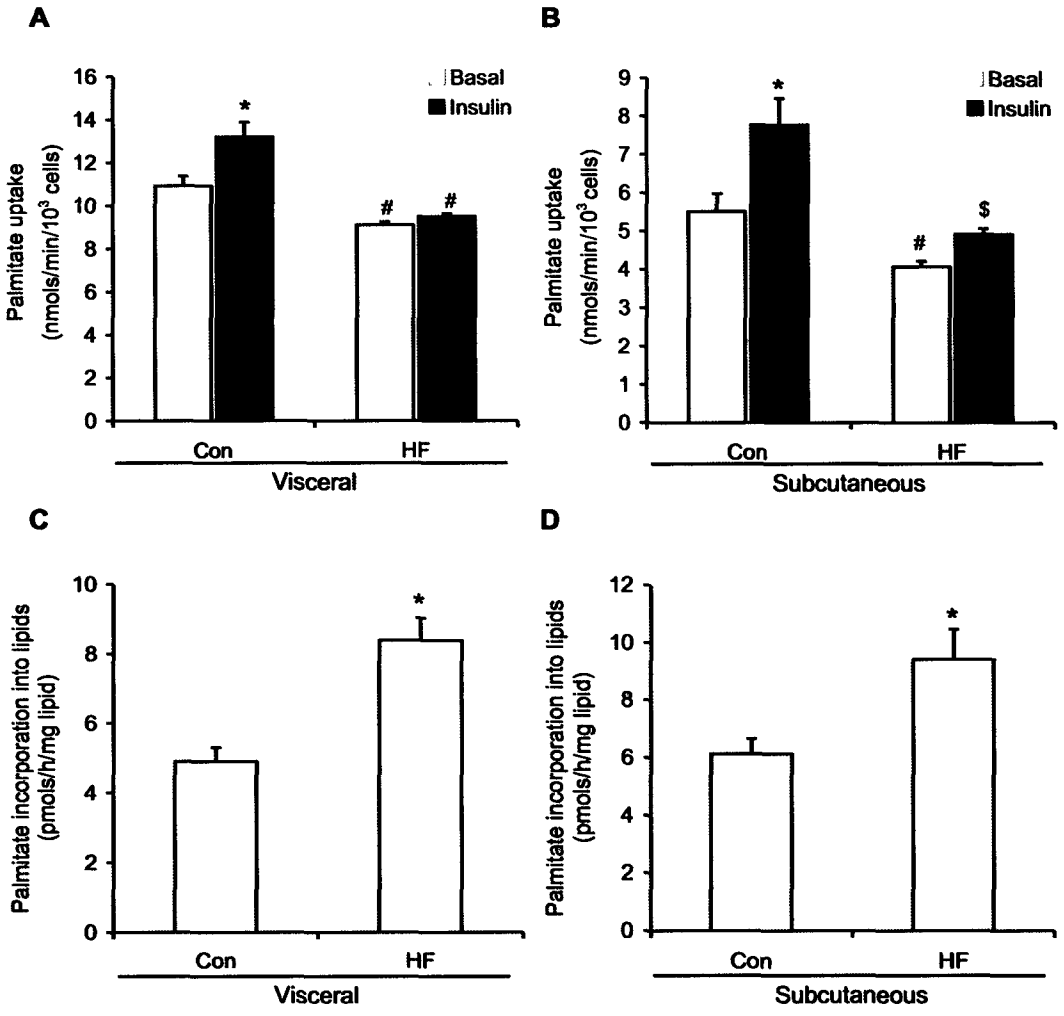

Figure 5-4. Palmitate uptake in VC **(A)** and SC **(B)** adipocytes isolated from control (Con) and mice on a high-fat (HF) diet for 8 weeks under basal and insulin-stimulated conditions and palmitate incorporation into lipids in VC **(C)** and SC **(D)** fat cells. Data were compiled from 2-3 independent experiments, with triplicates for each condition. Two way ANOVAs or unpaired t-tests were used for statistical analyses. Different symbols denote statistical differences between all other conditions, where $P<0.05$.

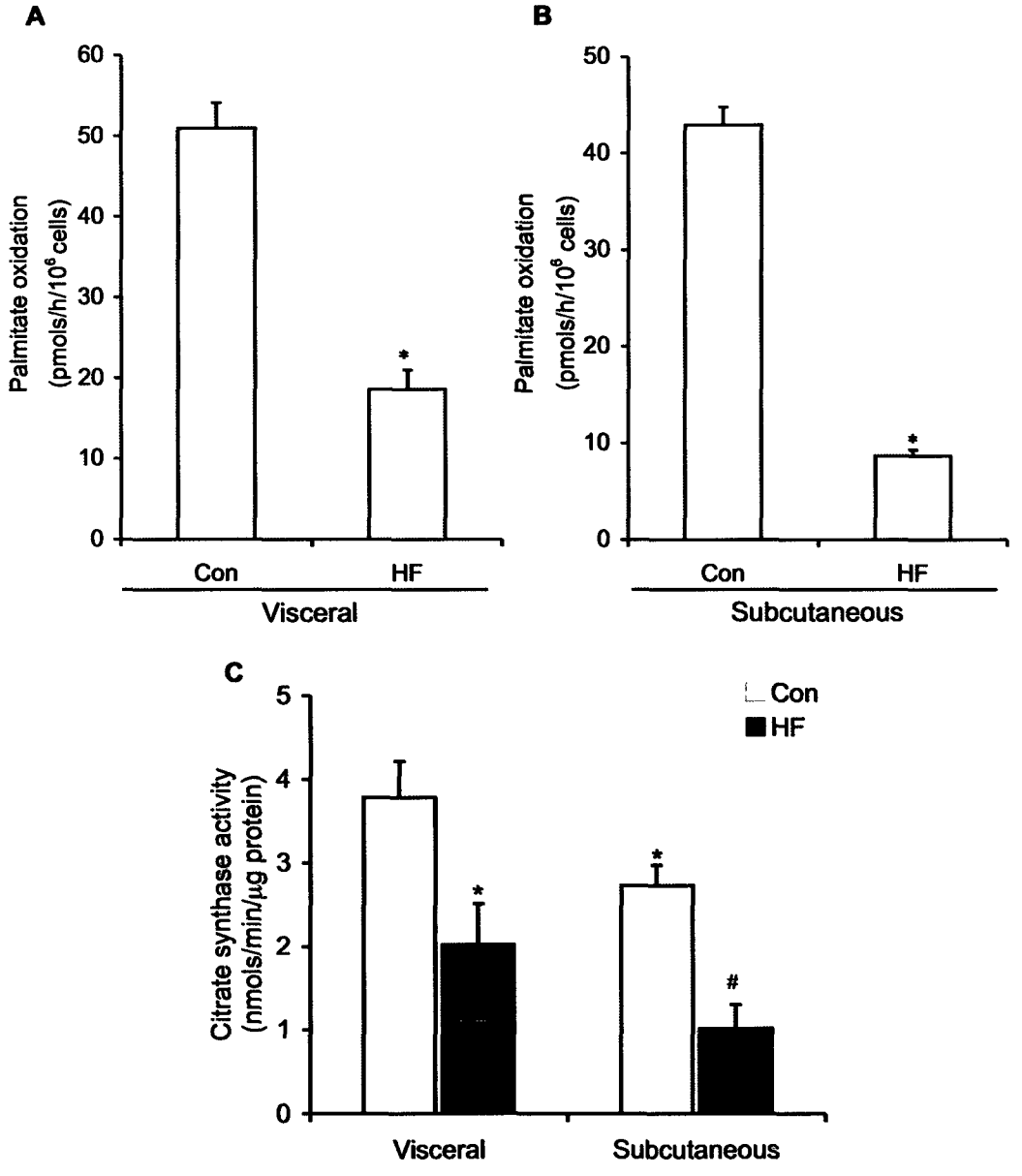

Figure 5-5. Palmitate oxidation in VC **(A)** and SC **(B)** adipocytes isolated from Con and HFD mice and citrate synthase activity **(C)**. Data are representative of 3 independent experiments, with a minimum of triplicates for each condition. Two-way ANOVA or unpaired t-tests were used for statistical analyses. *P<0.05 versus Con; #P<0.05 versus all other conditions.

quantitative PCR to determine whether the expression of genes involved in the regulation of lipolysis and lipid metabolism were altered in VC and SC adipose tissue from HFD mice. The mRNA levels of the α1 isoform of AMPK were decreased in VC and SC adipose tissue from HFD compared to control animals, whereas the expression of the α2 isoform remained unchanged (Table 5-3). Additionally, mRNA levels of other proteins involved in oxidative metabolism such as ACCα, cytochrome C oxidase subunit VIII (Cox8), PPARα, and PGC-1α were decreased in both VC (~57, 67, 72, and 57%, respectively) and SC (~43,73, 52, and 54%, respectively) adipose tissues from HFD mice (Table 5-3). Expression of CGI-58 was significantly up-regulated in both fat depots reaching 1.7-fold in VC and 1.8-fold in SC adipose tissues of HFD mice. The expression of adipose phospholipase A_2 ($AdPLA_2$) in VC and SC adipose tissues was significantly increased with HFD by 1.9- and 2.3-fold compared to control mice, respectively.

DISCUSSION

Here, we provide novel evidence that the increased basal but blunted epinephrine-stimulated lipolysis with HFD-induced obesity is mediated by impaired adrenergic receptor signaling, suppression of HSL phosphorylation, and up-regulation of ATGL content and CGI-58 expression. Phosphorylation of HSL at serine residues 563 and 660, which is required for PKA-mediated lipolysis (300), was potently suppressed by HFD in both visceral and subcutaneous fat tissues. Since ATGL functions essentially as a TAG lipase (42,288), up-regulation of ATGL content in combination with increased expression of its co-activator CGI-58 must have promoted TAG breakdown and formation of DAG.

Gene	Primer sequences (5' → 3')	Fold change relative to control diet	
		VC	SC
AMPKα1	F-TGACCGGACATAAAGTGGCTGTGA R-TGATGATGTGAGGGTGCCTGAACA	0.45 ± 0.01*	0.87 ± 0.03*
AMPKα2	F-TGGATCGCCAAATTATGCAGCACC R-AAGGGCATACAGGATGACACCACA	0.70 ± 0.25	1.01 ± 0.23
ACC-α	F-ACCTTACTGCCATCCCATGTGCTA R-GTGCCTGATGATCGCACGAACAAA	0.43 ± 0.07*	0.57 ± 0.05*
Cox 8	F-TCTCAGCCATAGTCGTTGGCTTCA R-CAACTTCATGCTGCGGAGCTCTTT	0.33 ± 0.01*	0.27 ± 0.01*
PGC-1α	F-ACCGTAAATCTGCGGGATGATGGA R-AGTCAGTTTCGTTCGACCTGCGTA	0.43 ± 0.07*	0.46 ± 0.09*
PPARα	F-ATGAAGAGGGCTGAGCGTAGGTAA R-TGCCGTTGTCTGTCACTGTCTGAA	0.28 ± 0.06*	0.48 ± 0.02*
CGI-58	F-TGTGCAGGACTCTTACTTGGCAGT R-GTTTCTTTGGGCAGACCGGTTTCT	1.70 ± 0.15*	1.98 ± 0.30*
AdPLA$_2$	F-ATAACAGTCTTTCCTGGCTGGCCT R-TCCATTTCTGTGTACCCAGGCTGT	1.94 ± 0.24*	2.28 ± 0.15*

Table 5-3: Quantitative PCR analysis of mRNA expression. F, forward; R, reverse. Fold changes in visceral (VC) and subcutaneous (SC) adipose tissues from high fat diet mice relative to control diet. Samples were run in duplicate on the plate, and data were compiled from 3-4 separate plates, with n=6-8 for each condition. GAPDH and β-actin were used as control genes. Unpaired t-tests were used for statistical analyses. *$P<0.05$ versus control diet.

This is supported by our data indicating that TAG lipase activity is increased in WAT from HFD mice. Conversely, HFD-induced suppression of HSL phosphorylation/activity impaired breakdown of DAG, thereby facilitating its accumulation in the WAT. This is evidenced by our findings that DAG content was significantly increased by 2.5- and 2.9-fold in visceral and subcutaneous WAT, respectively. This is also in line with previous studies in HSL knockout mice showing that in the absence of this lipase accumulation of DAG in WAT occurs (44).

Bypassing the adrenergic-receptor-mediated activation of adenylyl cyclases with forskolin fully rescued HFD-induced suppression of HSL phosphorylation at Ser 563 and 660 residues in visceral adipocytes. Interestingly, in HFD subcutaneous adipocytes, lipolysis was partially rescued by forskolin and this occurred in the absence of any detectable induction of HSL phosphorylation. Studies in HSL-null mice show residual lipolysis, indicating that this process is impaired by the lack HSL activity, although not entirely dependent on this lipase. Studies from other labs support these findings, where silencing HSL using siRNA diminished forskolin-stimulated lipolysis by 53%, while knocking down of ATGL resulted in ~90% reduction in glycerol release in differentiated human adipocytes (306). In line with these observations, we found that the ATGL content and the expression of its co-activator CGI-58 were both increased by HFD, which is compatible with increased lipolysis in HFD visceral and subcutaneous adipocytes exposed to forskolin. It is important to note that even though forskolin substantially increased lipolysis in HFD subcutaneous adipocytes, it was still limited to ~83% of the values obtained with control cells exposed to this agent. This indicates that although a

potent forskolin-induced lipolytic response could be obtained through up-regulation of ATGL and CGI-58, the lack of HSL phosphorylation/activation limited the ability of HFD subcutaneous adipocytes to fully respond to this agent. This is further supported by our findings that $HSL_{Ser563/660}$ was equally phosphorylated in HFD and control visceral adipocytes exposed to forskolin. Noteworthy, the lipolytic response of HFD adipocytes surpassed (1.67-fold) that of control VC cells treated with forskolin, even though no additional phosphorylation of HSL was observed.

The exposure of visceral and subcutaneous adipocytes from control and HFD mice to forskolin also demonstrated that signaling steps mediated by adrenergic receptors play an important role in determining the well-characterized differences in lipolytic rates between visceral and subcutaneous fat depots (295). This is evidenced by the fact that absolute values for lipolysis under basal and epinephrine-stimulation in control and HFD visceral fat cells were consistently higher than the values obtained with subcutaneous adipocytes. However, upon stimulation with forskolin, control subcutaneous lipolysis was 1.22-fold higher than in visceral control adipocytes. These findings demonstrate that subcutaneous adipocytes have the potential to elicit lipolytic responses that are similar or even higher than those of visceral adipocytes, but early signaling steps mediated by activation of adrenergic receptors appear to maintain a lower lipolytic rate in subcutaneous adipocytes from lean mice.

Besides HSL phosphorylation, the content of perilipin was also reduced in both fat depots with HFD. In HFD visceral WAT perilipin levels were hardly detectable, while in subcutaneous WAT the content of this protein was less than control, although still

abundantly present. Reduced perilipin content has been demonstrated to alter the normal break down of neutral lipids in fat cells. In fact, it has previously been reported that basal lipolysis is elevated, while isoproterenol-stimulated lipolysis is severely blunted in perilipin null mice (36). Based on these observations, it was proposed that perilipin exerts an important role in preventing lipases from accessing neutral lipid stores under basal conditions, while its presence is required for PKA-mediated lipolysis (36,307). In the absence of adrenergic stimulation, HSL is mainly located in the cytoplasm whereas perilipin is on the surface of the lipid droplet (308). Upon β-adrenergic stimulation, activated PKA phosphorylates HSL as well as perilipin (46,309). HSL then translocates to the lipid droplet and colocalizes with perilipin leading to enhancement in hydrolysis of neutral lipids (46,47,308), indicating that the interaction of perilipin and HSL is essential for the PKA-mediated effects on lipolysis (307,310). Our data are consistent with these observations, since the HFD-induced reduction in perilipin content coincided with 3.8- and 3.0-fold increases in basal lipolysis in visceral and subcutaneous fat cells, respectively, while epinephrine-stimulated lipolysis was equally and potently blunted in HFD adipocytes from both fat depots.

Another pathway that plays an important role in the regulation of lipolysis involves prostaglandins, particularly prostaglandin E_2 (PGE_2). PGE_2 levels are reported to be up-regulated in adipose tissue from obese humans, and acts on the EP3 receptor which signals through G_i-coupled protein receptors to reduce intracellular cAMP levels and potently inhibits lipolysis (311). In adipose tissue, PGE_2 is synthesized by adipose phospholipase A_2 ($AdPLA_2$), and is secreted by adipocytes (76). It was recently

demonstrated that ablation of $AdPLA_2$ in mice generates a phenotype that prevents obesity induced by HFD and elevates lipolysis, primarily through a decrease in PGE_2 production and content in WAT (49). In the HFD mice, we found a significant increase in $AdPLA_2$ expression in visceral and subcutaneous WAT, which is compatible with increased PGE_2 levels seen in obese individuals (76). Therefore, we hypothesized that over-activation of the EP3 receptor due to elevated prostaglandin secretion by HFD adipocytes could be responsible for the impairment in adrenergic receptor signaling and blunted catecholamine-induced lipolysis in visceral and subcutaneous adipocytes of HFD mice. Pre-incubation with the EP3 receptor antagonist L826266 increased basal lipolysis in control visceral and subcutaneous adipocytes. However, it did not alter the potent inhibitory effect of HFD on epinephrine-induced lipolysis. The reasons underlying this are unclear though it could be that after 8 weeks of HFD, the EP3 receptor was hyperactivated and acute incubation with L826266 was unable to overcome the powerful suppressive effect of the prolonged HFD on this pathway.

Although AMPK activation has been shown to exert an anti-lipolytic effect in WAT, its effect on metabolic processes under conditions of HFD have not yet been assessed. Here, we provide novel evidence that both phosphorylation and content of AMPK and its substrate ACC were strongly reduced in both visceral and subcutaneous fat tissue from HFD mice. Although this seems consistent with the fact that basal lipolysis is elevated, HFD completely abolished HSL phosphorylation on PKA targets Ser 563 and 660 with a concomitant reduction in AMPK activity. Therefore, the inhibition of catecholamine-induced lipolysis cannot be attributed to exacerbated

activation of this kinase by HFD. In fact, lower phosphorylation of ACC and HSL_{Ser565}, downstream targets of AMPK (179,302), is in line with the reduced activation of this kinase in visceral and subcutaneous fat depots of HFD mice. Furthermore, we have previously demonstrated that short- and long-term AICAR-induced AMPK activation reduces FA esterification (191,303). In the present study, we show that a reduction in AMPK signaling with HFD elicits the opposite effect, since FA incorporation into lipids was increased, while citrate synthase activity and palmitate oxidation were reduced, which is also compatible with facilitation of lipid storage in a condition of chronic energy surplus. Furthermore, it is fitting that under conditions of HFD the production of citrate is reduced, since the cells are exposed to an abundance of FAs and there is no need for the *de novo* lipid synthesis pathway to be activated. HFD not only reduced AMPK phosphorylation but also promoted insulin resistance in both fat depots. This was clearly demonstrated by the fact that insulin-stimulated palmitate uptake was inhibited by HFD in visceral and subcutaneous adipocytes. In this scenario, impairment of AMPK signaling must have facilitated the release of FAs by the WAT, since the anti-lipolytic effect of this kinase was attenuated.

To date, no studies have demonstrated whether the FA oxidative pathway in adipocytes is altered under conditions of diet-induced obesity. Here, we provide evidence that the oxidative capacity of both visceral and subcutaneous adipocytes was markedly decreased in fat cells from HFD mice. Although this maybe partly attributed to reduced palmitate uptake in adipocytes of HFD mice, changes in the expression of genes involved in oxidative metabolism were also altered. Gene expression of PGC-1α and PPARα,

which are critical regulators of mitochondrial biogenesis and energy expenditure (104), were significantly reduced in both visceral and subcutaneous WAT. Importantly, it has been recently shown that AMPK and another energy sensor, the NAD^+-dependent type III deactylase SIRT1, are necessary for PGC-1α activation (209). Therefore, chronic suppression of AMPK as seen in the WAT of HFD mice is consistent with a reduced ability of this tissue to up-regulate oxidative metabolism. Furthermore, recent studies from our lab indicated that AICAR-induced activation of AMPK for 15 hours increased gene expression of PGC-1α and PPARα, which drove lipid metabolism towards energy dissipation instead of storage (303). Although the WAT does not have high oxidative capacity, these differences in metabolism of FAs could have a major impact on whole body lipid metabolism, since fat tissue makes up a large proportion of body mass (15-20% and 20-30% in healthy men and women, respectively), particularly in obese individuals (more than 40%) (196). Although there is no evidence that FA oxidation in adipocytes increases as a means to cope with excess lipid load in obesity, our data suggest that the impairment of FA oxidation in WAT may further contribute to the accumulation of fat mass in both visceral and subcutaneous fat depots under conditions of HFD.

In summary, our results indicate that HFD-induced obesity disrupts signaling through major components of the lipolytic cascade in WAT (Figure 5-6). Specifically, HSL and perilipin are down-regulated, while ATGL and CGI-58 are up-regulated. This culminates in increased basal but severely blunted catecholamine-induced lipolysis and accumulation of DAG in visceral and subcutaneous fat depots. Additionally, impairment

of AMPK activity and down-regulation of PGC-1α and PPARα resulted in elevated esterification and reduced ability to oxidize FA in visceral and subcutaneous adipocytes (Figure 5-6). Altogether, these alterations in molecular regulation of lipolysis and FA metabolism give insight into the dysfunctional metabolic adaptations that occur with HFD in the WAT, and may help further our understanding of defective mechanisms that contribute to obesity and its related metabolic disorders.

ACKNOWLEDGEMENTS

The authors would like to thank Merck Frosst for their kind gift of L826266. This research was funded by an operating grant from the Canadian Institute of Health Research (CIHR) and by infrastructure grants from the Canada Foundation for Innovation (CFI) and the Ontario Research Fund (ORF) awarded to RBC. RBC is also a recipient of the CIHR New Investigator Award and the Early Research Award from the Ontario Ministry of Research and Innovation. MPG and NMA are supported by Doctoral and Masters CIHR Canadian Graduate Scholarships, respectively.

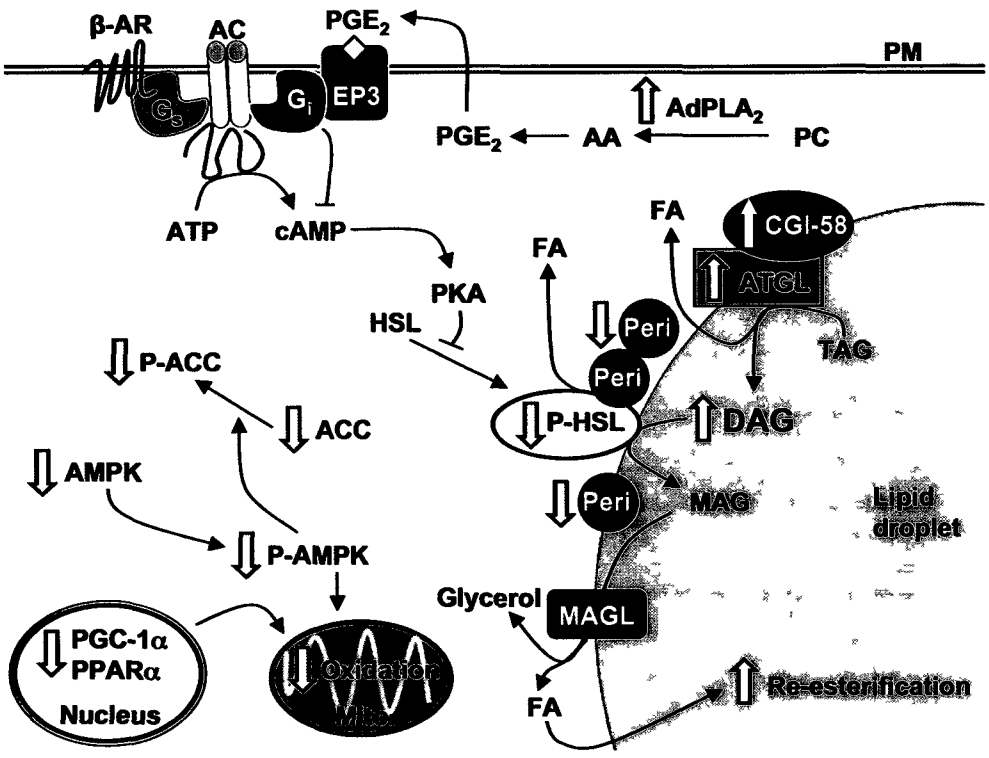

Figure 5-6. Summary of the effects of HFD on adipocyte lipolysis and metabolism. Arrows represent up- or down-regulation of activity, protein content, and/or expression. Lines without arrow heads denote inhibition. Under HFD, the effect of catecholamines on the β-adrenergic (β-AR) signaling cascade are blunted through reduced activation of the Gs-protein coupled receptor. This reduces PKA activation and inhibits phosphorylation of HSL. HFD also upregulates expression of $AdPLA_2$, which has been demonstrated to increased PGE_2 production, the primary ligand for the EP3 receptor. Since EP3 is coupled to an inhibitory G-protein (G_i), activation of this receptor further inhibits PKA under HFD conditions. Increase in ATGL content and CGI-58 expression also occurs with HFD to facilitate TAG breakdown, although subsequent decreased HSL phosphorylation/activity results in the accumulation of DAG. HFD-induced decreases in perilipin (Peri) content also seems to contribute to dysfunctional lipolysis in these cells. Reduction of AMPK content and phosphorylation by HFD is in line with reduced ACC and suppressed oxidation. The oxidative capacity of adipocytes is decreased with HFD, which is compatible with suppression of regulators of mitochondrial biogenesis such as PGC-1α and PPARα expression. AC, adenylyl cyclase; AA, arachidonic acid; PC, phosphatidylcholine; PM, plasma membrane; FA, fatty acid; MAG; monoacylglycerol; MAGL, MAG lipase; Mito, mitochondria.

CHAPTER 6:

Disruption of AMPKα1 signaling prevents AICAR-induced inhibition of AS160/TBC1D4 phosphorylation and glucose uptake in primary rat adipocytes

Mandeep P. Gaidhu, Robert L.S. Perry, Fawad Noor, Rolando B. Ceddia

School of Kinesiology and Health Science, York University – Toronto, Canada

Contribution of authors:

MPG organized and conducted all experiments, and wrote the manuscript. RLS designed and produced the adenovirus used for experiments and edited the manuscript. FN assisted with assays. RBC designed and assisted with experiments, and edited the manuscript.

Keywords: AS160/TBC1D4, AMPK, AICAR, glucose uptake, insulin, adipocytes

A version of this manuscript has been published in *Molecular Endocrinology.* (Copyright permission, Appendix C)

(Gaidhu MP, Perry RL, Noor F, Ceddia RB. Disruption of AMPKalpha1 signaling prevents AICAR-induced inhibition of AS160/TBC1D4 phosphorylation and glucose uptake in primary rat adipocytes. *Mol Endocrinol.* **24**:1434-40, 2010).

ABSTRACT

The aim of this study was to investigate the molecular mechanisms by which AMP-kinase (AMPK) activation inhibits basal and insulin-stimulated glucose uptake in primary adipocytes. Rat epididymal adipocytes were exposed to 5-aminoimidazole-4-carboxamide-1-β-D-ribofuranoside (AICAR) for 1h. Subsequently, basal and insulin-stimulated glucose uptake and the phosphorylation of AMPK, ACC, Akt, and the Akt substrate of 160kDa (AS160/TBC1D4) were determined. In order to investigate whether these effects of AICAR were mediated by AMPK activation, these parameters were also assessed in adipocytes either expressing LacZ (control) or a kinase dead AMPKα1 mutant (KD-AMPKα1). AICAR increased AMPK activation without affecting basal and insulin-stimulated Akt1/2 phosphorylation on Thr_{308} and Ser_{473} residues. However, AMPK activation suppressed the phosphorylation of AS160/TBC1D4 and its interaction with the 14-3-3 signal transduction regulatory protein, which was accompanied by significant reductions in plasma membrane GLUT4 content and glucose uptake under basal and insulin-stimulated conditions. Phosphorylation of Akt substrates GSK3α and β were unaltered by AICAR, indicating that the AMPK regulatory effects were specific to the AS160/TBC1D4 signaling pathway. Expression of the KD-AMPKα1 mutant fully prevented the suppression of AS160/TBC1D4 phosphorylation, plasma membrane GLUT4 content, and the inhibitory effect of AICAR-induced AMPK activation on basal and insulin-stimulated glucose uptake. This study is the first to provide evidence that disruption of AMPKα1 signaling prevents the suppressive effects of AMPK activation on

AS160/TBC1D4 phosphorylation and glucose uptake, indicating that insulin-signaling steps that are common to white adipose tissue and skeletal muscle regulation of glucose uptake are distinctly affected by AMPK activation.

INTRODUCTION

It has been demonstrated in skeletal muscle that AMPK activation leads to an increase in glucose uptake independently of insulin, suggesting an anti-diabetic effect of this enzyme (274,282,312). However, contrary to skeletal muscle, work from our lab (191) and others (190) has provided evidence that AICAR-induced AMPK activation causes a reduction in basal and insulin-stimulated glucose uptake and metabolism in adipocytes. These findings provide evidence that AMPK elicits tissue-specific effects and opposes the effects of insulin in white adipose tissue (WAT). However the molecular mechanisms underlying these effects have yet to be elucidated. It has been reported that in 3T3-L1 adipocytes neither tyrosine phosphorylation of insulin receptor substrates (IRS1/IRS2) nor phosphatidylinositol 3-kinase (PI-3kinase) recruitment were affected by AICAR (190), suggesting that a downstream target is responsible for inhibition of glucose uptake. In this context, a group of proteins containing a TBC domain (Tre-2/Bub2/Cdc16) present in most Rab GTPase-activating proteins (Rab-GAPs) emerged as potential targets for the regulation of glucose uptake by AMPK. Two particular members of this family, TBC1D1 and Akt substrate of 160kDa (AS160; also named TBC1D4), have been demonstrated to associate with GLUT4-containing membranes and are thought to be the point of convergence of the insulin and AMPK signaling pathways (313). When

phosphorylated, these Rab-GAP proteins release the inhibition on GLUT4 vesicles and allow translocation to the plasma membrane to facilitate glucose uptake (313). In WAT from mice TBC1D1 is undetectable, and its low expression in fully differentiated 3T3-L1 adipocytes suggests that the endogenous protein is unlikely to participate significantly in insulin-stimulated GLUT4 translocation and glucose uptake (314). However, AS160 is highly expressed in WAT, suggesting that this Rab-GAP plays a major role in glucose uptake in this tissue (22),(315). Based on the importance of AS160 in glucose transport in adipocytes and on our findings that AICAR causes an inhibition of glucose uptake in these cells (191), we hypothesized that AMPK impairs phosphorylation of AS160. To test this hypothesis, we used primary rat adipocytes either expressing LacZ (control) or a kinase dead mutant of the predominant α1 subunit of AMPK (KD-AMPKα1). We then assessed plasma membrane GLUT4 content, glucose uptake and the phosphorylation of AMPK, ACC, Akt, and AS160 in adipocytes acutely exposed (1h) to AICAR under basal and insulin-stimulated condition. The findings of this study advance our understanding of the molecular mechanisms underlying the inhibitory effect of AMPK activation on glucose uptake in fat cells with important implications for the regulation of white adipose tissue metabolism.

MATERIALS AND METHODS

Reagents – AICAR was purchased from Toronto Research Chemicals, Inc. (Toronto, Canada); cytochalasin B, di-`isononyl' phthalate, DMEM, and fatty acid free albumin, and MTT kit were obtained from Sigma-Aldrich (Oakville, Canada); 2-deoxy-D-glucose

was from Bioshop Canada; 2-[1,2-^{3}H]deoxy-D-glucose was purchased from GE Healthcare (Quebec City, Canada), and human insulin (Humulin® R) was from Eli Lily. The AdEasy XL Adenoviral Vector System Kit was purchased from Stratagene (La Jolla, USA). All other chemicals were of the highest grade available. Antibodies against P-ACC and P-AS160 were from Upstate (Charlottesville, USA). GLUT4 antibody was from Santa Cruz Biotechnology, Inc. (Santa Cruz, USA). Anti-HA monoclonal antibody supernatant was produced in the laboratory using the 12CA5 hybridoma cell line. All other antibodies were obtained from Cell Signaling Technology (Boston, USA).

Cloning of rat AMPKα1 and adenoviral production – AMPKα1 was cloned by RT-PCR (reverse transcription-polymerase chain reaction) using RNA extracted from male Wistar rat tissues and adenoviral production was prepared using the AdEasy XL Adenoviral Vector System. Mutagenesis of aspartic acid 157 to alanine (D157A) was done by overlapping PCR, rendering AMPKα1 kinase dead (KD-AMPKα1) (316). DNA fragments representing the amino-terminal (NT) and carboxyl-terminal (CT) halves were amplified using the following primer sets (NT: Forward 5' CCG GAA TTC CCA ATG GCC GAG AAG CAG AAG CAC GAC -3' and Reverse 5'– CCG CTC GAG TCA GTT GTA CAG GCA GCT GAG GAC CTC -3'; CT: Forward 5'- CCG GAA TTC CCA ATG CTG TAC AAC AGA AAC CAC CAG GAC C -3' and Reverse 5'- CCG CTC GAG TTA CTG TGC AAG AAT TTT AAT TAG ATT TGC -3'), cloned into the pcDNA3 plasmid backbone (Invitrogen) as EcoRI-XhoI fragments and sequenced at the York University Core Facility. Sequences matching Genbank Accession number

NM_019142 were used for subsequent cloning reactions. Full-length versions containing a single amino-terminal hemagglutinin-tag (HA-tag) were generated by three-way ligations into the pCAN-HA1 plasmid backbone as EcoRI/BsrGI (NT) and BsrGI/XhoI (CT) fragments and sequenced to confirm correct framing of the HA-tag with AMPKα1. Mutagenesis of aspartic acid 157 to alanine (D157A) was done by overlapping PCR mutagenesis using the forward and reverse NT primers detailed above paired with internal primers containing a GAC (Asp) to GCC (Ala) mutation (Forward: 5'-GAA TGC AAA GAT AGC C**GC C**TT CGG TCT TTC AAA CAT G-3' and Reverse: 5'-CAT GTT TGA AAG ACC GAA GGC **GGC** TAT CTT TGC ATT C-3'. Mutation is underlined). Positive clones were sequenced to confirm the presence of the mutation. Adenoviruses expressing HA-AMPKα1 D157A and LacZ were generated using the AdEasy XL Adenoviral System (Stratagene). Briefly, an Asp718/XhoI fragment representing the full-length HA-tagged AMPKα1 D157A was subcloned into the pShuttleCMV plasmid backbone. Plasmid DNA isolated from positive colonies was linearized with PmeI and electroporated into BJ5183-AD-1 bacterial stocks for recombination into the pADEasy plasmid backbone. Positive recombinants of both HA-AMPKα1 D157A and the control *LacZ* (provided with the kit) were used for large-scale DNA preparation. For primary virus production, linearized plasmid (PacI digested) was transiently transfected into AD-293 cells using the calcium phosphate method. Primary viral stocks were used for further viral amplification. Adenovirus-producing AD293 cells were harvested, lysed by 4 rounds of freeze/thaw lysis and viral supernatants were cleared by centrifugation and 0.45 μM filtering. Viral titers were determined using the immunocytochemically-based

AdEasy Viral Titer Kit (Stratagene) according to the provided instructions. Confirmation of viral efficacy was done by X-gal staining of LacZ infected cells or, detection of HA-tagged AMPKα1 D157A by immunoblotting with anti-HA monoclonal antibody on protein lysates from cells infected with HA-AMPK D157A expressing adenovirus.

Experimental animals and isolation/infection of primary adipocytes –Male albino rats (Wistar strain) weighing 175-200g were maintained on a 12/12-h light/dark cycle at 22°C and fed (*ad libitum*) standard laboratory chow. The protocol was approved by the York University Animal Care Ethics Committee. Fat cells were isolated (191,303) and subjected to adenoviral-mediated gene transfer (MOI of 250 pfu/cell) in 2mL of DMEM for 4h at 37°C with occasional agitation. Culture medium was adjusted to 6mL with DMEM supplemented with 1% serum and adipocytes were incubated for an additional 24h prior to use in experiments. Importantly, maintenance of adipocytes in culture for 24h was the minimum time required to obtain a significant and reproducible inhibition of AMPK activity using the adenovirus mediated over-expression of the KD-AMPKα1 mutant. Typical infection rates ranged from ~70-80% between independent experiments as determined by counting YFP-positive adipocytes using fluorescence microscopy. For adipocytes that were not infected, cells were isolated and left at 37°C for 24h prior to acute AICAR and insulin treatment in order to compare results with infected cells that are subjected to prolonged *in vitro* culture conditions.

Assessment of cytotoxicity and glucose uptake – Under all experimental conditions, adipocytes were exposed for 1h to AICAR (2mM) and subsequently assayed for

cytotoxicity using the MTT (3[-4,5-dimethylthiazol-2-yl]2,5idiphenyl tetrazolium bromide) assay kit (303). For glucose uptake, cells were treated as described above except cells were stimulated with insulin (100nM) in the final 20min of the incubation period. Glucose uptake was then assayed using 2-[1,2-^{3}H]deoxy-D-glucose (191).

Immunoprecipitations and immunoblotting – Adipocytes (~1 x 10^7 cells) were incubated for 1h in the absence or presence of AICAR (2mM), and stimulated with insulin (100nM) in the final 20min of incubation. Cells were immediately lysed and used for either SDS-PAGE analysis (191,303)Chapter 4, page 80) or immunoprecipitations (IPs). For IPs, 400μg of protein lysate was incubated with antibodies (1:100 dilution) and protein G sepharose beads on a rotator overnight at 4°C. Subsequently, IPs were gently centrifuged (4000rpm for 3min) and the supranatant was aspirated. Beads were washed with 150mM NaCl, 1mM EDTA pH 8.0, 50mM Tris-HCl pH 8.0, 0.1% NP-40 3 times, with a centrifugation step between each wash. Beads were then re-suspended in 30μL of Laemmli lysis buffer, boiled for 5min, and centrifuged at 13,000rpm for 3min. Supranatant was then subjected to SDS-PAGE analysis as described previously (191,303). All antibodies were diluted to 1:1000 with the exception of P-AMPK (1:500) and GLUT4 (1:500). Equal loading was confirmed with GAPDH (1:5000) and by Coomassie blue staining of gels.

Subcellular fractionation for the measurement of GLUT4 translocation – Translocation of GLUT4 to the plasma membrane was measured after subcellular fractionation of adipocytes as described previously (317). Briefly, after treatment of adipocytes, cells

were washed twice and re-suspended in TES buffer (20mM Tris-HCl, 1mM EDTA, and 8.7% sucrose, pH 7.4). Cells were lysed in a pre-cooled Potter-Elvehjem tissue homogenizer and then transferred to microtubes. Homogenate was centrifuged at 12,000rpm at room temperature for 1min, then at 0°C for 15min. Subsequently, the solidified fat cake and supranatant was removed and the resulting pellet was homogenized in 2mL of TES buffer, loaded onto a sucrose cushion (20mM Tris-HCl, 1mM EDTA, 38.5% sucrose), and centrifuged at 4°C for 60min at 100,000g in swinging bucket rotor (Sorvall S52-ST). The concentrated plasma membranes were collected from the top of the sucrose cushion, re-suspended in TES buffer and centrifuged at 31,000*g* for 60min at 4°C in a fixed angle rotor (Sorvall S55-A). The resulting pellet was re-suspended in lysis buffer and quantified for protein using the Bradford assay. Lysate was diluted 1:1 with Laemmli sample buffer and 10-20μg was used for western blotting analysis for GLUT4 content.

RESULTS

Cytotoxicity – Using the MTT assay we found that exposure of primary rat adipocytes to vehicle (PBS) or infection with adenovirus coding for LacZ or KD-AMPKα1 did not cause cell toxicity (Figure 6-1).

Effects of AICAR treatment on the phosphorylation and content of AMPK, ACC, and Akt – Exposure of adipocytes to insulin reduced AMPK and ACC phosphorylation. However, AICAR treatment for 1h equally increased AMPK and ACC phosphorylation under basal

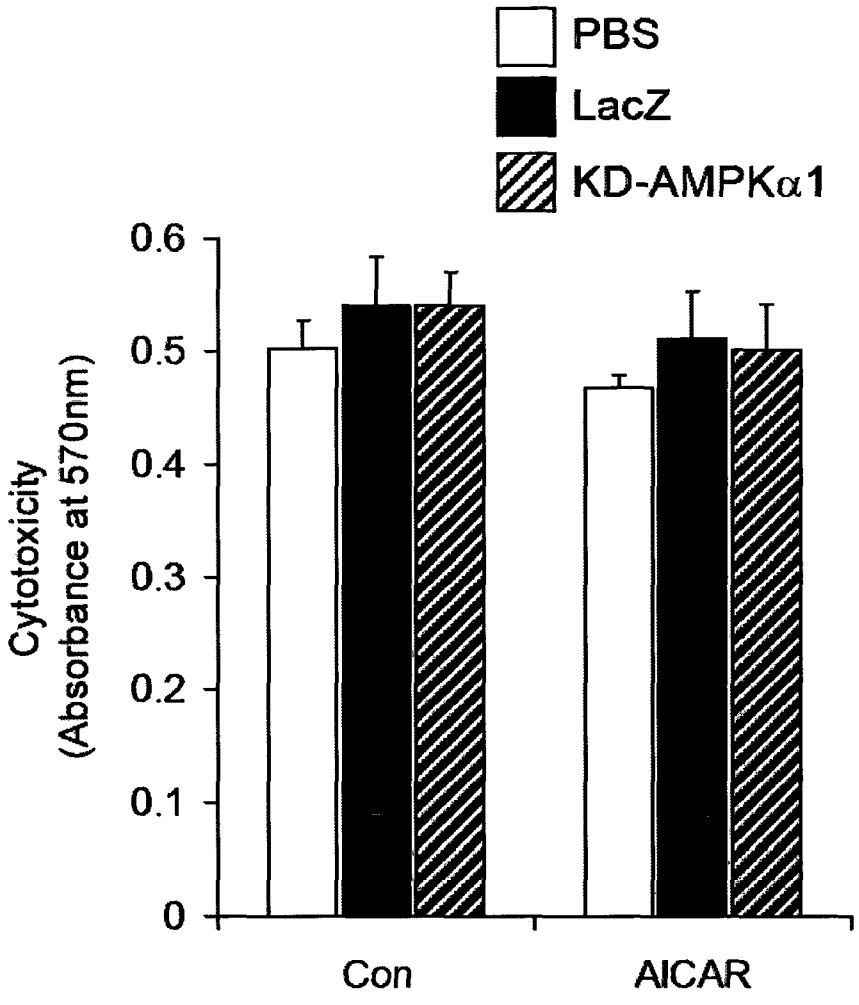

Figure 6-1. Effects of adenoviral infection and acute AICAR (2mM) incubation on adipocyte cytotoxicity. Cells were treated with either PBS (white bars), LacZ control virus (black bars), or virus encoding KD-AMPKα1 (hatched bars). Subsequently, adipocytes were exposed to AICAR for 1h prior to assessing for cytotoxicity using the MTT (3-(4,5-dimethylthiazol-2-yl)-2,5-diphenyl tetrasodium bromide) assay kit according to manufacturer's instructions.

and insulin-stimulated conditions (Figure 6-2A). No alterations were observed in the total content of AMPK and ACC under all treatment conditions (Figure 6-2A). As expected, insulin increased in Akt_{Thr308} and Akt_{Ser473} phosphorylation, respectively (Figure 6-2B). Treatment of adipocytes with AICAR did not affect either basal or insulin-stimulated phosphorylation of Akt_{Thr308} and Akt_{Ser473} (Figure 6-2B). We then tested the relative contributions of Akt1 and Akt2 in mediating signal transduction under basal and insulin-stimulated conditions in primary rat adipocytes. Western blot analysis revealed that Akt1 and Akt2 were both present in isolated primary adipocytes, and no alteration in the content of these proteins was observed in adipocytes under all treatment conditions (Figure 6-2C). However, it is important to notice that an upward shift in the Akt2 bands was observed in adipocytes exposed to insulin, although Akt1 did not elicit the same band-shift pattern in adipocytes stimulated with insulin (Figure 6-2C). This upward band shift of Akt2 coincided with increased phosphorylation of this protein on Thr308 and Ser473 residues (Figure 6-2D). Interestingly, while insulin-stimulated Ser473 phosphorylation was present in immunoprecipitations with both Akt1 and Akt2, we only detected Thr308 phosphorylation in Akt2 of insulin-stimulated adipocytes (Figure 6-2D). AICAR treatment under either basal or insulin-stimulated conditions did not affect band shift (Figure 6-2C) or the phosphorylation states of Akt1 and Akt2 (Figure 6-2D). See Figure 6-3 for quantification of blots in Figure 6-2.

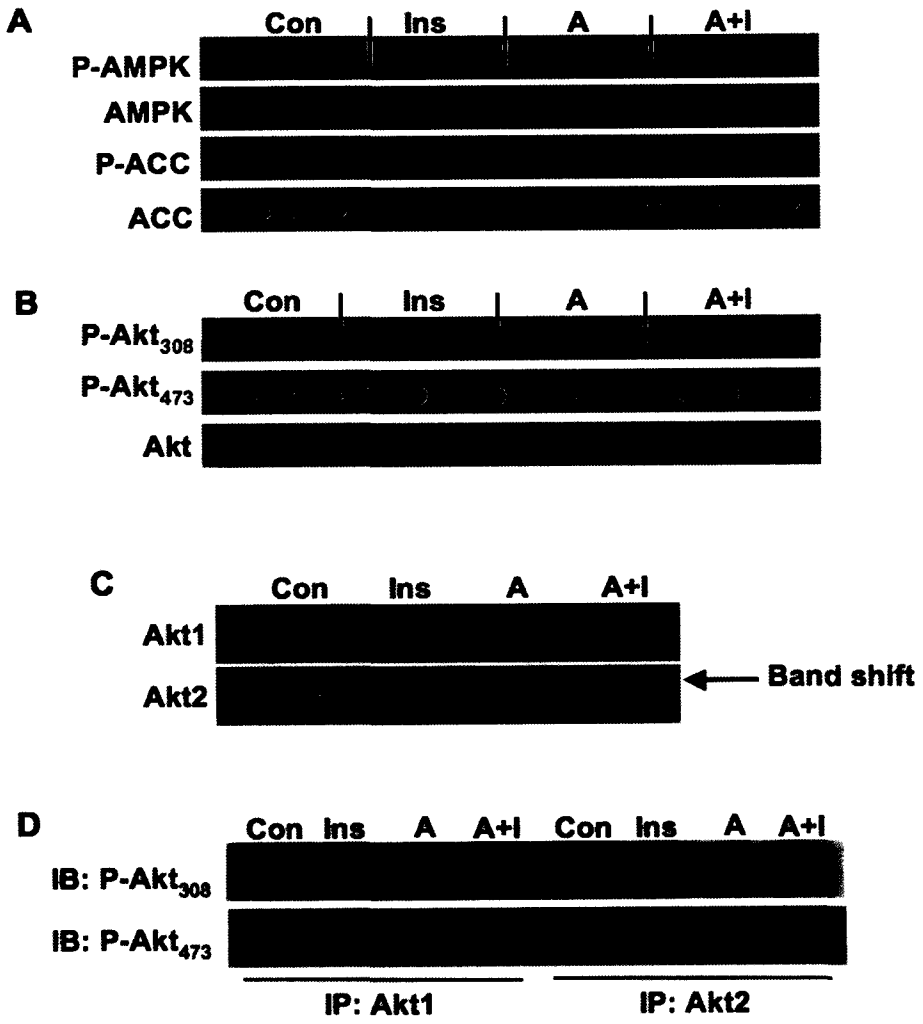

Figure 6-2. Representative blots showing the effects of AICAR (A; 2mM), insulin (Ins; 100nM), and AICAR plus insulin (A + I) on phosphorylation and content of AMPK, ACC, and Akt (Panel **A** and **B**). Total Akt1 and Akt2 content **(C)**. Phosphorylation of Akt1 and Akt2 at Thr308 and Ser473 **(D)**. Blots are representative of 2-3 independent experiments. Immunoprecipitations were performed in duplicate in 2 independent experiments. IP, immunoprecipitation; IB, immunoblot.

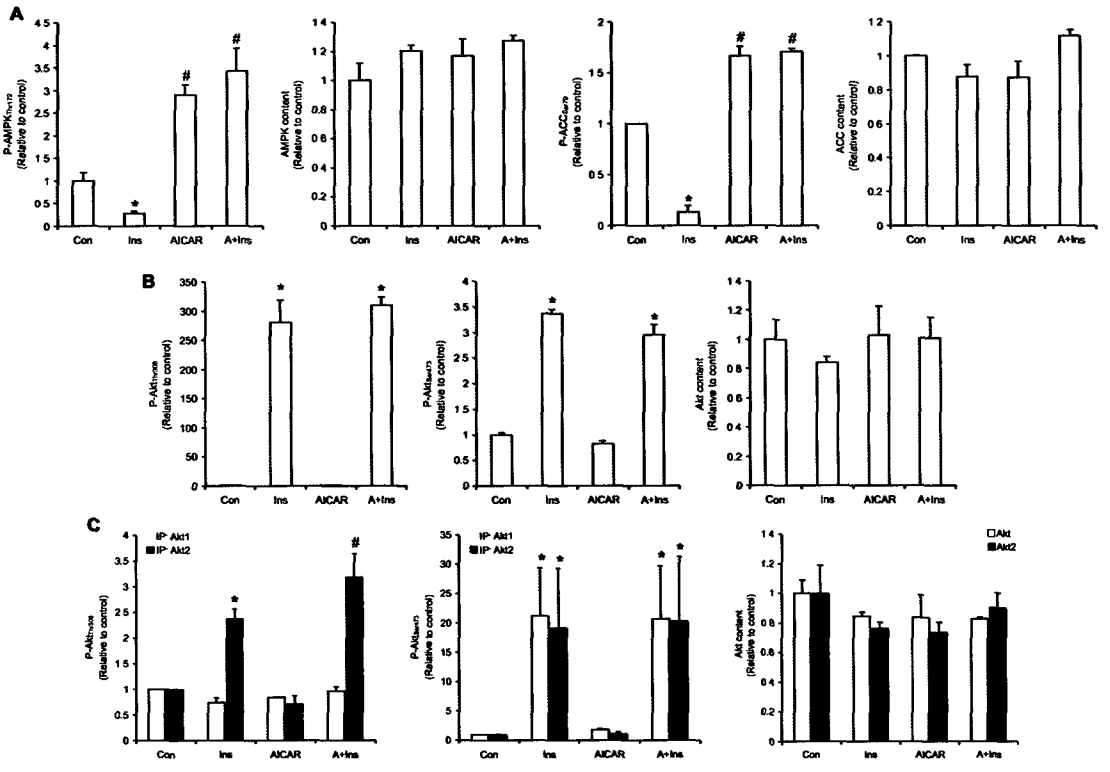

Figure 6-3. Quantification of western blots from Figure 6-2. Data were first normalized to LacZ control, and compiled from 2-3 independent experiments. One- and two-way ANOVA was used for statistical analyses with Tukey-Kramer and Bonferonni comparison post-hoc tests. *and $^{\#}P<0.05$ versus all other conditions.

Effects of AICAR on Akt targets (AS160 and GSK3α/β) and plasma membrane GLUT4 content – Since Akt phosphorylation was unaltered with AICAR treatment, we investigated downstream targets that could potentially be responsible for the inhibitory effect of AMPK activation on glucose uptake. As expected, AS160 phosphorylation was increased in the presence of insulin, while AICAR markedly suppressed this variable under insulin-stimulated conditions (Figure 6-4A). Immunoprecipitation of P-AS160 revealed that the insulin-induced association with the 14-3-3 family of regulatory proteins involved in signal transduction was also reduced by AICAR treatment (Figure 6-4B). Compatible with the role of AS160 in the trafficking of GLUT4-containing vesicles, measurement of GLUT4 content in the plasma membrane fraction of adipocytes was reduced with AICAR treatment under basal and insulin-stimulated conditions (Figure 6-4C). Importantly, phosphorylation and content of the Akt targets GSK3α and β isoforms were not suppressed by AICAR treatment (Figure 6-4D), demonstrating that AICAR-induced AMPK activation specifically affected the AS160 signaling pathway. See Figure 6-5 for quantification of blots in Figure 6-4.

Phosphorylation of AMPK, ACC and AS160, and glucose uptake in adipocytes expressing the KD-AMPKα1 – Since AS160 was altered with AICAR treatment, we infected adipocytes with an HA-tagged kinase dead (KD) version of AMPKα1 (316) in order to determine if these effects were indeed AMPK mediated. The HA-tag was only detected in KD-AMPKα1-expressing cells (Figure 6-6A), confirming expression of the mutant isoform. Furthermore, AICAR increased AMPK and ACC phosphorylation under

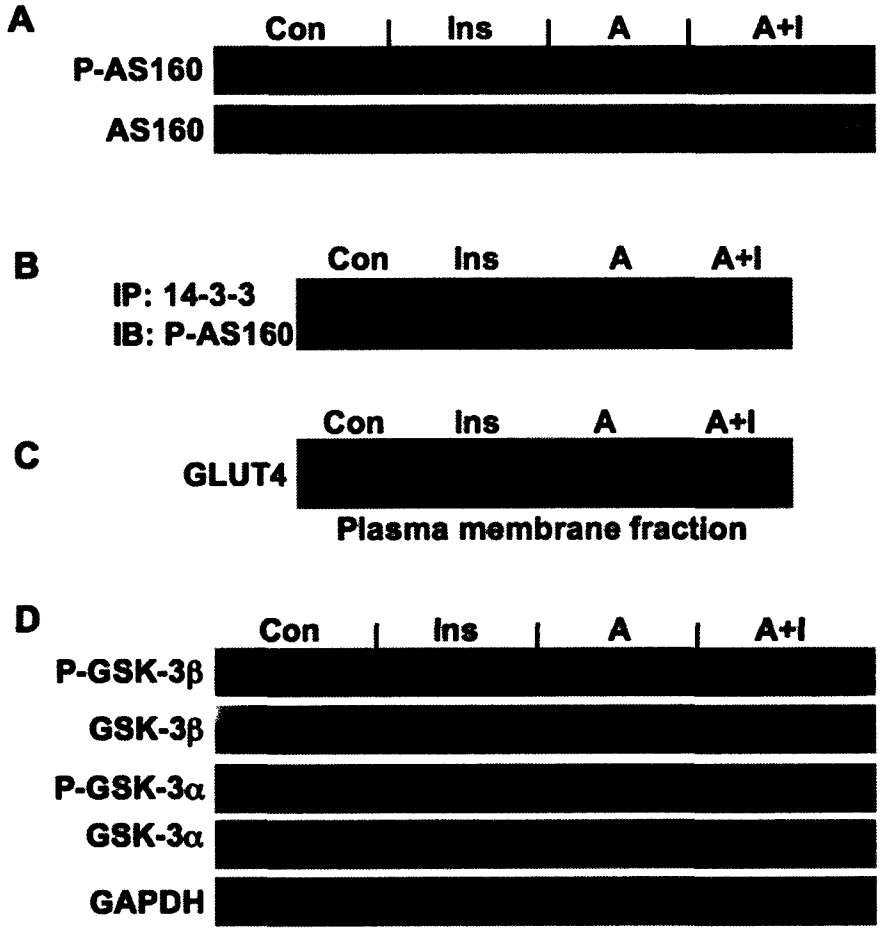

Figure 6-4. Effects of AICAR (A; 2mM) and insulin (Ins; 100nM) on phosphorylation of Akt substrates. AS160 phosphorylation and content **(A)** and co-immunoprecipitation of 14-3-3 **(B)**. GLUT4 content in the plasma membrane fraction of adipocytes **(C)**. Phosphorylation and content of GSK-3α and β **(D)**. Blots are representative of 2-3 independent experiments. Con, control.

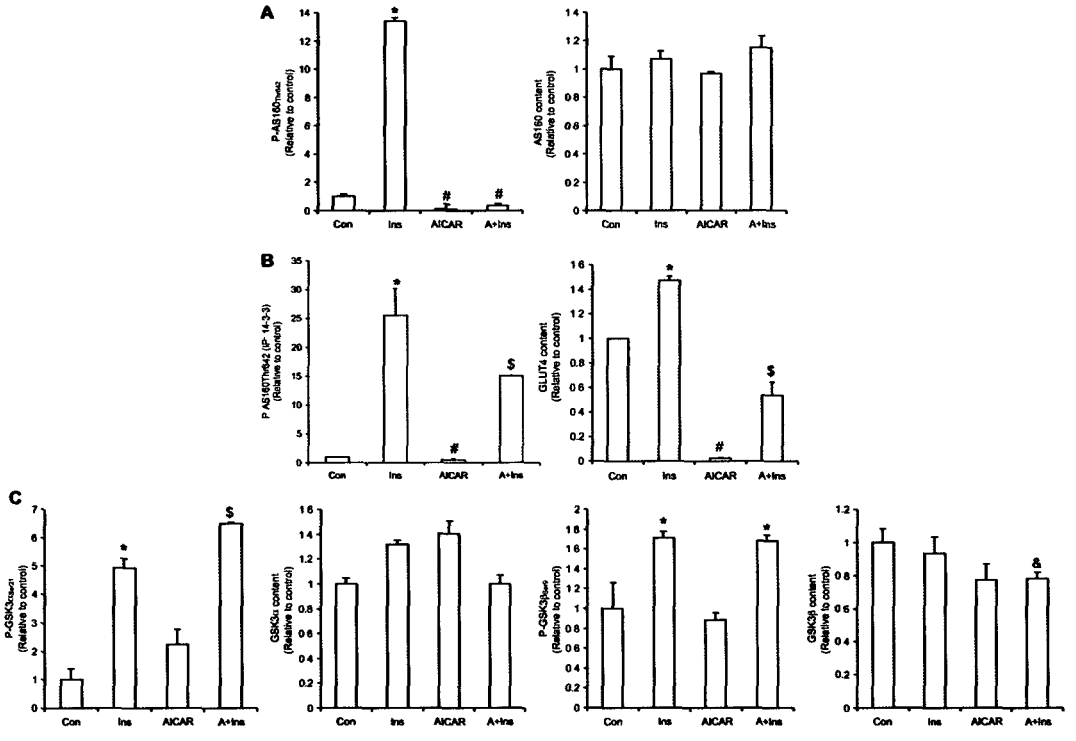

Figure 6-5. Quantification of western blots from Figure 6-4 in the manuscript. Data were first normalized to LacZ control, and compiled from 2-3 independent experiments. One-way ANOVA was used for statistical analyses with Tukey-Kramer multiple comparison post-hoc tests. *, $^{\#}$, and $^{\$}P<0.05$ versus all other conditions; $^{\&}P<0.05$ versus Con.

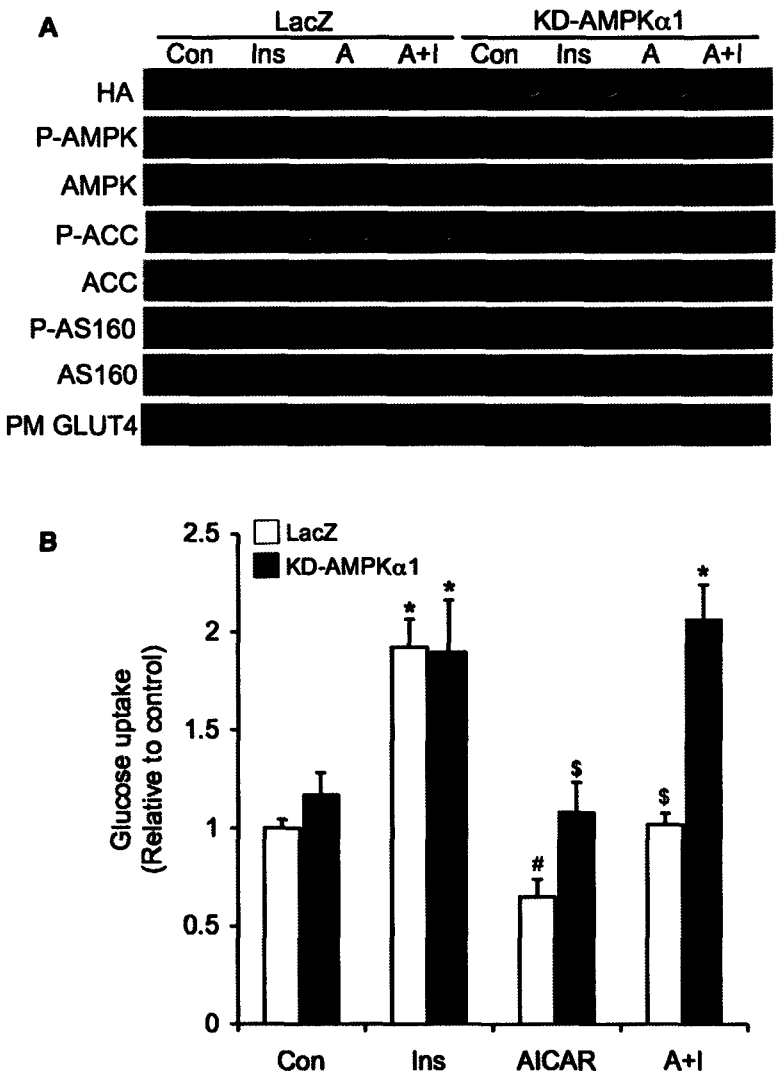

Figure 6-6. (A) Representative blots for content and phosphorylation of HA-tag, AMPK, ACC, AS160, and GLUT4 (plasma membrane fraction; PM) in cells expressing either LacZ control virus or the KD-AMPKα1 mutant in the presence of insulin (Ins, 100nM), AICAR (A, 2mM) and AICAR plus insulin (A+I). **(B)** Glucose uptake in under basal and insulin-stimulated conditions in cells infected with LacZ control virus or KD-AMPKα1 in the absence or presence of AICAR (2mM). Data were analyzed using two-way ANOVA with Tukey-Kramer post-hoc tests. * and $^{\#}P<0.05$ versus all other conditions; $^{\$}P<0.05$ versus LacZ cells exposed to Ins and AICAR, and versus KD-AMPKα1 in Ins and A+I conditions. Blots are representative of three to four independent experiments. The glucose uptake data were compiled from three independent experiments with triplicates in each assay.

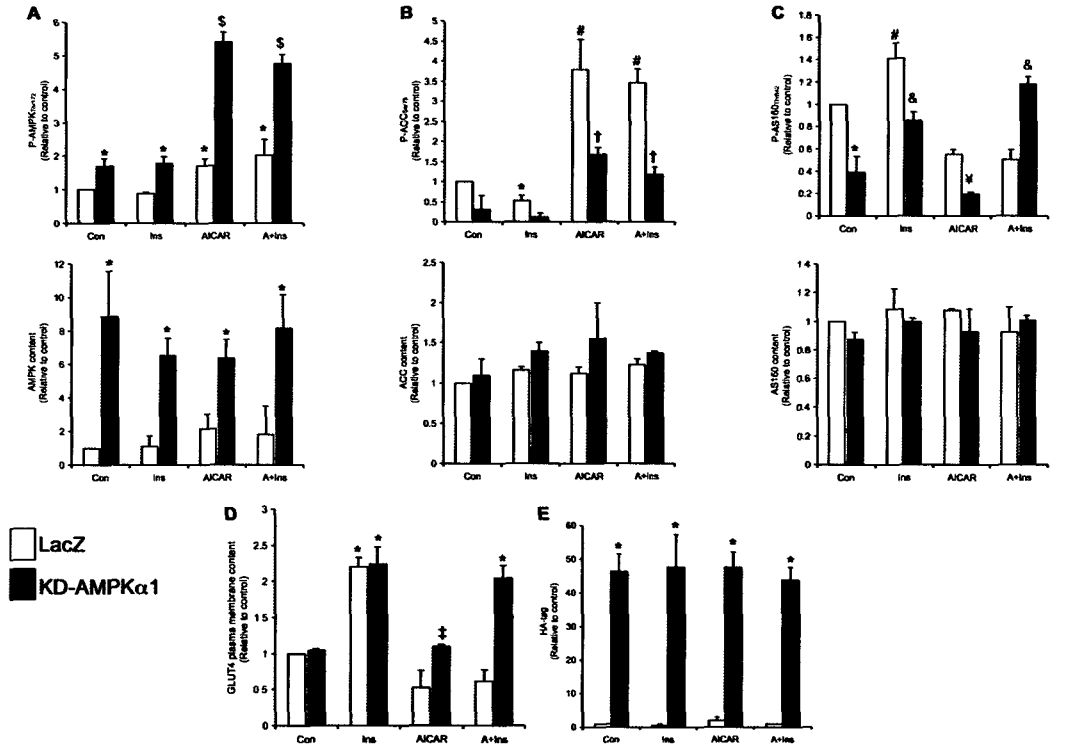

Figure 6-7. Quantification of western blots from Figure 6-7 in the manuscript. Data were first normalized to LacZ control, and compiled from 2-3 independent experiments. LacZ, white bars; KD-AMPKα1, black bars. Two-way ANOVA was used for statistical analyses with Bonferonni comparison post-hoc tests. $^{*}P<0.05$ versus all other conditions; $^{\#}P<0.05$ versus all other conditions; $^{\$}P<0.05$ versus all other conditions; $^{¥}P<0.05$ versus all LacZ conditions, and KD-AMPKα1 Ins, A+Ins conditions; $^{\dagger}P<0.05$ versus Ins, and LacZ A, A+Ins conditions; $^{\&}P<0.05$ versus all other conditions; $^{\ddagger}P=0.06$ versus LacZ AICAR.

basal and insulin-stimulated conditions in cells expressing LacZ (Figure 6-6A). As expected, phosphorylation of AMPK was increased in cells expressing the KD-AMPKα1, but the effect of this kinase on ACC phosphorylation was suppressed (Figure 6-6A). KD-AMPKα1 over-expression increased total AMPK, without altering ACC protein content (Figure 6-6A). AICAR inhibited basal and insulin-stimulated phosphorylation of AS160 in cells expressing LacZ. However, the expression of the KD-AMPKα1 mutant prevented AICAR-induced inhibition of AS160 phosphorylation (Figure 6-6A) and brought basal and insulin-stimulated glucose uptake back to control values (Figure 6-6B). In line with these findings, measurement of GLUT4 content in the plasma membrane fraction was reduced with AICAR treatment in LacZ-expressing adipocytes, and this effect was restored in cells with impaired AMPKα1 signaling (Figure 6A; see Figure 6-7 for quantification of blots in Figure 6-6A). It is important to note that prolonged maintenance of primary adipocytes in culture cause a reduction in the insulin-stimulated fold increase in glucose transport when compared to freshly isolated adipocytes. However, despite this limitation, we observed that AICAR-induced AMPK activation robustly and equally affected insulin-signaling steps and suppressed glucose uptake in adipocytes either freshly isolated (191); unpublished data) or maintained in culture for 24h.

DISCUSSION

We have previously demonstrated that acute AICAR-induced AMPK activation caused a marked reduction in basal and insulin-stimulated glucose uptake and

metabolism in primary rat adipocytes (191). However, the molecular mechanisms underlying these effects remained elusive. Since early steps of the insulin signaling pathway (IRS1/IRS2 tyrosine phosphorylation and PI-3kinase recruitment) were unaffected by AICAR in 3T3-L1 adipocytes (190), a downstream signaling target was expected to be regulated by AMPK. In this context, we hypothesized that the Rab-GAP AS160, which is a common target for Akt and AMPK (313), could play a major role in the inhibitory effect of AICAR on glucose uptake in adipocytes. In fact, AS160 has been demonstrated to play a pivotal role in insulin-mediated GLUT4 trafficking and regulating glucose uptake in adipocytes (22). Studies applying mutational analysis reveal that phosphorylation of the Ser588 and Thr642 residues of AS160 are critical for these effects (22). Although it has been shown that AS160 is important for insulin-stimulated glucose uptake in white adipocytes, no evidence has been provided that this protein is a direct substrate of AMPK in this tissue. Here, we provide novel evidence that AICAR-induced AMPK activation consistently and significantly reduced basal and insulin-stimulated $AS160_{Thr642}$ phosphorylation in primary rat adipocytes. This effect was independent of Akt, since the phosphorylation of Akt at the Thr308 and Ser473 residues were unaffected. In fact, by immunoprecipitating Akt1 and Akt2, we found that AICAR-induced AMPK activation did not have any effect on basal or insulin-stimulated phosphorylation of any of these Akt isoforms.

In order to better understand how AMPK activation leads to decreased AS160 phosphorylation, we assessed whether the effect of AICAR was specific to AS160 or also involved other Akt substrates. To address this, we determined the phosphorylation of

GSK-3, which is a direct target of Akt that is also phosphorylated under insulin-stimulated conditions. Our results revealed that AICAR treatment did not decrease GSK3α/β phosphorylation, providing evidence that the suppressive effect triggered by AMPK activation was specific to AS160 and its downstream signaling pathway. This is further supported by our findings that the interaction between AS160 with the 14-3-3 family of signal transduction regulatory proteins was impaired by AICAR treatment. Current evidence indicates that the binding of 14-3-3 to phosphorylated AS160 suppresses its Rab GAP activity and thereby facilitates the translocation of GLUT4 storage vesicles to the plasma membrane (318,319). We demonstrate here that direct measurement of GLUT4 content in the plasma membrane fraction of adipocytes treated with AICAR confirms that reduced interaction between AS160 and 14-3-3 prevents translocation of glucose transporters to the cell surface. Therefore, the binding of 14-3-3 to phosphorylated AS160 is an important step to promote influx of glucose into the cell. In this context, our findings of impaired AS160 phosphorylation and binding to 14-3-3 proteins are compatible with reduced basal and insulin-stimulated GLUT4 translocation to the plasma membrane and glucose uptake in AICAR-treated adipocytes. It is not clear how AMPK induces this specific inhibitory effect on AS160 phosphorylation. However, it could be due to AMPK-induced phosphorylation of an interacting factor that leads to decreased phosphorylation of AS160, or by directly affecting AS160 making it a less suitable substrate for Akt.

In order to demonstrate that the effects of AICAR were indeed caused by AMPK activation, we disrupted AMPK signaling with the mutated KD-version of the α1 subunit

of this kinase. This was confirmed by detection of the HA-tag and by the inhibition of AMPK-induced ACC phosphorylation. Overexpression of KD-AMPKα1 fully prevented the AICAR-induced suppression of insulin-stimulated $AS160_{Thr642}$ phosphorylation and glucose uptake. Our data is in agreement with previous observations that AS160 is the primary Rab-GAP involved in the regulation of GLUT4 translocation in 3T3-L1 adipocytes (314). In our system the expression of KD-AMPKα1 fully prevented the AICAR-induced inhibition of basal glucose uptake by isolated adipocytes, although we did not detect a concomitant increase in $AS160_{Thr642}$ phosphorylation in these cells. Interestingly, measurement of GLUT4 content in the plasma membrane fraction of adipocytes expressing KD-AMPKα1 indicated a restoration of these glucose transporters at the cell surface under basal and insulin-stimulated conditions when treated with AICAR. This suggests that AMPK could target alternative Rab-GAPs that were not detected by the polyclonal phospho-antibody against AS160 used in our experiments. Previous studies have demonstrated that in skeletal muscle at least two Rab-GAPs (AS160 and TBC1D1) participate in the regulation of GLUT4 trafficking and glucose uptake in response to AMPK activation and insulin stimulation (314). In skeletal muscle, it has been proposed that GLUT4 translocation stimulated by insulin is mainly regulated by AS160, while under AICAR treatment or contraction TBC1D1 is the major regulator of this process (314). This provides support to the concept that distinct AMPK-mediated mechanisms may govern glucose uptake under basal and insulin-stimulated conditions in adipocytes. However, because TBC1D1 expression has been reported to be very low in fully differentiated 3T3-L1 adipocytes and also undetected in mice WAT (314), it is

unlikely that this Rab-GAP is the alternative target of AMPK in our system. Therefore, future investigations are warranted to identify potential novel molecular targets by which basal and insulin-stimulated glucose uptake is regulated by AMPK in adipocytes.

It is important to note that differences clearly exist between primary and cultured 3T3-L1 adipocytes with respect to the role of AMPK in the regulation of glucose uptake. In fact, studies in 3T3-L1 adipocytes (190) demonstrate that AICAR causes an increase in basal glucose uptake but powerfully suppresses the insulin-stimulated effect on this variable, and we have confirmed these findings in our lab (data not shown). However, we have repeatedly demonstrated here and in previous studies (191) that in primary rat adipocytes, AICAR-induced AMPK activation inhibits both basal and insulin-stimulated glucose uptake. Therefore, it is important that future studies take into consideration that 3T3-L1 adipocytes respond differently from primary adipocytes when assessing the role of AMPK in the regulation of glucose uptake.

Our findings from the present study are in line with previous observations that AMPK activation has tissue-specific effects in skeletal muscle versus adipose tissue (Figure 6-8). Work from our lab (191) and others (293) have shown that activation of AMPK with AICAR elicits concomitant decreases in fatty acid synthesis and glucose incorporation into lipids, which is compatible with a reduction in glucose uptake seen in this study. The question that arises is how does AMPK differentially modulate glucose metabolism in skeletal muscle versus adipose tissue? It may be that AMPK targets a currently unidentified Akt-interacting factor present only in adipose tissue, which impairs the ability of Akt to recognize AS160 as a substrate. Our data indicate that this protein

specifically affects the ability of Akt to phosphorylate AS160, since other Akt targets such as GSK-3α/β were unaffected by AICAR treatment. However, we cannot rule out the possibility that AMPK could be regulating AS160 phosphorylation directly or via activation of phosphatases targeted towards Rab-GAPs. This prevents AS160 from being phosphorylated in the presence of AICAR under basal and insulin-stimulated conditions, leading to decreased glucose entry into the adipocyte. Conversely, disruption of AMPKα1 signaling allowed phosphorylation of AS160 to occur and fully prevented suppression of glucose uptake. In this context, identifying novel molecular targets that mediate the tissue-specific effects of AMPK activation on AS160 phosphorylation may be of great importance for the regulation of whole-body glucose disposal and energy homeostasis.

From a physiological perspective, the activation of AMPK in WAT occurs under conditions of cellular stress. This leads to activation of energy sparing mechanisms in order to increase intracellular ATP content. In line with this concept, the inhibition of glucose and fatty acid uptake induced by AMPK activation in adipocytes (191,303) may play an important role in reducing FA activation and esterification, which may serve to restrain intracellular ATP consumption. This study is the first to provide evidence that activation of AMPK with AICAR in primary rat adipocytes suppresses AS160 phosphorylation leading to inhibition of basal and insulin-stimulated GLUT4 translocation to the plasma membrane and subsequently glucose uptake. Disruption of AMPKα1 signaling fully prevented these effects, indicating that insulin-signaling steps

that are common to WAT and skeletal muscle regulation of glucose uptake are distinctly affected by AMPK activation in these tissues.

ACKNOWLEDGEMENTS

This research was funded by an operating grant from the Canadian Institute of Health Research (CIHR) and by infrastructure grants from the Canada Foundation for Innovation (CFI) and the Ontario Research Fund (ORF) awarded to RBC. RBC is also a recipient of the CIHR New Investigator Award and the Early Research Award from the Ontario Ministry of Research and Innovation. MPG was supported by a CIHR Doctoral Canadian Graduate Scholarship.

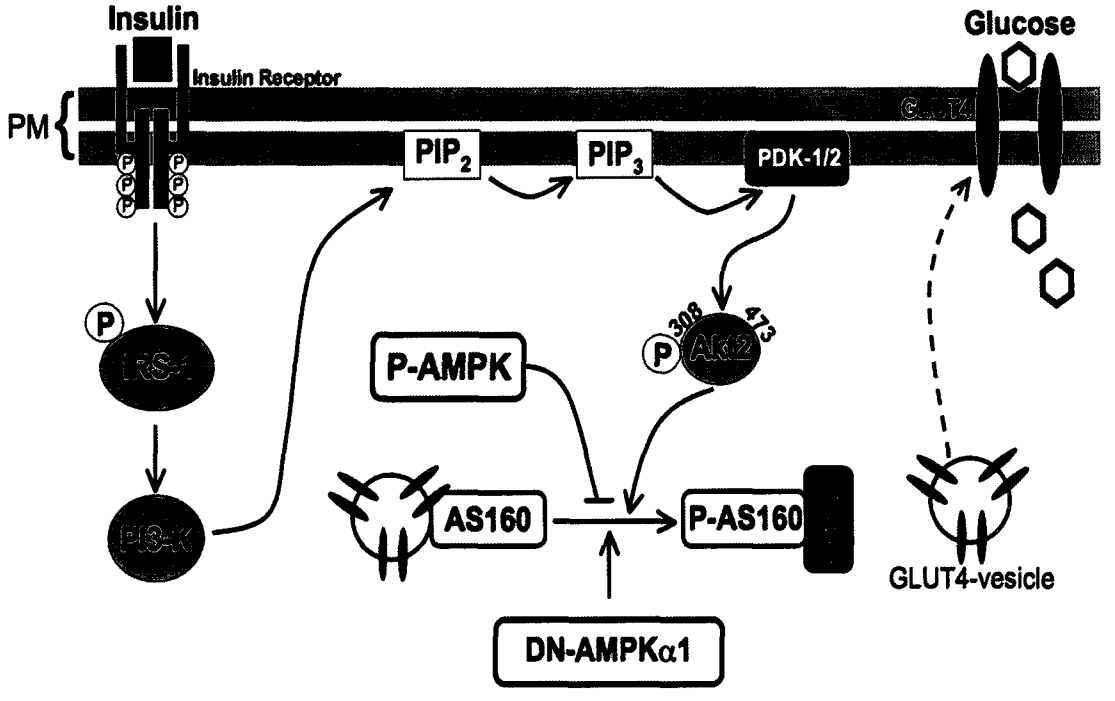

Figure 6-8. AMPK regulates glucose uptake in primary adipocytes. Under basal conditions, AS160 promotes intracellular retention of GLUT4-containing vesicles. When adipocytes are stimulated with insulin, this hormone binds to its receptor and elicits a cascade of events leading to phosphorylation/activation of Akt. This promotes phosphorylation of AS160, which interacts with 14-3-3 and releases the inhibitory effect on GLUT4 vesicles. GLUT4 is then translocated to the plasma membrane and facilitates glucose uptake into the cell. When AMPK is activated in adipocytes with AICAR, it prevents phosphorylation of AS160 and inhibits glucose uptake. Disruption of AMPKα1 signaling reverses the effects on AS160 phosphorylation and glucose uptake, indicating that AMPKα1 plays an important role in regulating glucose uptake in adipocytes.

CHAPTER 7:

Chronic AMP-kinase activation with AICAR reduces adiposity by remodeling adipocyte metabolism and increasing whole-body energy expenditure

Mandeep P. Gaidhu[1], Andrea Frontini[2], Steven Hung[1], Kathryn Pistor[1], Saverio Cinti[2], Rolando B. Ceddia[1]

[1] *Muscle Health Research Centre, York University, Toronto, ON, Canada.*

[2] *Department of Molecular Pathology and Innovative Therapies, School of Medicine, University of Ancona (Politecnica delle Marche), Ancona, Italy.*

Contribution of authors:

MPG organized, carried out all experiments, and wrote the manuscript. AF adminstered treatment, assisted with morphological analyses, and edited the manuscript. SH and KP assisted with administering treatment, operating the CLAMS, collecting blood samples, and conducting metabolic experiments. SC assisted with assessment of electron microscope images and edited the manuscript. RBC designed the experiments, helped conduct metabolic experiments, and edited the manuscript.

Keywords: AMPK, adipose tissue, metabolism, oxidation, energy expenditure

A version of this manuscript is under review at the *Journal of Lipid Research* (Manuscript #JLR/2011/015354)

ABSTRACT

This study investigated the effect of chronic AMP-kinase (AMPK) activation with 5-aminoimidazole-4-carboxamide-1-β-D-ribofuranoside (AICAR) on white adipose tissue (WAT) metabolism and the implications for visceral (VC) and subcutaneous (SC) adiposity, whole body-energy homeostasis, and hypothalamic leptin sensitivity. Male Wistar rats received daily single intraperitoneal injections of either saline or AICAR (0.7g/kg B.W.) for 4 and 8 weeks and pair-fed throughout the study. AICAR-treated rats had reduced adiposity with increased mitochondrial density in VC and SC fat pads, which was accompanied by reduced circulating leptin and time-dependent and depot-specific regulation of AMPK phosphorylation and fatty acid oxidation. Interestingly, the anorectic effect to exogenous leptin was more pronounced in AICAR-treated animals than controls. This corresponded to reductions in hypothalamic AMPK phosphorylation and suppressor of cytokine signaling 3 (SOCS3) content, while signal transducer and activator of transcription 3 (STAT3) phosphorylation was either unchanged or increased at 4 and 8 weeks in AICAR-treated rats. Ambulatory activity and whole-body energy expenditure (EE) were also increased with AICAR treatment. Altogether, chronic AICAR-induced AMPK activation increased WAT oxidative machinery, whole-body EE, and hypothalamic leptin sensitivity. This led to significant reductions in VC and SC adiposity without fully inducing energy-sparing mechanisms that oppose long-term fat loss.

INTRODUCTION

Successful treatment of obesity requires a continuous reduction in adiposity and maintenance of a healthy body weight. The conventional approaches used to achieve weight loss involve exercise and diet. However, as body fat is reduced through these approaches, energy-sparing mechanisms are activated and impose a major obstacle to long-term weight loss (4). Therefore, identifying strategies to overcome these energy-sparing mechanisms is crucial to improve the outcome of weight loss programs. One potential approach would be to remodel white adipose tissue (WAT) metabolism towards a highly metabolic brown adipose tissue (BAT) phenotype that shifts metabolism towards fat oxidation instead of storage, independently of altering whole-body energy expenditure (EE) through physical activity (320).

The acquisition of a "brown-like" phenotype by white adipocytes requires a substantial increase in mitochondrial content and up-regulation of the oxidative machinery in these cells. These functional changes could ultimately reduce fat storage and adipose tissue mass. In this context, one enzyme that is central to sense the energy state of the cell and regulate ATP production through fatty acid (FA) oxidation is AMP-kinase (AMPK). In its activated state, AMPK shuts down anabolic pathways and promotes catabolism by regulating the activity of key enzymes of intermediary metabolism (163). AMPK has also been shown to block adipocyte differentiation in the early stages by inhibiting clonal expansion, which is a critical step for adipogenesis to occur (229,230). Additionally, treatment of preadipocytes with pharmacological agents to activate AMPK prevents the expression of late adipogenic markers, fatty acid synthase,

acetyl-CoA carboxylase (ACC), and transcription factors PPARγ1/2 and C/EBPα which are required for the synthesis and storage of lipids in mature adipocytes (229,230). AMPK also phosphorylates and activates peroxisome proliferator-activated receptor (PPAR)-γ co-activator-1α (PGC-1α) and promotes mitochondrial biogenesis in skeletal muscle (209).

We have recently demonstrated that prolonged (15h) AICAR-induced AMPK activation increased mRNA expression of PPAR-γ and of its co-activator PGC-1α in isolated rat epididymal adipocytes (303). These cells also had ~4-fold higher than control expression of carnitine palmitoyl transferase-1b, which was accompanied by a 2-fold increase in palmitate oxidation and by a marked reduction in lipogenesis (303). Based on these observations, we hypothesized that chronic activation of AMPK *in vivo* could lead to a shift in WAT metabolism towards oxidation and lead to reduced adiposity. Additionally, the effects of chronic AMPK activation on remodeling WAT metabolism could potentially overcome the opposition to fat reduction triggered by the centrally-mediated activation of energy-sparing mechanisms as adiposity is reduced (321). Even though alterations in fat mass with chronic *in vivo* AICAR treatment in rodents have been previously reported (285,322,323), it is unknown whether these effects arise from direct structural and functional alterations in WAT or indirectly through alterations in whole-body energy homeostasis. Therefore, this study was designed to investigate the time-course effects of chronic *in vivo* AICAR-induced AMPK activation on VC and SC WAT metabolism, as well as on whole-body energy balance. Previous studies have demonstrated that major depot-specific differences exist with respect to metabolic

properties and plasticity under specific conditions (324). Thus, a goal of this study was also to determine whether VC and SC fat depots would elicit distinct responses to chronic AICAR-induced AMPK activation with regards to oxidative capacity. Furthermore, since alterations in fat mass also determine leptin expression and release by the WAT and this hormone exerts a major role in the regulation of whole-body EE (325), we assessed the time-course plasma profile of leptin. Phosphorylation and/or content of STAT3, AMPK, and SOCS3 were measured in the hypothalamus to assess leptin signaling in this tissue, as well as the anorectic response of AICAR-treated animals to exogenous leptin adminstration. This is the first study to provide evidence that chronic systemic pharmacological AMPK activation in rats remodels WAT metabolism by inducing mitochondrial biogenesis and promoting fat loss without inducing energy-sparing mechanisms. Importantly, this effect appears to be at least partially mediated by increased hypothalamic leptin sensitivity.

MATERIALS AND METHODS

Reagents – FA-free bovine serum albumin (BSA), free glycerol determination kit, glucose oxidase kit, isoproterenol, and palmitic acid were obtained from Sigma. [1-^{14}C]palmitic acid was from GE Healthcare Radiochemicals (Quebec City, Quebec). Leptin was measured using an ELISA from Millipore (Billerica, MA). AICAR was purchased from Toronto Research Chemicals (Toronto, Ontario). Recombinant rat leptin was obtained from Dr. A.F. Parlow at the National Hormone & Peptide Program (Torrance, CA). All antibodies were from Cell Signaling Technology Inc. (Beverly, MA)

unless noted otherwise. Phospho-acetyl-CoA carboxylase (P-ACC) was obtained from Upstate (Charlottesville, VA), and uncoupling protein 1 (UCP-1) was from Abcam (Cambridge, MA). All other chemicals were of the highest grade available.

In vivo *AICAR treatment and plasma analyses* – Male albino rats (Wistar strain) weighing 150–200 g, were maintained on a 12/12 h light/dark cycle at 22°C and fed standard laboratory chow *ad libitum*. Rats were given a single daily intraperitoneal injection of either saline or AICAR (0.7g/kg body weight) for 4 and 8 weeks. The dosage was chosen based on previous *in vivo* rat studies that used between 0.5 and 1.0g/kg body weight for chronic AICAR injections (285,303,323). Saline-injected rats were pair-fed to the AICAR-treated group to control for effects of altered food intake induced by the treatment. Control animals were pair-fed according to the average amount of chow consumed by the AICAR-treated animals the previous day. Pair-fed animals received one third of the total food in the morning (09:00) and the remaining two thirds immediately prior to lights off at 19:00 to avoid prolonged periods of fasting. Weekly blood samples were collected prior to daily injections from the saphenous vein and the plasma was frozen for later analyses of leptin.

Determination of in vivo *metabolic parameters* – The Comprehensive Laboratory Animal Monitoring System (CLAMS; Columbus Instruments, Inc. Ohio, USA) was used to perform all automated *in vivo* determinations as previously described (326). Briefly, the CLAMS measures oxygen consumption (VO_2), carbon dioxide production (VCO_2), and respiratory exchange ratio (RER). Each cage is also equipped with a system of infrared

beams that detects animal movement in the X and Z axes. Energy expenditure (EE) was calculated by multiplying the calorific value (CV= 3.815 + 1.232 × RER) by VO_2. Measurements using the CLAMS were performed on a weekly basis throughout the 8-week period. Animals were placed in the CLAMS at 10:00 immediately following the daily saline or AICAR injections. The first hour of data collected in the CLAMS was discarded, since it is the time required for the rats to fully acclimatize to the cage environment (326). The rats were monitored for a 24h-period encompassing the light (10:00-19:00 and 07:00-10:00) and dark (19:00-07:00) cycles.

Assessment of the anorectic response to leptin – Rats received daily injections of either saline or AICAR (0.7mg/kg b.w.) for 2 weeks. During this treatment period, control animals were pair-fed as described above. On the day of the test, food was removed from the cages at 07:00 and the animals were injected at 09:00 with either saline (control) or AICAR. Rats were fasted until the onset of the dark cycle (19:00; 12h fast). At this point, the animals were subdivided into 4 groups: control, leptin, AICAR, and AICAR plus leptin and then injected i.p. with either saline (control conditions) or recombinant rat leptin (5mg/kg b.w.). We used this dosage of leptin because it has been previously demonstrated to induce a significant reduction in food intake 4h post-injection in rats (327). In order to measure food intake, animals were placed in the CLAMS 15min post-leptin injection for 24h with *ad libitum* access to food.

Extraction of tissues and calculation of lean body mass (LBM) – Fat depots from subcutaneous-inguinal (ING), epididymal (EPI), and retroperitoneal (RP) regions were

quickly removed and weighed prior to being processed for various metabolic assays. Weights of all tissues were normalized per 100g of body weight. LBM was calculated as carcass weight with all skin, viscera and fat depots removed (326).

Isolation of adipocytes, and measurement of palmitate oxidation – After the 4 and 8-week treatment periods, fat depots from ING, EPI, and RP regions were quickly removed and adipocytes were isolated from each tissue as previously described (303,328). For palmitate oxidation, cells (5×10^5) were incubated in KRBH-3.5% containing 0.2μCi/mL of [1-^{14}C]palmitic acid, 200μM non-labeled palmitate, and 500μM of L-carnitine. Oxidation of palmitate was determined by collection of $^{14}CO_2$ (303,328).

Morphometric and ultrastructural analyses – Rats were anesthetized and transcardially perfused with 4% paraformaldehyde (PFA) in 0.1 M phosphate buffer (PB), pH 7.4. Subsequently, WAT depots were carefully dissected and postfixed by overnight immersion in the same fixative at 4°C. For light microscopy, tissues were washed in PB and dehydrated using an ethanol gradient, cleared in a solution of xylene, and embedded into paraffin blocks (329). Once embedded, 3μm thick sections were mounted onto glass slides, deparaffinized/rehydrated, and stained with hemotoxylin and eosin to assess morphological changes. Adipocyte size was calculated as the mean adipocyte area of 200 random adipocytes (100 per section) from each animal using the Nikon LUCIA Image program (version 4.61; Laboratory Imaging, Prague, Czech Republic). Tissue sections were observed with a Nikon Eclipse E800 light microscope using a 20X objective lens. Digital images were captured with a Nikon DXM 1200 camera. For electron microscopy,

small fragments of tissue were excised from perfused animals and placed into a solution consisting of 2% PFA + 2% glutaraldehyde in 0.1M PB, pH 7.4, overnight at 4°C. After primary fixation, tissues were placed in a solution of 1% osmium tetraoxide and 1% potassium ferrocyanide for 1h. Samples were then dehydrated using an acetone gradient and embedded in an Epon-Araldite mixture (329). Subsequently, ultrathin sections (50-65nm) were obtained with an MT-X ultratome (RMC; Tucson, AZ), stained with lead citrate, and examined with a CM10 transmission electron microscope (Philips; Eindhoven, The Netherlands). Mitochondrial and cytoplasmic areas were quantified using the LUCIA program from 30-40 images per tissue captured at 12,500X magnification. Mitochondrial density was determined as area of mitochondria occupying the area of cytoplasm.

Determination of content and phosphorylation of proteins by western blot – Fat depots were extracted and immediately snap frozen in liquid nitrogen. Immediately after decapitation, the hypothalamus was dissected using the optic tracts, the thalamus, and the mammillary body as landmarks, and then quickly frozen in liquid nitrogen and stored at -80°C. The tissues were homogenized in a buffer containing 25mM Tris-HCl and 25mM NaCl (pH 7.4), 1mM $MgCl_2$, 2.7mM KCl, 1% Triton-X, and protease and phosphatase inhibitors (0.5mM Na_3VO_4, 1mM NaF, 1μM leupeptin, 1μM pepstatin, and 20mM PMSF). Homogenates were centrifuged, the infranatant collected, and an aliquot was used to measure protein by the Bradford method. Samples were diluted 1:1 (vol/vol) with 2x Laemmli sample buffer, heated to 95°C for 5min, and subjected to SDS-PAGE. All

primary antibodies were used in a dilution of 1:1,000 except for P-AMPK (1:500). Equal loading was confirmed by both β-actin detection and Coomasie blue staining of gels.

RESULTS

Food intake, body weight, fat mass, and adipocyte morphology – A reduction in food intake with AICAR injections has been observed in previous studies in rodents (215), therefore food intake was measured on a daily basis in order to pair-feed control rats. Compared to *ad libitum*-fed rats, food intake was reduced by 10% and 3% after 4 and 8 weeks, respectively, in AICAR-treated rats. No differences in body weight or LBM were detected between control and AICAR-treated animals at any time point (data not shown). Analyses of WAT mass indicated that ING, RP, and EPI fat depots were reduced in AICAR-treated animals by 39%, 56%, and 43% after 4 weeks and by 22%, 47%, and 34% after 8 weeks, respectively (Figure 7-1). In ING and RP fat depots, adipocyte area was reduced by 33% and 37% at week 4 and by 37% and 42% at week 8, respectively (Figure 7-2A-C). Adipocyte area was unchanged in EPI fat pads after 4 weeks of AICAR treatment, but was 33% lower than controls after 8 weeks (Figure 7-2B). Western blot analyses of UCP-1 protein content (Figure 7-2D) and immunohistochemistry in WAT depots (Figure 7-3) indicated that AICAR treatment did not increase the prevalence of brown adipocytes within the WAT depots.

Mitochondrial density and morphology – For assessment of mitochondrial density and ultrastructural changes, we analyzed ING and RP fat pads as representative depots for SC and VC WAT, respectively. After 4 and 8 weeks of AICAR treatment, mitochondrial

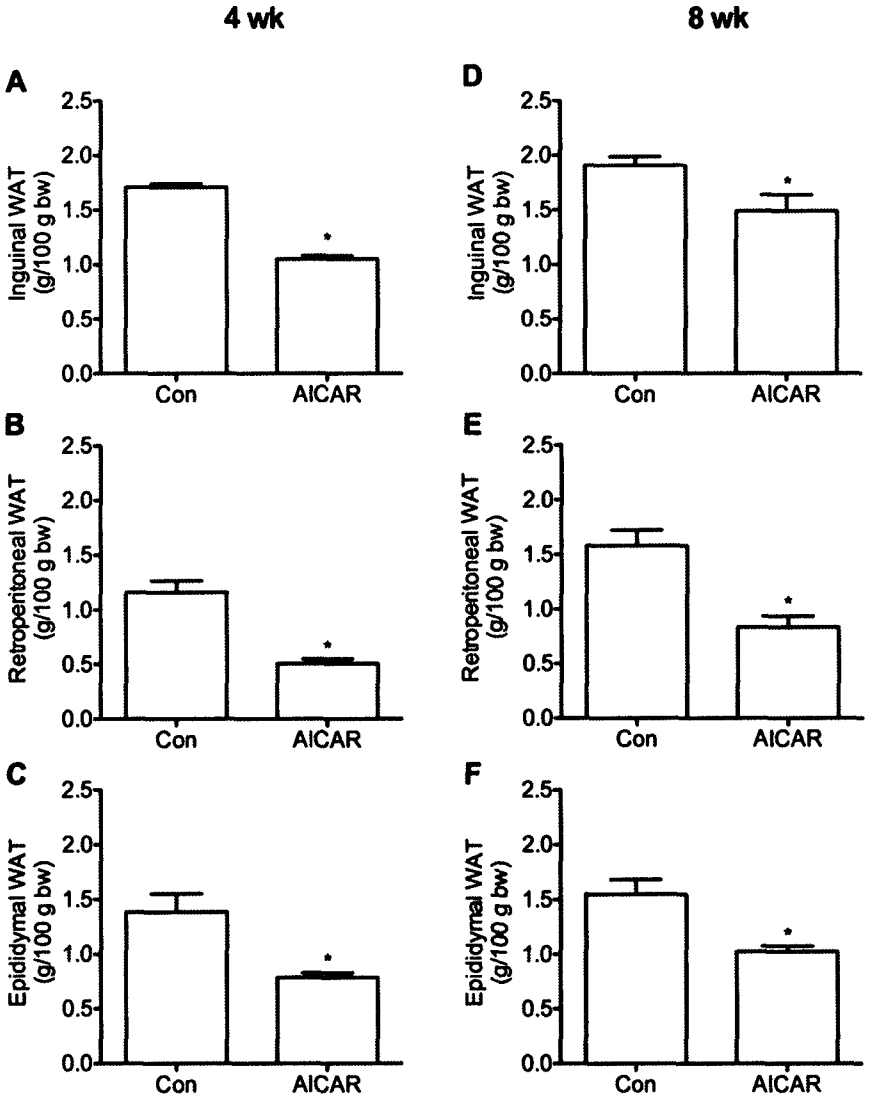

Figure 7-1. Fat pad mass of inguinal, retroperitoneal, and epididymal depots after 4 and 8 weeks of AICAR treatment (panels **A-C** and **D-F**, respectively). Fat pad mass was normalized to 100g of total body weight of the animal at the time of tissue harvest. N = 3-4 per group. $^{*}P<0.05$ vs. control (Con).

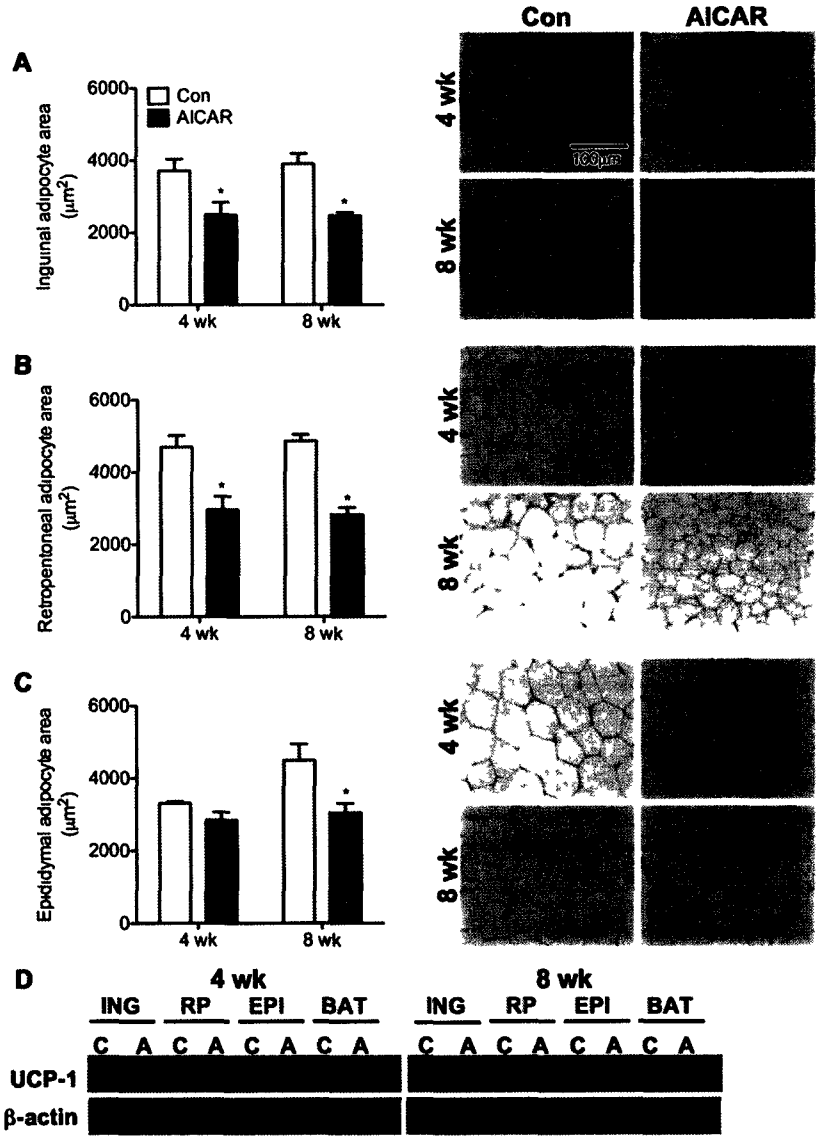

Figure 7-2. Measurement of adipocyte area in 4 and 8 week animals in inguinal **(A)**, retroperitoneal **(B)**, and epididymal **(C)** fat depots. All images were taken at 20X magnification and represent the same field of view for comparative purposes. The scale bar represents 100μm and applies to all panels. N=3 per group. Analysis of UCP-1 protein content in inguinal (ING), retroperitoneal (RP), epididymal (EPI), and brown adipose tissue (BAT) depots at 4 and 8 weeks **(D)**. Samples from control and AICAR-treated animals are denoted as 'C' and 'A', respectively. $^{*}P<0.05$ vs. respective control (Con) for 4 or 8 weeks.

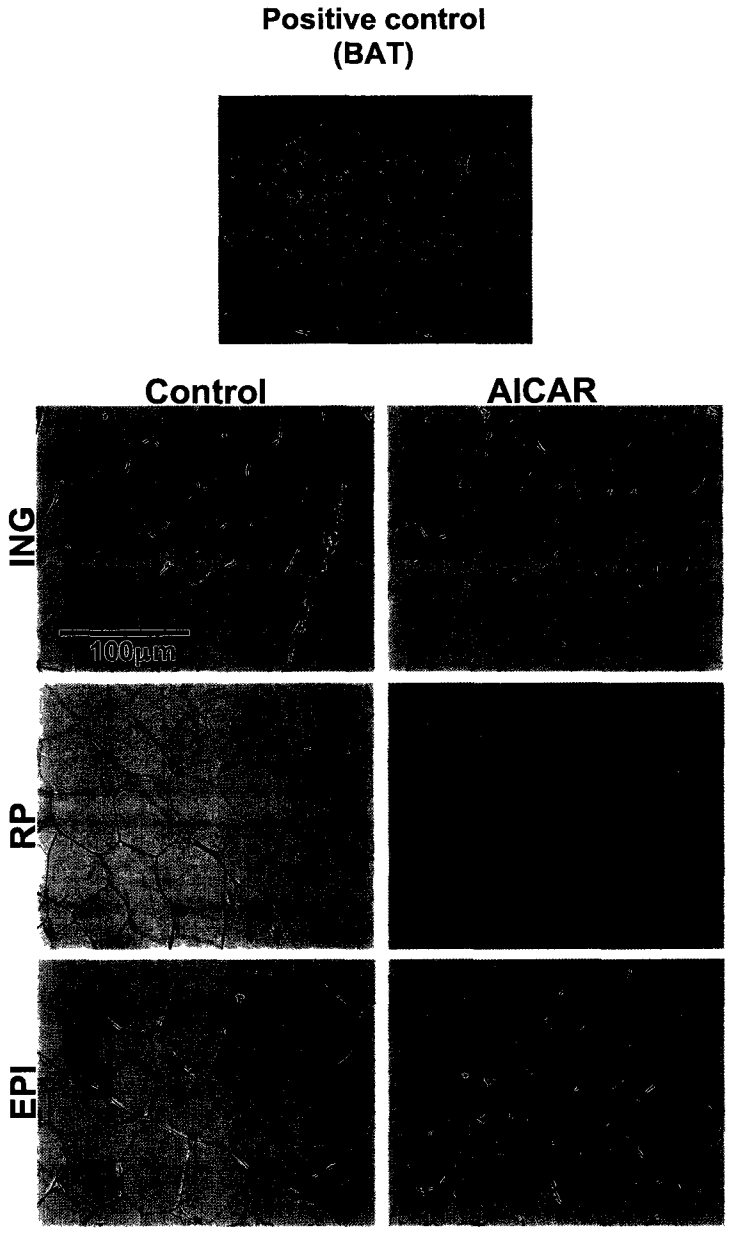

Figure 7-3. Immunohistochemistry on inguinal (ING), retroperitoneal (RP) and epididymal (EPI) fat depots for UCP-1 content. Brown adipose tissue (BAT) was used as a positive control for the primary antibody. Images are from animals treated for 8 weeks and show no change in UCP-1 staining in AICAR treated animals. Rats treated for 4 weeks also showed similar results. Scale bar represents 100µm.

density in both ING and RP WAT was increased by 1.78-fold and 2.45-fold and by 2.28-fold and 1.83-fold, respectively (Figure 7-4A-D). Additionally, electron microscopy analysis revealed that adipocytes from rats treated with AICAR for 4 or 8 weeks had mitochondria with more defined cristae when compared to adipocytes from control animals (Figure 7-4A-D, insets).

Effects of AICAR on AMPK and ACC phosphorylation and palmitate oxidation – As expected, AMPK phosphorylation (Thr172) increased in ING, RP, and EPI fat depots after 4 and 8 weeks of AICAR treatment. The most pronounced increase in AMPK phosphorylation was in the ING fat pads (Figure 7-5A). AMPK content in all fat depots was reduced in the AICAR group at week 4, an effect no longer present at week 8. ACC phosphorylation and protein content were markedly reduced at week 4 in ING, RP, and EPI fat pads; however the suppressive effect of AICAR on this variable was reversed at the 8-week time point with increased ACC content (Figure 7-5A). Palmitate oxidation increased in ING and RP adipocytes by ~1.46- and 1.84-fold, respectively, after 4 weeks of AICAR treatment, with no change observed in EPI cells (Figure 7-5B-D). Conversely, after 8 weeks of AICAR treatment intra-adipocyte palmitate oxidation reduced by 40%, 53%, and 48% in ING, RP, and EPI adipocytes, respectively (Figure 7-5E-G).

Whole-body EE, spontaneous ambulatory activity, and respiratory exchange ratio (RER) – Baseline values were collected prior to commencing the study and no differences existed between the two groups with respect to EE and ambulatory activity (data not shown). Time-course analysis revealed that EE increased by 8% at week 4 and then by

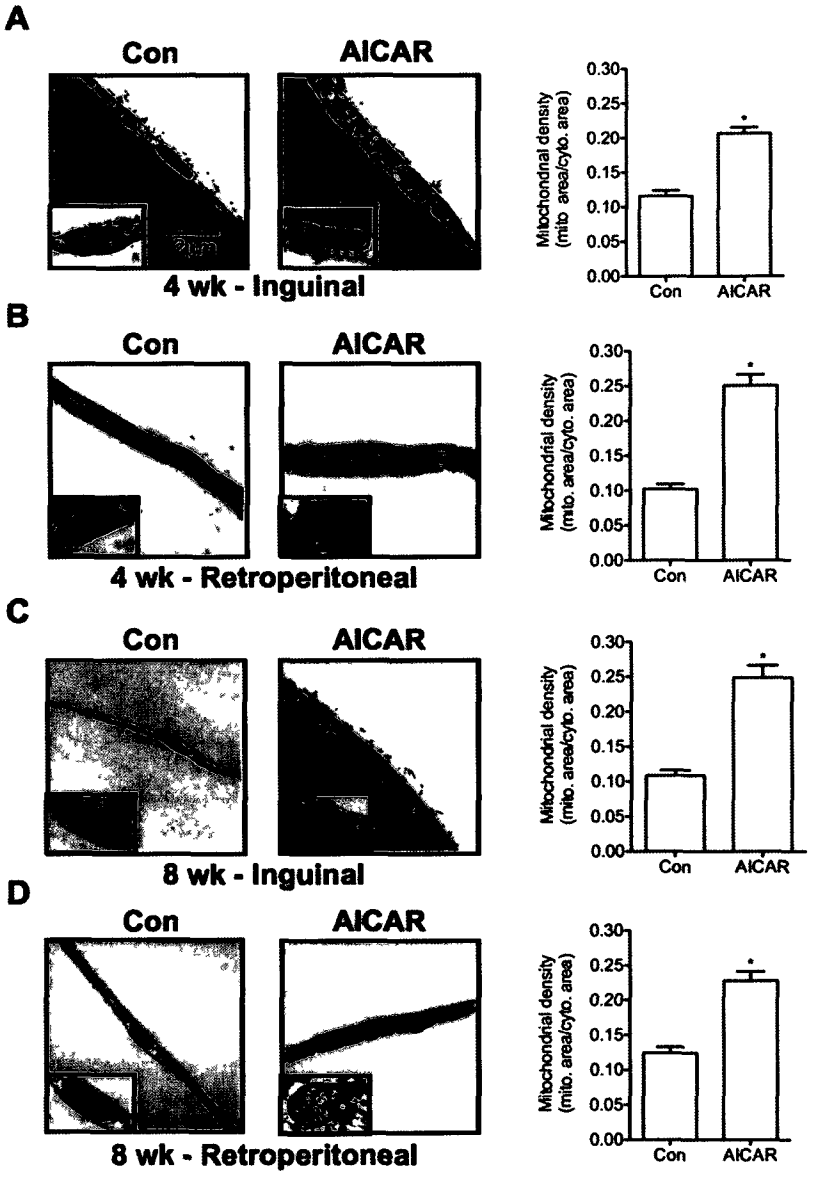

Figure 7-4. Mitochondrial density and morphology in inguinal (**A** and **C**) and retroperitoneal (**B** and **D**) fat depots at 4 and 8 weeks. Lipid droplet (LD). Arrows point to cristae within mitochondria (inset). All images were taken at 12,500X magnification, and insets are magnified. Scale bar represents 2μm and applies to all panels. N=3 per group. Unpaired t-tests. $^{*}P<0.05$ vs. control (Con).

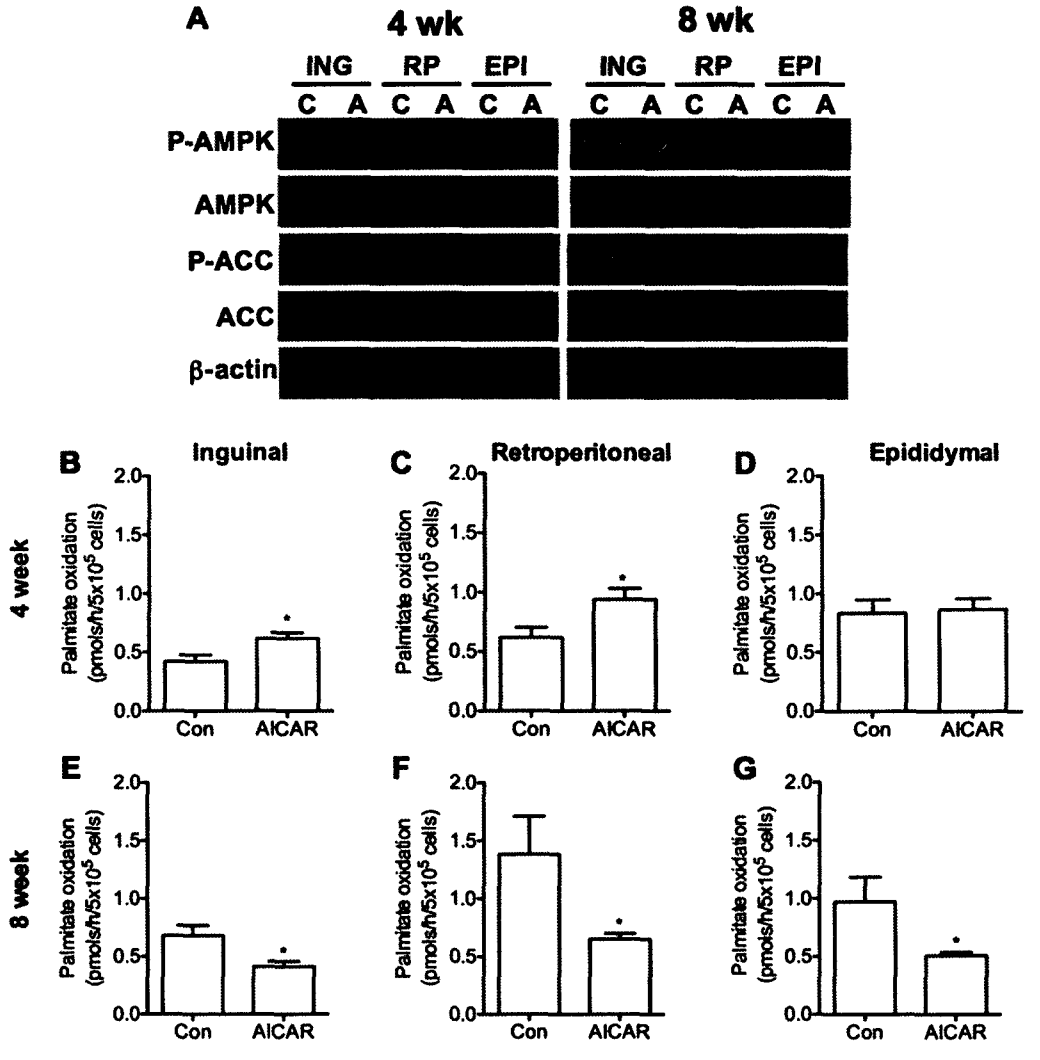

Figure 7-5. Phosphorylation and content of AMPK and ACC in inguinal (ING), retroperitoneal (RP), and epididymal (EPI) fat pads at 4 and 8 weeks **(A)**. Samples from control and AICAR-treated animals are denoted as 'C' and 'A', respectively. Blots are representative from N=3-4 per group. Palmitate oxidation in isolated adipocytes from ING (**B** and **E**), RP (**C** and **F**), and EPI (**D** and **G**) fat depots. Data are compiled from 4 independent experiments with N=4 per group, with triplicates in each assay performed. Unpaired t-tests. $^{*}P<0.05$ vs. control (Con).

16% at week 8 during the dark cycle in AICAR-treated rats (Figure 7-6A and B). This was also accompanied by 29 and 33% increases in dark cycle ambulatory activity as compared to controls in weeks 4 and 8, respectively (Figure 7-6C-D). RER was lower during the first light cycle (11:00 to 19:00) in AICAR-treated versus control rats (0.928 ± 0.007 vs 0.902 ± 0.011 and 0.925 ± 0.005 vs. 0.0.894 ± 0.015) ~8h subsequent to AICAR injection after 4 (Figure 7-7A-B) and 8 weeks (Figure 7-7C-D) respectively, indicating a shift towards fat oxidation in AICAR-treated animals. No differences in RER were detected between control and AICAR-treated rats during the dark cycle. However, during the second light cycle that preceded the daily AICAR injection (07:00 to 10:00), RER was lower in control than AICAR-treated animals (0.937 ± 0.005 vs 0.997 ± 0.002 and 0.949 ± 0.002 vs. 0.979 ± 0.003) after 4 and 8 weeks, respectively (Figure 7-7). This resulted from the pair-feeding procedure in which the control animals consumed their allotment of food before the end of the dark cycle leading to a reduction in RER.

Effects of AICAR on plasma measurements and hypothalamic leptin signaling – At weeks 4 and 8 of treatment, plasma leptin in AICAR-injected animals was lower than controls by 42% and 48%, respectively (Figure 7-8A). In the hypothalamus, STAT3 phosphorylation at tyrosine 705 was either unchanged or increased and AMPK phosphorylation was consistently reduced after 4 and 8 weeks of AICAR treatment, although the content of these proteins remained unchanged (Figure 7-8B). Hypothalamic SOCS3 content was also markedly reduced in the AICAR group at 4 and 8 weeks.

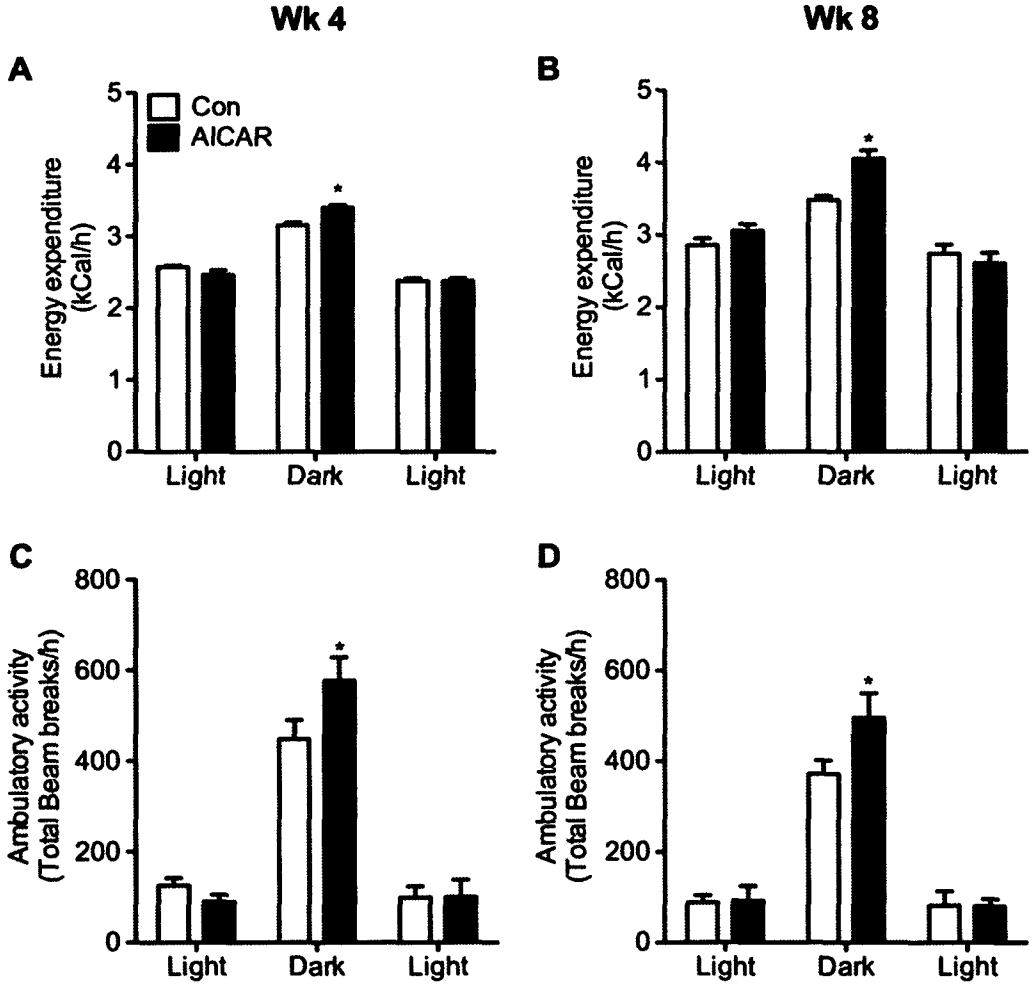

Figure 7-6. *In vivo* measurements of energy expenditure **(A-B)**, and ambulatory activity **(C-D)**. Rats were placed into the CLAMS for 24h after 4 and 8 weeks of treatment. Values from all animals were pooled an average for an N=4 per group. Data were analyzed based on light and dark cycles. The first light cycle occurred from 10am-7pm, where the animals were placed into the CLAMS immediately after their daily saline or AICAR injections. The dark cycle occurred from 7pm-7am, and the second light cycle is from 7am-10am in order to complete a full 24h cycle in the metabolic cages. Two-way ANOVA with Bonferroni post-hoc tests. *P<0.05 vs. control (Con) for each particular light/dark cycle.

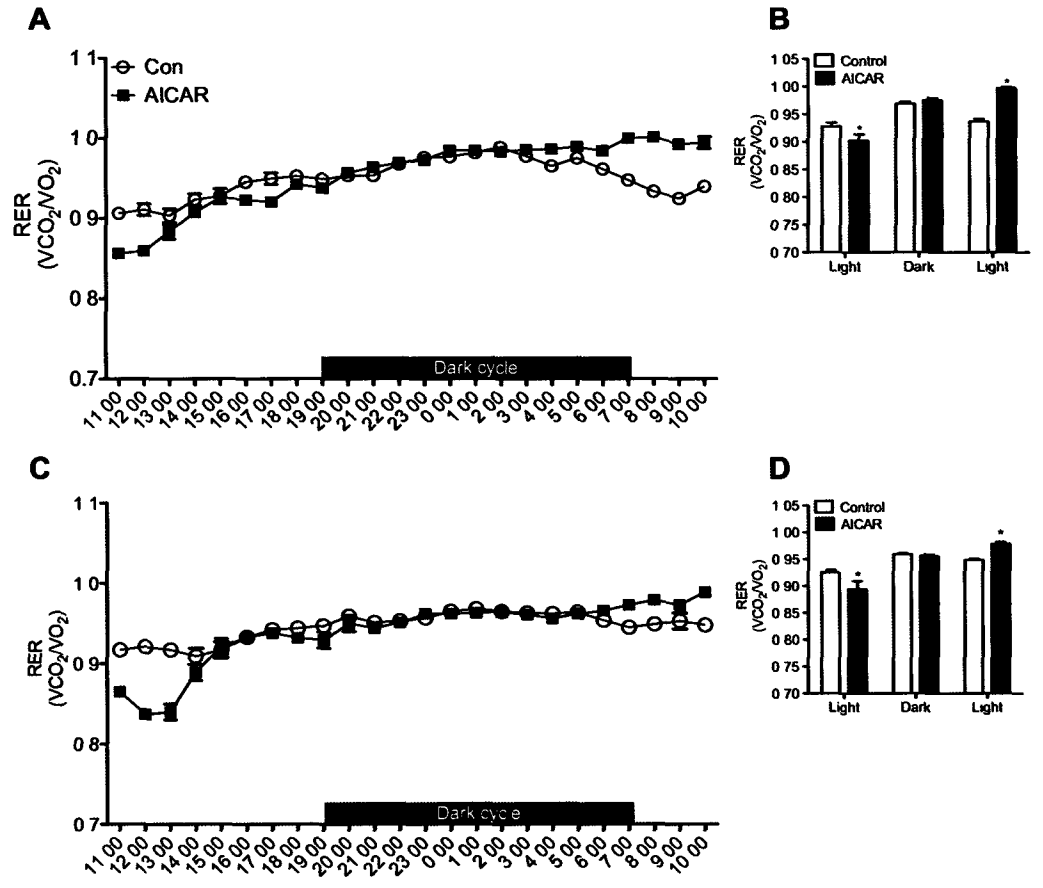

Figure 7-7. Respiratory exchange ratio (RER) after 4 **(A-B)** and 8 weeks **(C-D)** of AICAR treatment. Rats were placed into the CLAMS for 24h after 4 and 8 weeks of treatment. Panels **B** and **D** represent the average values for RER during the light and dark cycles and were analyzed using two-way ANOVA with Bonferroni post-hoc tests. *P<0.05 vs. control (Con) for each particular light/dark cycle.

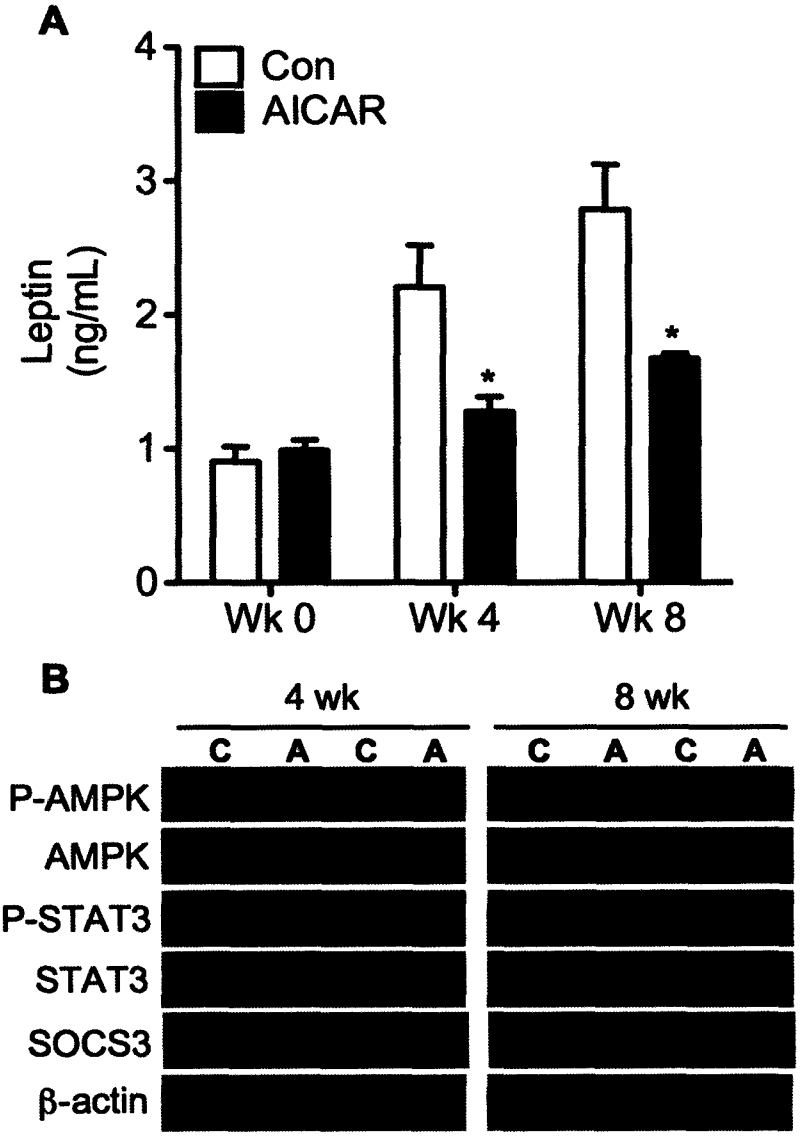

Figure 7-8. Levels of circulating leptin at weeks 0, 4, and 8 in control (Con) and AICAR treated animals (**A**). Assessment of phosphorylation and content of AMPK and SOCS3 in the hypothalami of rats at 4 and 8 weeks (**B**). N=4-8 for leptin concentrations. N=4 for western blot data. Control and AICAR-treated animals are denoted as 'C' and 'A', respectively. Two-way ANOVA with Bonferroni post-hoc tests. * and $^{\#}P<0.05$ vs. all other conditions.

Effects of AICAR on the anorexic response to leptin – We found that in the absence of leptin administration (saline injected in lieu of leptin), AICAR animals showed a 30% reduction in food intake after 4 hours compared to control rats (Table 7-1). This confirmed our previous observations that this drug caused an anorexic effect in these animals. When injected with leptin, control rats ate 35% less after 4h compared to saline-injected controls, indicating a robust response to leptin administration. Interestingly, when injected with both AICAR and leptin, animals exhibited a further significant reduction in food intake of 23% compared to animals treated with AICAR alone. This equated to a profound ~46% reduction in food intake when compared to control animals injected with saline. No differences in food intake were detected between all groups over a 24h period (Table 7-1).

DISCUSSION

Here, we report novel findings that chronic AICAR-induced AMPK activation promotes alterations in adipose tissue metabolism that leads to reduced VC and SC adiposity in rats. These effects were characterized by increased mitochondrial density and by the presence of mitochondria with more defined cristae in WAT of AICAR-treated animals. This was also accompanied by time-dependent up-regulation of FA oxidation in inguinal and retroperitoneal but not in epididymal adipocytes, indicating that not all VC fat depots change their metabolic profile in response to chronic AMPK activation. Our observations are in line with previous reports that epididymal fat is more "resistant" to morphological and metabolic changes compared to inguinal and retroperitoneal fat

	Food intake (g/4h)		Food intake (g/24h)	
	Saline	**Leptin**	**Saline**	**Leptin**
Control	12.50 ± 1.54	8.19 ± 1.28*	29.40 ± 0.90	27.92 ± 0.87
AICAR	8.74 ± 0.20*	6.76 ± 0.34$^{\#}$	26.86 ± 2.00	28.80 ± 0.65

Table 7-1. Food intake in control and AICAR-treated rats injected without or with leptin. Animals were injected on a daily basis with either saline (vehicle) or AICAR (0.7mg/kg b.w.) for 2 weeks. Subsequently, rats were fasted for 12h prior to injection with either saline or leptin and re-fed *ad libitum*. Food intake was monitored 4 and 24h post-leptin injection as a measure of sensitivity to the anorexic effects of leptin. N=4 for each condition. *P<0.05 compared to Control-Saline; $^{\#}$P<0.05 compared to Control-Saline and AICAR-Saline conditions.

depots, which have greater plasticity and ability to change metabolic function upon stimulation (324). Interestingly, although AICAR treatment reduced food intake and increased energy expenditure, these animals still gained fat mass between the 4 and 8-week period similar to control animals. From an energy balance perspective, this could be due to the attenuated anorexic effect of AICAR at the 8 week time point (~3% reduction in food intake) compared to 4 weeks (~10% reduction in food intake). Additionally, the suppression of intra-adipocyte oxidation observed at 8 weeks would also prevent depletion of lipid content from the WAT. Therefore, the increase in energy expenditure must have been counteracted by the above factors and could help explain why AICAR-treated animals still gained fat mass between the 4 and 8 week time period.

A surprising finding of this study was that the ability of adipocytes to oxidize FAs was increased and reduced after 4 and 8 weeks of AICAR treatment, respectively. This occurred despite the fact that mitochondrial density was augmented at both time points, indicating that the activity of the oxidative machinery was regulated differently during the course of treatment. The precise mechanisms underlying these differences are not clear. It may be at least partially explained by the fact that the initial adaptive responses to AMPK activation in WAT were driven to shift towards oxidation of FAs. This is supported by our previous observations that oxidation of endogenous and exogenous FAs was increased, while the costly processes of FA esterification and lipogenesis were potently suppressed in isolated adipocytes under prolonged AICAR exposure (303). Increased AMPK phosphorylation combined with undetectable levels of ACC protein is compatible with up-regulation of FA oxidation seen after 4 weeks of AICAR treatment.

However, FA oxidation was reduced at week 8, despite increased mitochondrial content in VC and SC adipocytes from AICAR-treated rats. The large reduction in intraadipocyte FA oxidation could represent an adaptive response to accommodate the increased demand for the supply of FA to peripheral tissues, particularly skeletal muscles. In fact, skeletal muscles have been previously demonstrated to significantly increase their ability to oxidize fat upon chronic AICAR-induced AMPK activation (330,331). Therefore, the reduction in intra-adipocyte FA oxidation seems compatible with the increased systemic demand for FA in AICAR-treated rats.

As expected with AICAR treatment, P-AMPK was increased in all fat depots at both 4 and 8 weeks, regardless of alterations in protein content. Surprisingly, AICAR treatment did not induce phosphorylation of ACC as expected, as this enzyme is a well-known downstream target of AMPK. However, the profound decrease in total ACC content at 4 weeks in AICAR treated animals would serve as a limiting factor for phosphorylation of this protein. In fact, it has been demonstrated in 3T3-L1 adipocytes that the content and/or activity of ACC are decreased in cells treated with various AMPK agonists, along with other adipogenic markers required for differentiation of preadipocytes into mature fat cells (229,230). In our study, animals begin AICAR treatment at ~6-7 weeks in age, which may have affected adipogenesis in preadipocytes present in the WAT. Interestingly, at 8 weeks there was a rebound in ACC protein content with AICAR treatment, although phosphorylation of this enzyme still remained suppressed in all fat depots. It is possible that the reemergence of ACC after 8 weeks of treatment was part of the adaptive metabolic response involved in the time-dependent down-regulation of FA

oxidation under conditions of reduced adiposity. Importantly, we also observed that ACC phosphorylation was not induced despite marked increases in AMPK phosphorylation at week 8 of AICAR treatment. This suggests that AMPK-independent mechanisms regulated ACC activity as adipocyte lipid content reduced with AICAR treatment. Work in our laboratory with adipocytes has demonstrated that certain metabolic effects of AICAR in WAT such as FA oxidation and glucose uptake are indeed mediated by AMPK (191,332). However, since our treatment is *in vivo* and delivered systemically, we must acknowledge that AMPK-independent effects may be taking place resulting in changes to parameters affecting whole-body metabolism.

Our immunohistochemistry and western blot analyses for the presence of UCP-1 in VC and SC fat depots demonstrated that brown adipogenesis by either transdifferentiation of white into brown adipocytes or recruitment of brown adipocyte precursors present within WAT was not induced with chronic AICAR-induced AMPK activation. Moreover, histological analysis excluded the development of UCP-1 negative multilocular adipocytes. Considering that AMPK is activated under conditions of ATP depletion and it acts to restore intracellular energy levels (163), it is compatible that UCP-1 content and activity was not up-regulated. This would allow substrate oxidation to be diverted towards ATP synthesis instead of non-shivering thermogenesis, ultimately serving to restore cellular energy levels. Therefore, our data provide evidence that the increased oxidative machinery of adipocytes exposed to chronic AICAR-induced AMPK activation did not result from white adipocytes converting to brown adipocytes. The absence of AMPK-induced BAT within WAT depots in our study is at odds with recent

studies that have demonstrated this effect in mice exposed to chronic AICAR treatment (215). Species differences (mice versus rats), duration of AICAR treatment (2 weeks versus 4 and 8 weeks), dosage (0.5mg/g b.w. versus 0.7mg/g b.w.) and frequency of injections (3 versus 7 days a week) could explain the different responses to chronic AICAR treatment between these studies.

The observed elevation in whole-body energy expenditure after 4 (8%) and 8 weeks (16%) of AICAR treatment seems to be mainly driven by increased dark cycle locomotor activity. In fact, this variable was significantly increased by 29% and 33% after 4 and 8 weeks of AICAR treatment, respectively, which is in line with studies where AICAR-injected mice elicited enhanced exercise capacity (323). Increased substrate oxidation by itself in skeletal muscle and liver did not seem to have contributed to increase energy expenditure in AICAR-treated rats. This is based on the fact that energy expenditure was only increased in AICAR-treated rats during the dark cycle when RER data indicated that there was no difference in substrate oxidation between the pair-fed controls and AICAR-treated rats. Importantly, others have also shown that the increases in mitochondrial FA oxidation do not necessarily lead to elevated whole-body energy expenditure (320).

It has repeatedly been demonstrated in rodents and humans that a reduction in fat mass is almost invariably followed by activation of energy-sparing mechanisms, which causes resistance to continuous long-term reduction in adiposity (68,325,333). At the whole-body level, these energy-sparing mechanisms could counteract and offset potential fat-reducing effects induced by remodeling white adipocyte metabolism towards a more oxidative phenotype. The activation of energy-sparing mechanisms under conditions of

reduced adiposity has been attributed to a drop in circulating leptin, since exogenous replacement of this hormone to pre-weight loss values reverses this adaptive response (68). In order to exert its effects on energy balance (334), leptin must bind to its receptor (LepR), permitting STAT3 to dock onto the LepR. STAT3 is then phosphorylated, homodimerizes, and enters the nucleus to promote the expression of genes that inhibit food intake and increase energy expenditure. It also promotes the expression of SOCS3, which serves as a negative feedback regulator of leptin signaling. Therefore, while activation of AMPK in the hypothalamus induces food intake and favors weight gain, inhibition of this kinase by leptin blocks these centrally-mediated effects on energy balance (231,238). Based on these observations, we hypothesized that energy-sparing mechanisms would be activated in AICAR-treated rats. This could occur by AICAR directly increasing hypothalamic AMPK activity, since previous studies have demonstrated that this drug can cross the blood brain barrier with limited permeability (335). Alternatively, AICAR could indirectly lead to activation of energy-sparing mechanisms by reducing circulating leptin as a consequence of fat loss induced by prolonged AMPK activation in SC and VC fat depots. Time-course analyses revealed that circulating leptin indeed dropped ~40% in AICAR-treated rats when compared to pair-fed controls, which was compatible with the differences in adiposity between the groups. However, phosphorylation of hypothalamic AMPK was reduced, while STAT3 phosphorylation was either the same or increased in AICAR-injected animals when compared to controls after 4 and 8 weeks. Furthermore, these effects were accompanied by marked reductions in the content of SOCS3 in the hypothalamus. These findings

indicated that leptin sensitivity in this tissue was actually increased with systemic AICAR-induced AMPK activation. In line with this hypothesis, our data suggest that with respect to the anorexic effects of leptin, AICAR-treated animals showed a greater sensitivity to this hormone compared to their control counterparts. This is corroborated with our hypothalamic signaling data indicating that P-AMPK was reduced in AICAR-treated rats. Interestingly, leptin has been demonstrated to play a major role in relaying to the hypothalamus information regarding the amount of energy stored in the organism, allowing the central nervous system (CNS) to regulate non-exercise activity thermogenesis accordingly (333,336,337). Therefore, the increases in ambulatory activity and EE observed in this study could also be attributed to enhanced CNS leptin sensitivity. Further studies are required to investigate possible direct actions of AICAR on specific hypothalamic sites involved in the control of food intake and energy homeostasis.

Altogether, our novel findings provide evidence that significant reductions in adiposity may be achieved through systemic pharmacological AMPK activation. Based on our data, this approach causes neither WAT to BAT transdifferentiation nor recruitment of brown adipocyte precursors within WAT. Rather, it increases the oxidative machinery in white adipocytes and induces remodeling of WAT metabolism toward a catabolic state. Importantly, the adipose-reducing effects of chronic AICAR-induced AMPK activation increased hypothalamic leptin sensitivity, and thus did not trigger the typical centrally-mediated adaptive responses that oppose long-term weight loss.

ACKNOWLEDGEMENTS

The authors state no conflict or duality of interest in regards to this work. This research was funded by an operating grant from the Canadian Institute of Health Research (CIHR MOP - 86538) and by infrastructure grants from the Canada Foundation for Innovation (CFI) and the Ontario Research Fund (ORF) awarded to RBC. RBC is also a recipient of the CIHR New Investigator Award and the Early Research Award from the Ontario Ministry of Research and Innovation. The morphometry and imaging portions of the study were funded by a Scientific Research Grant (RSA) of Università Politecnica delle Marche to SC. MPG was supported in part by the CIHR Michael Smith Foreign Study Supplement, and is currently supported by the Canadian Diabetes Association (CDA) Doctoral Student Research Award. AF is supported by an Italian foundation for Research and Development (Fondazione Cariverona). The authors would like to thank Cristina Maria Zingaretti from the University of Ancona, for her technical expertise in acquiring transmission electron microscope images.

CHAPTER 8: STUDY LIMITATIONS

Although all experiments were designed to control as many variables as possible, we must acknowledge that limitations exist in every study executed.

In this dissertation (chapters 4, 6, and 7), we must take into account the possibility that AICAR, like other pharmacological agents, exerts effects independent of AMPK activation. For example, in skeletal muscle of AMPK$\beta_2^{-/-}$ mice, the effect of AICAR on glucose uptake was blunted, while no change in FA oxidation occurred, indicating that AICAR increased the latter independently of AMPKβ_2 (338). Work from our laboratory also suggests that not all metabolic parameters that are altered with AICAR treatment are mediated by AMPK, such as glucose oxidation. Furthermore, although it has been demonstrated that short term treatment with AICAR does not alter the AMP:ATP in the cell, longer exposure of hepatocytes have been shown to inhibit mitochondrial complex 1 thereby activating AMPK indirectly . Importantly, our *in vitro* work has indicated that the effects of AICAR on FA oxidation and glucose uptake in adipocytes are indeed mediated by AMPK (191,332). However, in our *in vivo* studies, we must acknowledge that since the treatment is being delivered systemically, AMPK-independent effects may be taking place in other tissues, resulting in changes to parameters that affect whole-body metabolism. New small molecule agonists such as A-769662, which are not adenosine analogs, have been designed in an attempt to increase specificity with regards to activation of AMPK (266). Also, tissue-specific and conditional transgenic and knockout mice models have also been developed as tools that can give insight into the specificity of various AMPK activators.

In chapter 7, it must be considered that with a small sample size (N=3-4) the variability between animals, particularly in regards to the *in vivo* data, limits our ability to draw more definitive conclusions with respect to whole-body energy homeostasis. However, it is important to point out that two independent experiments were carried out with 4 AICAR-treated and 4 pair-fed animals per group (total of 8 animals per condition) and alterations in food intake and fat mass were consistently reproduced. Unfortunately, the *in vivo* metabolic analysis using the CLAMS could not be performed in all 8 animals. This occurred because one of the experiments was carried out in Italy for morphologic analysis of tissues and the CLAMS was not available at the time for *in vivo* measurements. Despite these limitations, all treated animals demonstrated the phenotype as expected based on published literature and previous work carried out in our laboratory. Therefore, a small sample size may in fact be underestimating the effects of chronic AICAR-induced AMPK activation in these animals. In order to increase the statistical power in this particular study, another group of animals will be required.

Our rationale for using rats was based on the fact that these animals more closely resemble humans with regards to *in vivo* metabolic parameters when compared to mice. Mice have a much higher metabolic rate than rats and humans, which makes it more difficult to obtain stable and reliable *in vivo* data using indirect calorimetry. However, the lack of available genetically modified rats imposes a limitation on investigating certain mechanistic aspects of AICAR treatment. The use of mice such as the *ob/ob* and *db/db* models commercially available may allow us to investigate whether the effects of long-term AICAR treatment are mediated by increased leptin sensitivity. Furthermore, the use

of mice will give access to different transgenic and knockout models of various AMPK subunits that can directly address questions regarding molecular mechanisms of action that lead to certain metabolic alterations.

CHAPTER 9: SUMMARY AND CONCLUSIONS

The studies presented here were designed to investigate the role of AMPK in adipocyte metabolism and whether activation of this enzyme could promote energy dissipation versus lipid storage in fat cells. Since excessive WAT deposits are characteristic of obesity, the evidence obtained from our work could help identify whether AMPK or other pathways affected by this enzyme could be potential targets for the development of drugs to treat obesity.

We first utilized an *in vitro* approach in order to address the role of AMPK in lipid partitioning, and the molecular mechanisms that were governing these processes (Objective #1) (303). We determined that in WAT, chronic pharmacological activation of AMPK exerted distinct time-dependent regulation of HSL and ATGL in order to regulate lipolysis. Since the primary function of WAT is to store energy when in excess and provision substrate under conditions of higher energy demand, understanding the role of AMPK in lipolysis is important in identifying mechanisms that could be malfunctioning in conditions such as obesity. Furthermore, we determined that expression of genes (i.e. PGC-1α, PPARα, PPARδ, CPT-1) that promote lipid utilization were up-regulated in adipocytes exposed to AICAR for 15h, and this was accompanied by increased intra-adipocyte FA oxidation. Interestingly, when we examined these parameters in a diet-induced obesity model (Objective #2) (328), impairment of AMPK activity and down-regulation of PGC-1α and PPARα resulted in elevated esterification and reduced ability to oxidize FA in VC and SC adipocytes. Additionally, the regulation of lipolysis by AMPK through HSL and ATGL gives insight into the magnitude by which AMPK can

control and prevent excessive release of FAs into the circulation. This is of particular importance under obese conditions, where FA release is excessive and results in insulin-resistance and subsequently type 2 diabetes.

The role of AMPK is also important when considering glucose metabolism since glucose is necessary for the costly process of FA re-esterification. Therefore, it is compatible that our lab (191,303) and others (190) have shown that AMPK activation suppresses glucose uptake in adipocytes. We were interested in the molecular mechanisms by which AMPK inhibits glucose uptake in WAT, and whether this enzyme was absolutely required for the regulation of this process. We provide the first evidence demonstrating that AICAR-induced AMPK activation suppresses glucose uptake by impairing phosphorylation of AS160 and preventing GLUT4 translocation to the plasma membrane (Objective #3) (332). Disruption of AMPKα1 signaling reversed these effects, indicating that AMPKα1 plays an important role in regulating glucose levels in the WAT in order to suppress lipid storage.

Our final objective (Objective #4) was an *in vivo* study that integrated the effects of systemic AMPK activation on whole-body metabolism as well as tissue-specific analyses on WAT function and structure. Data collected using metabolic cages indicate that energy expenditure and ambulatory activity are increased in rats treated with AICAR despite profound reductions in adiposity, suggesting that the compensatory mechanisms commonly seen with weight loss are not activated in these animals. This may be partially mediated by increased hypothalamic leptin sensitivity, since AICAR treated animals had less circulating leptin yet P-STAT3 levels that were similar or higher than controls. We

also show novel evidence that AICAR treatment induces a higher mitochondrial density in visceral and subcutaneous fat depots through direct quantification of mitochondria, which supports our previous study showing increased expression of markers involved in mitochondrial biogenesis (303).

Considering all of our studies assessing the role of AMPK using *in vitro* and *in vivo* approaches in WAT, our data clearly indicate that chronic activation of AMPK promotes energy dissipation and suppresses fat storage. Importantly, the absence of AMPK activity under diet-induced obesity conditions suggests that impaired activity of this enzyme is involved in dysfunctional lipid handling seen in obesity. Altogether, our findings support the hypothesis that AMPK could be a molecular target for developing novel and effective strategies to treat obesity and its related metabolic disorders.

CHAPTER 10: FUTURE DIRECTIONS

Does activation of AMPK using nutritional supplements elicit the same metabolic changes seen with the use of AICAR?

Our data clearly indicate the beneficial effects of chronic AICAR treatment on reducing adiposity without inducing the energy-sparing mechanisms commonly associated with weight loss. However, bioavailability of AICAR is low when administered orally, and requires intravenous delivery in order to enter the circulation at effective doses. Thus, identification of compounds that stimulate AMPK activity through nutrition have become of great therapeutic interest. In this context, resveratrol is a natural polyphenol compound present in grapes and red wine. Studies have shown that resveratrol activates AMPK indirectly by inhibiting ATP synthase and by reducing cellular ATP levels (339). Recent *in vivo* studies have demonstrated that the negative effects of HF diet on health can be alleviated by supplementing the diet of mice with resveratrol, while this effect was absent in AMPKα1-deficient mice (340). Therefore, we are interested in testing whether nutritional delivery of resveratrol can elicit the same metabolic effects and structural changes within the WAT as seen with chronic AICAR treatment. Resveratrol will be administered to male Wistar rats (~200g starting weight) through a specially formulated diet containing 0.04% resveratrol in standard chow from Dyets Inc. (Bethlehem, PA) (272,340). Diet will be administered for 4 and 8 weeks with control animals fed standard chow. Prior to the end of treatment, animals will be placed in metabolic cages to assess *in vivo* metabolic parameters (RER, VO_2, VCO_2, energy expenditure, ambulatory activity). After treatment, rats will be sacrificed, the adipose

tissue weighed and extracted to assess the following parameters: ***1)*** *palmitate oxidation;* ***2)*** *mitochondrial content;* ***3)*** *expression of genes involved in oxidative metabolism;* ***4)*** *basal and catecholamine-stimulated lipolysis;* ***5)*** *analyses of proteins involved in the lipolytic pathway;* ***6)*** *plasma measurements of FAs, leptin, and glucose.* This work will provide insight into whether activation of AMPK using a nutritional aid is sufficient to reduce adiposity and promote energy dissipation versus storage in the WAT. Additionally, *in vivo* metabolic data will allow us to determine whether energy-sparing mechanisms are activated with resveratrol-induced AMPK activation.

What regions of the hypothalamus are activated in response to chronic AICAR treatment?

Treatment with AICAR for 4 and 8 weeks in rats elicited a reduction in food intake, and increase in energy expenditure despite reductions in adiposity. Analyses of leptin signaling in the hypothalamus indicated that phosphorylation of STAT3 was unchanged or increased in AICAR treated animals, despite lower levels of circulating leptin. Additionally, phosphorylation of AMPK was reduced, which is compatible with a reduction in food intake. However, it is unclear what specific regions/circuits of the hypothalamus were altered in response to AICAR treatment. This is important, since the ventromedial/dorsomedial/paraventricular hypothalamus, and arcuate nucleus have increased AMPK activity in response to fasting or via pharmacological action, with other areas of the hypothalamus being unaffected (231,238,241,341). To address this question, male Wistar rats (~200g starting weight) treated with either saline or AICAR (0.7mg/kg b.w.) for 4 and 8 weeks will be sacrificed and the entire brain carefully excised. The brain

is then fixed in 4% paraformaldehyde for 24h, and transferred to a 30% sucrose solution for cryoprotection for 48h. Using a cryostat, 8μm sections of the brain will be taken, using an atlas for reference to determine location of hypothalamic nuclei. The most suitable sections for IHC analyses will be confirmed using Nissl staining on serial sections. IHC procedures are described elsewhere on floating sections (342), and we will use this procedure to analyze the following proteins using commercially available antibodies: ***1)*** *Δ-fosB, which is present after chronic activation of neuronal circuits;* ***2)*** *phosphorylation and content of AMPK and ACC;* ***3)*** *β-endorphin and melanocyte-stimulating hormone as products of POMC;* ***4)*** *prepro-NPY and NPY.* Analyses of these neuropeptides and their abundance/phosphorylation in various regions in the hypothalamus will give insight into the potential mechanisms by which AICAR treatment reduces food intake and increases energy expenditure.

REFERENCES

1. Shields, M., C. MD and C.L. Ogden. 2011. Adult Obesity Prevalence in Canada and the United States. *National Center for Health Statistics* **56**:1-8.
2. Shields, M. 2008. Nutrition: Findings from the Canadian Community Health Survey - Measured Obesity: Overweight Canadian children and adolescents. *Statistics Canada Catalogue No 82-620-MWE* **1**:1-34.
3. Anis, A.H., W. Zhang, N. Bansback, D.P. Guh, Z. Amarsi and C.L. Birmingham. 2010. Obesity and overweight in Canada: an updated cost-of-illness study. *Obes Rev* **11**:31-40.
4. Rosenbaum, M. and R.L. Leibel. 1998. The physiology of body weight regulation: relevance to the etiology of obesity in children. *Pediatrics* **101**:525-539.
5. Leibel, R.L., M. Rosenbaum and J. Hirsch. 1995. Changes in energy expenditure resulting from altered body weight. *N Engl J Med* **332**:621-628.
6. Connolly, H.M., J.L. Crary, M.D. McGoon, D.D. Hensrud, B.S. Edwards, W.D. Edwards and H.V. Schaff. 1997. Valvular heart disease associated with fenfluramine-phentermine. *N Engl J Med* **337**:581-588.
7. Chen, S.P., M.H. Tang, S.W. Ng, W.T. Poon, A.Y. Chan and T.W. Mak. 2010. Psychosis associated with usage of herbal slimming products adulterated with sibutramine: a case series. *Clin Toxicol (Phila)* **48**:832-838.
8. Peterson, E., A. Stoebner, J. Weatherill and E. Kutscher. 2008. Case of acute psychosis from herbal supplements. *S D Med* **61**:173-177.
9. Pittler, M.H., K. Schmidt and E. Ernst. 2005. Adverse events of herbal food supplements for body weight reduction: systematic review. *Obes Rev* **6**:93-111.
10. Cinti, S. 2009. Transdifferentiation properties of adipocytes in the Adipose Organ. *Am J Physiol Endocrinol Metab* **297**:E977-E986.
11. Fruhbeck, G. 2008. Overview of adipose tissue and its role in obesity and metabolic disorders. *Methods Mol Biol* **456**:1-22.
12. Bays, H.E., J.M. Gonzalez-Campoy, G.A. Bray, A.E. Kitabchi, D.A. Bergman, A.B. Schorr, H.W. Rodbard and R.R. Henry. 2008. Pathogenic potential of adipose tissue and metabolic consequences of adipocyte hypertrophy and increased visceral adiposity. *Expert Rev Cardiovasc Ther* **6**:343-368.
13. Leibel, R.L. 2008. Molecular physiology of weight regulation in mice and humans. *Int J Obes (Lond)* **32 Suppl 7**:S98-108.
14. DiGirolamo, M. and J.B. Fine. 2001. Cellularity measurements. *Methods Mol Biol* **155**:65-75.
15. Forest, C., J. Tordjman, M. Glorian, E. Duplus, G. Chauvet, J. Quette, E.G. Beale and B. Antoine. 2003. Fatty acid recycling in adipocytes: a role for glyceroneogenesis and phosphoenolpyruvate carboxykinase. *Biochem Soc Trans* **31**:1125-1129.
16. Ducluzeau, P.H., L.M. Fletcher, H. Vidal, M. Laville and J.M. Tavare. 2002. Molecular mechanisms of insulin-stimulated glucose uptake in adipocytes. *Diabetes Metab* **28**:85-92.

17. Taniguchi, C.M., B. Emanuelli and C.R. Kahn. 2006. Critical nodes in signalling pathways: insights into insulin action. *Nat Rev Mol Cell Biol* **7**:85-96.
18. Wang, T., Y. Zang, W. Ling, B.E. Corkey and W. Guo. 2003. Metabolic partitioning of endogenous fatty acid in adipocytes. *Obes Res* **11**:880-887.
19. Zeigerer, A., M.A. Lampson, O. Karylowski, D.D. Sabatini, M. Adesnik, M. Ren and T.E. McGraw. 2002. GLUT4 retention in adipocytes requires two intracellular insulin-regulated transport steps. *Mol Biol Cell* **13**:2421-2435.
20. Miinea, C.P., H. Sano, S. Kane, E. Sano, M. Fukuda, J. Peranen, W.S. Lane and G.E. Lienhard. 2005. AS160, the Akt substrate regulating GLUT4 translocation, has a functional Rab GTPase-activating protein domain. *Biochem J* **391**:87-93.
21. Zerial, M. and H. McBride. 2001. Rab proteins as membrane organizers. *Nat Rev Mol Cell Biol* **2**:107-117.
22. Sano, H., S. Kane, E. Sano, C.P. Miinea, J.M. Asara, W.S. Lane, C.W. Garner and G.E. Lienhard. 2003. Insulin-stimulated phosphorylation of a Rab GTPase-activating protein regulates GLUT4 translocation. *J Biol Chem* **278**:14599-14602.
23. Olswang, Y., H. Cohen, O. Papo, H. Cassuto, C.M. Croniger, P. Hakimi, S.M. Tilghman, R.W. Hanson and L. Reshef. 2002. A mutation in the peroxisome proliferator-activated receptor gamma-binding site in the gene for the cytosolic form of phosphoenolpyruvate carboxykinase reduces adipose tissue size and fat content in mice. *Proc Natl Acad Sci U S A* **99**:625-630.
24. Franckhauser, S., S. Munoz, A. Pujol, A. Casellas, E. Riu, P. Otaegui, B. Su and F. Bosch. 2002. Increased fatty acid re-esterification by PEPCK overexpression in adipose tissue leads to obesity without insulin resistance. *Diabetes* **51**:624-630.
25. Cesar, T.B., M.R. Oliveira, C.H. Mesquita and R.C. Maranhao. 2006. High cholesterol intake modifies chylomicron metabolism in normolipidemic young men. *J Nutr* **136**:971-976.
26. Kiens, B. 2006. Skeletal muscle lipid metabolism in exercise and insulin resistance. *Physiol Rev* **86**:205-243.
27. Hamilton, J.A. and F. Kamp. 1999. How are free fatty acids transported in membranes? Is it by proteins or by free diffusion through the lipids? *Diabetes* **48**:2255-2269.
28. Ball, E.G. 1966. Regulation of fatty acid synthesis in adipose tissue. *Adv Enzyme Regul* **4**:3-18.
29. Ruderman, N.B., A.K. Saha, D. Vavvas and L.A. Witters. 1999. Malonyl-CoA, fuel sensing, and insulin resistance. *Am J Physiol* **276**:E1-E18.
30. Munday, M.R. 2002. Regulation of mammalian acetyl-CoA carboxylase. *Biochem Soc Trans* **30**:1059-1064.
31. Frayn, K.N., F. Karpe, B.A. Fielding, I.A. Macdonald and S.W. Coppack. 2003. Integrative physiology of human adipose tissue. *Int J Obes Relat Metab Disord* **27**:875-888.
32. Neumann-Haefelin, C., A. Beha, J. Kuhlmann, U. Belz, M. Gerl, M. Quint, G. Biemer-Daub, M. Broenstrup, M. Stein, E. Kleinschmidt, H.L. Schaefer, D. Schmoll, W. Kramer, H.P. Juretschke and A.W. Herling. 2004. Muscle-type

specific intramyocellular and hepatic lipid metabolism during starvation in wistar rats. *Diabetes* **53**:528-534.

33. Romijn, J.A., E.F. Coyle, L.S. Sidossis, A. Gastaldelli, J.F. Horowitz, E. Endert and R.R. Wolfe. 1993. Regulation of endogenous fat and carbohydrate metabolism in relation to exercise intensity and duration. *Am J Physiol* **265**:E380-91.
34. Tansey, J.T., C. Sztalryd, E.M. Hlavin, A.R. Kimmel and C. Londos. 2004. The central role of perilipin A in lipid metabolism and adipocyte lipolysis. *IUBMB Life* **56**:379-385.
35. Lafontan, M. and M. Berlan. 1993. Fat cell adrenergic receptors and the control of white and brown fat cell function. *J Lipid Res* **34**:1057-1091.
36. Tansey, J.T., C. Sztalryd, J. Gruia-Gray, D.L. Roush, J.V. Zee, O. Gavrilova, M.L. Reitman, C.X. Deng, C. Li, A.R. Kimmel and C. Londos. 2001. Perilipin ablation results in a lean mouse with aberrant adipocyte lipolysis, enhanced leptin production, and resistance to diet-induced obesity. *Proc Natl Acad Sci U S A* **98**:6494-6499.
37. Granneman, J.G., H.P. Moore, R. Krishnamoorthy and M. Rathod. 2009. Perilipin controls lipolysis by regulating the interactions of ab-hydrolase containing 5 (Abhd5) and adipose trigylceride lipase (ATGL). *J Biol Chem* **284**:34538-34544.
38. Subramanian, V., A. Rothenberg, C. Gomez, A.W. Cohen, A. Garcia, S. Bhattacharyya, L. Shapiro, G. Dolios, R. Wang, M.P. Lisanti and D.L. Brasaemle. 2004. Perilipin A mediates the reversible binding of CGI-58 to lipid droplets in 3T3-L1 adipocytes. *J Biol Chem* **279**:42062-42071.
39. Yamaguchi, T., N. Omatsu, S. Matsushita and T. Osumi. 2004. CGI-58 interacts with perilipin and is localized to lipid droplets. Possible involvement of CGI-58 mislocalization in Chanarin-Dorfman syndrome. *J Biol Chem* **279**:30490-30497.
40. Marcinkiewicz, A., D. Gauthier, A. Garcia and D.L. Brasaemle. 2006. The phosphorylation of serine 492 of perilipin a directs lipid droplet fragmentation and dispersion. *J Biol Chem* **281**:11901-11909.
41. Steinberg, G.R., B.E. Kemp and M.J. Watt. 2007. Adipocyte triglyceride lipase expression in human obesity. *Am J Physiol Endocrinol Metab* **293**:E958-64.
42. Zimmermann, R., J.G. Strauss, G. Haemmerle, G. Schoiswohl, R. Birner-Gruenberger, M. Riederer, A. Lass, G. Neuberger, F. Eisenhaber, A. Hermetter and R. Zechner. 2004. Fat mobilization in adipose tissue is promoted by adipose triglyceride lipase. *Science* **306**:1383-1386.
43. Haemmerle, G., A. Lass, R. Zimmermann, G. Gorkiewicz, C. Meyer, J. Rozman, G. Heldmaier, R. Maier, C. Theussl, S. Eder, D. Kratky, E.F. Wagner, M. Klingenspor, G. Hoefler and R. Zechner. 2006. Defective lipolysis and altered energy metabolism in mice lacking adipose triglyceride lipase. *Science* **312**:734-737.
44. Haemmerle, G., R. Zimmermann, M. Hayn, C. Theussl, G. Waeg, E. Wagner, W. Sattler, T.M. Magin, E.F. Wagner and R. Zechner. 2002. Hormone-sensitive lipase deficiency in mice causes diglyceride accumulation in adipose tissue, muscle, and testis. *J Biol Chem* **277**:4806-4815.

45. Watt, M.J., A.G. Holmes, S.K. Pinnamaneni, A.P. Garnham, G.R. Steinberg, B.E. Kemp and M.A. Febbraio. 2006. Regulation of HSL serine phosphorylation in skeletal muscle and adipose tissue. *Am J Physiol Endocrinol Metab* **290**:E500-8.
46. Su, C.L., C. Sztalryd, J.A. Contreras, C. Holm, A.R. Kimmel and C. Londos. 2003. Mutational analysis of the hormone-sensitive lipase translocation reaction in adipocytes. *J Biol Chem* **278**:43615-43619.
47. Wang, H., L. Hu, K. Dalen, H. Dorward, A. Marcinkiewicz, D. Russel, D. Gong, C. Londos, T. Yamaguchi, C. Holm, M.A. Rizzo, D. Brasaemle and C. Sztalryd. 2009. Activation of hormone-sensitive lipase requires two steps: protein phosphorylation and binding to the PAT-1 domain of lipid droplet coat proteins. *J Biol Chem* **284**:32116-32125.
48. Fredrikson, G., H. Tornqvist and P. Belfrage. 1986. Hormone-sensitive lipase and monoacylglycerol lipase are both required for complete degradation of adipocyte triacylglycerol. *Biochim Biophys Acta* **876**:288-293.
49. Jaworski, K., M. Ahmadian, R.E. Duncan, E. Sarkadi-Nagy, K.A. Varady, M.K. Hellerstein, H.Y. Lee, V.T. Samuel, G.I. Shulman, K.H. Kim, S. de Val, C. Kang and H.S. Sul. 2009. AdPLA ablation increases lipolysis and prevents obesity induced by high-fat feeding or leptin deficiency. *Nat Med* **15**:159-168.
50. Strong, P., R.A. Coleman and P.P. Humphrey. 1992. Prostanoid-induced inhibition of lipolysis in rat isolated adipocytes: probable involvement of EP3 receptors. *Prostaglandins* **43**:559-566.
51. Borglum, J.D., G. Vassaux, B. Richelsen, D. Gaillard, C. Darimont, G. Ailhaud and R. Negrel. 1996. Changes in adenosine A1- and A2-receptor expression during adipose cell differentiation. *Mol Cell Endocrinol* **117**:17-25.
52. Galic, S., J.S. Oakhill and G.R. Steinberg. 2010. Adipose tissue as an endocrine organ. *Mol Cell Endocrinol* **316**:129-139.
53. Zhang, Y., R. Proenca, M. Maffei, M. Barone, L. Leopold and J.M. Friedman. 1994. Positional cloning of the mouse obese gene and its human homologue. *Nature* **372**:425-432.
54. Halaas, J.L., K.S. Gajiwala, M. Maffei, S.L. Cohen, B.T. Chait, D. Rabinowitz, R.L. Lallone, S.K. Burley and J.M. Friedman. 1995. Weight-reducing effects of the plasma protein encoded by the obese gene. *Science* **269**:543-546.
55. Heymsfield, S.B., A.S. Greenberg, K. Fujioka, R.M. Dixon, R. Kushner, T. Hunt, J.A. Lubina, J. Patane, B. Self, P. Hunt and M. McCamish. 1999. Recombinant leptin for weight loss in obese and lean adults: a randomized, controlled, dose-escalation trial. *JAMA* **282**:1568-1575.
56. Roth, J.D., B.L. Roland, R.L. Cole, J.L. Trevaskis, C. Weyer, J.E. Koda, C.M. Anderson, D.G. Parkes and A.D. Baron. 2008. Leptin responsiveness restored by amylin agonism in diet-induced obesity: evidence from nonclinical and clinical studies. *Proc Natl Acad Sci U S A* **105**:7257-7262.
57. Vaisse, C., J.L. Halaas, C.M. Horvath, J.E.J. Darnell, M. Stoffel and J.M. Friedman. 1996. Leptin activation of Stat3 in the hypothalamus of wild-type and ob/ob mice but not db/db mice. *Nat Genet* **14**:95-97.

58. Friedman, J.M. and J.L. Halaas. 1998. Leptin and the regulation of body weight in mammals. *Nature* **395**:763-770.
59. Wen, Z., Z. Zhong and J.E.J. Darnell. 1995. Maximal activation of transcription by Stat1 and Stat3 requires both tyrosine and serine phosphorylation. *Cell* **82**:241-250.
60. Bjorbak, C., H.J. Lavery, S.H. Bates, R.K. Olson, S.M. Davis, J.S. Flier and M.G.J. Myers. 2000. SOCS3 mediates feedback inhibition of the leptin receptor via Tyr985. *J Biol Chem* **275**:40649-40657.
61. Stanley, B.G., S.E. Kyrkouli, S. Lampert and S.F. Leibowitz. 1986. Neuropeptide Y chronically injected into the hypothalamus: a powerful neurochemical inducer of hyperphagia and obesity. *Peptides* **7**:1189-1192.
62. Bewick, G.A., J.V. Gardiner, W.S. Dhillo, A.S. Kent, N.E. White, Z. Webster, M.A. Ghatei and S.R. Bloom. 2005. Post-embryonic ablation of AgRP neurons in mice leads to a lean, hypophagic phenotype. *FASEB J* **19**:1680-1682.
63. Elias, C.F., C. Aschkenasi, C. Lee, J. Kelly, R.S. Ahima, C. Bjorbaek, J.S. Flier, C.B. Saper and J.K. Elmquist. 1999. Leptin differentially regulates NPY and POMC neurons projecting to the lateral hypothalamic area. *Neuron* **23**:775-786.
64. Belgardt, B.F., T. Okamura and J.C. Bruning. 2009. Hormone and glucose signalling in POMC and AgRP neurons. *J Physiol* **587**:5305-5314.
65. Balthasar, N., R. Coppari, J. McMinn, S.M. Liu, C.E. Lee, V. Tang, C.D. Kenny, R.A. McGovern, S.C.J. Chua, J.K. Elmquist and B.B. Lowell. 2004. Leptin receptor signaling in POMC neurons is required for normal body weight homeostasis. *Neuron* **42**:983-991.
66. Erickson, J.C., G. Hollopeter and R.D. Palmiter. 1996. Attenuation of the obesity syndrome of ob/ob mice by the loss of neuropeptide Y. *Science* **274**:1704-1707.
67. Maffei, M., J. Halaas, E. Ravussin, R.E. Pratley, G.H. Lee, Y. Zhang, H. Fei, S. Kim, R. Lallone, S. Ranganathan, P.A. Kern and J.M. Friedman. 1995. Leptin levels in human and rodent: measurement of plasma leptin and ob RNA in obese and weight-reduced subjects. *Nat Med* **1**:1155-1161.
68. Rosenbaum, M., E.M. Murphy, S.B. Heymsfield, D.E. Matthews and R.L. Leibel. 2002. Low dose leptin administration reverses effects of sustained weight-reduction on energy expenditure and circulating concentrations of thyroid hormones. *J Clin Endocrinol Metab* **87**:2391-2394.
69. Hada, Y., T. Yamauchi, H. Waki, A. Tsuchida, K. Hara, H. Yago, O. Miyazaki, H. Ebinuma and T. Kadowaki. 2007. Selective purification and characterization of adiponectin multimer species from human plasma. *Biochem Biophys Res Commun* **356**:487-493.
70. Kadowaki, T. and T. Yamauchi. 2005. Adiponectin and adiponectin receptors. *Endocr Rev* **26**:439-451.
71. Yamauchi, T., J. Kamon, H. Waki, Y. Terauchi, N. Kubota, K. Hara, Y. Mori, T. Ide, K. Murakami, N. Tsuboyama-Kasaoka, O. Ezaki, Y. Akanuma, O. Gavrilova, C. Vinson, M.L. Reitman, H. Kagechika, K. Shudo, M. Yoda, Y. Nakano, K. Tobe, R. Nagai, S. Kimura, M. Tomita, P. Froguel and T. Kadowaki. 2001. The fat-

derived hormone adiponectin reverses insulin resistance associated with both lipoatrophy and obesity. *Nat Med* **7**:941-946.

72. Yu, J.G., S. Javorschi, A.L. Hevener, Y.T. Kruszynska, R.A. Norman, M. Sinha and J.M. Olefsky. 2002. The effect of thiazolidinediones on plasma adiponectin levels in normal, obese, and type 2 diabetic subjects. *Diabetes* **51**:2968-2974.
73. Yamauchi, T., J. Kamon, Y. Ito, A. Tsuchida, T. Yokomizo, S. Kita, T. Sugiyama, M. Miyagishi, K. Hara, M. Tsunoda, K. Murakami, T. Ohteki, S. Uchida, S. Takekawa, H. Waki, N.H. Tsuno, Y. Shibata, Y. Terauchi, P. Froguel, K. Tobe, S. Koyasu, K. Taira, T. Kitamura, T. Shimizu, R. Nagai and T. Kadowaki. 2003. Cloning of adiponectin receptors that mediate antidiabetic metabolic effects. *Nature* **423**:762-769.
74. Yamauchi, T., Y. Nio, T. Maki, M. Kobayashi, T. Takazawa, M. Iwabu, M. Okada-Iwabu, S. Kawamoto, N. Kubota, T. Kubota, Y. Ito, J. Kamon, A. Tsuchida, K. Kumagai, H. Kozono, Y. Hada, H. Ogata, K. Tokuyama, M. Tsunoda, T. Ide, K. Murakami, M. Awazawa, I. Takamoto, P. Froguel, K. Hara, K. Tobe, R. Nagai, K. Ueki and T. Kadowaki. 2007. Targeted disruption of AdipoR1 and AdipoR2 causes abrogation of adiponectin binding and metabolic actions. *Nat Med* **13**:332-339.
75. Bonnard, C., A. Durand, H. Vidal and J. Rieusset. 2008. Changes in adiponectin, its receptors and AMPK activity in tissues of diet-induced diabetic mice. *Diabetes Metab* **34**:52-61.
76. Fain, J.N., A.K. Madan, M.L. Hiler, P. Cheema and S.W. Bahouth. 2004. Comparison of the release of adipokines by adipose tissue, adipose tissue matrix, and adipocytes from visceral and subcutaneous abdominal adipose tissues of obese humans. *Endocrinology* **145**:2273-2282.
77. Brockhaus, M., H.J. Schoenfeld, E.J. Schlaeger, W. Hunziker, W. Lesslauer and H. Loetscher. 1990. Identification of two types of tumor necrosis factor receptors on human cell lines by monoclonal antibodies. *Proc Natl Acad Sci U S A* **87**:3127-3131.
78. Hotamisligil, G.S., D.L. Murray, L.N. Choy and B.M. Spiegelman. 1994. Tumor necrosis factor alpha inhibits signaling from the insulin receptor. *Proc Natl Acad Sci U S A* **91**:4854-4858.
79. Hotamisligil, G.S., N.S. Shargill and B.M. Spiegelman. 1993. Adipose expression of tumor necrosis factor-alpha: direct role in obesity-linked insulin resistance. *Science* **259**:87-91.
80. Uysal, K.T., S.M. Wiesbrock and G.S. Hotamisligil. 1998. Functional analysis of tumor necrosis factor (TNF) receptors in TNF-alpha-mediated insulin resistance in genetic obesity. *Endocrinology* **139**:4832-4838.
81. Xu, H., J.K. Sethi and G.S. Hotamisligil. 1999. Transmembrane tumor necrosis factor (TNF)-alpha inhibits adipocyte differentiation by selectively activating TNF receptor 1. *J Biol Chem* **274**:26287-26295.
82. Chen, H., O. Charlat, L.A. Tartaglia, E.A. Woolf, X. Weng, S.J. Ellis, N.D. Lakey, J. Culpepper, K.J. Moore, R.E. Breitbart, G.M. Duyk, R.I. Tepper and J.P. Morgenstern. 1996. Evidence that the diabetes gene encodes the leptin receptor:

identification of a mutation in the leptin receptor gene in db/db mice. *Cell* **84**:491-495.
83. Mohamed-Ali, V., S. Goodrick, A. Rawesh, D.R. Katz, J.M. Miles, J.S. Yudkin, S. Klein and S.W. Coppack. 1997. Subcutaneous adipose tissue releases interleukin-6, but not tumor necrosis factor-alpha, in vivo. *J Clin Endocrinol Metab* **82**:4196-4200.
84. Feve, B. and J.P. Bastard. 2009. The role of interleukins in insulin resistance and type 2 diabetes mellitus. *Nat Rev Endocrinol* **5**:305-311.
85. Senn, J.J., P.J. Klover, I.A. Nowak and R.A. Mooney. 2002. Interleukin-6 induces cellular insulin resistance in hepatocytes. *Diabetes* **51**:3391-3399.
86. Rotter, V., I. Nagaev and U. Smith. 2003. Interleukin-6 (IL-6) induces insulin resistance in 3T3-L1 adipocytes and is, like IL-8 and tumor necrosis factor-alpha, overexpressed in human fat cells from insulin-resistant subjects. *J Biol Chem* **278**:45777-45784.
87. Somm, E., E. Henrichot, A. Pernin, C.E. Juge-Aubry, P. Muzzin, J.M. Dayer, M.J. Nicklin and C.A. Meier. 2005. Decreased fat mass in interleukin-1 receptor antagonist-deficient mice: impact on adipogenesis, food intake, and energy expenditure. *Diabetes* **54**:3503-3509.
88. Fasshauer, M., S. Kralisch, M. Klier, U. Lossner, M. Bluher, J. Klein and R. Paschke. 2003. Adiponectin gene expression and secretion is inhibited by interleukin-6 in 3T3-L1 adipocytes. *Biochem Biophys Res Commun* **301**:1045-1050.
89. Trujillo, M.E., S. Sullivan, I. Harten, S.H. Schneider, A.S. Greenberg and S.K. Fried. 2004. Interleukin-6 regulates human adipose tissue lipid metabolism and leptin production in vitro. *J Clin Endocrinol Metab* **89**:5577-5582.
90. Morisset, A.S., C. Huot, D. Legare and A. Tchernof. 2008. Circulating IL-6 concentrations and abdominal adipocyte isoproterenol-stimulated lipolysis in women. *Obesity (Silver Spring)* **16**:1487-1492.
91. Wallenius, V., K. Wallenius, B. Ahren, M. Rudling, H. Carlsten, S.L. Dickson, C. Ohlsson and J.O. Jansson. 2002. Interleukin-6-deficient mice develop mature-onset obesity. *Nat Med* **8**:75-79.
92. Febbraio, M.A., N. Hiscock, M. Sacchetti, C.P. Fischer and B.K. Pedersen. 2004. Interleukin-6 is a novel factor mediating glucose homeostasis during skeletal muscle contraction. *Diabetes* **53**:1643-1648.
93. Carey, A.L., G.R. Steinberg, S.L. Macaulay, W.G. Thomas, A.G. Holmes, G. Ramm, O. Prelovsek, C. Hohnen-Behrens, M.J. Watt, D.E. James, B.E. Kemp, B.K. Pedersen and M.A. Febbraio. 2006. Interleukin-6 increases insulin-stimulated glucose disposal in humans and glucose uptake and fatty acid oxidation in vitro via AMP-activated protein kinase. *Diabetes* **55**:2688-2697.
94. Steensberg, A., C.P. Fischer, M. Sacchetti, C. Keller, T. Osada, P. Schjerling, G. van Hall, M.A. Febbraio and B.K. Pedersen. 2003. Acute interleukin-6 administration does not impair muscle glucose uptake or whole-body glucose disposal in healthy humans. *J Physiol* **548**:631-638.

95. Stenlof, K., I. Wernstedt, T. Fjallman, V. Wallenius, K. Wallenius and J.O. Jansson. 2003. Interleukin-6 levels in the central nervous system are negatively correlated with fat mass in overweight/obese subjects. *J Clin Endocrinol Metab* **88**:4379-4383.
96. Jansson, J.O., K. Wallenius, I. Wernstedt, C. Ohlsson, S.L. Dickson and V. Wallenius. 2003. On the site and mechanism of action of the anti-obesity effects of interleukin-6. *Growth Horm IGF Res* **13 Suppl A**:S28-32.
97. Cinti, S. 2001. The adipose organ: morphological perspectives of adipose tissues. *Proc Nutr Soc* **60**:319-328.
98. Cannon, B. and J. Nedergaard. 2004. Brown adipose tissue: function and physiological significance. *Physiol Rev* **84**:277-359.
99. Cypess, A.M., S. Lehman, G. Williams, I. Tal, D. Rodman, A.B. Goldfine, F.C. Kuo, E.L. Palmer, Y.H. Tseng, A. Doria, G.M. Kolodny and C.R. Kahn. 2009. Identification and importance of brown adipose tissue in adult humans. *N Engl J Med* **360**:1509-1517.
100. van Marken Lichtenbelt, W.D., J.W. Vanhommerig, N.M. Smulders, J.M. Drossaerts, G.J. Kemerink, N.D. Bouvy, P. Schrauwen and G.J. Teule. 2009. Cold-activated brown adipose tissue in healthy men. *N Engl J Med* **360**:1500-1508.
101. Rosen, E.D. and O.A. MacDougald. 2006. Adipocyte differentiation from the inside out. *Nat Rev Mol Cell Biol* **7**:885-896.
102. Rosen, E.D., P. Sarraf, A.E. Troy, G. Bradwin, K. Moore, D.S. Milstone, B.M. Spiegelman and R.M. Mortensen. 1999. PPAR gamma is required for the differentiation of adipose tissue in vivo and in vitro. *Mol Cell* **4**:611-617.
103. Larrouy, D., H. Vidal, F. Andreelli, M. Laville and D. Langin. 1999. Cloning and mRNA tissue distribution of human PPARgamma coactivator-1. *Int J Obes Relat Metab Disord* **23**:1327-1332.
104. Puigserver, P., Z. Wu, C.W. Park, R. Graves, M. Wright and B.M. Spiegelman. 1998. A cold-inducible coactivator of nuclear receptors linked to adaptive thermogenesis. *Cell* **92**:829-839.
105. Leone, T.C., J.J. Lehman, B.N. Finck, P.J. Schaeffer, A.R. Wende, S. Boudina, M. Courtois, D.F. Wozniak, N. Sambandam, C. Bernal-Mizrachi, Z. Chen, J.O. Holloszy, D.M. Medeiros, R.E. Schmidt, J.E. Saffitz, E.D. Abel, C.F. Semenkovich and D.P. Kelly. 2005. PGC-1alpha deficiency causes multi-system energy metabolic derangements: muscle dysfunction, abnormal weight control and hepatic steatosis. *PLoS Biol* **3**:e101.
106. Tiraby, C., G. Tavernier, C. Lefort, D. Larrouy, F. Bouillaud, D. Ricquier and D. Langin. 2003. Acquirement of brown fat cell features by human white adipocytes. *J Biol Chem* **278**:33370-33376.
107. Seale, P., S. Kajimura, W. Yang, S. Chin, L.M. Rohas, M. Uldry, G. Tavernier, D. Langin and B.M. Spiegelman. 2007. Transcriptional control of brown fat determination by PRDM16. *Cell Metab* **6**:38-54.
108. Kajimura, S., P. Seale, K. Kubota, E. Lunsford, J.V. Frangioni, S.P. Gygi and B.M. Spiegelman. 2009. Initiation of myoblast to brown fat switch by a PRDM16-C/EBP-beta transcriptional complex. *Nature* **460**:1154-1158.

109. Seale, P., B. Bjork, W. Yang, S. Kajimura, S. Chin, S. Kuang, A. Scime, S. Devarakonda, H.M. Conroe, H. Erdjument-Bromage, P. Tempst, M.A. Rudnicki, D.R. Beier and B.M. Spiegelman. 2008. PRDM16 controls a brown fat/skeletal muscle switch. *Nature* **454**:961-967.
110. Seale, P., H.M. Conroe, J. Estall, S. Kajimura, A. Frontini, J. Ishibashi, P. Cohen, S. Cinti and B.M. Spiegelman. 2011. Prdm16 determines the thermogenic program of subcutaneous white adipose tissue in mice. *J Clin Invest* **121**:96-105.
111. Cinti, S. 2002. Adipocyte differentiation and transdifferentiation: plasticity of the adipose organ. *J Endocrinol Invest* **25**:823-835.
112. Barbatelli, G., I. Murano, L. Madsen, Q. Hao, M. Jimenez, K. Kristiansen, J.P. Giacobino, R. De Matteis and S. Cinti. 2010. The emergence of cold-induced brown adipocytes in mouse white fat depots is determined predominantly by white to brown adipocyte transdifferentiation. *Am J Physiol Endocrinol Metab* **298**:E1244-53.
113. Murano, I., G. Barbatelli, A. Giordano and S. Cinti. 2009. Noradrenergic parenchymal nerve fiber branching after cold acclimatisation correlates with brown adipocyte density in mouse adipose organ. *J Anat* **214**:171-178.
114. Ghorbani, M., T.H. Claus and J. Himms-Hagen. 1997. Hypertrophy of brown adipocytes in brown and white adipose tissues and reversal of diet-induced obesity in rats treated with a beta3-adrenoceptor agonist. *Biochem Pharmacol* **54**:121-131.
115. Himms-Hagen, J., A. Melnyk, M.C. Zingaretti, E. Ceresi, G. Barbatelli and S. Cinti. 2000. Multilocular fat cells in WAT of CL-316243-treated rats derive directly from white adipocytes. *Am J Physiol Cell Physiol* **279**:C670-81.
116. Fukui, Y., S. Masui, S. Osada, K. Umesono and K. Motojima. 2000. A new thiazolidinedione, NC-2100, which is a weak PPAR-gamma activator, exhibits potent antidiabetic effects and induces uncoupling protein 1 in white adipose tissue of KKAy obese mice. *Diabetes* **49**:759-767.
117. Okamoto, Y., H. Higashiyama, J.X. Rong, M.J. McVey, M. Kinoshita, S. Asano and M.K. Hansen. 2007. Comparison of mitochondrial and macrophage content between subcutaneous and visceral fat in db/db mice. *Exp Mol Pathol* **83**:73-83.
118. Petrovic, N., T.B. Walden, I.G. Shabalina, J.A. Timmons, B. Cannon and J. Nedergaard. 2010. Chronic Peroxisome Proliferator-activated Receptor {gamma} (PPAR{gamma}) Activation of Epididymally Derived White Adipocyte Cultures Reveals a Population of Thermogenically Competent, UCP1-containing Adipocytes Molecularly Distinct from Classic Brown Adipocytes. *J Biol Chem* **285**:7153-7164.
119. Orci, L., W.S. Cook, M. Ravazzola, M.Y. Wang, B.H. Park, R. Montesano and R.H. Unger. 2004. Rapid transformation of white adipocytes into fat-oxidizing machines. *Proc Natl Acad Sci U S A* **101**:2058-2063.
120. Ceddia, R.B., W.N.J. William, F.B. Lima, P. Flandin, R. Curi and J.P. Giacobino. 2000. Leptin stimulates uncoupling protein-2 mRNA expression and Krebs cycle activity and inhibits lipid synthesis in isolated rat white adipocytes. *Eur J Biochem* **267**:5952-5958.

121. Kopecky, J., G. Clarke, S. Enerback, B. Spiegelman and L.P. Kozak. 1995. Expression of the mitochondrial uncoupling protein gene from the aP2 gene promoter prevents genetic obesity. *J Clin Invest* **96**:2914-2923.
122. Gale, E.A. 2011. Therapy: The second time as farce: rosiglitazone and the regulators. *Nat Rev Endocrinol* **7**:5-6.
123. Lundgren, M., M. Svensson, S. Lindmark, F. Renstrom, T. Ruge and J.W. Eriksson. 2007. Fat cell enlargement is an independent marker of insulin resistance and 'hyperleptinaemia'. *Diabetologia* **50**:625-633.
124. Molina, J.M., T.P. Ciaraldi, D. Brady and J.M. Olefsky. 1989. Decreased activation rate of insulin-stimulated glucose transport in adipocytes from obese subjects. *Diabetes* **38**:991-995.
125. Wueest, S., R.A. Rapold, J.M. Rytka, E.J. Schoenle and D. Konrad. 2009. Basal lipolysis, not the degree of insulin resistance, differentiates large from small isolated adipocytes in high-fat fed mice. *Diabetologia* **52**:541-546.
126. Monteiro, R., P.M. de Castro, C. Calhau and I. Azevedo. 2006. Adipocyte size and liability to cell death. *Obes Surg* **16**:804-806.
127. Roden, M. 2004. How free fatty acids inhibit glucose utilization in human skeletal muscle. *News Physiol Sci* **19**:92-96.
128. Heilbronn, L., S.R. Smith and E. Ravussin. 2004. Failure of fat cell proliferation, mitochondrial function and fat oxidation results in ectopic fat storage, insulin resistance and type II diabetes mellitus. *Int J Obes Relat Metab Disord* **28 Suppl 4**:S12-21.
129. Wang, Z., S. Zhu, J. Wang, R.N.J. Pierson and S.B. Heymsfield. 2003. Whole-body skeletal muscle mass: development and validation of total-body potassium prediction models. *Am J Clin Nutr* **77**:76-82.
130. DeFronzo, R.A., E. Ferrannini, Y. Sato, P. Felig and J. Wahren. 1981. Synergistic interaction between exercise and insulin on peripheral glucose uptake. *J Clin Invest* **68**:1468-1474.
131. Stefan, N., K. Kantartzis and H.U. Haring. 2008. Causes and metabolic consequences of Fatty liver. *Endocr Rev* **29**:939-960.
132. Randle, P.J., P.B. Garland, C.N. Hales and E.A. Newsholme. 1963. The glucose fatty-acid cycle. Its role in insulin sensitivity and the metabolic disturbances of diabetes mellitus. *Lancet* **1**:785-789.
133. Roden, M., T.B. Price, G. Perseghin, K.F. Petersen, D.L. Rothman, G.W. Cline and G.I. Shulman. 1996. Mechanism of free fatty acid-induced insulin resistance in humans. *J Clin Invest* **97**:2859-2865.
134. Boden, G., X. Chen, J. Ruiz, J.V. White and L. Rossetti. 1994. Mechanisms of fatty acid-induced inhibition of glucose uptake. *J Clin Invest* **93**:2438-2446.
135. Dresner, A., D. Laurent, M. Marcucci, M.E. Griffin, S. Dufour, G.W. Cline, L.A. Slezak, D.K. Andersen, R.S. Hundal, D.L. Rothman, K.F. Petersen and G.I. Shulman. 1999. Effects of free fatty acids on glucose transport and IRS-1-associated phosphatidylinositol 3-kinase activity. *J Clin Invest* **103**:253-259.

136. Griffin, M.E., M.J. Marcucci, G.W. Cline, K. Bell, N. Barucci, D. Lee, L.J. Goodyear, E.W. Kraegen, M.F. White and G.I. Shulman. 1999. Free fatty acid-induced insulin resistance is associated with activation of protein kinase C theta and alterations in the insulin signaling cascade. *Diabetes* **48**:1270-1274.
137. Itani, S.I., N.B. Ruderman, F. Schmieder and G. Boden. 2002. Lipid-induced insulin resistance in human muscle is associated with changes in diacylglycerol, protein kinase C, and IkappaB-alpha. *Diabetes* **51**:2005-2011.
138. Faulds, G., M. Ryden, I. Ek, H. Wahrenberg and P. Arner. 2003. Mechanisms behind lipolytic catecholamine resistance of subcutaneous fat cells in the polycystic ovarian syndrome. *J Clin Endocrinol Metab* **88**:2269-2273.
139. Reynisdottir, S., H. Wahrenberg, K. Carlstrom, S. Rossner and P. Arner. 1994. Catecholamine resistance in fat cells of women with upper-body obesity due to decreased expression of beta 2-adrenoceptors. *Diabetologia* **37**:428-435.
140. Bederman, I.R. and S.F. Previs. 2008. Hormonal regulation of intracellular lipolysis in C57BL/6J mice: effect of diet-induced adiposity and data normalization. *Metabolism* **57**:1405-1413.
141. Portillo, M.P., E. Simon, M.A. Garcia-Calonge and A.S. Del Barrio. 1999. Effect of high-fat diet on lypolisis in isolated adipocytes from visceral and subcutaneous WAT. *Eur J Nutr* **38**:177-182.
142. Jocken, J.W. and E.E. Blaak. 2008. Catecholamine-induced lipolysis in adipose tissue and skeletal muscle in obesity. *Physiol Behav* **94**:219-230.
143. Elizalde, M., M. Ryden, V. van Harmelen, P. Eneroth, H. Gyllenhammar, C. Holm, S. Ramel, A. Olund, P. Arner and K. Andersson. 2000. Expression of nitric oxide synthases in subcutaneous adipose tissue of nonobese and obese humans. *J Lipid Res* **41**:1244-1251.
144. Martinez-Botas, J., J.B. Anderson, D. Tessier, A. Lapillonne, B.H. Chang, M.J. Quast, D. Gorenstein, K.H. Chen and L. Chan. 2000. Absence of perilipin results in leanness and reverses obesity in Lepr(db/db) mice. *Nat Genet* **26**:474-479.
145. Fain, J.N., C.W. Leffler, G.S.J. Cowan, C. Buffington, L. Pouncey and S.W. Bahouth. 2001. Stimulation of leptin release by arachidonic acid and prostaglandin E(2) in adipose tissue from obese humans. *Metabolism* **50**:921-928.
146. Cinti, S. 2005. The adipose organ. *Prostaglandins Leukot Essent Fatty Acids* **73**:9-15.
147. Yang, X. and U. Smith. 2007. Adipose tissue distribution and risk of metabolic disease: does thiazolidinedione-induced adipose tissue redistribution provide a clue to the answer? *Diabetologia* **50**:1127-1139.
148. Ross, R., L. Leger, D. Morris, J. de Guise and R. Guardo. 1992. Quantification of adipose tissue by MRI: relationship with anthropometric variables. *J Appl Physiol* **72**:787-795.
149. Martin, A.D., V. Janssens, D. Caboor, J.P. Clarys and M.J. Marfell-Jones. 2003. Relationships between visceral, trunk and whole-body adipose tissue weights by cadaver dissection. *Ann Hum Biol* **30**:668-677.

150. Jensen, M.D. 2008. Role of body fat distribution and the metabolic complications of obesity. *J Clin Endocrinol Metab* **93**:S57-63.
151. Albu, J.B., A.J. Kovera and J.A. Johnson. 2000. Fat distribution and health in obesity. *Ann N Y Acad Sci* **904**:491-501.
152. Meek, S.E., K.S. Nair and M.D. Jensen. 1999. Insulin regulation of regional free fatty acid metabolism. *Diabetes* **48**:10-14.
153. Fried, S.K., T. Tittelbach, J. Blumenthal, U. Sreenivasan, L. Robey, J. Yi, S. Khan, C. Hollender, A.S. Ryan and A.P. Goldberg. 2010. Resistance to the antilipolytic effect of insulin in adipocytes of African-American compared to Caucasian postmenopausal women. *J Lipid Res* **51**:1193-1200.
154. Bolinder, J., L. Kager, J. Ostman and P. Arner. 1983. Differences at the receptor and postreceptor levels between human omental and subcutaneous adipose tissue in the action of insulin on lipolysis. *Diabetes* **32**:117-123.
155. Tavernier, G., J. Galitzky, P. Valet, A. Remaury, A. Bouloumie, M. Lafontan and D. Langin. 1995. Molecular mechanisms underlying regional variations of catecholamine-induced lipolysis in rat adipocytes. *Am J Physiol* **268**:E1135-42.
156. Engfeldt, P. and P. Arner. 1988. Lipolysis in human adipocytes, effects of cell size, age and of regional differences. *Horm Metab Res Suppl* **19**:26-29.
157. Sztalryd, C. and F.B. Kraemer. 1994. Differences in hormone-sensitive lipase expression in white adipose tissue from various anatomic locations of the rat. *Metabolism* **43**:241-247.
158. Palou, M., J. Sanchez, T. Priego, A.M. Rodriguez, C. Pico and A. Palou. 2010. Regional differences in the expression of genes involved in lipid metabolism in adipose tissue in response to short- and medium-term fasting and refeeding. *J Nutr Biochem* **21**:23-33.
159. Berndt, J., S. Kralisch, N. Kloting, K. Ruschke, M. Kern, M. Fasshauer, M.R. Schon, M. Stumvoll and M. Bluher. 2008. Adipose triglyceride lipase gene expression in human visceral obesity. *Exp Clin Endocrinol Diabetes* **116**:203-210.
160. Large, V., P. Arner, S. Reynisdottir, J. Grober, V. Van Harmelen, C. Holm and D. Langin. 1998. Hormone-sensitive lipase expression and activity in relation to lipolysis in human fat cells. *J Lipid Res* **39**:1688-1695.
161. Jensen, M.D. 2007. Adipose tissue metabolism -- an aspect we should not neglect? *Horm Metab Res* **39**:722-725.
162. Stumvoll, M., B.J. Goldstein and T.W. van Haeften. 2005. Type 2 diabetes: principles of pathogenesis and therapy. *Lancet* **365**:1333-1346.
163. Hardie, D.G. 2007. AMP-activated/SNF1 protein kinases: conserved guardians of cellular energy. *Nat Rev Mol Cell Biol* **8**:774-785.
164. Elbing, K., E.M. Rubenstein, R.R. McCartney and M.C. Schmidt. 2006. Subunits of the Snf1 kinase heterotrimer show interdependence for association and activity. *J Biol Chem* **281**:26170-26180.
165. McBride, A., S. Ghilagaber, A. Nikolaev and D.G. Hardie. 2009. The glycogen-binding domain on the AMPK beta subunit allows the kinase to act as a glycogen sensor. *Cell Metab* **9**:23-34.

166. Xiao, B., R. Heath, P. Saiu, F.C. Leiper, P. Leone, C. Jing, P.A. Walker, L. Haire, J.F. Eccleston, C.T. Davis, S.R. Martin, D. Carling and S.J. Gamblin. 2007. Structural basis for AMP binding to mammalian AMP-activated protein kinase. *Nature* **449**:496-500.
167. Xiao, B., M.J. Sanders, E. Underwood, R. Heath, F.V. Mayer, D. Carmena, C. Jing, P.A. Walker, J.F. Eccleston, L.F. Haire, P. Saiu, S.A. Howell, R. Aasland, S.R. Martin, D. Carling and S.J. Gamblin. 2011. Structure of mammalian AMPK and its regulation by ADP. *Nature* **472**:230-233.
168. Hancock, C.R., E. Janssen and R.L. Terjung. 2006. Contraction-mediated phosphorylation of AMPK is lower in skeletal muscle of adenylate kinase-deficient mice. *J Appl Physiol* **100**:406-413.
169. Scott, J.W., S.A. Hawley, K.A. Green, M. Anis, G. Stewart, G.A. Scullion, D.G. Norman and D.G. Hardie. 2004. CBS domains form energy-sensing modules whose binding of adenosine ligands is disrupted by disease mutations. *J Clin Invest* **113**:274-284.
170. Suter, M., U. Riek, R. Tuerk, U. Schlattner, T. Wallimann and D. Neumann. 2006. Dissecting the role of 5'-AMP for allosteric stimulation, activation, and deactivation of AMP-activated protein kinase. *J Biol Chem* **281**:32207-32216.
171. Baas, A.F., J. Boudeau, G.P. Sapkota, L. Smit, R. Medema, N.A. Morrice, D.R. Alessi and H.C. Clevers. 2003. Activation of the tumour suppressor kinase LKB1 by the STE20-like pseudokinase STRAD. *EMBO J* **22**:3062-3072.
172. Boudeau, J., A.F. Baas, M. Deak, N.A. Morrice, A. Kieloch, M. Schutkowski, A.R. Prescott, H.C. Clevers and D.R. Alessi. 2003. MO25alpha/beta interact with STRADalpha/beta enhancing their ability to bind, activate and localize LKB1 in the cytoplasm. *EMBO J* **22**:5102-5114.
173. Hawley, S.A., J. Boudeau, J.L. Reid, K.J. Mustard, L. Udd, T.P. Makela, D.R. Alessi and D.G. Hardie. 2003. Complexes between the LKB1 tumor suppressor, STRAD alpha/beta and MO25 alpha/beta are upstream kinases in the AMP-activated protein kinase cascade. *J Biol* **2**:28.
174. Sakamoto, K., O. Goransson, D.G. Hardie and D.R. Alessi. 2004. Activity of LKB1 and AMPK-related kinases in skeletal muscle: effects of contraction, phenformin, and AICAR. *Am J Physiol Endocrinol Metab* **287**:E310-7.
175. Hawley, S.A., D.A. Pan, K.J. Mustard, L. Ross, J. Bain, A.M. Edelman, B.G. Frenguelli and D.G. Hardie. 2005. Calmodulin-dependent protein kinase kinase-beta is an alternative upstream kinase for AMP-activated protein kinase. *Cell Metab* **2**:9-19.
176. Momcilovic, M., S.P. Hong and M. Carlson. 2006. Mammalian TAK1 activates Snf1 protein kinase in yeast and phosphorylates AMP-activated protein kinase in vitro. *J Biol Chem* **281**:25336-25343.
177. Herrero-Martin, G., M. Hoyer-Hansen, C. Garcia-Garcia, C. Fumarola, T. Farkas, A. Lopez-Rivas and M. Jaattela. 2009. TAK1 activates AMPK-dependent cytoprotective autophagy in TRAIL-treated epithelial cells. *EMBO J* **28**:677-685.

178. Garton, A.J. and S.J. Yeaman. 1990. Identification and role of the basal phosphorylation site on hormone-sensitive lipase. *Eur J Biochem* **191**:245-250.
179. Anthony, N.M., M.P. Gaidhu and R.B. Ceddia. 2009. Regulation of visceral and subcutaneous adipocyte lipolysis by acute AICAR-induced AMPK activation. *Obesity (Silver Spring)* **17**:1312-1317.
180. Daval, M., F. Diot-Dupuy, R. Bazin, I. Hainault, B. Viollet, S. Vaulont, E. Hajduch, P. Ferre and F. Foufelle. 2005. Anti-lipolytic action of AMP-activated protein kinase in rodent adipocytes. *J Biol Chem* **280**:25250-25257.
181. Yin, W., J. Mu and M.J. Birnbaum. 2003. Role of AMP-activated protein kinase in cyclic AMP-dependent lipolysis In 3T3-L1 adipocytes. *J Biol Chem* **278**:43074-43080.
182. Koh, H.J., M.F. Hirshman, H. He, Y. Li, Y. Manabe, J.A. Balschi and L.J. Goodyear. 2007. Adrenaline is a critical mediator of acute exercise-induced AMP-activated protein kinase activation in adipocytes. *Biochem J* **403**:473-481.
183. Gauthier, M.S., H. Miyoshi, S.C. Souza, J.M. Cacicedo, A.K. Saha, A.S. Greenberg and N.B. Ruderman. 2008. AMP-activated protein kinase is activated as a consequence of lipolysis in the adipocyte: potential mechanism and physiological relevance. *J Biol Chem* **283**:16514-16524.
184. Brooks, B., J.R. Arch and E.A. Newsholme. 1982. Effects of hormones on the rate of the triacylglycerol/fatty acid substrate cycle in adipocytes and epididymal fat pads. *FEBS Lett* **146**:327-330.
185. Bergeron, R., S.F. Previs, G.W. Cline, P. Perret, R.R.r. Russell, L.H. Young and G.I. Shulman. 2001. Effect of 5-aminoimidazole-4-carboxamide-1-beta-D-ribofuranoside infusion on in vivo glucose and lipid metabolism in lean and obese Zucker rats. *Diabetes* **50**:1076-1082.
186. Narbonne, P. and R. Roy. 2009. Caenorhabditis elegans dauers need LKB1/AMPK to ration lipid reserves and ensure long-term survival. *Nature* **457**:210-214.
187. Musi, N., T. Hayashi, N. Fujii, M.F. Hirshman, L.A. Witters and L.J. Goodyear. 2001. AMP-activated protein kinase activity and glucose uptake in rat skeletal muscle. *Am J Physiol Endocrinol Metab* **280**:E677-684.
188. Jessen, N., R. Pold, E.S. Buhl, L.S. Jensen, O. Schmitz and S. Lund. 2003. Effects of AICAR and exercise on insulin-stimulated glucose uptake, signaling, and GLUT-4 content in rat muscles. *J Appl Physiol* **94**:1373-1379.
189. Yamaguchi, S., H. Katahira, S. Ozawa, Y. Nakamichi, T. Tanaka, T. Shimoyama, K. Takahashi, K. Yoshimoto, M.O. Imaizumi, S. Nagamatsu and H. Ishida. 2005. Activators of AMP-activated protein kinase enhance GLUT4 translocation and its glucose transport activity in 3T3-L1 adipocytes. *Am J Physiol Endocrinol Metab* **289**:E643-E649.
190. Salt, I.P., J.M. Connell and G.W. Gould. 2000. 5-aminoimidazole-4-carboxamide ribonucleoside (AICAR) inhibits insulin-stimulated glucose transport in 3T3-L1 adipocytes. *Diabetes* **49**:1649-1656.
191. Gaidhu, M.P., S. Fediuc and R.B. Ceddia. 2006. 5-Aminoimidazole-4-carboxamide-1-beta-D-ribofuranoside-induced AMP-activated protein kinase phosphorylation

inhibits basal and insulin-stimulated glucose uptake, lipid synthesis, and fatty acid oxidation in isolated rat adipocytes. *J Biol Chem* **281**:25956-25964.

192. Kramer, H.F., C.A. Witczak, N. Fujii, N. Jessen, E.B. Taylor, D.E. Arnolds, K. Sakamoto, M.F. Hirshman and L.J. Goodyear. 2006. Distinct signals regulate AS160 phosphorylation in response to insulin, AICAR, and contraction in mouse skeletal muscle. *Diabetes* **55**:2067-2076.
193. Reshef, L., Y. Olswang, H. Cassuto, B. Blum, C.M. Croniger, S.C. Kalhan, S.M. Tilghman and R.W. Hanson. 2003. Glyceroneogenesis and the triglyceride/fatty acid cycle. *J Biol Chem* **278**:30413-30416.
194. Abu-Elheiga, L., D.B. Almarza-Ortega, A. Baldini and S.J. Wakil. 1997. Human acetyl-CoA carboxylase 2. Molecular cloning, characterization, chromosomal mapping, and evidence for two isoforms. *J Biol Chem* **272**:10669-10677.
195. Castle, J.C., Y. Hara, C.K. Raymond, P. Garrett-Engele, K. Ohwaki, Z. Kan, J. Kusunoki and J.M. Johnson. 2009. ACC2 is expressed at high levels in human white adipose and has an isoform with a novel N-terminus. *PLoS One* **4**:e4369.
196. Ceddia, R.B. 2005. Direct metabolic regulation in skeletal muscle and fat tissue by leptin: implications for glucose and fatty acids homeostasis. *Int J Obes (Lond)* **29**:1175-1183.
197. Park, H., V.K. Kaushik, S. Constant, M. Prentki, E. Przybytkowski, N.B. Ruderman and A.K. Saha. 2002. Coordinate regulation of malonyl-CoA decarboxylase, sn-glycerol-3-phosphate acyltransferase, and acetyl-CoA carboxylase by AMP-activated protein kinase in rat tissues in response to exercise. *J Biol Chem* **277**:32571-32577.
198. Winder, W.W., J. Arogyasami, R.J. Barton, I.M. Elayan and P.R. Vehrs. 1989. Muscle malonyl-CoA decreases during exercise. *J Appl Physiol* **67**:2230-2233.
199. Saha, A.K., A.J. Schwarsin, R. Roduit, F. Masse, V. Kaushik, K. Tornheim, M. Prentki and N.B. Ruderman. 2000. Activation of malonyl-CoA decarboxylase in rat skeletal muscle by contraction and the AMP-activated protein kinase activator 5-aminoimidazole-4-carboxamide-1-beta -D-ribofuranoside. *J Biol Chem* **275**:24279-24283.
200. Habinowski, S.A., M. Hirshman, K. Sakamoto, B.E. Kemp, S.J. Gould, L.J. Goodyear and L.A. Witters. 2001. Malonyl-CoA decarboxylase is not a substrate of AMP-activated protein kinase in rat fast-twitch skeletal muscle or an islet cell line. *Arch Biochem Biophys* **396**:71-79.
201. Abu-Elheiga, L., M.M. Matzuk, K.A. Abo-Hashema and S.J. Wakil. 2001. Continuous fatty acid oxidation and reduced fat storage in mice lacking acetyl-CoA carboxylase 2. *Science* **291**:2613-2616.
202. Abu-Elheiga, L., W. Oh, P. Kordari and S.J. Wakil. 2003. Acetyl-CoA carboxylase 2 mutant mice are protected against obesity and diabetes induced by high-fat/high-carbohydrate diets. *Proc Natl Acad Sci U S A* **100**:10207-10212.
203. Oh, W., L. Abu-Elheiga, P. Kordari, Z. Gu, T. Shaikenov, S.S. Chirala and S.J. Wakil. 2005. Glucose and fat metabolism in adipose tissue of acetyl-CoA carboxylase 2 knockout mice. *Proc Natl Acad Sci U S A* **102**:1384-1389.

204. Pimenta, A.S., M.P. Gaidhu, S. Habib, M. So, S. Fediuc, M. Mirpourian, M. Musheev, R. Curi and R.B. Ceddia. 2008. Prolonged exposure to palmitate impairs fatty acid oxidation despite activation of AMP-activated protein kinase in skeletal muscle cells. *J Cell Physiol* **217**:478-485.
205. Chen, M.B., A.J. McAinch, S.L. Macaulay, L.A. Castelli, P.E. O'brien, J.B. Dixon, D. Cameron-Smith, B.E. Kemp and G.R. Steinberg. 2005. Impaired activation of AMP-kinase and fatty acid oxidation by globular adiponectin in cultured human skeletal muscle of obese type 2 diabetics. *J Clin Endocrinol Metab* **90**:3665-3672.
206. Salt, I., J.W. Celler, S.A. Hawley, A. Prescott, A. Woods, D. Carling and D.G. Hardie. 1998. AMP-activated protein kinase: greater AMP dependence, and preferential nuclear localization, of complexes containing the alpha2 isoform. *Biochem J* **334**:177-187.
207. Bergeron, R., J.M. Ren, K.S. Cadman, I.K. Moore, P. Perret, M. Pypaert, L.H. Young, C.F. Semenkovich and G.I. Shulman. 2001. Chronic activation of AMP kinase results in NRF-1 activation and mitochondrial biogenesis. *Am J Physiol Endocrinol Metab* **281**:E1340-E1346.
208. Canto, C. and J. Auwerx. 2009. PGC-1alpha, SIRT1 and AMPK, an energy sensing network that controls energy expenditure. *Curr Opin Lipidol* **20**:98-105.
209. Canto, C., Z. Gerhart-Hines, J.N. Feige, M. Lagouge, L. Noriega, J.C. Milne, P.J. Elliott, P. Puigserver and J. Auwerx. 2009. AMPK regulates energy expenditure by modulating NAD+ metabolism and SIRT1 activity. *Nature* **458**:1056-1060.
210. Zong, H., J.M. Ren, L.H. Young, M. Pypaert, J. Mu, M.J. Birnbaum and G.I. Shulman. 2002. AMP kinase is required for mitochondrial biogenesis in skeletal muscle in response to chronic energy deprivation. *Proc Natl Acad Sci U S A* **99**:15983-15987.
211. Jager, S., C. Handschin, J. St-Pierre and B.M. Spiegelman. 2007. AMP-activated protein kinase (AMPK) action in skeletal muscle via direct phosphorylation of PGC-1alpha. *Proc Natl Acad Sci U S A* **104**:12017-12022.
212. Civitarese, A.E., S. Carling, L.K. Heilbronn, M.H. Hulver, B. Ukropcova, W.A. Deutsch, S.R. Smith and E. Ravussin. 2007. Calorie restriction increases muscle mitochondrial biogenesis in healthy humans. *PLoS Med* **4**:e76.
213. Ferrara, N., B. Rinaldi, G. Corbi, V. Conti, P. Stiuso, S. Boccuti, G. Rengo, F. Rossi and A. Filippelli. 2008. Exercise training promotes SIRT1 activity in aged rats. *Rejuvenation Res* **11**:139-150.
214. Sutherland, L.N., M.R. Bomhof, L.C. Capozzi, S.A. Basaraba and D.C. Wright. 2009. Exercise and adrenaline increase PGC-1{alpha} mRNA expression in rat adipose tissue. *J Physiol* **587**:1607-1617.
215. Vila-Bedmar, R., M. Lorenzo and S. Fernandez-Veledo. 2010. Adenosine 5'-monophosphate-activated protein kinase-mammalian target of rapamycin cross talk regulates brown adipocyte differentiation. *Endocrinology* **151**:980-992.
216. Houseknecht, K.L., C.A. Baile, R.L. Matteri and M.E. Spurlock. 1998. The biology of leptin: a review. *J Anim Sci* **76**:1405-1420.

217. Pelleymounter, M.A., M.J. Cullen, M.B. Baker, R. Hecht, D. Winters, T. Boone and F. Collins. 1995. Effects of the obese gene product on body weight regulation in ob/ob mice. *Science* **269**:540-543.
218. Ceddia, R.B., W.N.J. William and R. Curi. 1998. Leptin increases glucose transport and utilization in skeletal muscle in vitro. *Gen Pharmacol* **31**:799-801.
219. Ceddia, R.B., W.N.J. William and R. Curi. 1999. Comparing effects of leptin and insulin on glucose metabolism in skeletal muscle: evidence for an effect of leptin on glucose uptake and decarboxylation. *Int J Obes Relat Metab Disord* **23**:75-82.
220. Ceddia, R.B., W.N.J. William, F.B. Lima and R. Curi. 1998. Leptin inhibits insulin-stimulated incorporation of glucose into lipids and stimulates glucose decarboxylation in isolated rat adipocytes. *J Endocrinol* **158**:R7-9.
221. William, W.N.J., R.B. Ceddia and R. Curi. 2002. Leptin controls the fate of fatty acids in isolated rat white adipocytes. *J Endocrinol* **175**:735-744.
222. Chen, G., K. Koyama, X. Yuan, Y. Lee, Y.T. Zhou, R. O'Doherty, C.B. Newgard and R.H. Unger. 1996. Disappearance of body fat in normal rats induced by adenovirus-mediated leptin gene therapy. *Proc Natl Acad Sci U S A* **93**:14795-14799.
223. Minokoshi, Y., Y.B. Kim, O.D. Peroni, L.G. Fryer, C. Muller, D. Carling and B.B. Kahn. 2002. Leptin stimulates fatty-acid oxidation by activating AMP-activated protein kinase. *Nature* **415**:339-343.
224. Arita, Y., S. Kihara, N. Ouchi, M. Takahashi, K. Maeda, J. Miyagawa, K. Hotta, I. Shimomura, T. Nakamura, K. Miyaoka, H. Kuriyama, M. Nishida, S. Yamashita, K. Okubo, K. Matsubara, M. Muraguchi, Y. Ohmoto, T. Funahashi and Y. Matsuzawa. 1999. Paradoxical decrease of an adipose-specific protein, adiponectin, in obesity. *Biochem Biophys Res Commun* **257**:79-83.
225. Yamauchi, T., J. Kamon, Y. Minokoshi, Y. Ito, H. Waki, S. Uchida, S. Yamashita, M. Noda, S. Kita, K. Ueki, K. Eto, Y. Akanuma, P. Froguel, F. Foufelle, P. Ferre, D. Carling, S. Kimura, R. Nagai, B.B. Kahn and T. Kadowaki. 2002. Adiponectin stimulates glucose utilization and fatty-acid oxidation by activating AMP-activated protein kinase. *Nat Med* **8**:1288-1295.
226. Rattan, R., S. Giri, A.K. Singh and I. Singh. 2005. 5-Aminoimidazole-4-carboxamide-1-beta-D-ribofuranoside inhibits cancer cell proliferation in vitro and in vivo via AMP-activated protein kinase. *J Biol Chem* **280**:39582-39593.
227. Zhou, J., W. Huang, R. Tao, S. Ibaragi, F. Lan, Y. Ido, X. Wu, Y.O. Alekseyev, M.E. Lenburg, G.F. Hu and Z. Luo. 2009. Inactivation of AMPK alters gene expression and promotes growth of prostate cancer cells. *Oncogene* **28**:1993-2002.
228. Giri, S., R. Rattan, E. Haq, M. Khan, R. Yasmin, J.S. Won, L. Key, A.K. Singh and I. Singh. 2006. AICAR inhibits adipocyte differentiation in 3T3L1 and restores metabolic alterations in diet-induced obesity mice model. *Nutr Metab (Lond)* **3**:31.
229. Habinowski, S.A. and L.A. Witters. 2001. The effects of AICAR on adipocyte differentiation of 3T3-L1 cells. *Biochem Biophys Res Commun* **286**:852-856.

230. Zhou, Y., D. Wang, Q. Zhu, X. Gao, S. Yang, A. Xu and D. Wu. 2009. Inhibitory effects of A-769662, a novel activator of AMP-activated protein kinase, on 3T3-L1 adipogenesis. *Biol Pharm Bull* **32**:993-998.
231. Minokoshi, Y., T. Alquier, N. Furukawa, Y.B. Kim, A. Lee, B. Xue, J. Mu, F. Foufelle, P. Ferre, M.J. Birnbaum, B.J. Stuck and B.B. Kahn. 2004. AMP-kinase regulates food intake by responding to hormonal and nutrient signals in the hypothalamus. *Nature* **428**:569-574.
232. Loftus, T.M., D.E. Jaworsky, G.L. Frehywot, C.A. Townsend, G.V. Ronnett, M.D. Lane and F.P. Kuhajda. 2000. Reduced food intake and body weight in mice treated with fatty acid synthase inhibitors. *Science* **288**:2379-2381.
233. Hu, Z., S.H. Cha, S. Chohnan and M.D. Lane. 2003. Hypothalamic malonyl-CoA as a mediator of feeding behavior. *Proc Natl Acad Sci U S A* **100**:12624-12629.
234. Shimokawa, T., M.V. Kumar and M.D. Lane. 2002. Effect of a fatty acid synthase inhibitor on food intake and expression of hypothalamic neuropeptides. *Proc Natl Acad Sci U S A* **99**:66-71.
235. Obici, S., Z. Feng, A. Arduini, R. Conti and L. Rossetti. 2003. Inhibition of hypothalamic carnitine palmitoyltransferase-1 decreases food intake and glucose production. *Nat Med* **9**:756-761.
236. Wolfgang, M.J., T. Kurama, Y. Dai, A. Suwa, M. Asaumi, S. Matsumoto, S.H. Cha, T. Shimokawa and M.D. Lane. 2006. The brain-specific carnitine palmitoyltransferase-1c regulates energy homeostasis. *Proc Natl Acad Sci U S A* **103**:7282-7287.
237. Andersson, U., K. Filipsson, C.R. Abbott, A. Woods, K. Smith, S.R. Bloom, D. Carling and C.J. Small. 2004. AMP-activated protein kinase plays a role in the control of food intake. *J Biol Chem* **279**:12005-12008.
238. Gao, S., K.P. Kinzig, S. Aja, K.A. Scott, W. Keung, S. Kelly, K. Strynadka, S. Chohnan, W.W. Smith, K.L. Tamashiro, E.E. Ladenheim, G.V. Ronnett, Y. Tu, M.J. Birnbaum, G.D. Lopaschuk and T.H. Moran. 2007. Leptin activates hypothalamic acetyl-CoA carboxylase to inhibit food intake. *Proc Natl Acad Sci U S A* **104**:17358-17363.
239. Claret, M., M.A. Smith, R.L. Batterham, C. Selman, A.I. Choudhury, L.G. Fryer, M. Clements, H. Al-Qassab, H. Heffron, A.W. Xu, J.R. Speakman, G.S. Barsh, B. Viollet, S. Vaulont, M.L. Ashford, D. Carling and D.J. Withers. 2007. AMPK is essential for energy homeostasis regulation and glucose sensing by POMC and AgRP neurons. *J Clin Invest* **117**:2325-2336.
240. McCrimmon, R.J., X. Fan, H. Cheng, E. McNay, O. Chan, M. Shaw, Y. Ding, W. Zhu and R.S. Sherwin. 2006. Activation of AMP-activated protein kinase within the ventromedial hypothalamus amplifies counterregulatory hormone responses in rats with defective counterregulation. *Diabetes* **55**:1755-1760.
241. McCrimmon, R.J., M. Shaw, X. Fan, H. Cheng, Y. Ding, M.C. Vella, L. Zhou, E.C. McNay and R.S. Sherwin. 2008. Key role for AMP-activated protein kinase in the ventromedial hypothalamus in regulating counterregulatory hormone responses to acute hypoglycemia. *Diabetes* **57**:444-450.

242. Han, S.M., C. Namkoong, P.G. Jang, I.S. Park, S.W. Hong, H. Katakami, S. Chun, S.W. Kim, J.Y. Park, K.U. Lee and M.S. Kim. 2005. Hypothalamic AMP-activated protein kinase mediates counter-regulatory responses to hypoglycaemia in rats. *Diabetologia* **48**:2170-2178.
243. Mangano, D.T., Y. Miao, I.C. Tudor and C. Dietzel. 2006. Post-reperfusion myocardial infarction: long-term survival improvement using adenosine regulation with acadesine. *J Am Coll Cardiol* **48**:206-214.
244. Bullough, D.A., C. Zhang, A. Montag, K.M. Mullane and M.A. Young. 1994. Adenosine-mediated inhibition of platelet aggregation by acadesine. A novel antithrombotic mechanism in vitro and in vivo. *J Clin Invest* **94**:1524-1532.
245. Drew, B.G. and B.A. Kingwell. 2008. Acadesine, an adenosine-regulating agent with the potential for widespread indications. *Expert Opin Pharmacother* **9**:2137-2144.
246. Gadalla, A.E., T. Pearson, A.J. Currie, N. Dale, S.A. Hawley, M. Sheehan, W. Hirst, A.D. Michel, A. Randall, D.G. Hardie and B.G. Frenguelli. 2004. AICA riboside both activates AMP-activated protein kinase and competes with adenosine for the nucleoside transporter in the CA1 region of the rat hippocampus. *J Neurochem* **88**:1272-1282.
247. Viollet, B., B. Guigas, J. Leclerc, S. Hebrard, L. Lantier, R. Mounier, F. Andreelli and M. Foretz. 2009. AMPK in the regulation of hepatic energy metabolism: from physiology to therapeutic perspectives. *Acta Physiol (Oxf)* **196**:81-98.
248. Kim, Y.D., K.G. Park, Y.S. Lee, Y.Y. Park, D.K. Kim, B. Nedumaran, W.G. Jang, W.J. Cho, J. Ha, I.K. Lee, C.H. Lee and H.S. Choi. 2008. Metformin inhibits hepatic gluconeogenesis through AMP-activated protein kinase-dependent regulation of the orphan nuclear receptor SHP. *Diabetes* **57**:306-314.
249. Boon, H., M. Bosselaar, S.F. Praet, E.E. Blaak, W.H. Saris, A.J. Wagenmakers, S.L. McGee, C.J. Tack, P. Smits, M. Hargreaves and L.J. van Loon. 2008. Intravenous AICAR administration reduces hepatic glucose output and inhibits whole body lipolysis in type 2 diabetic patients. *Diabetologia* **51**:1893-1900.
250. Cuthbertson, D.J., J.A. Babraj, K.J. Mustard, M.C. Towler, K.A. Green, H. Wackerhage, G.P. Leese, K. Baar, M. Thomason-Hughes, C. Sutherland, D.G. Hardie and M.J. Rennie. 2007. 5-aminoimidazole-4-carboxamide 1-beta-D-ribofuranoside acutely stimulates skeletal muscle 2-deoxyglucose uptake in healthy men. *Diabetes* **56**:2078-2084.
251. Dixon, R., J. Gourzis, D. McDermott, J. Fujitaki, P. Dewland and H. Gruber. 1991. AICA-riboside: safety, tolerance, and pharmacokinetics of a novel adenosine-regulating agent. *J Clin Pharmacol* **31**:342-347.
252. Albrektsen, T., K.S. Frederiksen, W.E. Holmes, E. Boel, K. Taylor and J. Fleckner. 2002. Novel genes regulated by the insulin sensitizer rosiglitazone during adipocyte differentiation. *Diabetes* **51**:1042-1051.
253. Guan, H.P., Y. Li, M.V. Jensen, C.B. Newgard, C.M. Steppan and M.A. Lazar. 2002. A futile metabolic cycle activated in adipocytes by antidiabetic agents. *Nat Med* **8**:1122-1128.

254. Fediuc, S., A.S. Pimenta, M.P. Gaidhu and R.B. Ceddia. 2008. Activation of AMP-activated protein kinase, inhibition of pyruvate dehydrogenase activity, and redistribution of substrate partitioning mediate the acute insulin-sensitizing effects of troglitazone in skeletal muscle cells. *J Cell Physiol* **215**:392-400.
255. LeBrasseur, N.K., M. Kelly, T.S. Tsao, S.R. Farmer, A.K. Saha, N.B. Ruderman and E. Tomas. 2006. Thiazolidinediones can rapidly activate AMP-activated protein kinase in mammalian tissues. *Am J Physiol Endocrinol Metab* **291**:E175-81.
256. Saha, A.K., P.R. Avilucea, J.M. Ye, M.M. Assifi, E.W. Kraegen and N.B. Ruderman. 2004. Pioglitazone treatment activates AMP-activated protein kinase in rat liver and adipose tissue in vivo. *Biochem Biophys Res Commun* **314**:580-585.
257. Bajaj, M., S. Suraamornkul, L.J. Hardies, L. Glass, N. Musi and R.A. DeFronzo. 2007. Effects of peroxisome proliferator-activated receptor (PPAR)-alpha and PPAR-gamma agonists on glucose and lipid metabolism in patients with type 2 diabetes mellitus. *Diabetologia* **50**:1723-1731.
258. Kubota, N., Y. Terauchi, T. Kubota, H. Kumagai, S. Itoh, H. Satoh, W. Yano, H. Ogata, K. Tokuyama, I. Takamoto, T. Mineyama, M. Ishikawa, M. Moroi, K. Sugi, T. Yamauchi, K. Ueki, K. Tobe, T. Noda, R. Nagai and T. Kadowaki. 2006. Pioglitazone ameliorates insulin resistance and diabetes by both adiponectin-dependent and -independent pathways. *J Biol Chem* **281**:8748-8755.
259. Galuska, D., L.A. Nolte, J.R. Zierath and H. Wallberg-Henriksson. 1994. Effect of metformin on insulin-stimulated glucose transport in isolated skeletal muscle obtained from patients with NIDDM. *Diabetologia* **37**:826-832.
260. Zhou, G., R. Myers, Y. Li, Y. Chen, X. Shen, J. Fenyk-Melody, M. Wu, J. Ventre, T. Doebber, N. Fujii, N. Musi, M.F. Hirshman, L.J. Goodyear and D.E. Moller. 2001. Role of AMP-activated protein kinase in mechanism of metformin action. *J Clin Invest* **108**:1167-1174.
261. Bell, D.S. and F. Ovalle. 2004. Outcomes of initiation of therapy with once-daily combination of a thiazolidinedione and a biguanide at an early stage of type 2 diabetes. *Diabetes Obes Metab* **6**:363-366.
262. Owen, M.R., E. Doran and A.P. Halestrap. 2000. Evidence that metformin exerts its anti-diabetic effects through inhibition of complex 1 of the mitochondrial respiratory chain. *Biochem J* **348 Pt 3**:607-614.
263. Brunmair, B., K. Staniek, F. Gras, N. Scharf, A. Althaym, R. Clara, M. Roden, E. Gnaiger, H. Nohl, W. Waldhausl and C. Furnsinn. 2004. Thiazolidinediones, like metformin, inhibit respiratory complex I: a common mechanism contributing to their antidiabetic actions? *Diabetes* **53**:1052-1059.
264. Zhou, G., I.K. Sebhat and B.B. Zhang. 2009. AMPK Activators - Potential Therapeutics for Metabolic and Other Diseases. *Acta Physiol (Oxf)*
265. Cool, B., B. Zinker, W. Chiou, L. Kifle, N. Cao, M. Perham, R. Dickinson, A. Adler, G. Gagne, R. Iyengar, G. Zhao, K. Marsh, P. Kym, P. Jung, H.S. Camp and E. Frevert. 2006. Identification and characterization of a small molecule AMPK activator that treats key components of type 2 diabetes and the metabolic syndrome. *Cell Metab* **3**:403-416.

266. Scott, J.W., B.J. van Denderen, S.B. Jorgensen, J.E. Honeyman, G.R. Steinberg, J.S. Oakhill, T.J. Iseli, A. Koay, P.R. Gooley, D. Stapleton and B.E. Kemp. 2008. Thienopyridone drugs are selective activators of AMP-activated protein kinase beta1-containing complexes. *Chem Biol* **15**:1220-1230.
267. Turner, N., J.Y. Li, A. Gosby, S.W. To, Z. Cheng, H. Miyoshi, M.M. Taketo, G.J. Cooney, E.W. Kraegen, D.E. James, L.H. Hu, J. Li and J.M. Ye. 2008. Berberine and its more biologically available derivative, dihydroberberine, inhibit mitochondrial respiratory complex I: a mechanism for the action of berberine to activate AMP-activated protein kinase and improve insulin action. *Diabetes* **57**:1414-1418.
268. Zang, M., S. Xu, K.A. Maitland-Toolan, A. Zuccollo, X. Hou, B. Jiang, M. Wierzbicki, T.J. Verbeuren and R.A. Cohen. 2006. Polyphenols stimulate AMP-activated protein kinase, lower lipids, and inhibit accelerated atherosclerosis in diabetic LDL receptor-deficient mice. *Diabetes* **55**:2180-2191.
269. Breen, D.M., T. Sanli, A. Giacca and E. Tsiani. 2008. Stimulation of muscle cell glucose uptake by resveratrol through sirtuins and AMPK. *Biochem Biophys Res Commun* **374**:117-122.
270. Um, J.H., S.J. Park, H. Kang, S. Yang, M. Foretz, M.W. McBurney, M.K. Kim, B. Viollet and J.H. Chung. 2010. AMP-activated protein kinase-deficient mice are resistant to the metabolic effects of resveratrol. *Diabetes* **59**:554-563.
271. Ajmo, J.M., X. Liang, C.Q. Rogers, B. Pennock and M. You. 2008. Resveratrol alleviates alcoholic fatty liver in mice. *Am J Physiol Gastrointest Liver Physiol* **295**:G833-42.
272. Baur, J.A., K.J. Pearson, N.L. Price, H.A. Jamieson, C. Lerin, A. Kalra, V.V. Prabhu, J.S. Allard, G. Lopez-Lluch, K. Lewis, P.J. Pistell, S. Poosala, K.G. Becker, O. Boss, D. Gwinn, M. Wang, S. Ramaswamy, K.W. Fishbein, R.G. Spencer, E.G. Lakatta, D. Le Couteur, R.J. Shaw, P. Navas, P. Puigserver, D.K. Ingram, R. de Cabo and D.A. Sinclair. 2006. Resveratrol improves health and survival of mice on a high-calorie diet. *Nature* **444**:337-342.
273. Shang, J., L.L. Chen, F.X. Xiao, H. Sun, H.C. Ding and H. Xiao. 2008. Resveratrol improves non-alcoholic fatty liver disease by activating AMP-activated protein kinase. *Acta Pharmacol Sin* **29**:698-706.
274. Long, Y.C. and J.R. Zierath. 2006. AMP-activated protein kinase signaling in metabolic regulation. *J Clin Invest* **116**:1776-1783.
275. Hardie, D.G. 2007. AMP-activated protein kinase as a drug target. *Annu Rev Pharmacol Toxicol* **47**:185-210.
276. Wang, M.Y., L. Orci, M. Ravazzola and R.H. Unger. 2005. Fat storage in adipocytes requires inactivation of leptin's paracrine activity: implications for treatment of human obesity. *Proc Natl Acad Sci U S A* **102**:18011-18016.
277. Canova, N., D. Lincova and H. Farghali. 2005. Inconsistent role of nitric oxide on lipolysis in isolated rat adipocytes. *Physiol Res* **54**:387-393.
278. Dole, V.P. and H. Meinertz. 1960. Microdetermination of long-chain fatty acids in plasma and tissues. *J Biol Chem* **235**:2595-2599.

279. Bligh, E.G. and W.J. Dyer. 1959. A rapid method of total lipid extraction and purification. *Can J Biochem Physiol* **37**:911-917.
280. Alp, P.R., E.A. Newsholme and V.A. Zammit. 1976. Activities of citrate synthase and NAD+-linked and NADP+-linked isocitrate dehydrogenase in muscle from vertebrates and invertebrates. *Biochem J* **154**:689-700.
281. Preiss, J., C.R. Loomis, W.R. Bishop, R. Stein, J.E. Niedel and R.M. Bell. 1986. Quantitative measurement of sn-1,2-diacylglycerols present in platelets, hepatocytes, and ras- and sis-transformed normal rat kidney cells. *J Biol Chem* **261**:8597-8600.
282. Fediuc, S., M.P. Gaidhu and R.B. Ceddia. 2006. Inhibition of insulin-stimulated glycogen synthesis by 5-aminoimidasole-4-carboxamide-1-beta-d-ribofuranoside-induced adenosine 5'-monophosphate-activated protein kinase activation: interactions with Akt, glycogen synthase kinase 3-3alpha/beta, and glycogen synthase in isolated rat soleus muscle. *Endocrinology* **147**:5170-5177.
283. Pold, R., L.S. Jensen, N. Jessen, E.S. Buhl, O. Schmitz, A. Flyvbjerg, N. Fujii, L.J. Goodyear, C.F. Gotfredsen, C.L. Brand and S. Lund. 2005. Long-term AICAR administration and exercise prevents diabetes in ZDF rats. *Diabetes* **54**:928-934.
284. Song, X.M., M. Fiedler, D. Galuska, J.W. Ryder, M. Fernstrom, A.V. Chibalin, H. Wallberg-Henriksson and J.R. Zierath. 2002. 5-Aminoimidazole-4-carboxamide ribonucleoside treatment improves glucose homeostasis in insulin-resistant diabetic (ob/ob) mice. *Diabetologia* **45**:56-65.
285. Winder, W.W., B.F. Holmes, D.S. Rubink, E.B. Jensen, M. Chen and J.O. Holloszy. 2000. Activation of AMP-activated protein kinase increases mitochondrial enzymes in skeletal muscle. *J Appl Physiol* **88**:2219-2226.
286. Danguir, J. and S. Nicolaidis. 1980. Circadian sleep and feeding patterns in the rat: possible dependence on lipogenesis and lipolysis. *Am J Physiol* **238**:E223-30.
287. Fredrikson, G., P. Stralfors, N.O. Nilsson and P. Belfrage. 1981. Hormone-sensitive lipase from adipose tissue of rat. *Methods Enzymol* **71 Pt C**:636-646.
288. Schweiger, M., R. Schreiber, G. Haemmerle, A. Lass, C. Fledelius, P. Jacobsen, H. Tornqvist, R. Zechner and R. Zimmermann. 2006. Adipose triglyceride lipase and hormone-sensitive lipase are the major enzymes in adipose tissue triacylglycerol catabolism. *J Biol Chem* **281**:40236-40241.
289. Zimmermann, R., G. Haemmerle, E.M. Wagner, J.G. Strauss, D. Kratky and R. Zechner. 2003. Decreased fatty acid esterification compensates for the reduced lipolytic activity in hormone-sensitive lipase-deficient white adipose tissue. *J Lipid Res* **44**:2089-2099.
290. Duncan, R.E., M. Ahmadian, K. Jaworski, E. Sarkadi-Nagy and H.S. Sul. 2007. Regulation of lipolysis in adipocytes. *Annu Rev Nutr* **27**:79-101.
291. Carrasco, S. and I. Merida. 2007. Diacylglycerol, when simplicity becomes complex. *Trends Biochem Sci* **32**:27-36.
292. Daval, M., F. Foufelle and P. Ferre. 2006. Functions of AMP-activated protein kinase in adipose tissue. *J Physiol* **574**:55-62.

293. Sullivan, J.E., K.J. Brocklehurst, A.E. Marley, F. Carey, D. Carling and R.K. Beri. 1994. Inhibition of lipolysis and lipogenesis in isolated rat adipocytes with AICAR, a cell-permeable activator of AMP-activated protein kinase. *FEBS Lett* **353**:33-36.
294. Koistinen, H.A., D. Galuska, A.V. Chibalin, J. Yang, J.R. Zierath, G.D. Holman and H. Wallberg-Henriksson. 2003. 5-amino-imidazole carboxamide riboside increases glucose transport and cell-surface GLUT4 content in skeletal muscle from subjects with type 2 diabetes. *Diabetes* **52**:1066-1072.
295. Arner, P. 2005. Human fat cell lipolysis: biochemistry, regulation and clinical role. *Best Pract Res Clin Endocrinol Metab* **19**:471-482.
296. Bergman, R.N., S.P. Kim, I.R. Hsu, K.J. Catalano, J.D. Chiu, M. Kabir, J.M. Richey and M. Ader. 2007. Abdominal obesity: role in the pathophysiology of metabolic disease and cardiovascular risk. *Am J Med* **120**:S3-8; discussion S29-32.
297. Mauriege, P., J. Galitzky, M. Berlan and M. Lafontan. 1987. Heterogeneous distribution of beta and alpha-2 adrenoceptor binding sites in human fat cells from various fat deposits: functional consequences. *Eur J Clin Invest* **17**:156-165.
298. Large, V. and P. Arner. 1998. Regulation of lipolysis in humans. Pathophysiological modulation in obesity, diabetes, and hyperlipidaemia. *Diabetes Metab* **24**:409-418.
299. Lafontan, M. and D. Langin. 2009. Lipolysis and lipid mobilization in human adipose tissue. *Prog Lipid Res* **48**:275-297.
300. Anthonsen, M.W., L. Ronnstrand, C. Wernstedt, E. Degerman and C. Holm. 1998. Identification of novel phosphorylation sites in hormone-sensitive lipase that are phosphorylated in response to isoproterenol and govern activation properties in vitro. *J Biol Chem* **273**:215-221.
301. Shen, W.J., S. Patel, V. Natu and F.B. Kraemer. 1998. Mutational analysis of structural features of rat hormone-sensitive lipase. *Biochemistry* **37**:8973-8979.
302. Garton, A.J., D.G. Campbell, D. Carling, D.G. Hardie, R.J. Colbran and S.J. Yeaman. 1989. Phosphorylation of bovine hormone-sensitive lipase by the AMP-activated protein kinase. A possible antilipolytic mechanism. *Eur J Biochem* **179**:249-254.
303. Gaidhu, M.P., S. Fediuc, N.M. Anthony, M. So, M. Mirpourian, R.L. Perry and R.B. Ceddia. 2009. Prolonged AICAR-induced AMP-kinase activation promotes energy dissipation in white adipocytes: novel mechanisms integrating HSL and ATGL. *J Lipid Res* **50**:704-715.
304. Lass, A., R. Zimmermann, G. Haemmerle, M. Riederer, G. Schoiswohl, M. Schweiger, P. Kienesberger, J.G. Strauss, G. Gorkiewicz and R. Zechner. 2006. Adipose triglyceride lipase-mediated lipolysis of cellular fat stores is activated by CGI-58 and defective in Chanarin-Dorfman Syndrome. *Cell Metab* **3**:309-319.
305. Granneman, J.G., H.P. Moore, R.L. Granneman, A.S. Greenberg, M.S. Obin and Z. Zhu. 2007. Analysis of lipolytic protein trafficking and interactions in adipocytes. *J Biol Chem* **282**:5726-5735.
306. Bezaire, V., A. Mairal, C. Ribet, C. Lefort, A. Girousse, J. Jocken, J. Laurencikiene, R. Anesia, A.M. Rodriguez, M. Ryden, B.M. Stenson, C. Dani, G. Ailhaud, P.

Arner and D. Langin. 2009. Contribution of Adipose Triglyceride Lipase and Hormone-sensitive Lipase to Lipolysis in Human hMADS Adipocytes. *J Biol Chem* **284**:18282-18291.
307. Brasaemle, D.L. 2007. Thematic review series: adipocyte biology. The perilipin family of structural lipid droplet proteins: stabilization of lipid droplets and control of lipolysis. *J Lipid Res* **48**:2547-2559.
308. Sztalryd, C., G. Xu, H. Dorward, J.T. Tansey, J.A. Contreras, A.R. Kimmel and C. Londos. 2003. Perilipin A is essential for the translocation of hormone-sensitive lipase during lipolytic activation. *J Cell Biol* **161**:1093-1103.
309. Miyoshi, H., J.W.n. Perfield, S.C. Souza, W.J. Shen, H.H. Zhang, Z.S. Stancheva, F.B. Kraemer, M.S. Obin and A.S. Greenberg. 2007. Control of adipose triglyceride lipase action by serine 517 of perilipin A globally regulates protein kinase A-stimulated lipolysis in adipocytes. *J Biol Chem* **282**:996-1002.
310. Moore, H.P., R.B. Silver, E.P. Mottillo, D.A. Bernlohr and J.G. Granneman. 2005. Perilipin targets a novel pool of lipid droplets for lipolytic attack by hormone-sensitive lipase. *J Biol Chem* **280**:43109-43120.
311. Wolf, G. 2009. Adipose-specific phospholipase as regulator of adiposity. *Nutr Rev* **67**:551-554.
312. Carling, D. 2005. AMP-activated protein kinase: balancing the scales. *Biochimie* **87**:87-91.
313. Sakamoto, K. and G.D. Holman. 2008. Emerging role for AS160/TBC1D4 and TBC1D1 in the regulation of GLUT4 traffic. *Am J Physiol Endocrinol Metab* **295**:E29-37.
314. Chavez, J.A., W.G. Roach, S.R. Keller, W.S. Lane and G.E. Lienhard. 2008. Inhibition of GLUT4 translocation by Tbc1d1, a Rab GTPase-activating protein abundant in skeletal muscle, is partially relieved by AMP-activated protein kinase activation. *J Biol Chem* **283**:9187-9195.
315. Eguez, L., A. Lee, J.A. Chavez, C.P. Miinea, S. Kane, G.E. Lienhard and T.E. McGraw. 2005. Full intracellular retention of GLUT4 requires AS160 Rab GTPase activating protein. *Cell Metab* **2**:263-272.
316. Stein, S.C., A. Woods, N.A. Jones, M.D. Davison and D. Carling. 2000. The regulation of AMP-activated protein kinase by phosphorylation. *Biochem J* **345 Pt 3**:437-443.
317. Joost, H.G. and A. Schurmann. 2001. Subcellular fractionation of adipocytes and 3T3-L1 cells. *Methods Mol Biol* **155**:77-82.
318. Larance, M., G. Ramm and D.E. James. 2008. The GLUT4 code. *Mol Endocrinol* **22**:226-233.
319. Ramm, G., M. Larance, M. Guilhaus and D.E. James. 2006. A role for 14-3-3 in insulin-stimulated GLUT4 translocation through its interaction with the RabGAP AS160. *J Biol Chem* **281**:29174-29180.
320. Hoehn, K.L., N. Turner, M.M. Swarbrick, D. Wilks, E. Preston, Y. Phua, H. Joshi, S.M. Furler, M. Larance, B.D. Hegarty, S.J. Leslie, R. Pickford, A.J. Hoy, E.W. Kraegen, D.E. James and G.J. Cooney. 2010. Acute or chronic upregulation of

mitochondrial fatty acid oxidation has no net effect on whole-body energy expenditure or adiposity. *Cell Metab* **11**:70-76.

321. Gaidhu, M.P. and R.B. Ceddia. 2011. The role of adenosine monophosphate kinase in remodeling white adipose tissue metabolism. *Exerc Sport Sci Rev* **39**:102-108.
322. Buhl, E.S., N. Jessen, R. Pold, T. Ledet, A. Flyvbjerg, S.B. Pedersen, O. Pedersen, O. Schmitz and S. Lund. 2002. Long-term AICAR administration reduces metabolic disturbances and lowers blood pressure in rats displaying features of the insulin resistance syndrome. *Diabetes* **51**:2199-2206.
323. Narkar, V.A., M. Downes, R.T. Yu, E. Embler, Y.X. Wang, E. Banayo, M.M. Mihaylova, M.C. Nelson, Y. Zou, H. Juguilon, H. Kang, R.J. Shaw and R.M. Evans. 2008. AMPK and PPARdelta agonists are exercise mimetics. *Cell* **134**:405-415.
324. Frontini, A. and S. Cinti. 2010. Distribution and development of brown adipocytes in the murine and human adipose organ. *Cell Metab* **11**:253-256.
325. Leibel, R.L. 2008. Energy in, energy out, and the effects of obesity-related genes. *N Engl J Med* **359**:2603-2604.
326. Araujo, R.L., B.M. Andrade, A.S. Padron, M.P. Gaidhu, R.L. Perry, D.P. Carvalho and R.B. Ceddia. 2010. High-fat diet increases thyrotropin and oxygen consumption without altering circulating 3,5,3'-triiodothyronine (T3) and thyroxine in rats: the role of iodothyronine deiodinases, reverse T3 production, and whole-body fat oxidation. *Endocrinology* **151**:3460-3469.
327. Patterson, C.M., S.G. Bouret, A.A. Dunn-Meynell and B.E. Levin. 2009. Three weeks of postweaning exercise in DIO rats produces prolonged increases in central leptin sensitivity and signaling. *Am J Physiol Regul Integr Comp Physiol* **296**:R537-48.
328. Gaidhu, M.P., N.M. Anthony, P. Patel, T.J. Hawke and R.B. Ceddia. 2010. Dysregulation of lipolysis and lipid metabolism in visceral and subcutaneous adipocytes by high-fat diet: role of ATGL, HSL, and AMPK. *Am J Physiol Cell Physiol* **298**:C961-71.
329. Cinti, S., M.C. Zingaretti, R. Cancello, E. Ceresi and P. Ferrara. 2001. Morphologic techniques for the study of brown adipose tissue and white adipose tissue. *Methods Mol Biol* **155**:21-51.
330. Smith, A.C., C.R. Bruce and D.J. Dyck. 2005. AMP kinase activation with AICAR simultaneously increases fatty acid and glucose oxidation in resting rat soleus muscle. *J Physiol* **565**:537-546.
331. Merrill, G.F., E.J. Kurth, D.G. Hardie and W.W. Winder. 1997. AICA riboside increases AMP-activated protein kinase, fatty acid oxidation, and glucose uptake in rat muscle. *Am J Physiol* **273**:E1107-12.
332. Gaidhu, M.P., R.L. Perry, F. Noor and R.B. Ceddia. 2010. Disruption of AMPKalpha1 signaling prevents AICAR-induced inhibition of AS160/TBC1D4 phosphorylation and glucose uptake in primary rat adipocytes. *Mol Endocrinol* **24**:1434-1440.

333. Rosenbaum, M., R. Goldsmith, D. Bloomfield, A. Magnano, L. Weimer, S. Heymsfield, D. Gallagher, L. Mayer, E. Murphy and R.L. Leibel. 2005. Low-dose leptin reverses skeletal muscle, autonomic, and neuroendocrine adaptations to maintenance of reduced weight. *J Clin Invest* **115**:3579-3586.
334. Bates, S.H., W.H. Stearns, T.A. Dundon, M. Schubert, A.W. Tso, Y. Wang, A.S. Banks, H.J. Lavery, A.K. Haq, E. Maratos-Flier, B.G. Neel, M.W. Schwartz and M.G.J. Myers. 2003. STAT3 signalling is required for leptin regulation of energy balance but not reproduction. *Nature* **421**:856-859.
335. Marangos, P.J., T. Loftus, J. Wiesner, T. Lowe, E. Rossi, C.E. Browne and H.E. Gruber. 1990. Adenosinergic modulation of homocysteine-induced seizures in mice. *Epilepsia* **31**:239-246.
336. Novak, C.M. and J.A. Levine. 2007. Central neural and endocrine mechanisms of non-exercise activity thermogenesis and their potential impact on obesity. *J Neuroendocrinol* **19**:923-940.
337. Nogueiras, R., M. Lopez, R. Lage, D. Perez-Tilve, P. Pfluger, H. Mendieta-Zeron, M. Sakkou, P. Wiedmer, S.C. Benoit, R. Datta, J.Z. Dong, M. Culler, M. Sleeman, A. Vidal-Puig, T. Horvath, M. Treier, C. Dieguez and M.H. Tschop. 2008. Bsx, a novel hypothalamic factor linking feeding with locomotor activity, is regulated by energy availability. *Endocrinology* **149**:3009-3015.
338. Steinberg, G.R., H.M. O'Neill, N.L. Dzamko, S. Galic, T. Naim, R. Koopman, S.B. Jorgensen, J. Honeyman, K. Hewitt, Z.P. Chen, J.D. Schertzer, J.W. Scott, F. Koentgen, G.S. Lynch, M.J. Watt, B.J. van Denderen, D.J. Campbell and B.E. Kemp. 2010. Whole body deletion of AMP-activated protein kinase {beta}2 reduces muscle AMPK activity and exercise capacity. *J Biol Chem* **285**:37198-37209.
339. Hawley, S.A., F.A. Ross, C. Chevtzoff, K.A. Green, A. Evans, S. Fogarty, M.C. Towler, L.J. Brown, O.A. Ogunbayo, A.M. Evans and D.G. Hardie. 2010. Use of cells expressing gamma subunit variants to identify diverse mechanisms of AMPK activation. *Cell Metab* **11**:554-565.
340. Lagouge, M., C. Argmann, Z. Gerhart-Hines, H. Meziane, C. Lerin, F. Daussin, N. Messadeq, J. Milne, P. Lambert, P. Elliott, B. Geny, M. Laakso, P. Puigserver and J. Auwerx. 2006. Resveratrol improves mitochondrial function and protects against metabolic disease by activating SIRT1 and PGC-1alpha. *Cell* **127**:1109-1122.
341. Kubota, N., W. Yano, T. Kubota, T. Yamauchi, S. Itoh, H. Kumagai, H. Kozono, I. Takamoto, S. Okamoto, T. Shiuchi, R. Suzuki, H. Satoh, A. Tsuchida, M. Moroi, K. Sugi, T. Noda, H. Ebinuma, Y. Ueta, T. Kondo, E. Araki, O. Ezaki, R. Nagai, K. Tobe, Y. Terauchi, K. Ueki, Y. Minokoshi and T. Kadowaki. 2007. Adiponectin stimulates AMP-activated protein kinase in the hypothalamus and increases food intake. *Cell Metab* **6**:55-68.
342. Frontini, A., P. Bertolotti, C. Tonello, A. Valerio, E. Nisoli, S. Cinti and A. Giordano. 2008. Leptin-dependent STAT3 phosphorylation in postnatal mouse hypothalamus. *Brain Res* **1215**:105-115.

APPENDIX A: OTHER CONTRIBUTIONS

During my Doctoral tenure, I made the following contributions not included in my Dissertation:

1. So M, Gaidhu MP, Maghdoori B, Ceddia RB. 2011. Analysis of time-dependent adaptations in whole-body energy balance in obesity induced by high-fat diet in rats. *Lipids Health Dis.* **10**:99.
2. **Gaidhu MP**, Ceddia RB. 2011. The Role of AMP-Kinase in Remodeling White Adipose Tissue Metabolism. *Exerc Sport Sci Rev.* **39**:102-8, 2011.
3. Gonzalez R, Reingold BK, Gao X, **Gaidhu MP**, Tsushima R, Unniappan S. Nesfatin-1 Exerts a Direct, Glucose-Dependent Insulinotropic Action on Mouse Islet Beta and MIN6 Cells. *J Endocrinol.* **208**: R9-R16, 2011.
4. Araujo RL, Andrade BM, Padrón AS, **Gaidhu MP**, Perry RLS, Carvalho DP, Ceddia RB. High-fat diet increases TSH and oxygen consumption without altering circulating T3 and T4 in rats: The role of iodothyronine deiodinases, rT3 production, and whole-body fat oxidation. *Endocrinology.* **151**:3460-9, 2010.
5. **Gaidhu MP**, Ceddia RB. 2009. Remodeling glucose and lipid metabolism through AMPK activation: relevance for treating obesity and Type 2 diabetes. *Clin. Lipidol.* **4**:465-477.
6. Anthony NM, **Gaidhu MP**, Ceddia RB. Regulation of visceral and subcutaneous adipocyte lipolysis by acute AICAR-induced AMPK activation. *Obesity* **17**:1312-7, 2009.
7. Pimenta AS, **Gaidhu MP (co-first author)**, Habib S, So M, Fediuc S, Mirpourian M, Musheev M, Curi R, Ceddia RB. Prolonged exposure to palmitate impairs fatty acid oxidation despite activation of AMP-activated protein kinase in skeletal muscle cells. *J. Cell. Physiol.* **217**:478-85, 2008.
8. Fediuc S, Pimenta A, **Gaidhu MP**, Ceddia RB. Activation of AMP-activated protein kinase, inhibition of pyruvate dehydrogenase activity, and redistribution of substrate partitioning mediate the acute insulin-sensitizing effects of troglitazone in skeletal muscle cells. *J. Cell. Physiol.* **215**:392-400, 2008.

APPENDIX B: ADDITIONAL DATA

		Wk 0	Wk 4	Wk 8
Glucose (mM)	**Con**	7.88 ± 0.14	7.68 ± 0.40	6.28 ± 0.29
	AICAR	7.82 ± 0.24	6.14 ± 0.16*	4.95 ± 0.48*
NEFAs (mM)	**Con**	0.53 ± 0.05	0.28 ± 0.02	0.15 ± 0.02
	AICAR	0.46 ± 0.05	0.16 ± 0.02*	0.50 ± 0.08*

Table B-1. Time-course effects of AICAR-induced AMPK activation on plasma glucose and NEFAs in animals chronically treated with AICAR. Non-esterified fatty acids (NEFAs). Week 0 (Wk 0), week 1 (Wk 1), week 4 (Wk 4), and week 8 (Wk 8). Data expressed as Mean ± SEM. N = 4-8 per group. Unpaired t-tests. *P<0.05 vs. control (Con).

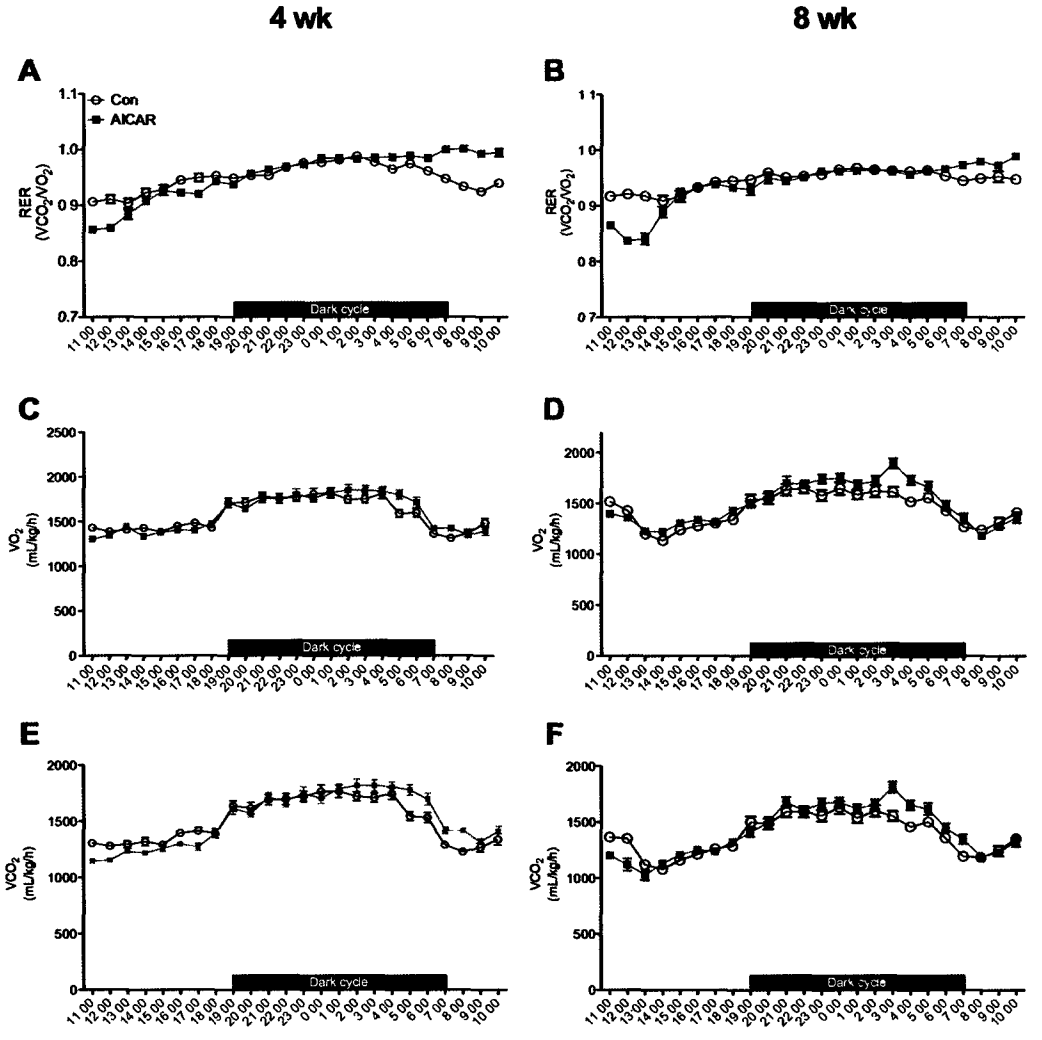

Figure B-1. *In vivo* measurements of respiratory exchange ratio (RER) **(A-B)**, oxygen consumption (VO_2) **(C-D)** and carbon dioxide production (VCO_2) **(E-F)**. Rats were placed into the CLAMS for 24h after 4 and 8 weeks of treatment. Values from all animals were pooled an average for an N=4 per group.

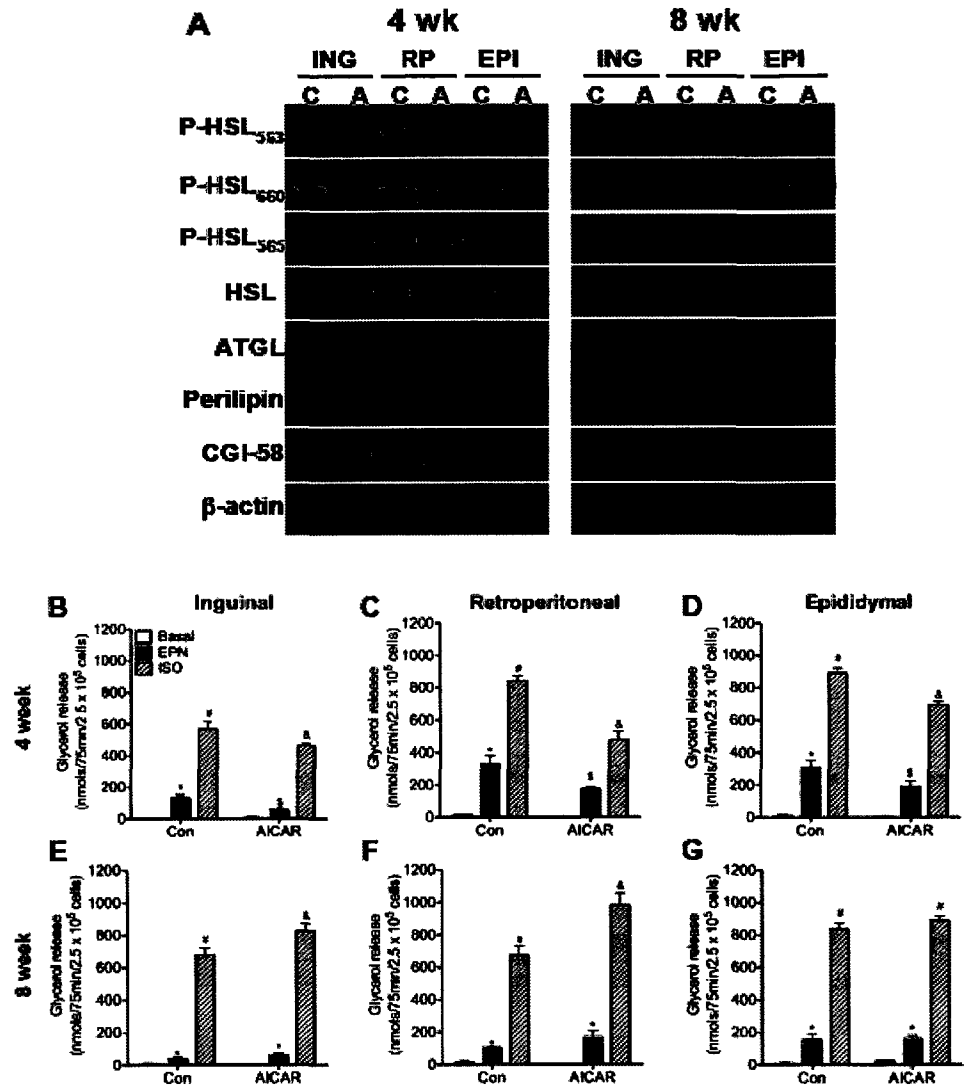

Figure B-2. Phosphorylation and content of HSL, ATGL, CGI-58, and perilipin in inguinal (ING), retroperitoneal (RP), and epididymal (EPI) fat pads at 4 and 8 weeks **(A)**. Samples from control and AICAR-treated animals are denoted as 'C' and 'A', respectively. Measurement of glycerol release to assess lipolysis under basal, epinephrine-(EPN), and isoproterenol (ISO)-stimulated conditions in isolated adipocytes from ING (**B** and **E**), RP (**C** and **F**), and EPI (**D** and **G**) fat depots. Data are compiled from 4 independent experiments with N=4 per group with triplicates in each assay performed. Two-way ANOVA with Bonferroni post-hoc tests. Symbols denote statistical significance ($P<0.05$) versus all other conditions.

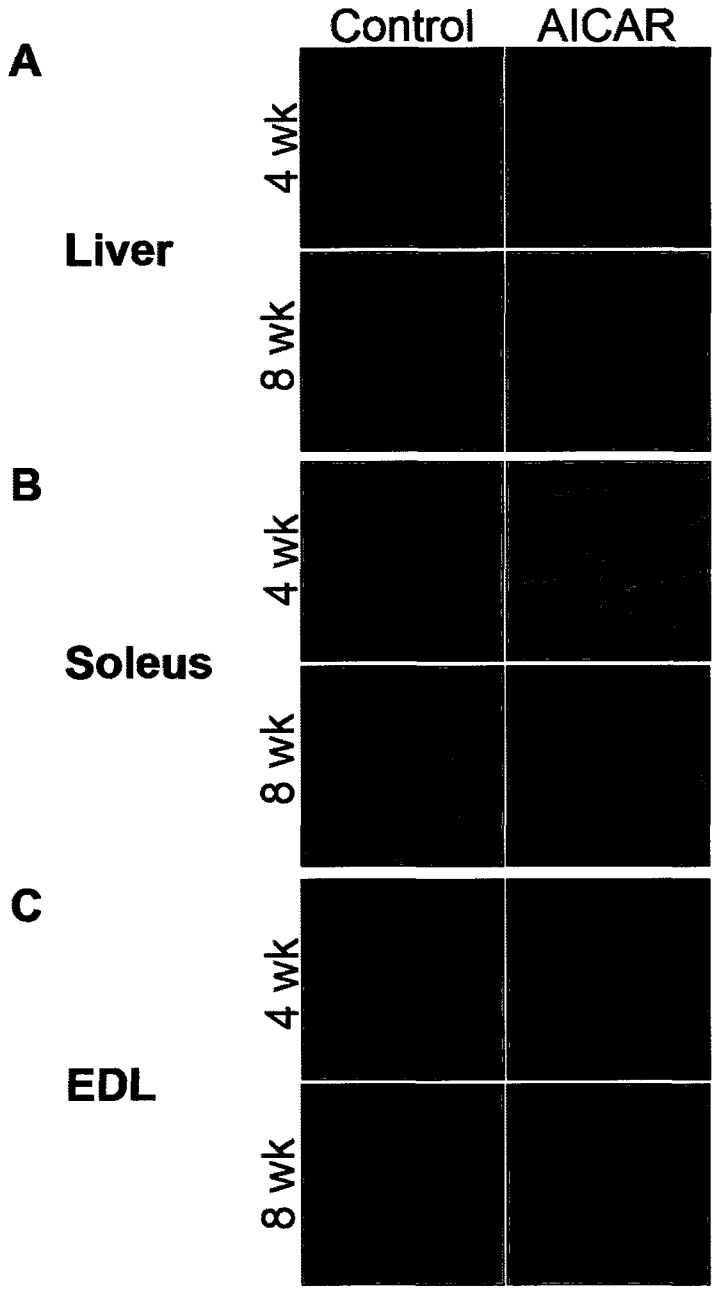

Figure B-3. Histology of liver **(A)**, soleus **(B)**, and extensor digitorum longus (EDL) **(C)** muscles. Sections (3μm) were deparaffinized and stained with hemotoxylin/eosin. Muscle samples are all cross-sectional.

APPENDIX C: COPYRIGHT PERMISSIONS

Chapter 5: Permission granted from the Americal Physiology Society

Request for Permission to Reproduce Previously Published Material

(please save this file to your desktop, fill out, save again, and e-mail to permissions@the-aps.org)

Your Name: Mandeep Pinky Gaidhu E-mail: pinky.gaidhu@gmail.com

Affiliation: York University

University Address (for PhD students): 357 Bethune College, York University, 4700 Keele Street, Toronto, ON M3J 1P3

Description of APS material to be reproduced (check all that apply):

- ☐ Figure
- ☐ Table
- ☐ Partial Article
- ☑ Full Article
- ☐ Abstract
- ☐ Book Chapter
- Other (please describe):

Are you an author of the APS material to be reproduced? ⊙ Yes ○ No

Please provide all applicable information about the APS material you wish to use:

Author(s): MP Gaidhu, NM Anthony, P Patel, TJ Hawke, RB Ceddia

Article or Chapter Title: Dysregulation of lipolysis and lipid metabolism in visceral and subcutaneous adipo

Journal or Book Title: Journal of Lipid Research Am J Physiol Cell Physiol

Volume: 298 Page No(s): C961-71 Figure No(s): 6 1-6 Table No(s): 3 1-3

Year: 2010 DOI: 10 1152/ajpcell.00547 2009

(If you are reproducing figures or tables from more than one article, please fill out and send a separate form for each citation)

Please provide all applicable information about where the APS material will be used:

How will the APS material be used? (please select from drop-down list) Dissertation

If "other," please describe:

Title of publication or meeting where APS material will be used (if used in an article or book chapter, please provide the journal name or book title as well as the article/chapter title):

The role of AMP-kinase in regulating and remodeling adipocyte metabolism
This article will be Chapter 5 of this dissertation

Publisher (if journal or book): Library and Archives of Canada

URL (if website):

Date of Meeting or Publication: 2011

Will readers be charged for the material: ○ Yes ⊙ No

Additional Information:

Entire article to be used solely for the purpose of dissertaion, Chapter 5.

APPROVED
By pripka at 9:26 am, Jun 20, 2011

THE AMERICAN PHYSIOLOGICAL SOCIETY
9650 Rockville Pike, Bethesda, MD 20814-3991

Permission is granted for use of the material specified above, provided the publication is credited as the source, including the words "used with permission."

Rita Scheman
Publications Manager & Executive Editor

Chapter 6: Permission granted from the Endocrine Society

Subject: Granted - Copyright Permission Request
Date: Sunday, June 19, 2011 10:44 AM
From: permissions@endo-society.org
To: <pinky.gaidhu@gmail.com>
Cc: <permissions@endo-society.org>
Conversation: Granted - Copyright Permission Request

The Endocrine Society
8401 Connecticut Avenue, Suite 900
Chevy Chase, MD 20815-5817
Telephone: 301-941-0200
Fax: 301-941-0259
www.endo-society.org <http://www.endo-society.org>
TIN Number: 73-0531256

Form was submitted by: pinky.gaidhu@gmail.com

Original author to publish in a Dissertation.

Date: June 19, 2011
Reference Number:

Name: Mandeep PInky Gaidhu
Organization: York University
Department:
Address: 4700 Keele Street
City, State and Postal Code: Toronto, Ontario M3J1P3
Country: Canada
Phone: 416 736 2100 x20426
Fax:
Email: pinky.gaidhu@gmail.com

Journal: Molecular Endocrinology
Author Name: MP Gaidhu
Title: Disruption of AMPKalpha1 signaling prevents AICAR-induced AS160/TBC1D4 phosphorylation and glucose uptake in primary rat adipocytes
Year: 2010
Volume: 24
Page Range: 1434-40